A DISSERTATION FOR THE DEGREE OF DOCTOR OF PHILOSOPHY

Azobenzene-Based Acrylic Resin System as a Photo-Responsive Switchable Pressure-Sensitive Adhesive for Electronic Device Transfer Process

일렉트로닉 디바이스 전사 공정을 위한 광 반응형 점착력 가변형 아조벤젠 기반 아크릴 점착소재

Advisor: Hyun-Joong Kim

by

Tae-Hyung Lee

PROGRAM IN ENVIRONMENTAL MATERIALS SCIENCE

GRADUATE SCHOOL

SEOUL NATIONAL UNIVERSITY

AUGUST, 2022

서울대학교 SEOUL NATIONAL UNIVERSITY

SEOUL NATIONAL UNIVERSITY

GRADUATE SCHOOL

PROGRAM IN ENVIRONMENTAL MATERIALS SCIENCE

We hereby recommend the thesis by
Tae-Hyung Lee

Entitled

Azobenzene-Based Acrylic Resin System as a Photo-Responsive Switchable Pressure-Sensitive Adhesive for Electronic Device Transfer Process

Be accepted in fulfillment of the requirements for the degree of doctor of philosophy

June, 2022

Committee on Final Examination

Chairman _____
Prof. Minsang Kwon

Co-Chairman _____
Prof. Hyun-Joong Kim

Member _____
Ph. D. Ick-Kyung Sung

Member _____
Ph. D. Youngdo Kim

Member _____
Ph. D. Seungman Kim

서울대학교 SEOUL NATIONAL UNIVERSITY

Abstract

Azobenzene-Based Acrylic Resin System as a Photo-Responsive Switchable Pressure-Sensitive Adhesive for Electronic Device Transfer Process

Tae-Hyung Lee
Program in Environmental Materials Science
Graduate School
Seoul National University

Many researchers have studied switchable adhesives that can switch adhesive properties based on external stimuli. The switchable adhesive has high adhesive force when it attaches to an adherent. However, its adhesive force is decreased in response to external stimuli for detaching process. The switchable adhesive is used in our daily lives or the medical industry for convenience of use. However, the material has recently been required in the advanced manufacturing process of electric and electronic industries for temporary bonding or transfer processes. Previously studied materials achieve adhesion switchability under restricted conditions (hydration, heat and long switching times), and some materials have limitations related to reuse because of irreversible reactions or residue formation on substrates.

In this study, azobenzene moiety was used for photo-responsive material. Switchable adhesives were fabricated by mixing the azobenzene-containing acrylic polymer and low molecular weight azobenzene compounds. The photo-responsive switchable adhesive had a non-sticky surface in an initial state.

서울대학교 SEOUL NATIONAL UNIVERSITY

However, its adhesive force was activated with 365 nm ultraviolet (UV) light irradiation and returned to the initial state with visible light irradiation. The adhesion switching was repeatable, and the repeatability was confirmed up to 30 times without changes in adhesive force.

The adhesion switching mechanism was found. The photo-isomerization between trans- and cis-azobenzene by UV and visible lights induced the dissolution and re-formation of crystalline structures of the azobenzene compounds. The transition in crystalline structures accompanied transitions in mechanical properties, surface energy and glass transition temperature (T_g) of the switchable PSA, resulting in the switching in adhesive force. Various azobenzene compounds were synthesized, including hydrocarbon substituents with different chain lengths. By studying the switchable PSAs with the azobenzene compounds, it was found that the degree of the solidity of the crystalline structures of the azobenzene compounds determines the UV irradiation intensity and time required for the adhesion switching.

A UV laser system was used as a light source for the adhesion switching test. The laser system enables precise micro-patterning and a fast process. This study applied a switchable adhesive containing a UV absorber to the laser process. The UV absorber prevented surface damage caused by a high-energy laser beam. Although there was no linear relationship between the energy density or power of the laser and the adhesion switching properties, the optimum process conditions could be obtained in specific ranges of energy density and power. Micro-patterned adhesion switching of the switchable PSA was possible with the process conditions, and a selective mini-LED transfer process was successfully implemented.

서울대학교

The above studies proposed novel switchable PSAs containing azobenzene moiety. The switchable PSAs were photo-responsive, rapid and reusable. In addition, the applicability to the selective transfer process of microscopic electronic devices, including mini-LED, by the laser process was proposed.

Keywords: pressure-sensitive adhesive, switchable PSA, photo-responsive, azobenzene, photo-isomerization, mini-LED, UV laser, transfer process

Student Number: 2013-21131

서울대학교 SEOUL NATIONAL UNIVERSITY

Table of Contents

서울대학교 SEOUL NATIONAL UNIVERSITY

Chapter 2

Photo-responsive, Switchable, Pressure-Sensitive Adhesives Containing Azobenzene Moiety

서울대학교 SEOUL NATIONAL UNIVERSITY

서울대학교

Chapter 3

Influence of Hydrocarbon Chain Length of Azo-compounds in Photo-responsive Adhesion Switching Efficiency

서울대학교 SEOUL NATIONAL UNIVERSITY

서울대학교 SEOUL NATIONAL UNIVERSITY

Chapter 4

UV Laser Process for Adhesion Switching and Selective Mini-LED Transfer

서울대학교 SEOUL NATIONAL UNIVERSITY

서울대학교 SEOUL NATIONAL UNIVERSITY

서울대학교 SEOUL NATIONAL UNIVERSITY

List of Tables

서울대학교 SEOUL NATIONAL UNIVERSITY

List of Figures

서울대학교 SEOUL NATIONAL UNIVERSITY

서울대학교

서울대학교

서울대학교 SEOUL NATIONAL UNIVERSITY

서울대학교

서울대학교 SEOUL NATIONAL UNIVERSITY

서울대학교 SEOUL NATIONAL UNIVERSITY

서울대학교
Seoul National University

Chapter 1

Introduction

서울대학교
SEOUL NATIONAL UNIVERSITY

1. Introduction

1.1 Pressure-Sensitive Adhesives

The adhesive is a polymeric material used to attach two substrates and is generally recognized as a material applied in a liquid state and cured into a solid by moisture, heat and light to form adhesion. The curing process is an irreversible chemical reaction that makes a cross-linked network between polymer chains constituting the adhesive. Hot-melt and pressure-sensitive adhesive (PSA) are exceptional types of adhesives. The hot-melt adhesive with thermoplastic polymer is applied to the substrate in a melted state by heating. It forms adhesion through a liquid to a solid phase transition. The PSA is a material that maintains its stickiness at using temperature and can form adhesion without chemical reaction or phase transition (Creton, *et al.*, 2016). Because of the convenient usage of the PSA, it has been used in various fields from our daily life to the electric and electronic and medical industry.

For the stickiness of the PSA at using temperature, the glass transition temperature (T_g) of the PSA must be 25-45°C lower than the using temperature (Creton, 2003). The T_g is a unique characteristic of an amorphous polymer. The polymer's molecular segment consisting of several molecular repeating units has mobility at this temperature. It cannot induce a complete transition in the material's phase, but the segmental movement of the polymer cause transition in mechanical properties of the polymer from a glassy to a rubbery state. Because of the low T_g, the PSA is in the rubbery state at the using temperature. The molecular mobility of the rubbery PSA enables physical permeation to the substrate and enlarges the surface area for chemical interaction between the PSA and adherent. Consequently, the PSA can form adhesion with the adherent

서울대학교

at usage temperature due to its low T_g.

In addition, viscoelastic properties have also been discussed as an important factor for the PSA's adhesion characteristics. Macosko defined frequency ranges of adhesive fabrication processes and test methods in the master curve of the PSA **(Figure 1-1a)** (Macosko, 1977). Chang published a study of the viscoelastic windows of the PSA based on Macosko's frequency ranges (Chang, 1991). Chang evaluated the viscoelastic properties of various PSAs in the frequency range of the peel and creep test, 10^{-1} sec^{-1} to 10^{2} sec^{-1}, as a reference range. It was found that most PSAs had a storage modulus (G') and loss modulus (G") between 10^{3} and 10^{6} Pa at the frequency range.

Furthermore, the frequency-modulus graph was divided into five areas to define the classification of the PSAs with viscoelastic characteristics **(Figure 1-1b)**. As described in the previous paragraph, the influence of the T_g in the adhesion can be explained by focusing on the surficial phenomena such as physical permeation and enlargement of chemical surface interaction. However, the viscoelastic properties are related to both surficial and bulk characteristics in the adhesion phenomena. In adhesion, the bulk property is expressed as cohesive strength. To maintain adhesive force at usage temperature, the PSA should have adequately high cohesive force without losing wettability at the interface. The viscoelastic windows can explain it.

Consequently, the PSA has unique properties that can form adhesion with the adherent in using temperature without curing or phase transition when it has low T_g and proper viscoelastic properties. However, in other words, it means that the PSA, whose T_g and viscoelastic properties are determined by the chemical structure and manufacturing process, has fixed adhesive strength.

서울대학교 SEOUL NATIONAL UNIVERSITY

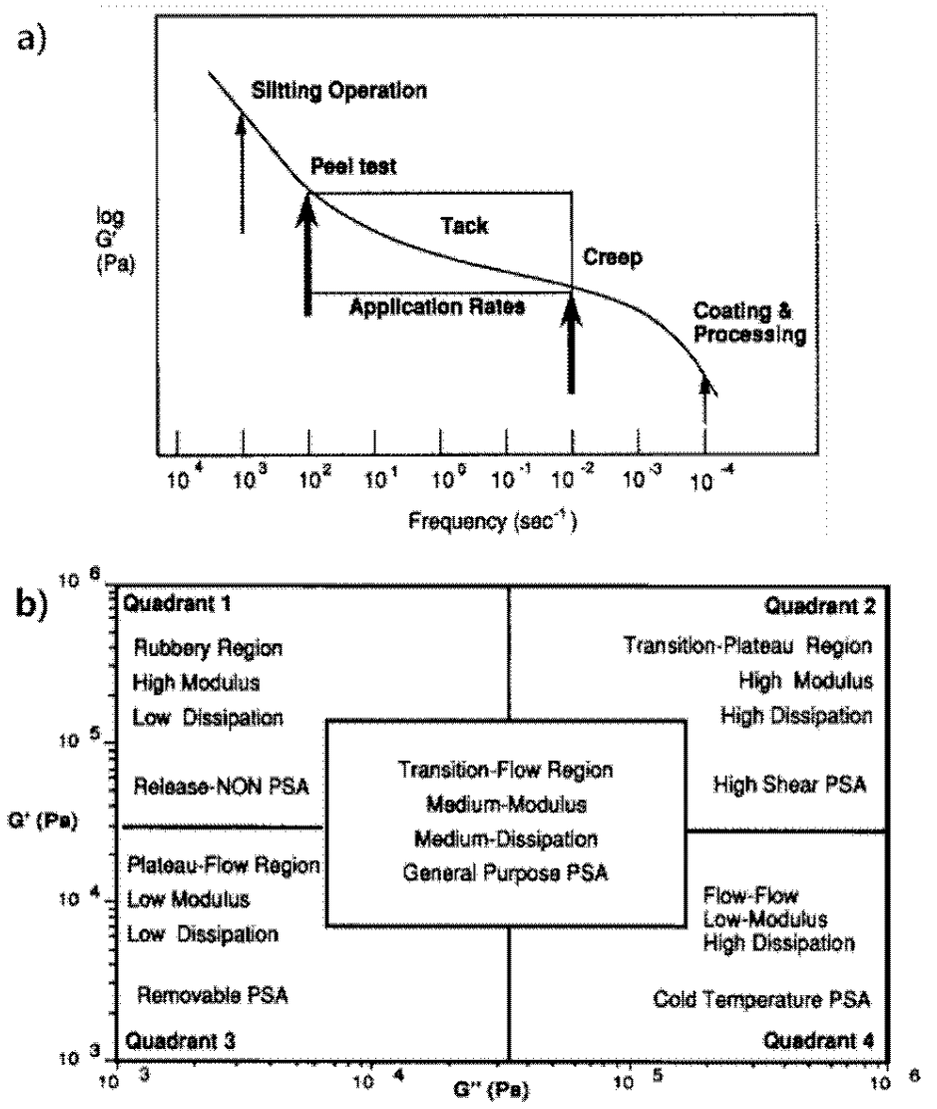

Figure 1-1. a) Frequency ranges of adhesive formulation processes and test methods on the viscoelastic master curve of the PSA (Macosko, 1977), b) Viscoelastic window of the PSAs (Chang, 1991).

서울대학교

1.2 Switchable Adhesives

Many researchers have studied adhesives to improve their adhesive strength or realize multi-functions such as thermal conductivity, electrical conductivity, high/low dielectric properties, optically clear properties or stretchability while having a fixed adhesive strength. However, recently, researchers have been interested in adhesives having controllable adhesive strength for convenience of use or advanced manufacturing processes. These kinds of adhesives are called switchable adhesives or dynamic adhesives. The changes in the switchable adhesives' physical, chemical or geometrical characteristics responding to external stimuli lead to switching of adhesive strength. Croll et al. defined these external stimuli as mechanical, electromagnetic, fluidic and thermal stimuli as switching triggers (Croll, *et al.*, 2019). Researchers introduced various stimuli-responsive dynamic chemical linkage, interaction or transitions in conformation and configuration to the adhesives for inducing changes in physical, chemical and geometrical properties.

Many researchers have studied various switching triggers and switchable adhesive systems. The studies can be classified by switching mechanisms as reversible host-guest interaction (Nakamura, *et al.*, 2014, Yamaguchi, *et al.*, 2012, Zheng, *et al.*, 2012, Zheng, *et al.*, 2013), a transition of coordination complexes with metal-ion (Gao, *et al.*, 2019, Heinzmann, *et al.*, 2014, Nakamura, *et al.*, 2014), the conformational transition of the polymer (La Spina, *et al.*, 2007), a transition of the crystalline structure of liquid crystal elastomer (Cho, *et al.*, 2003, De Crevoisier, *et al.*, 1999, Ohzono, *et al.*, 2019, Ohzono, *et al.*, 2020), photo-isomerization of azobenzene moiety (Akiyama, *et al.*, 2014, Yamaguchi, *et al.*, 2012) and irreversible crosslinking (Boyne, *et al.*, 2001, Ebe, *et al.*, 2003). Also, the switching triggers are heat (Cho, *et al.*, 2003, De Crevoisier, *et al.*, 1999, Heinzmann, *et al.*, 2014, Ohzono, *et al.*, 2019, Ohzono,

서울대학교

et al., 2020), solvent (Zheng, *et al.*, 2012), PH control (La Spina, *et al.*, 2007, Zheng, *et al.*, 2013), light (Akiyama, *et al.*, 2014, Boyne, *et al.*, 2001, Ebe, *et al.*, 2003, Gao, *et al.*, 2019, Heinzmann, *et al.*, 2014, Ohzono, *et al.*, 2020, Yamaguchi, *et al.*, 2012) and magnetic field (Testa, *et al.*, 2020).

The performance of the switchable adhesives can be evaluated by 'how wide its controllable adhesive force range is' and 'how quickly the adhesive force can be switched'. These can be expressed as a switching ratio and switching time (Croll, *et al.*, 2019). The switching ratio is the ratio between the maximum adhesion force (F_{max}) and the minimum adhesion force (F_{min}) of the switchable adhesives. The F_{max} and F_{min} also mean the switched on/off adhesive forces, respectively. The switching time means the stimuli application time required for adhesion switching. Although it depends on the application, researchers have studied switchable adhesives with a high switching ratio and low switching time. According to the two parameters, Croll et al. collect many studies on the switchable adhesive **(Figure 1-2)**.

서울대학교

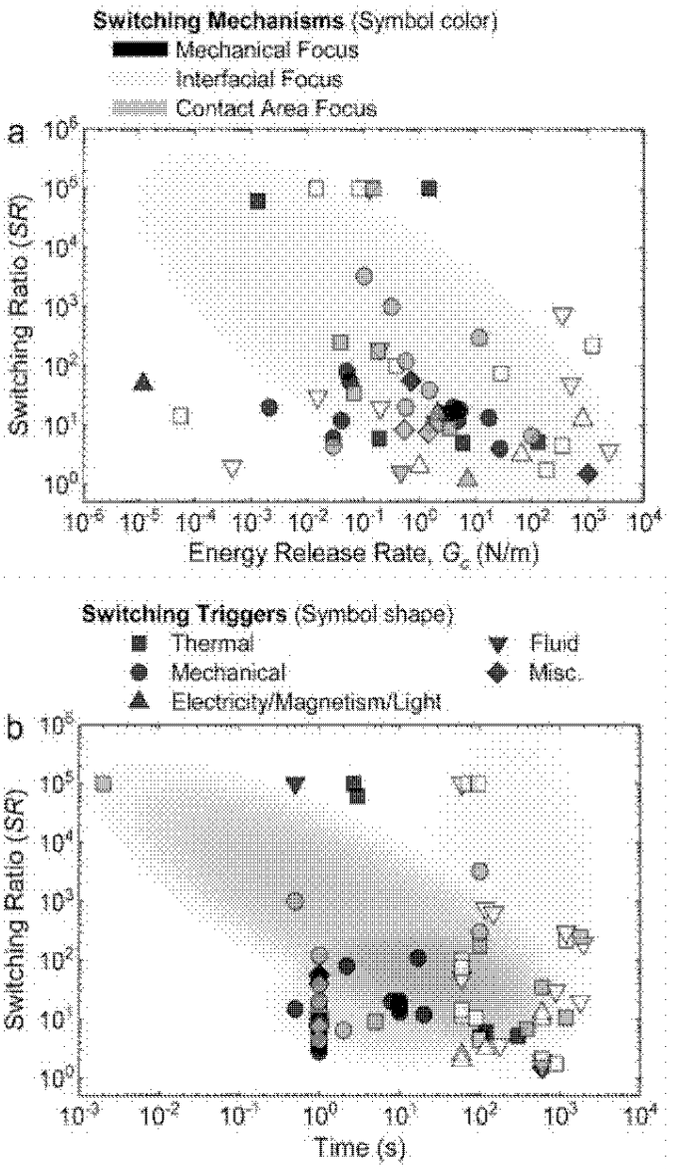

Figure 1-2. Adhesion switching performance of the reported switchable adhesives (Croll, *et al.*, 2019).

서울대학교

1.3 Adhesion Switching Mechanism

Adhesion is the state in which two substances adhere to each other, and it is formed at the interface of two materials when they come into contact with each other. In this case, the adhesion can be mainly approached by surface chemistry. However, the adhesion force can be evaluated when the substrates are separated. Therefore, many studies have tried to understand the adhesion by fracture mechanics (Maugis, *et al.*, 1980). The adhesion fracture mechanics consider not only surface chemistry but also complex factors such as bulk properties of adhesive and substrate, surface area, and fracture modes.

Understanding the complex adhesion phenomena is a prerequisite for the design of switchable adhesives because it is closely related to the adhesion switching mechanism. Croll et al. reported the adhesion switching mechanisms of switchable adhesives (Croll, *et al.*, 2019). They classified the switching mechanisms into three factors: contact area change, mechanics and near interface properties **(Figure 1-3)**. In the case of adhesion switching by changing the contact area between the adhesive and adherent, external stimuli induce a change in the surface morphology of the adhesives. The adhesive force per unit area does not change. The mechanics factor means compliance and modulus, i.e. bulk properties of the adhesives. The transition in adhesive's bulk properties affects both interfacial and cohesive properties and induces a change in adhesive force by mechanical factor. Finally, the factor of near interface refers to the adhesion switching caused by property change at the interface between the adhesive and adherent. The phenomenon at the interface between the adhesive and substrate is generally represented by the work of adhesion (ω).

$$\omega = \gamma_a + \gamma_s - \gamma_{as}$$

서울대학교 SEOUL NATIONAL UNIVERSITY

γ_a, γ_s and γ_{as} are the surface energy of adhesive, substrate and interface, respectively. The work of adhesion is a thermodynamic concept applied to separating two substances. Because it is governed by surface energy, the surface chemistry of adhesive and adherent determines the work of adhesion. Consequently, transition in surface chemistry responded to switching triggers also can cause adhesion switching of the switchable adhesives.

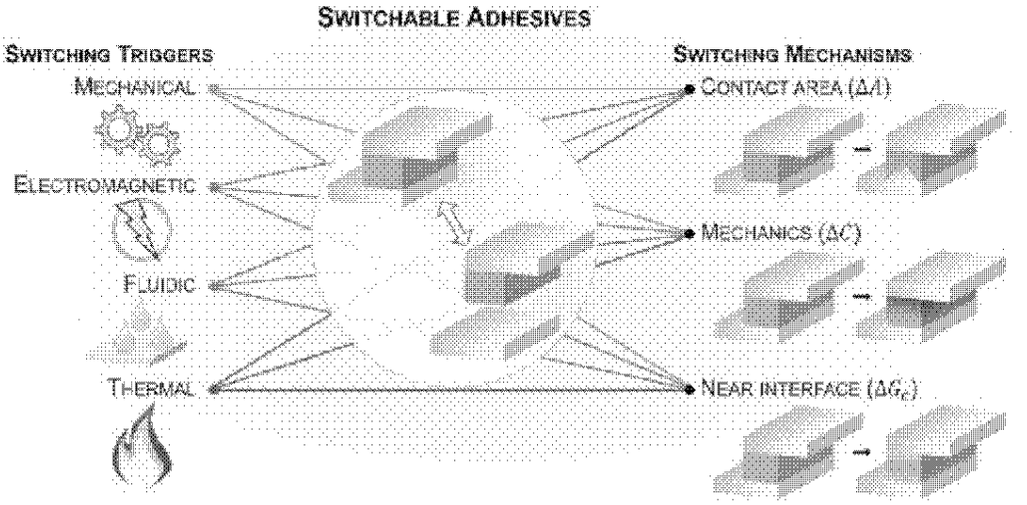

Figure 1-3. The definition of the switchable adhesives suggested by Croll et al. (Croll, *et al.*, 2019).

The adhesion switching resulting from physical, chemical and geometrical changes has a switching mechanism to change the characteristics of the material itself. However, even if the adhesive characteristics are maintained, the adhesive strength can be evaluated differently depending on the test methods and conditions, i.e. the fracture modes and conditions. The evaluation methods are based on the direction of external forces such as tension, compression and shear. If force is applied to a parallel direction of the interface, the adhesives can hold significant stress, but it can be peeled with a much lower force if the force is applied to a vertical direction. Tack, peel and lap shear tests are

서울대학교

representative methods for evaluating adhesion force according to the fracture direction **(Figure 1-4)**. There are different variables depending on the methods, and the extent of each variable's influence on the adhesive force is also different. The representative models of each test method are presented in the next paragraph. Some factors applied as adhesion switching mechanisms can be derived through the equations.

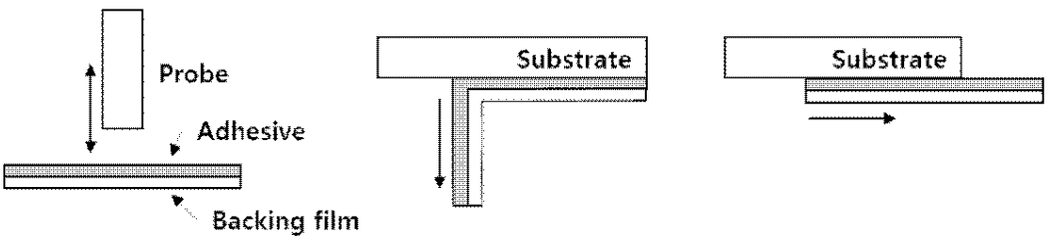

Figure 1-4. Schematic illustration of the adhesion test methods. Probe tack, 90° peel and lap shear test from the left.

1.3.1. Probe Tack

The tack test is classified into loop tack, ball tack and probe tack according to the type of material contacting the adhesive, and the probe tack method with a cylindrical probe is mostly used. The probe is separated vertically from the adhesive surface after the flat bottom probe contacts the adhesive with specific pressure and time. External factors less influence this method, and the adhesion strength is determined mainly by the adhesive's bulk properties and work of adhesion between the probe and adhesive surface. A representative model was reported by Kendall (Kendall, 1971).

서울대학교

$$F_t = \sqrt{\frac{8\pi}{(1-\nu^2)} E\omega a^3}$$

F_t is probe tack force, ν is Poisson's ratio of the adhesive, E is Young's modulus, and a is adhesion area. The above equation assumes that the thickness of the adhesive is infinite. When the adhesive is thin, the equation is modified as

$$F_t = \sqrt{\frac{2\pi E\omega a^4}{t}}$$

where t is the thickness of adhesive. Simplifying this correlation as

$$F_t \propto \sqrt{\frac{E\omega}{t}} a^2$$

According to the above equations, the probe tack force is determined by modulus, work of adhesion, adhesive thickness, and contact area. The modulus, work of adhesion and adhesion area correspond to Croll's switching mechanism, i. e. mechanics, near interface and contact area, respectively. The contact area is a dominant factor for tack force, and the force is proportional to the square root of the modulus and work of adhesion.

서울대학교

1.3.2. Peel

Since the adhesive has different peel strength depending on a peel-off angle, it is common to name an evaluation method such as the 90° peel test and 180° peel test according to the peeling angle. For the preparation of the peel test specimen, the adhesive is coated to backing film in most cases. When the adhesive is peeled off from the adherent with the backing film, not only characteristics of the adhesive itself but also the physical properties of the backing film engage in peel strength. Unlike tack and shear tests, which are affected by the adhesive area, the peel strength is affected by adhesion width since it is separated from the interface line between adhesive and adherent. The representative model for the peel test is as follows (Kendall, 1975).

$$F_p = Etb[\sqrt{(1-cos\theta)^2 + \frac{2\omega}{Et}} - (1-cos\theta)]$$

F_p, b and θ are the peel force, the adhesion width and the peeling angle, respectively. Kendall's model shows the influence of adhesive properties and peeling angle on the peel force. However, it does not consider factors related to the backing film. The thickness of the backing film determines the radius of curvature of the adhesive, and the physical properties of the backing film are reflected in the peel force due to bending and tensile deformation during the peeling test. For this reason, several models include additional factors related to the backing film (Saito, 1985, 畑, *et al.*, 1947).

서울대학교 SEOUL NATIONAL UNIVERSITY

$$F_p = \frac{\omega b}{\frac{\rho}{\rho + t_{bf}} - cos\theta}$$

$$F_p(1 - cos\theta) + \frac{{F_p}^2}{2t_{bf}E_{bf}} = \omega b$$

ρ is the radius of curvature, t_{bf} is the thickness of the backing film, and E_{bf} is Young's modulus of the backing film.

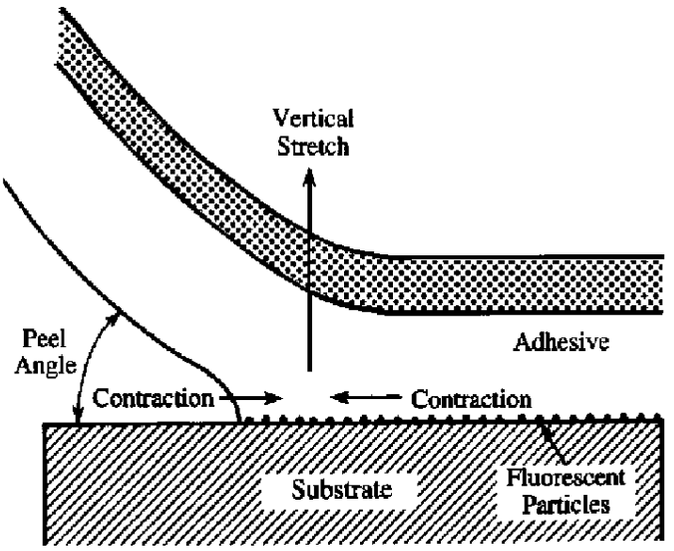

Figure 1-5. Schematic illustration of various deformations in the peel test (Sperling, 2005).

서울대학교

1.3.3. Shear

Shear is a mode in which force is applied parallel to the interface, and the adhesive can withstand the highest stress. For this reason, the backing film's physical properties can greatly influence the measured value, and in some cases, the physical properties of the substrate can also affect the results. The representative model of shear mode assumes a structure in which adhesive is sandwiched between two rigid substrates to reduce variables (Suh, *et al.*, 2007).

$$F_s = \sqrt{2G\omega a^2 b^2 / t}$$

G is the shear modulus of adhesive, and a is the length of the adhesion area. When the adhesive film is attached to the substrate, the modulus and thickness of the backing film should be additionally considered.

1.3.4. Wetting

Most of the models mentioned above assume an equilibrium adhesion state between adhesive and adherent. However, the wetting process has to be preceded to reach the equilibrium state. The work of adhesion determines the wetting of liquid on a solid surface. However, even in the wetting of the liquid onto the solid substrate, the viscosity of the liquid acts as a force to resist the spread of the liquid (Härth, *et al.*, 2012). In the same context, the wetting by the surface energy of the polymer adhesive is resisted by the modulus (Donatas, 1999). Therefore, the wetting of the adhesive to adherent can be determined by surface energy and modulus of the adhesive, and the magnitude of wetting can

서울대학교 SEOUL NATIONAL UNIVERSITY

lead to different results from the prediction by the adhesion models.

1.3.5. Frequency Dependence of Adhesive

Since the adhesive consists of a viscoelastic polymer, it has a frequency dependence. It means that the physical properties of polymer vary with the frequency of external force. The frequency dependence is a physical phenomenon related to the diffusion of polymers and time (Sperling, 2005). When the frequency is high, that is, stress or strain is applied with high speed to polymer, it can't secure enough time to make a molecular movement. Therefore, the material has a higher modulus under high-frequency stress. It is closely related that a polymer has a lower modulus at high temperatures and a higher modulus at lower temperatures. The adhesion force is changed depending on the separating speed from the substrate.

Peng et al. published a study about adhesive force change by peeling rate **(Figure 6)** (Peng, *et al.*, 2014). They conducted peel tests with various peeling angles and rates. In all 45°, 60° and 90° peel tests, the peel-off force increased with the increasing peeling rate. It means that the adhesive force can be controlled only with separation speed. In addition, they also presented the influence of adhesive thickness on the peel test with experimental data.

서울대학교

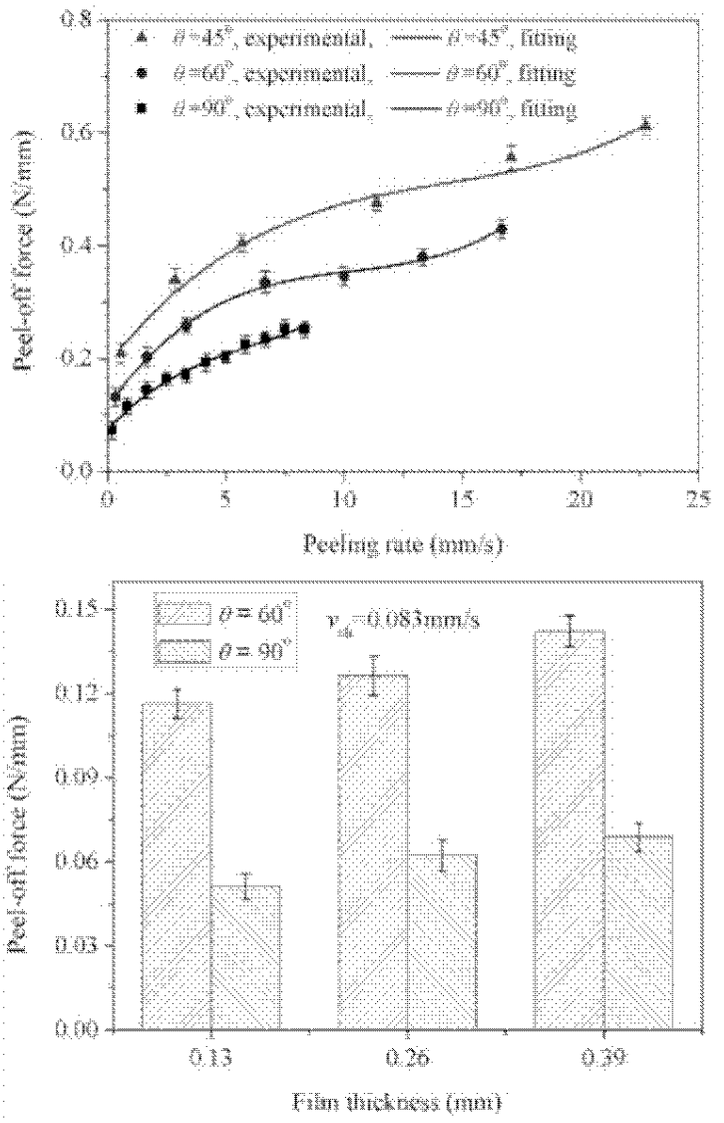

Figure 1-6. Peeling rate, peeling angle and film thickness dependence of adhesive (Peng, *et al.*, 2014).

서울대학교

1.3.6. Summary of the Influence of Adhesion Switching Factors

Understanding adhesion phenomena is to understand the adhesion formation mechanism and influence factors determining adhesive force. The factors are applied as switching factors for designing switchable adhesives. In addition to the Croll et al. mentioned factors such as contact area (A), mechanics (E or C) and near interface (ω), the adhesion switching factors obtained through various models and studies are adhesive thickness (t), peeling angle (θ), characteristics of backing film (t_{bf}, E_{bf}, ρ) and test speed. The influence of each factor, excluding some factors that were irreversibly determined during the adhesive preparation process, is briefly summarized in **Table 1-1**. '+' and '-' mean the influence on adhesion force when the value of the factor increases.

As mentioned above, the contact area and work of adhesion are positive factors for adhesive force in all adhesion models. Although modulus is also positive to adhesive force in every model, it also acts as a negative factor when the wetting process is considered. High modulus restricts adhesive's wetting to adherent, which causes a reduction in the actual contact area in the adhesion of identical dimension adhesives. In addition, test speed induces modulus variation by the frequency dependence of adhesive, which is a positive factor for adhesive force. If peeling angle or test speed is used as adhesion switching factors, it will be a way to induce adhesion switching with changes in the external environment rather than designing trigger-responsive materials. However, this simple method may have a limited adhesion control range. Therefore, stimuli-responsive switchable adhesives have been studied.

서울대학교

Table 1-1. Summary of the effects of adhesion switching factors

Factors	Influence
Contact area	+
Modulus (Compliance)	+ (Adhesion equilibrium state) - (Before adhesion equilibrium state)
Work of adhesion	+
Peeling angle	- (0° to 90°) + (90° to 180°)
Test speed	+

1.4. Introduction of Azobenzene Moiety

The stimuli-responsive switchable adhesives require dynamic chemical linkage or unique chemical structures, and the response of these elements to external stimuli should induce changes in the physical and chemical properties of the adhesives.

As the stimuli-responsive element, azobenzene moiety was used in this study. Azobenzene, an azo compound having two benzene groups, is a representative photo-reactive moiety that exists as a trans-form in a stable state and isomerizes to a cis-form by exposure to ultraviolet (UV) light. After activation as a cis-form, it returns to the trans-azobenzene by visible light irradiation. This process is called photo-isomerization **(Figure 1-7)**. The photo-isomerization of azobenzene has the advantages of high quantum yields and low photo-bleaching, and it occurs in a picosecond timescale (Beharry, *et al.*, 2011).

서울대학교 SEOUL NATIONAL UNIVERSITY

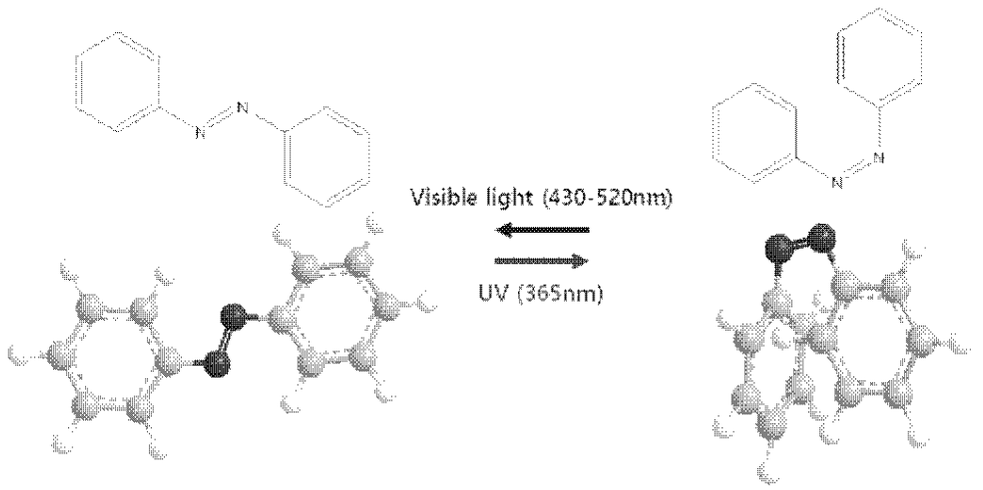

Figure 1-7. Photo-isomerization of the azobenzene moiety and three-dimensional chemical structures of trans- and cis-isomer.

Two isomers of azobenzene have mechanically and chemically different characteristics. Trans-azobenzene molecules can be arranged easily by intermolecular pi-pi interaction because of their two aromatic groups and planar structure. However, cis-azobenzene has a three-dimensionally twisted structure, and it sterically hinders intermolecular stacking. Since the difference in intermolecular stacking, photo-isomerization of azobenzene can accompany the phase transition between solid and liquid **(Figure 1-8)** (Norikane, *et al.*, 2016). In addition, the cis-form has a relatively higher molecular dipole moment because it loses the symmetric structure of the trans-form. There is also a transition in the UV-visible absorption spectrum by photo-isomerization. Trans-form has the main absorption band at a UV wavelength of 300–350nm, whereas cis-azobenzene mainly absorbs visible light of 400–450nm (Beharry and Woolley, 2011). It also can be confirmed visually in their color **(Figure 1-8)**. Since these differences between trans- and cis-azobenzene can change materials' physical and chemical properties, they have been widely used in photo-responsive actuators, molecular robotics and surface modification

서울대학교

(Goulet-Hanssens, *et al.*, 2020).

Because azobenzene is sufficiently non-reactive, it can be modified into various structures by substituting a reactive group in phenyl groups (Barrett, *et al.*, 2007). By the modification, it can be introduced as a pendant of various polymers such as acrylate (Morino, *et al.*, 1998), methacrylate (Shin, *et al.*, 2019), imide (Agolini, *et al.*, 1970), ester (Hvilsted, *et al.*, 1995), ether (Bignozzi, *et al.*, 1999) and acetylene (Izumi, *et al.*, 2000). Furthermore, azobenzene groups can be introduced directly into the backbone chain (Izumi, *et al.*, 2000). Due to the high usability, azobenzene can be easily introduced into the acrylic polymer, one of the primary materials of adhesive, for photo-responsive properties.

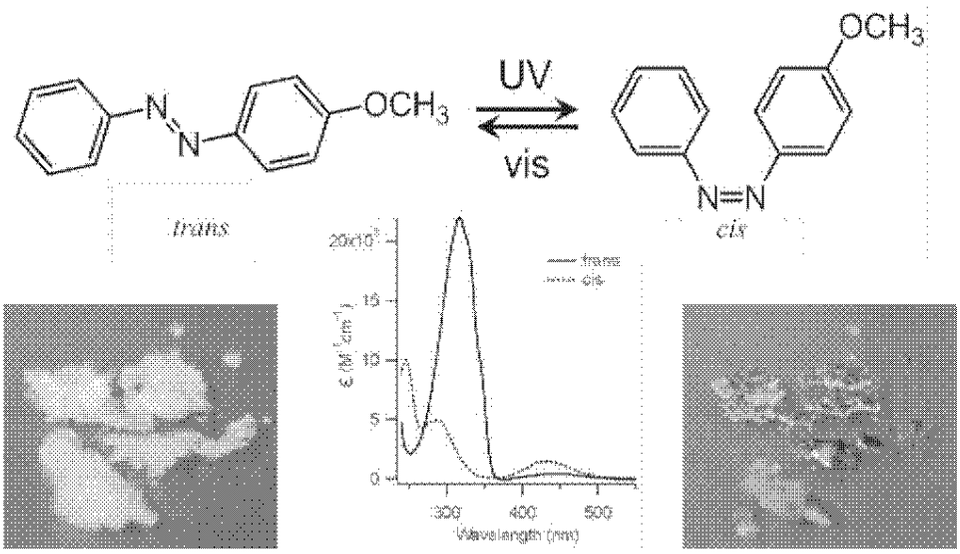

Figure 1-8. Changes in phase, color and UV-Vis absorption spectrum between trans- and cis-azobenzene (Beharry and Woolley, 2011, Norikane, *et al.*, 2016).

서울대학교

1.5. Electronic Device Transfer Process

The electronic device transfer process can be called transfer printing in a broad category. One of the motivations for recent studies on transfer printing is the complex manufacturing processes of flexible and stretchable electronic devices. Rigid devices are manufactured by forming circuits and other components on inorganic substrates. The circuits are formed on the substrate through a lithography process, and devices are repeatedly exposed to high temperatures and chemicals for etching during the process. However, flexible and stretchable devices are fabricated with flexible organic substrates. Since the organic substrates are vulnerable to high temperatures and chemicals, it is impossible to directly form circuits on the organic substrates (Linghu, *et al.*, 2018). Therefore, the manufacturing process for flexible and stretchable devices requires an additional process for transferring the inorganic components from inorganic substrate to organic substrate. This process is called transfer printing.

In addition to the flexible device manufacturing process, transfer printing is also applied for transferring tiny devices. The transfer printing process has recently emerged as an important issue in manufacturing next-generation display panels, i.e. mini- and micro-LED (Light Emitting Diode) displays. The micro-LED display has advantages such as high brightness, energy efficiency, fast response and longer lifetime compared to OLED display. Unlike OLED display, which is manufactured by depositing self-luminous organic materials on a substrate, the micro-LED display is manufactured by transferring micro-sized inorganic LEDs to the panel. For high-resolution displays, millions to tens of millions of micro-LEDs are transferred to a single display panel. The transfer process must be fast, precise and high yield; it is considered a major hurdle in micro-LED display manufacturing. To realize this process, a material that can

서울대학교

pick up many LEDs and drop them on demand is required, and various switchable adhesives have been studied as the material. (Choi, *et al.*, 2017, Kim, *et al.*, 2019, Li, *et al.*, 2020, Meitl, *et al.*, 2005, Pan, *et al.*, 2020). Some of the representative technologies are listed in **Table 1-2**.

Table 1-2. Summary of micro-LED mass transfer technologies (Ding, *et al.*, 2019, Li, *et al.*, 2020).

Methods	**Switching triggers or mechanisms**	**Transfer rate**	**Manufacturing time**	
			4k-75 inch display	**2k mobile phone**
Elastomer Stamp	Frequency dependence	1M units/hr	25 hrs	11 hrs
Roll Printing	Frequency dependence	1000 units/sec	7 hrs	3 hrs
Laser Release	Additional cross-linking	100M units/hr	0.25 hrs	0.11 hrs
Liquid Assembly	Gravity & fluid force	50M units/hr	0.50 hrs	0.22 hrs
Magnetic Stamp	Magnetic force	0.9M units/hr	27 hrs	12 hrs
Electrostatic Stamp	Electrostatic force	12M units/hr	2 hrs	0.92 hrs

서울대학교 SEOUL NATIONAL UNIVERSITY

2. Literature review

2.1. Heat Triggered Switchable Adhesives

Phase transition is a simple way to realize adhesion switching. Hot-melt adhesive is the adhesive whose adhesive strength is controlled by heat-induced phase transition. Several thermoplastics have been used as a hot-melt adhesive. After applying to substrate with melted state, it has adhesive force by solidification. It can be separated by reheating. Therefore, hot-melt adhesive can be classified as the switchable adhesive that responds to a thermal stimulus. However, since the phase transition temperature is generally high, it has not been studied as switchable adhesives. In addition, although the adhesion force of PSA changes depending on the temperature, it isn't easy to use as a switchable adhesive because the temperature range for sufficient adhesion switching is 60-70 °C (Zosel, 1985).

For this reason, researchers have been studying liquid crystal adhesive whose adhesion property changes in a low and narrow temperature range. Crevoisier et al. polymerized acrylic polymer having a crystalline side chain by copolymerizing 50% of an acrylic monomer having a long perfluoroalkyl side chain (C_2H_4-C_8F_{17}) and 50% of a methacrylic monomer having a long alkyl chain ($C_{17}H_{35}$) (De Crevoisier, *et al.*, 1999). This material changed from a rigid smectic phase to a soft isotropic phase causing tackiness of the surface **(Figure 1-9a)**. As a result of the tack measurement, it could be confirmed that adhesion force occurred rapidly in a narrow temperature range of 2 °C, but when the temperature rose, the adhesion strength rapidly decreased again **(Figure 1-9b)**.

서울대학교 SEOUL NATIONAL UNIVERSITY

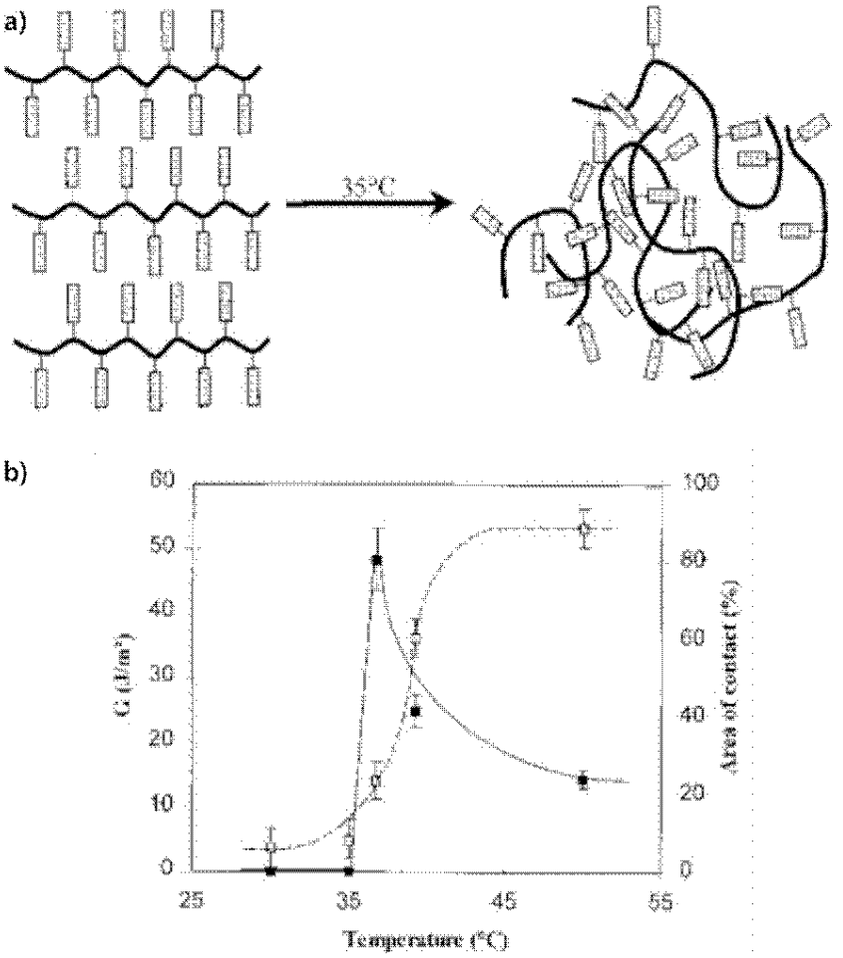

Figure 1-9. a) Phase transition of the side-chain crystalline polymer from smectic to isotropic phase, b) Tack results of the thermal switchable adhesive according to temperature (De Crevoisier, *et al.*, 1999).

서울대학교

Some researchers have used liquid crystalline polymers for thermal-responsive switchable adhesive, and recently, Ohzono et al. reported liquid crystalline adhesive using a liquid crystal elastomer (LCE). It incorporated a liquid crystalline structure into the polymer backbone chain (Ohzono, *et al.*, 2019). The LCE was prepared by copolymerizing RM82, di-functional acrylate, multi-functional acrylate and thiol monomer through a thiol-acrylate Michael addition reaction **(Figure 1-10a)**. This polymer has a nematic phase at room temperature. A phase transition occurs from the nematic to the isotropic phase when the temperature increases. The LCE adhesive had high adhesive force in its nematic phase, and the adhesive force decreased with phase transition to the isotropic state **(Figure 1-10b)**. This paper explained that the viscoelastic properties predominately affected adhesion force, and the nematic state had appropriate physical properties as PSA. However, the adhesion force of this LCE did not decrease to zero even in the isotropic phase, and the switching ratio, about 3, was not high enough.

서울대학교

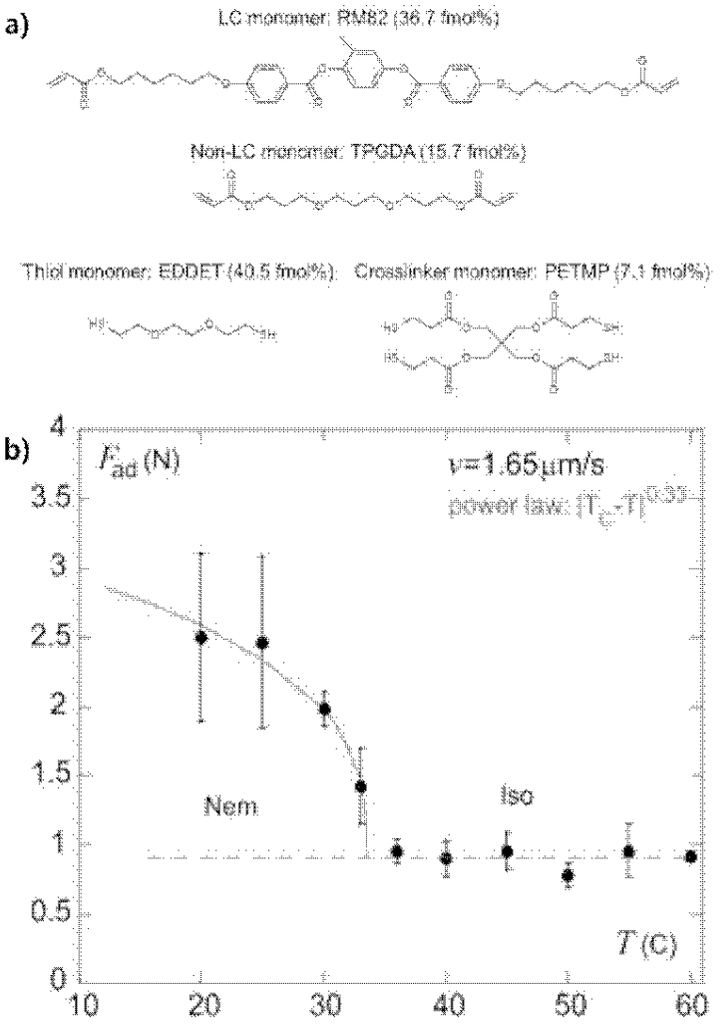

Figure 1-10. a) Materials for polymerizing nematic LCE switchable adhesive, b) Tack results of the thermal switchable adhesive according to temperature (Ohzono, *et al.*, 2019).

서울대학교
SEOUL NATIONAL UNIVERSITY

While the studies mentioned above used heat-induced phase transition, some studies used a heat-triggered geometrical change of polymer as an adhesion switching mechanism. Eisenhaure et al. studied microstructured shape memory polymer for switchable adhesive (Eisenhaure, *et al.*, 2013). This material induced adhesion switching through the change of adhesion area caused by shape memory characteristics. A pad having pyramid-shaped micro-tips was prepared by curing diglycidyl ether of bisphenol A epoxy, poly(propylene glycol) bis(2-aminopropyl) ether and neopentyl glycol diglycidyl ether (1:1:1 molar ratio) in a mold. This material had a high modulus of 2.5 GPa at below 35 °C, but the modulus decreased to 10 MPa above 65 °C. When the pad is attached to the substrate with pressure after heating above T_g, the entire pad area could contact the substrate due to the deformation of the micro-tips. Then, the adhesion was maintained when the temperature was lowered below T_g. However, when the temperature was raised again, the shape of the micro-tip was recovered by the shape memory characteristic. As a result, the pad could be separated from the substrate by decreasing the adhesion area **(Figure 1-11)**.

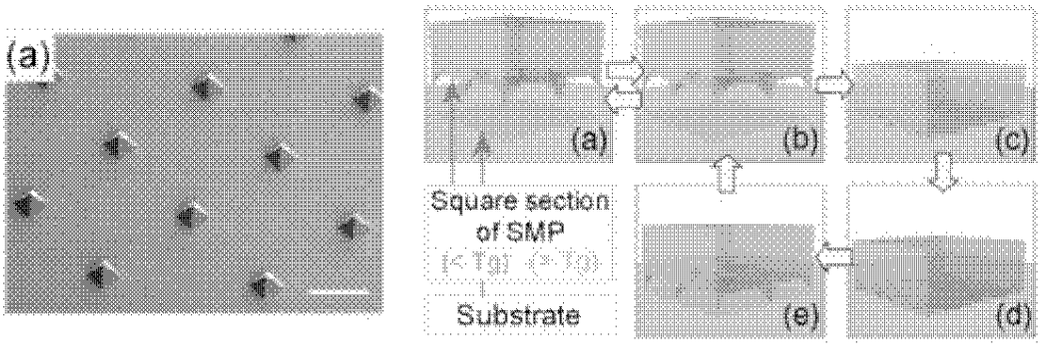

Figure 1-11. Microstructured shape-memory pad and adhesion switching mechanism (Eisenhaure, *et al.*, 2013).

서울대학교

2.2. Light Triggered Switchable Adhesives

Adhesion switching characteristic by light irradiation is a widely applied technique to PSA, and the switching mechanism is additional crosslinking of acrylic PSA (Boyne, *et al.*, 2001, Ebe, *et al.*, 2003, Lee, *et al.*, 2015). In Boyne's research, acrylic polymer with an acrylate group as a pendant was polymerized for a medical PSA that can easily be separated from the skin. Additional crosslinking was carried out by visible light irradiation using a visible light photo-initiator (Boyne, *et al.*, 2001). Dicing tape is a representative type of switchable PSA. It is used for the dicing process of silicon wafers. The wafer is fixed on dicing tape and cut into small-sized wafer chips during the dicing process. Since this dicing tape needs to be easily separated after dicing, Ebo et al. conducted a study to reduce the adhesion force of the dicing tape by additional curing (Ebe, *et al.*, 2003). A UV photo-initiator was used to initiate the crosslinking of acrylate functional groups. Lee et al. prepared temporary bonding and debonding (TBDB) adhesive for the back-grinding process of silicon wafers with a similar mechanism (Lee, *et al.*, 2015). When the UV laser was irradiated to the adhesive, additional crosslinking was performed by converting light energy into thermal energy caused by a UV absorber. However, the exact switching mechanism was not clear. There is an argument that the reduction of tackiness due to additional crosslinking is a switching mechanism, but the reduction of the adhesion area due to shrinkage by the additional reaction is considered more reasonable. The biggest limitation of adhesion switching by additional crosslinking is that repeatable adhesion switching is impossible because of the irreversibility of the crosslinking reaction.

Other studies using light as a trigger used photo-responsive moieties that change the structure in response to light or coordination complexes of metals that can be dissociated by photo-stimulus. Yamaguchi et al. fabricated a host

서울대학교

hydrogel containing cyclodextrin and a guest gel containing azobenzene **(Figure 1-12a)** (Yamaguchi, *et al.*, 2012). Cyclodextrin and azobenzene are dynamic host-guest reaction compounds. Azobenzene can be inserted into the hydrophobic hole of the donut-shaped cyclodextrin. However, when the azobenzene isomerizes into a cis-form by UV light irradiation, it is released from cyclodextrin by a three-dimensionally bent structure and polarity. The host and guest hydrogels can be attached in a stable state and separated by UV light by the dynamic host-guest reaction **(Figure 1-12b)**. Gao et al. spread polyacrylic acid (PAA) solution and Fe^{3+} ions on the surface of two hydrogels to form adhesion through coordination complexes between Fe^{3+} ions and carboxyl groups **(Figure 1-12c)** (Gao, *et al.*, 2019). The coordination complexes can be dissociated by reducing Fe^{3+} to Fe^{2+} when irradiating UV light. The dynamic host-guest reaction and coordination complex are reversible. However, these systems have a limitation in that these can be realized only in a hydrated circumstance.

서울대학교

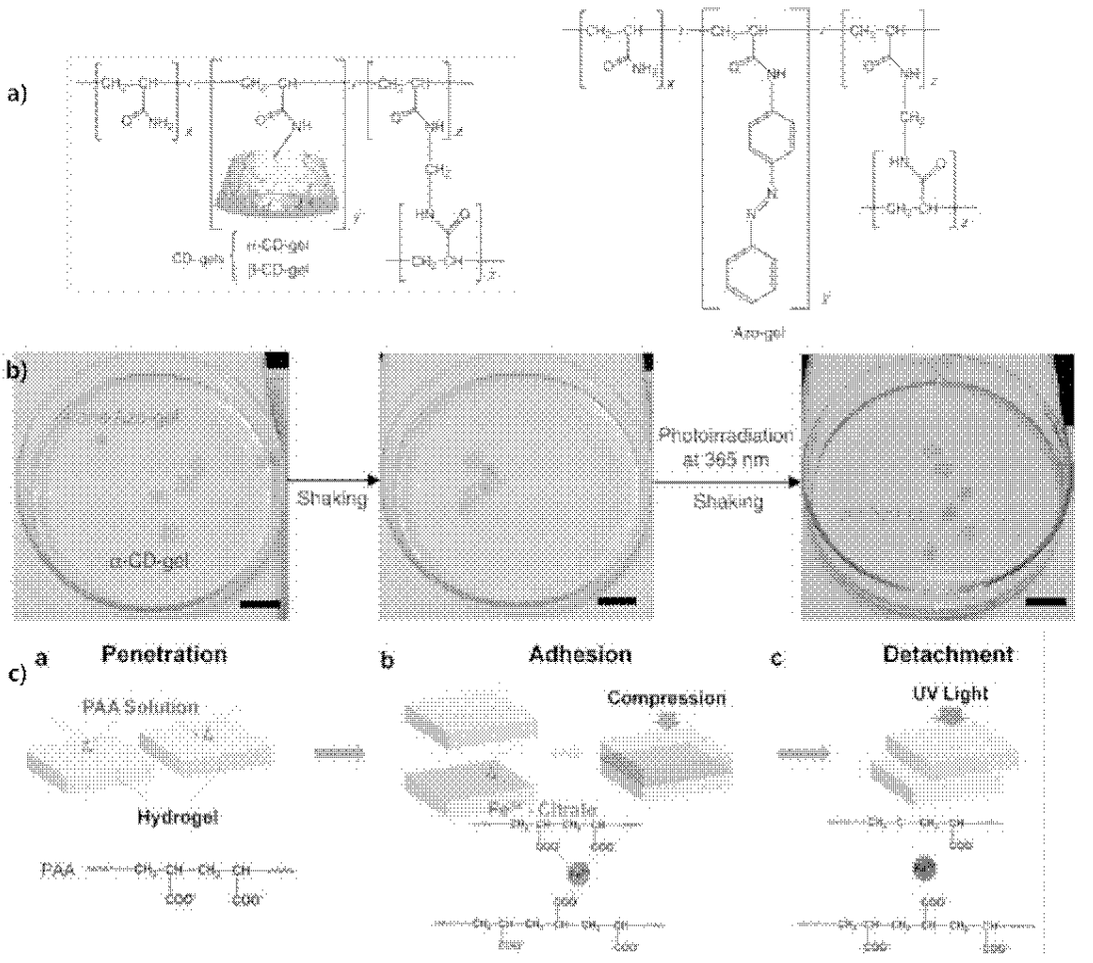

Figure 1-12. a) Chemical structures of cyclodextrin-containing host hydrogel and azobenzene-containing guest hydrogel, b) Adhesion switching between the host and guest hydrogel by UV irradiation (Yamaguchi, *et al.*, 2012), c) Adhesion switching mechanism using coordination complex of metal and carboxylic acid (Gao, *et al.*, 2019).

서울대학교 SEOUL NATIONAL UNIVERSITY

2.3. Switchable Adhesives with Other Triggers

Spina et al. reported switchable adhesive using changes in the interaction of polyelectrolytes depending on pH conditions (La Spina, *et al.*, 2007). They modified the surface of the polydimethylsiloxane (PDMS) substrate with a poly[2-(dimethylamino)ethyl methacrylate] brush and observed the difference in adhesion between the modified PDMS substrate and poly(methacrylic acid) (PMAA) hydrogel according to pH values. In the acidic condition, 3–7 of pH range, they had high adhesion characteristics because of their opposite charges between brush and PMAA gel. However, the separation between brush and gel was observed at lower pH conditions, below 2.

Zheng et al. realized a switchable adhesion system through a guest hydrogel containing pyrenyl and a host hydrogel containing α-, β- and γ-cyclodextrin, respectively (Zheng, *et al.*, 2012). The trigger was a mixed solvent of water and dimethyl sulfoxide (DMSO). The pyrenyl group forms dimers in aqueous conditions because of high hydrophobicity and low water solubility. Therefore, the ratio of the monomer and dimer of the pyrenyl structure was varied according to the ratio of water and DMSO. The donut-shaped α-, β- and γ-cyclodextrin are distinguished by the number of repeating units; This makes the hole size of each cyclodextrin different. Due to the hole sizes of each cyclodextrin, the monomers and dimers of pyrenyl have selectivity with cyclodextrins to form macroscopic assemblies. Therefore, the guest hydrogel formed adhesion with other host hydrogels according to the mixing ratio of the solvent. However, these two systems are also possible only in aqueous or solution conditions.

서울대학교

2.4. Azobenzene-containing Switchable Adhesives

The Akiyama and Kihara research group has researched switchable adhesives, including azobenzene moiety. They studied the light-induced phase transition of various structures of azobenzene derivatives in their early study (Akiyama, *et al.*, 2012). Azobenzene that does not have any substituents on its aromatic groups does not have sufficient free volume for photo-induced phase transition when it forms a crystalline structure. Therefore, they modified the chemical structure of azobenzene to make photo-induced phase transition possible.

Afterward, they polymerized azobenzene-containing acrylic polymers and conducted studies to apply the phase transition phenomenon of the polymer by UV and visible light to switchable adhesives **(Figure 1-13)** (Akiyama, *et al.*, 2014, Akiyama, *et al.*, 2016, Ito, *et al.*, 2018, Ito, *et al.*, 2018, Ito, *et al.*, 2019, Ito, *et al.*, 2019). Most of their studies adopted controlled radical polymerization such as ATRP or RAFT to polymerize well definable polymer or block copolymer. The polymers had a lower molecular weight (under 20,000) than general acrylic adhesive for photo-induced phase transition.

The azobenzene-containing switchable adhesive can be switched in a dried environment and in a short time by light. This switchable adhesive motivated this study since dry and fast adhesion switching is advantageous for the electronic device transfer process. However, the previously studied adhesives were separated from the substrate through a solid-to-liquid phase transition, which can induce problems such as substrate residue and non-reusability.

서울대학교

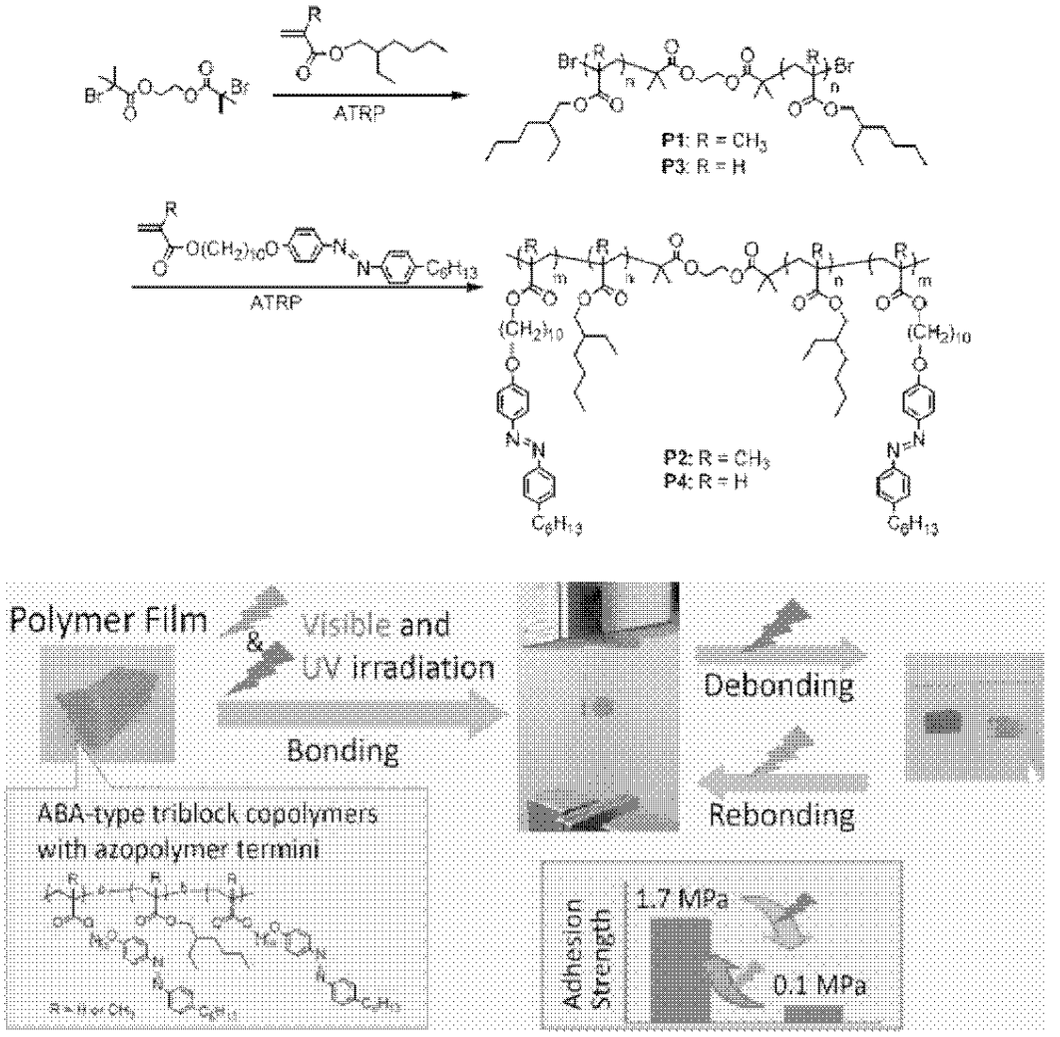

Figure 1-13. Polymerization of azobenzene-containing switchable adhesive and its adhesion switching test (Ito, *et al.*, 2018).

서울대학교

3. Objectives

The switching triggers used in the previously studied switchable adhesive systems were heat, light, pH and solvent. Photo-stimulation was considered the most suitable trigger for the electronic device transfer process. Other stimuli have limitations such as damaging the device, requirement of water or solvent or long process time, while light makes a fast process possible without damaging the device. In addition, a selective transfer process is possible since partial irradiation is possible using a photomask or local irradiation. Therefore, we carried out a study about photo-responsive materials in this study.

Many studies have adopted the hydrogel system for switchable adhesion systems. Since the hydrogel is a cross-linked polymer swollen by the water, its molecular movement is freer than the dried polymer. Therefore, it is easy to realize adhesion switching induced by stimuli-responsive chemical structure or dynamic linkage with hydrogel. However, in the hydrogel system, moisture can be evaporated and unstable in high and low temperatures, so there are many restrictions on the usage environment. Furthermore, hydrated materials cannot be used in the electronic device manufacturing process. Therefore, dried switchable adhesive was studied in this research.

The studies in azobenzene-containing switchable adhesives satisfied the above conditions, i.e. photo-responsive and dried materials. The studies used phase transition of low molecular weight azobenzene-containing polymer as a switching mechanism. In this case, adhesion is formed by solidifying adhesive after applying liquefied adhesive to the substrate, and it is separated through re-liquefaction by UV light irradiation. However, the re-liquefied adhesive remains on the surface of the substrate, and it causes contamination of the device and the non-reusability of the adhesive. In addition, when the devices

서울대학교 SEOUL NATIONAL UNIVERSITY

are attached to liquefied adhesive, the alignment of the devices may be disturbed due to the flow of the adhesive.

As a result, in this research, 1) photo-responsive, 2) switchable in the dried state and 3) reusable switchable PSA was studied.

3.1. Polymerization of Azobenzene-containing Acrylic Polymer

It was tried to modify the residue problem and polymerize acrylic polymer with low T_g for properties of PSA. Therefore, it was intended to polymerize a high molecular weight azobenzene-containing acrylic polymer (Azo-polymer) as a matrix polymer of switchable PSA. Acrylic polymer is the primary material for PSA because it has a wide selection of monomers and can be copolymerized easily with various monomers. It is also easy to control the T_g of polymer. The typical composition of acrylic PSA is listed in **Table 1-3**. Butyl acrylate (BA) is selected as the base monomer for low T_g and the simple chemical structure of switchable PSA. An acrylic monomer including azobenzene moiety (Azo-acrylic monomer) was synthesized to introduce the azobenzene groups into the acrylic polymer. The monomer also has an aliphatic chain between the acrylic group and azobenzene moiety to secure mobility and arrangement of azobenzene, as shown in **Figure 1-14**. Then, BA and Azo-acrylic monomer were copolymerized through free-radical polymerization to obtain Azo-polymer. Consequently, one of the objectives of this study was to polymerize the azobenzene-containing polymer that has relatively high molecular weight and low T_g.

서울대학교

Table 1-3. Composition of standard acrylic PSA.

	Major monomers	Proportion	Function
Alkyl acrylate (T_g < 0°C)	2-ethylhexyl acrylate, Butyl acrylate	70~90 wt%	- Base monomer - Lowering T_g
Alkyl acrylate (T_g > 0°C)	Isobornyl acrylate, Methyl methacrylate, Cyclohexyl acrylate	5~15 wt%	- Improving modulus and cohesion force
Functional acrylate	2-Hydroxyethyl acrylate, Acrylic acid	5~15 wt%	- Improving modulus, cohesion force, and chemical interaction with a substrate - Crosslinking site

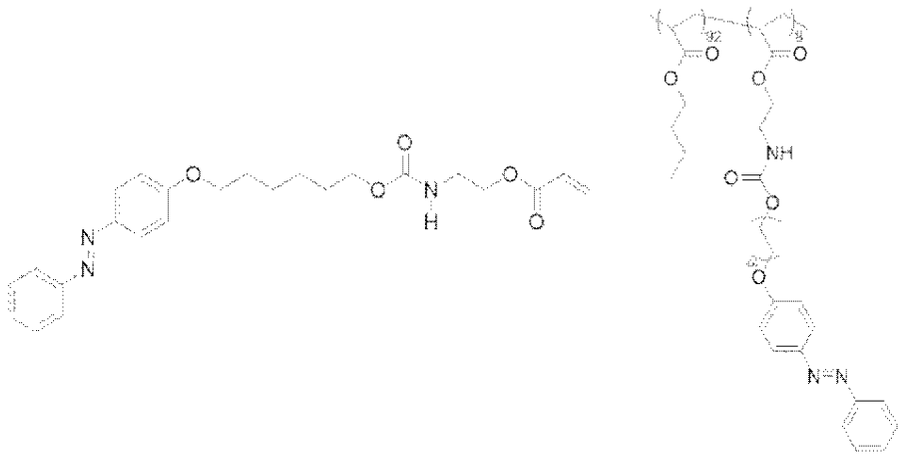

Figure 1-14. Azobenzene-containing acrylic monomer (Azo-acrylic monomer) and acrylic polymer (Azo-polymer).

서울대학교 Seoul National University

3.2. Synthesis of Low Molecular Weight Azobenzene Compounds

Previous studies in azobenzene-containing switchable adhesive introduced high content of azobenzene moiety in the polymer. However, in this study, it was intended to polymerize low T_g polymer. The content of azobenzene moiety in Azo-polymer was not sufficient to form molecular arrangement that can cause the switching of physical and chemical properties of the switchable PSA such as modulus and surface energy. Therefore, low molecular weight azobenzene compounds were synthesized to prepare mixtures with the matrix polymer. The chemical structures of four types of azobenzene compounds are shown in **Figure 1-15**. The low molecular weight compounds were designed according to a hydrocarbon chain length of the aliphatic substituent. The difference in chain length was expected to affect the interaction between the compound molecules or between the compound and the azobenzene moiety in the polymer. The switchable PSAs were prepared by mixing these four azobenzene compounds and Azo-polymer. The tendency of adhesion and switching characteristics depending on the structures of the compound were studied.

서울대학교

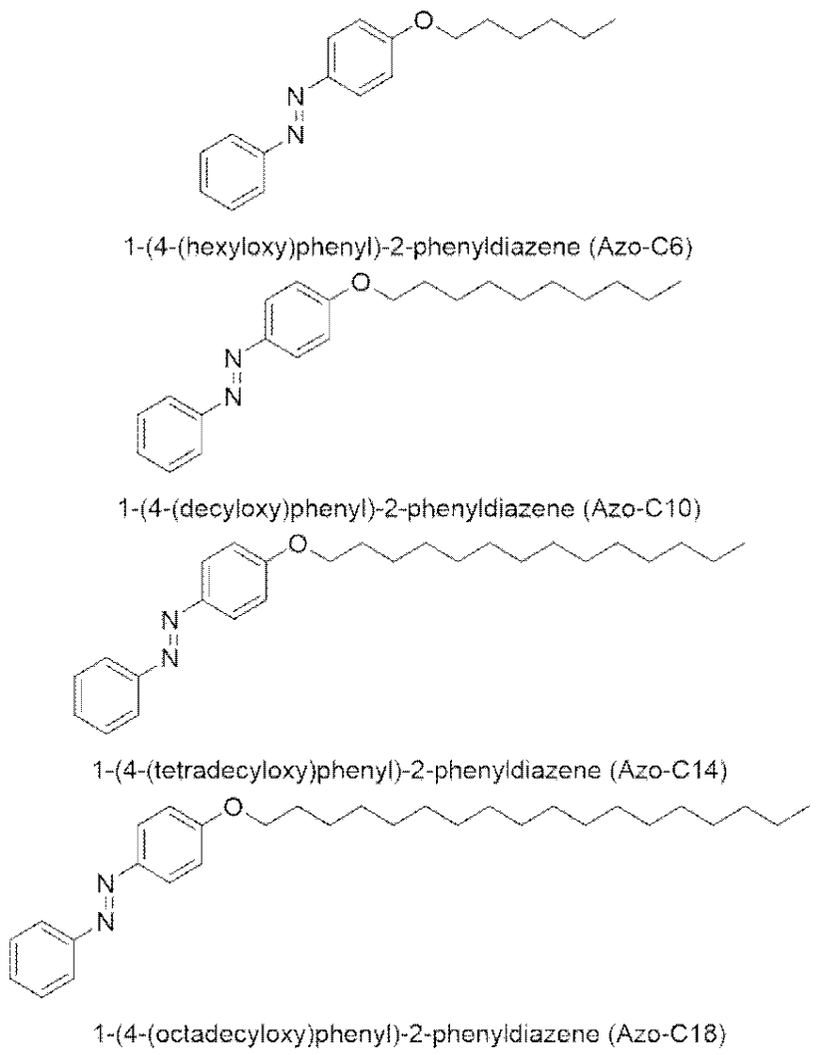

Figure 1-15. Chemical structures of low molecular weight azobenzene compound according to hydrocarbon chain length.

서울대학교 SEOUL NATIONAL UNIVERSITY

3.3. Fast and Selective Adhesion Switching by UV Laser Light Source

This study used an LED lamp of 365nm wavelength as a UV light source. After evaluating the properties of the switchable PSAs and defining the adhesion switching mechanism using an LED light source, it was tried to apply a laser light source for a faster and more exquisite process. Laser has a well-refined single wavelength and high directivity. It also can focus light on a narrow area. Since high energy can be quickly irradiated on a very small area, it was expected that local adhesion switching and a faster process could be performed by using a laser light source. The local adhesion switching would enable the selective transfer of micro-sized electronic devices.

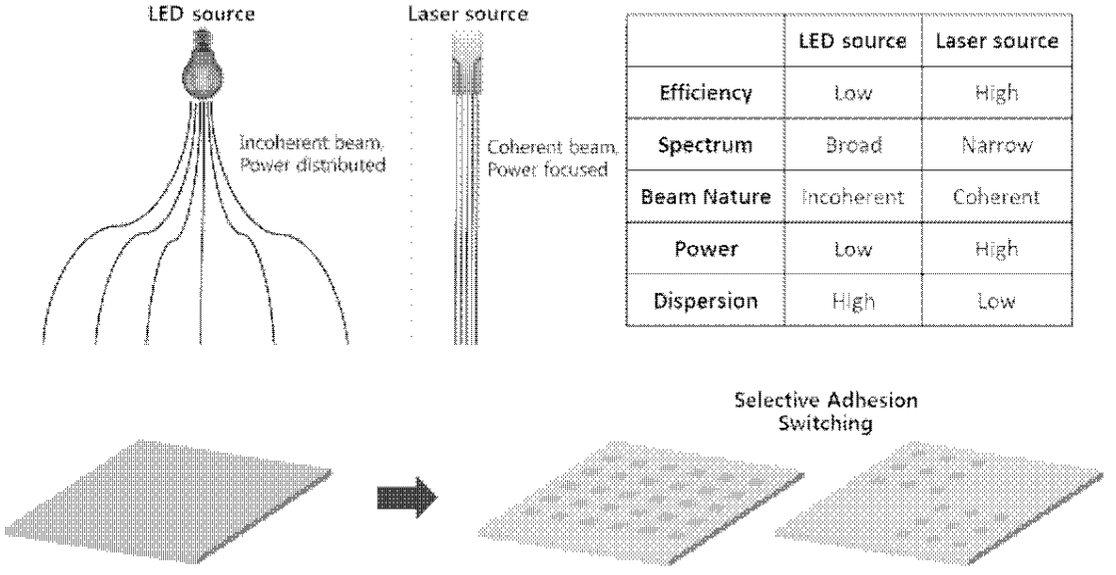

	LED source	Laser source
Efficiency	Low	High
Spectrum	Broad	Narrow
Beam Nature	Incoherent	Coherent
Power	Low	High
Dispersion	High	Low

Figure 1-16. Differences between LED and laser light source and schematic illustration of selective adhesion switching.

서울대학교
SEOUL NATIONAL UNIVERSITY

Chapter 2

Photo-responsive, Switchable, Pressure-Sensitive Adhesives Containing Azobenzene Moiety

서울대학교 SEOUL NATIONAL UNIVERSITY

1. Introduction

Pressure-sensitive adhesives (PSAs) are different from conventional adhesives in terms of the adhesion mechanism. PSAs do not require the influence of heat, the presence of a solvent or a phase change to adhere to the substrate at room temperature (Creton and Ciccotti, 2016). This advantage allows PSAs to be used for attaching dissimilar substrates, which has extended their applicability to areas beyond those related to daily life and general industrial use to automobile, electrical and electronic, and biomedical industries (Creton, 2003, Webster, 1997).

The adhesive strength of PSAs is related to their surface energy and physical property (Donatas, 1999). Therefore, the adhesive strength is kept constant in a fixed environment (where the temperature, humidity and detaching rate are constant) because the surface energy and physical property are determined when the PSA is formed. Recently, adhesives with controllable adhesive properties have found applications in the electrical, electronics and medical industries. The properties of these materials allow them to get easily released from the surface based on user demands, even if the adhesives were well attached to the substrates before being released. Such PSAs are called dynamic adhesives (Ohzono, *et al.*, 2019) or switchable adhesives. Croll et al. defined switchable adhesives as materials that exhibit adhesion switching by changing the contact area, interfacial property and material compliance (Croll, *et al.*, 2019).

Many researchers have studied stimuli-responsive materials. Mechanisms that enable switching include reversible host-guest interactions (Yamaguchi, *et al.*, 2012, Zheng, *et al.*, 2013), a transition of coordination complexes with metal ions (Gao, *et al.*, 2019, Heinzmann, *et al.*, 2014, Nakamura, *et al.*, 2014),

서울대학교

a conformational transition of polymers (La Spina, *et al.*, 2007), hydrogel swelling using water (Yi, *et al.*, 2018), a transition of the crystalline structure of liquid crystal elastomers (Cho, *et al.*, 2003, De Crevoisier, *et al.*, 1999, Ohzono, *et al.*, 2019, Ohzono, *et al.*, 2020), photo-isomerization of azobenzene moiety (Akiyama, *et al.*, 2014, Yamaguchi, *et al.*, 2012) and irreversible cross-linking (Boyne, *et al.*, 2001, Ebe, *et al.*, 2003). External stimuli (e.g., mechanical, thermal, and electromagnetic) that enable switching are called switching triggers (Croll, *et al.*, 2019). These include heat (Cho, *et al.*, 2003, De Crevoisier, *et al.*, 1999, Ohzono, *et al.*, 2019), solvents (Zheng, *et al.*, 2012), water (Yi, *et al.*, 2018), pH control (Zheng, *et al.*, 2013) and light (Ebe, *et al.*, 2003, Heinzmann, *et al.*, 2014, Yamaguchi, *et al.*, 2012). However, some of the abovementioned trigger systems only work in an aqueous environment or do not exhibit the property of repeatability. In addition, the heating process can damage the substrate, which affects its application. Therefore, we focus on developing a switchable PSA that can be used repeatedly in a dry state using light as the switching trigger.

Recently, displays manufactured using small inorganic light-emitting diodes (LEDs; size: < 100 μm) are considered the next-generation displays. The small inorganic LEDs are also known as mini-LEDs or micro-LEDs. Compared to conventional liquid crystal displays or organic LED displays, mini- and micro-LEDs exhibit higher contrast and have faster response times, a longer lifespan and higher energy efficiency (Ding, *et al.*, 2019). However, they cannot be fabricated directly on the display panel and require the transfer of millions of individual LEDs to the panel (Li, *et al.*, 2020). Transfer can be achieved using kinetically controlled polydimethylsiloxane (PDMS) stamps (Kim, *et al.*, 2009, Meitl, *et al.*, 2005), thermal release films (Yan, *et al.*, 2017), laser-driven processes (Eisenhaure, *et al.*, 2016, Saeidpourazar, *et al.*, 2012), ultraviolet (UV) tapes (Pan, *et al.*, 2020) and magnetorheological elastomers (Kim, *et al.*, 2019).

서울대학교

The kinetically modulated PDMS stamp is a representative transfer method that exploits the frequency dependence of the viscoelastic material to transfer devices by varying the speeds of the picking and releasing processes. However, the adhesive force can only be adjusted within a limited range. Surface contamination can hinder the process (Linghu, *et al.*, 2018). Moreover, it is not possible to selectively switch the property of adhesion. Other methods have limitations such as using heat stimuli which can damage the device, difficulty to reuse and narrow adhesion range. Thus, materials that exhibit selective adhesion switching, wide modulation range and reusability should be developed.

We used the azobenzene moiety (a representative photo-responsive unit) for designing a switchable PSA that satisfies the abovementioned conditions. Researchers have previously used the azobenzene moiety for developing switchable adhesives and achieving adhesion switching by exploiting the properties of hydrogel systems (Yamaguchi, *et al.*, 2012), phase transition (Akiyama, *et al.*, 2014, Akiyama, *et al.*, 2016, Ito, *et al.*, 2019, Kortekaas, *et al.*, 2020) or softening(Ito, *et al.*, 2018). Early studies on switchable adhesives exploiting phase transition properties in the presence of azobenzene units were conducted using sugar alcohol derivatives containing multi-azobenzene moiety (Akiyama, *et al.*, 2014). Later, studies using acrylic homopolymers (Akiyama, *et al.*, 2016, Ito, *et al.*, 2018) or block copolymers (Ito, *et al.*, 2018, Ito, *et al.*, 2019) with azobenzene side chains were conducted. These materials can be liquefied or softened by irradiating them with UV light. The process results in the loss of adhesive strength. However, liquefaction and softening-based debonding cannot be used to realize the LED transfer process because the residue can contaminate the device.

Therefore, we fabricated a switchable PSA using a mixture of acrylic polymer and aliphatic low molecular weight compound (containing the

서울대학교

azobenzene moiety). The adhesion property of this PSA can be "switched on" in the presence of UV radiation and "switched off" in the presence of visible light (Vis) radiation. The switching process does not proceed through the solid-to-liquid phase transition step. To the best of our knowledge, there are no reports on a switchable PSA whose adhesive strength can be repeatedly and selectively "switched on and off" for realizing the mini- or micro-LED transfer process under conditions of short light irradiation. We successfully realized an electronic device transfer process and transferred mini-LEDs from a carrier PSA to a PDMS substrate using the fabricated switchable PSA. The selective transfer was also achieved by partial adhesion switching using a photomask. Our novel and switchable PSA can be potentially used to realize the transfer process of mini-LEDs, micro-LEDs, micro-scale inorganic circuits and semiconductors.

서울대학교

2. Experimental

2.1. Materials

4-Phenylazophenol (PAP, 98%), dibutyltin dilaurate (DBTDL, 95%) and butyl acrylate (BA, >99%) were purchased from Sigma-Aldrich. Potassium carbonate (>99%), potassium iodide (>99.5%), 6-chloro-1-hexanol (>96%) and 1-chlorotetradecane (>98) were purchased from Tokyo Chemical Industry Co., Ltd. 2,2'-Azobisisobutyronitrile (AIBN, 98%), 2-butanone (MEK, 99.5%) and ethyl acetate (EA, 99.5%) were purchased from Samchun Chemicals Co., Ltd. N,N-Dimethylformamide (DMF, >99.5%) was purchased from Daejung Chemicals & Metals Co., Ltd. Karenz AOI (2-isocyanatoethyl acrylate, Showa Denko) was used as the isocyanate-containing acrylic monomer. SYLGARD 184 (Dow Corning) was used as the PDMS acceptor in the mini-LED transfer test.

2.2. Synthesis of Azobenzene-containing Acrylic Monomer and Low Molecular Weight Compound

2.2.1. 6-(4-(Phenyldiazenyl)phenoxy)hexan-1-ol

The method used in Zhou's study was employed (Zhou, *et al.*, 2016). PAP (3.586 g, 0.018 mol) and potassium carbonate (2.488 g, 0.018 mol) were dissolved in DMF (15 mL) by stirring for 30 min at room temperature. After that, potassium iodide (7.5 mg, 0.045 mmol) and 6-chloro-1-hexanol (3.689 g, 0.027 mol) were added to the PAP solution. The solution was stirred and kept at 110 °C for 24 h. The reaction mixture was poured into diethyl ether and

서울대학교

washed with water three times. After drying diethyl ether with air, the residue was precipitated with water. The precipitate was dried at room temperature under a vacuum condition after filtering. The dried compound was washed with n-hexane to obtain a yellow powder.

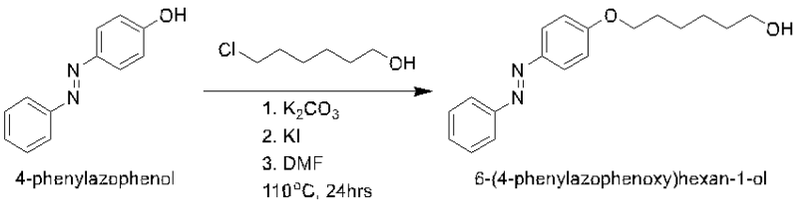

Figure 2-1. Synthesis of 6-(4-(Phenyldiazenyl)phenoxy)hexan-1-ol.

2.2.2. 2-((((6-(4-(Phenyldiazenyl)phenoxy)hexyl)oxy)carbonyl)amino)ethyl acrylate (Azo-acrylate)

6-(4-(Phenyldiazenyl)phenoxy)hexan-1-ol (2.000 g, 0.007 mol) was dissolved in MEK (15 mL). 2-Isocyanatoethyl acrylate (1.976 g, 0.014 mol) was added to the solution, and the solution was stirred at 40 °C under an atmosphere of N_2. After that, DBTDL (0.019 g) was added to the solution. The temperature of the reaction mixture was maintained at 40 °C for 6 h. The reaction mixture was then poured into cold n-hexane (300 mL), and the mixture was filtered. This process was repeated three times. The filtered compound was dried at room temperature under vacuum to obtain the product.

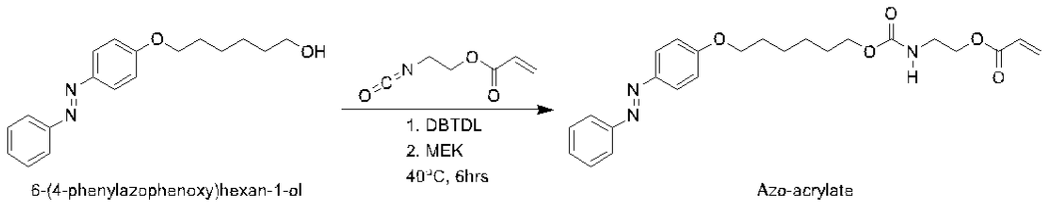

Figure 2-2. Synthesis of Azo-acrylate.

서울대학교

2.2.3. 1-Phenyl-2-(4-(tetradecyloxy)phenyl)diazene (Azo-M)

To synthesize Azo-M, the method for the synthesis of 6-(4-(phenyldiazenyl)phenoxy)hexan-1-ol was followed, but 1-chlorotetradecane was used instead of 6-chloro-1-hexanol.

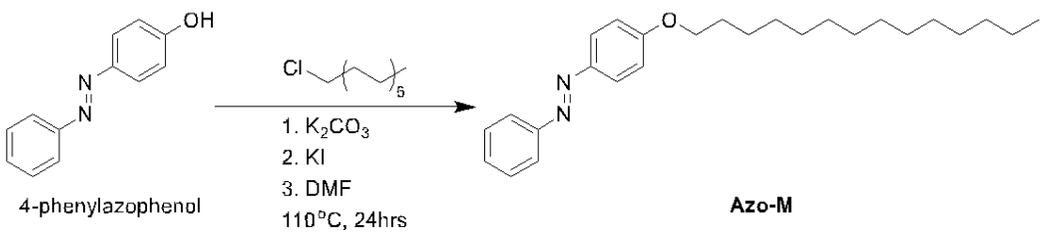

Figure 2-3. Synthesis of Azo-M.

2.3. Polymerization of the BA/Azo-acrylate Co-polymer (Azo-polymer)

After removing the inhibitor of BA using neutral aluminum oxide, BA (1.5 g, 0.012 mol) and Azo-acrylate (0.572 g, 1.3 mmol) were added to EA (5 mL). After stirring the mixture for 1 min at 70 °C to dissolve the Azo-acrylate powder, N2 gas was blown into the solution for 20 min at room temperature. AIBN (0.01 g) was added to the solution, and the solution was stirred at 70 °C for 1.5 h. Tetrahydrofuran (THF, 5 mL) was poured into the polymerized solution to prevent gelation caused by the interaction between the azobenzene moieties. The polymer solution was washed and dissolved with methanol and THF, respectively. The process was repeated thrice. The dissolved solution was poured on a silicone-release film and dried at 70 °C.

서울대학교

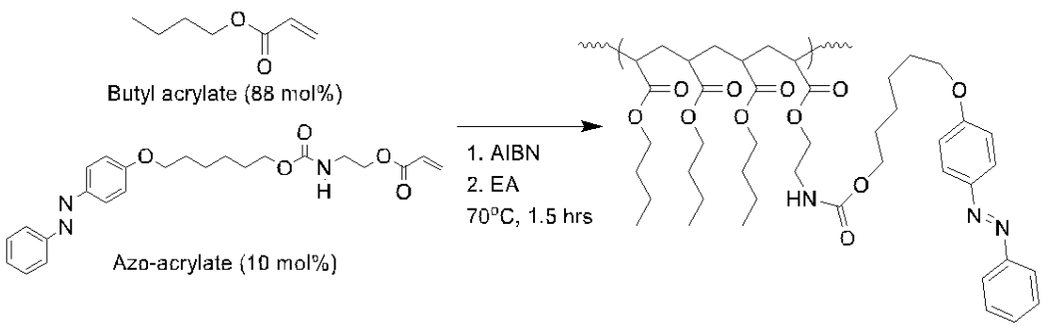

Figure 2-4. Polymerization of Azo-polymer.

2.4. Preparation of the Switchable PSA Specimens

The dried Azo-polymer (0.1 g) was dissolved in THF (1 mL). Azo-M (4, 8 and 12 mol%) was added to the Azo-polymer solution. The Azo-M content was calculated based on the number of all monomers present in the polymer. The solution was mixed using a vortex mixer. After that, the solution was cast on a PET film (corona-treated, 50 μm) with a film applicator (wet thickness: 120 μm). The film was dried at 100 °C over 20 min in a convection oven. The thickness of the dried PSA was 6–7 μm measured with a digital micrometer (S-Mike_Pro, Sylvac). The rigid-body pendulum-type physical properties testing (RPT), lap shear test, X-ray diffraction (XRD) and polarized optical microscopy (POM) specimens were cast on other substrates following the method previously mentioned (RPT: steel plate; lap shear test: silicone-release film; XRD, POM: slide glass).

서울대학교

2.5. Preparation of the PDMS Acceptor

The PDMS resin and curing agent (resin : curing agent = 10 : 0.5) were mixed using a paste mixer (ARE-310, THINKY) operated at 2,000 rpm. The process proceeded for 3 min (mixing: 2 min, deforming: 1 min). The mixture was poured into a petri dish, and the sample was cured at 80 °C (curing time: 12 h).

2.6. Characterization

2.6.1. Nuclear Magnetic Resonance (NMR) Spectroscopy

The NMR spectra were recorded using a 400 MHz NMR spectrometer (JNM-ECX400, JEOL) operated at room temperature. Tetramethylsilane ($\delta = 0$ ppm) was used as the reference for determining chemical shift.

2.6.2. UV and Visible Light Sources

A 365 nm LED UV lamp was used for UV irradiation (intensity: 120 mW/cm^2). A 50 W white LED lamp was used to irradiate Vis to the samples. UV was irradiated from the direction in which the PSA surface was exposed. Meanwhile, Vis was irradiated to the backside of the film to avoid the shading of the attached substrate.

서울대학교 SEOUL NATIONAL UNIVERSITY

2.6.3. Adhesion Switchability Test

The probe tack and peel strength were measured using a texture analyzer (TA.XT plus, Stable Micro Systems) at 25 °C (RH: 50 ± 10%). A cylindrical probe (stainless steel, diameter: 5 mm) was used for the probe tack test. The UV and visible light irradiated specimens were measured after 10 s and 30 s for temperature stabilization. After the probe was in contact (100 g_f) for 1 s, it was detached at a speed of 10 mm/s. The test speed for the peel test was 5 mm/s, and the test angle was 180°. The width of the PSA specimen was 10 mm. The specimen was attached to a silicon wafer substrate by applying pressure using a 2 kg rubber roller. All experiments were repeated five times, and the average value was used.

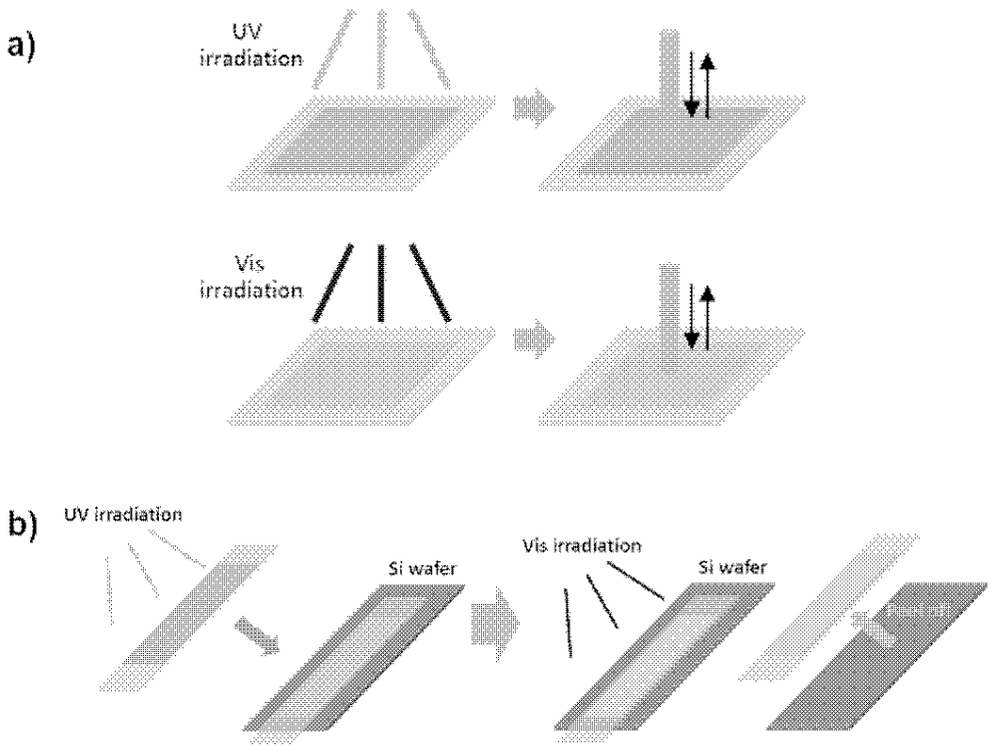

Figure 2-5. Schematic illustration of adhesion switching evaluation methods with a) probe tack and b) peel test.

서울대학교 SEOUL NATIONAL UNIVERSITY

The adhesion switching test was also conducted as a 90° peel test. The silicon wafer was used as the substrate for the test. The 2 kg rubber roller was also used to attach the PSA specimen with a width of 10 mm to the substrate. Two small-sized binder clips (2.5 g each) were applied to the ends of the PSA specimen.

2.6.4. UV/Vis Spectroscopy

The UV/Vis absorption spectra were recorded using a UV/Vis spectrometer (OPTIZEN Alpha, K LAB). The wavelength scan range was between 200–700 nm. The 50 μm PET film used as the backing film of the PSA was considered the baseline of the spectrum. The PSA was then measured as coated on the PET film.

2.6.5. Rigid-body Pendulum Type Physical Properties Test (RPT)

The logarithmic damping ratio of the switchable PSAs was measured following the RPT (RPT-3000W, A&D Company) method. The rigid-body pendulum and edge were FRB-400 and round type (RBP-040). The pendulum weight, including the edge, was 109 g. The steel plate coated with switchable PSAs was placed on a specimen mount. After putting the pendulum on the surface of the PSA, the lower part of the pendulum containing a magnet was attracted to 0.1° for 2 s by magnetic force. After removing the magnetic force, the pendulum oscillated freely, and the attenuation of the amplitude was detected for 8 s by the displacement sensor. The sequence, attraction and oscillation, was recorded repeatedly for 5 min. The reduction of the amplitude was used for calculating the logarithmic damping ratio (Δ) as

서울대학교

$$\Delta = [\ln(A_1/A_2) + \ln(A_2/A_3) + \ln(A_3/A_4) + \cdots + \ln(A_n/A_{n+1})]/n,$$

where A denotes the amplitude, and n denotes the number of oscillation waves (Chiu, *et al.*, 2007).

2.6.6. Shear Modulus

The shear modulus was measured by conducting a lap shear test using dynamic mechanical analysis (DMA, Q800, TA Instruments). The size of the poly(methyl methacrylate) (PMMA) substrate was 6 mm × 20 mm × 1 mm (width × length × thickness), and the adhesion area was 6 mm × 10 mm (width × length). The thicknesses of PSAs cast on silicone-release film were 6–7 μm measured with the digital micrometer. The PSA was attached between two PMMA substrates after UV irradiation. A shorter PMMA (6 mm × 6 mm × 1 mm) was attached to the end of each substrate using instant adhesive. Vis was irradiated through the transparent PMMA substrate to test the Vis irradiated specimen. The test was conducted using the strain ramp mode of the DMA at 25 °C. The test speed was 1%/s. All measurements were taken three times, and the average value was used.

서울대학교

2.6.7. Water Contact Angle Measurement

The water contact angle was measured using a drop shape analyzer (DSA 100, KRÜSS). It controlled the water volume at 5 μL. The contact angle was measured 10 s after dropping the water sample. Measurements were taken five times (for each specimen), and the average value was used.

2.6.8. X-ray Diffraction (XRD) and Differential Scanning Calorimetry (DSC)

The XRD patterns of the switchable PSA and Azo-M were recorded using a high-resolution XRD machine (Rigaku SmartLab; CuKα radiation) in the range of 5–40° at 25 °C. The DSC curve was obtained using Q200 DSC (TA Instruments). After heating to 250 °C, the data were recorded when the sample was cooled to 0 °C and re-heated at 10 °C/min.

서울대학교

3. Results and Discussion

3.1. Results of Synthesis and Polymerization

3.1.1. Synthesis of 6-(4-(Phenyldiazenyl)phenoxy)hexan-1-ol

The yield of synthesis of 6-(4-(Phenyldiazenyl)phenoxy)hexan-1-ol was 76.1%. The chemical structure was defined by the ^{1}H-NMR spectrum **(Figure 2-6)**. It was confirmed that the starting material, PAP, did not exist in the compound through the absence of a peak near 10 ppm corresponding to phenol of PAP. The analysis of the NMR spectrum is as follows.

δ = 7.86 (dd, 4H, Ar H), 7.55 (dt, 3H, Ar H), 7.12 (m, 2H, Ar H), 4.08 (t, 2H, OCH_2), 3.41 (m, 2H, $\underline{CH_2}OH$), 1.75 (m, 2H, $OCH_2\underline{CH_2}$), 1.41 (m, 6H, $OCH_2CH_2\underline{CH_2CH_2CH_2}$)

3.1.2. Synthesis of Azo-acrylate

The yield of the synthesis of Azo-acrylate was 84.0%. The chemical structure was defined by the ^{1}H-NMR spectrum **(Figure 2-7)**. The analysis of the NMR spectrum is as follows.

δ = 7.82 (dd, 4H, Ar H), 7.51 (dt, 3H, Ar H), 7.23 (m, 1H, NH), 7.08 (m, 2H, Ar H), 6.30 (m, 1H, C=CH), 6.11 (m, 1H, C=CH), 5.90 (m, 1H, C=CH), 4.04 (m, 4H, Ar-OCH_2, $NHCH_2\underline{CH_2}$), 3.92 (t, 2H, $\underline{CH_2}OOCNH$), 3.21 (m, 2H, $NH\underline{CH_2}$), 1.71 (m, 2H, Ar-$OCH_2\underline{CH_2}$), 1.42 (m, 6H, Ar-$OCH_2CH_2\underline{CH_2CH_2CH_2}$)

서울대학교

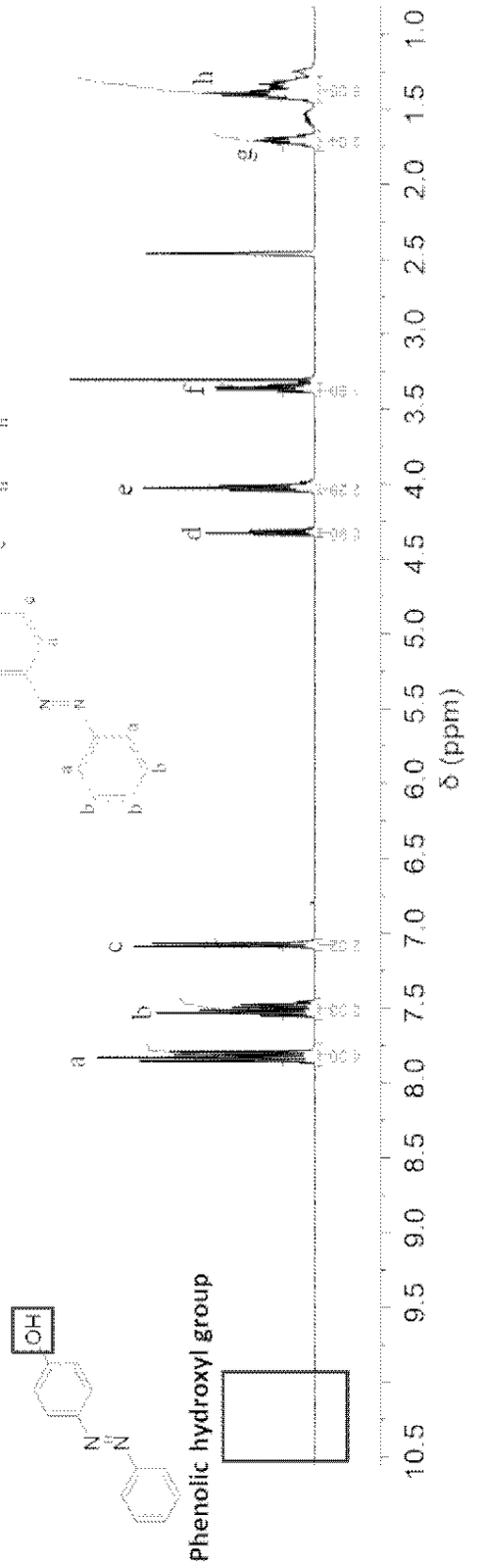

Figure 2-6. ^{1}H-NMR spectrum of 6-(4-(phenyldiazenyl)phenoxy)hexan-1-ol.

서울대학교

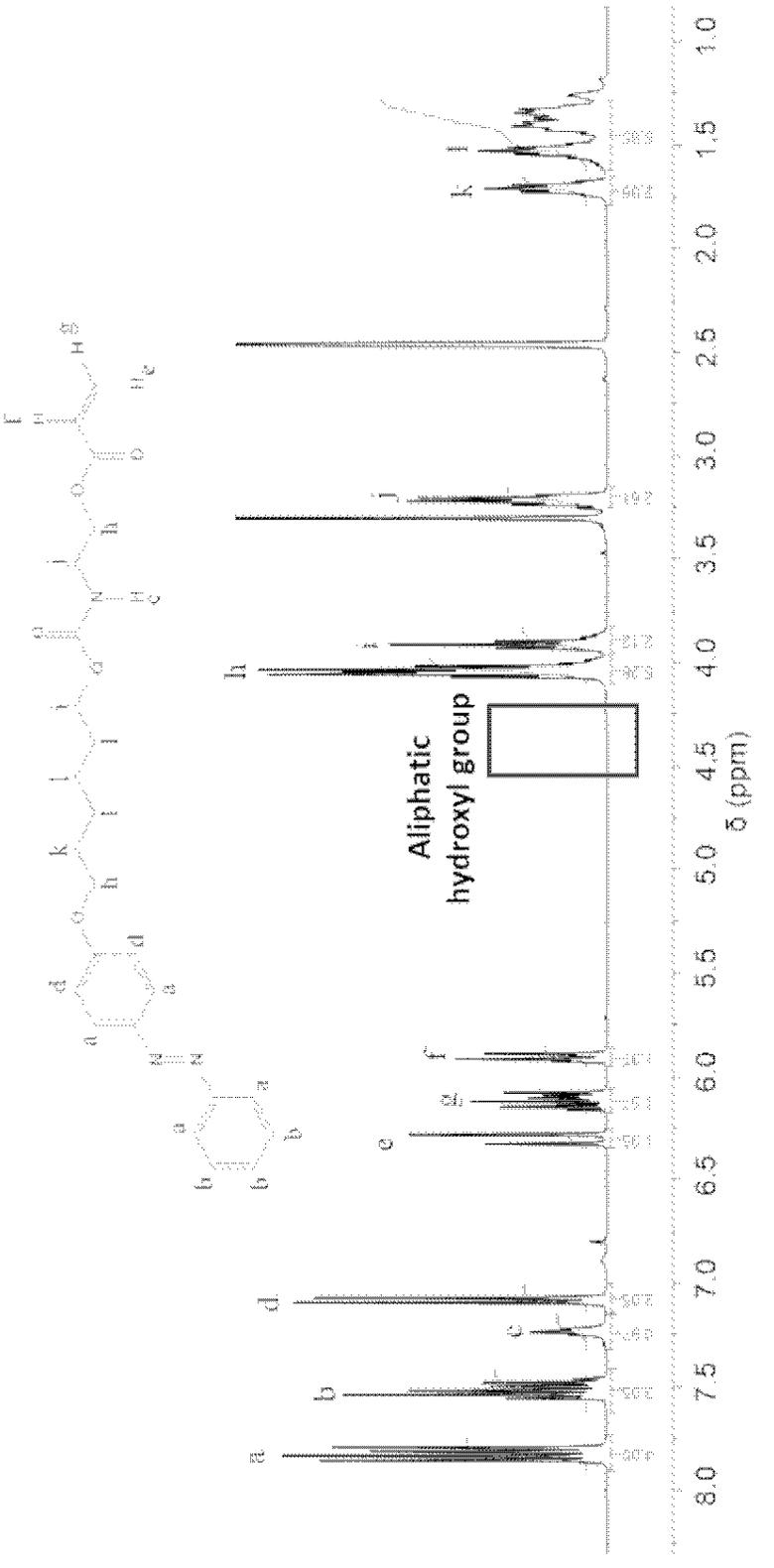

Figure 2-7. ^{1}H-NMR spectrum of Azo-acrylate.

세한대학교

3.1.3. Synthesis of Azo-M

The yield of the synthesis of Azo-M was 48.6%. The chemical structure was defined by the ^{1}H-NMR spectrum **(Figure 2-8)**. It was confirmed that the starting material, PAP, did not exist in the compound through the absence of a peak near 10 ppm corresponding to phenol of PAP. The analysis of the NMR spectrum is as follows.

δ = 7.88 (dd, 4H, Ar H), 7.46 (dt, 3H, Ar H), 6.99 (m, 2H, Ar H), 4.04 (t, 2H, OCH_2), 1.81 (m, 2H, $OCH_2\underline{CH_2}$), 1.47 (m, 2H, $OCH_2CH_2\underline{CH_2}$), 1.29 (m, 20H, $OCH_2CH_2CH_2(\underline{CH_2})_{10}$), 0.87 (t, 3H, $CH_2\underline{CH_3}$)

서울대학교 SEOUL NATIONAL UNIVERSITY

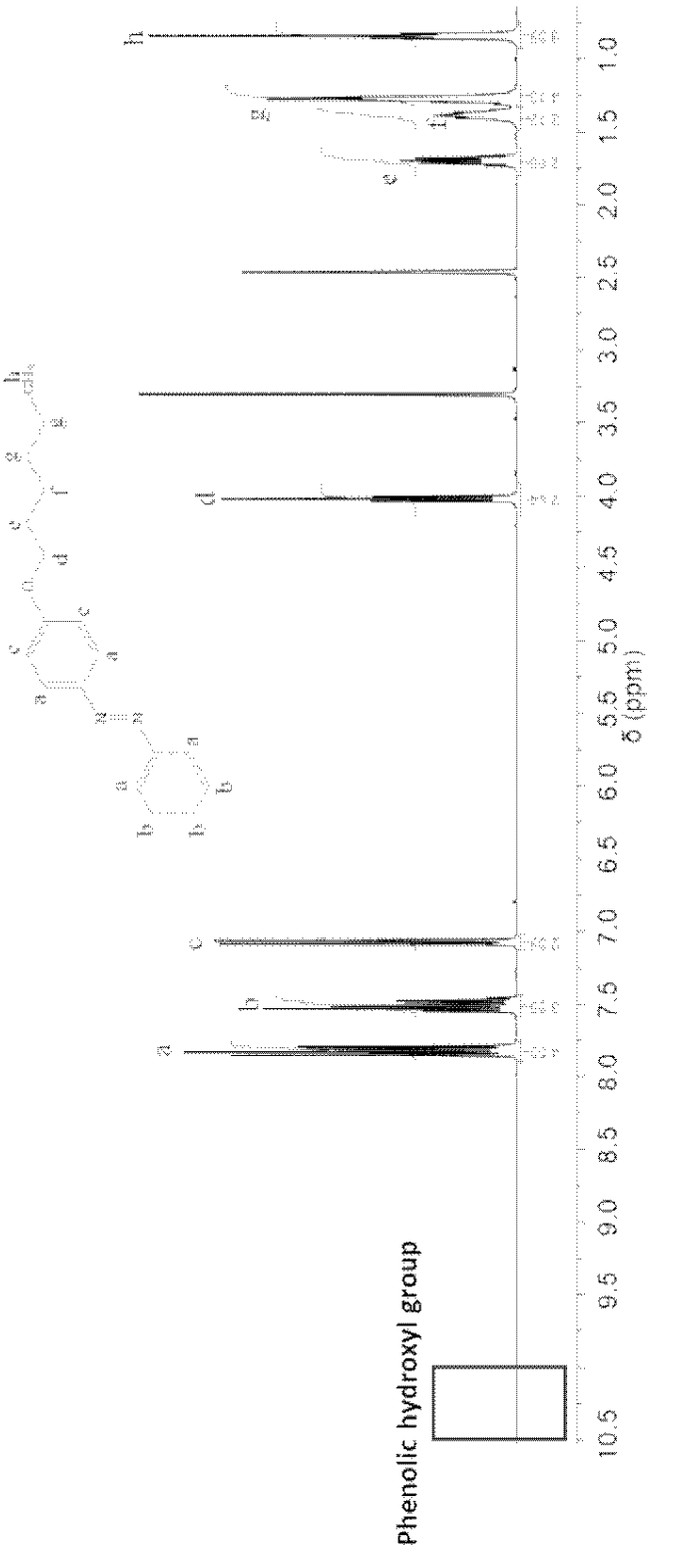

Figure 2-8. ^{1}H-NMR spectrum of Azo-M.

서울대학교

3.1.4. Polymerization of Azo-polymer

Unreacted BA and Azo-acrylate in polymerized Azo-polymer solution were removed by washing with methanol and THF. The ^{1}H-NMR spectrum of Azo-polymer is shown in **Figure 2-9**. The removal of unreacted monomers was confirmed through the absence of acrylate's double bond at 5.5-6.5 ppm of the NMR spectrum.

The ratio of azobenzene containing side group included in the polymerized chains among 10 mol% of azo-acrylate added for polymerization was calculated through the NMR spectrum, and the equation is as follows:

$$C_{azo} = \frac{I_{7.89ppm}/4}{I_{0.88ppm}/3 + I_{7.89ppm}/4}$$

where C_{azo} denotes the content of Azo-acrylate in washed Azo-polymer, $I_{7.89ppm}$ denotes the intensity of peak at 7.89 ppm corresponding to the azobenzene side chain, and $I_{0.88ppm}$ denotes the intensity of peak at 0.88 ppm corresponding to CH_3 of the butyl side chain. The calculated C_{azo} was 8 mol%.

The Azo-polymer's Mn, Mw and PDI measured with gel permeation chromatography (GPC) were 39,900, 147,400 and 3.8, respectively.

서울대학교

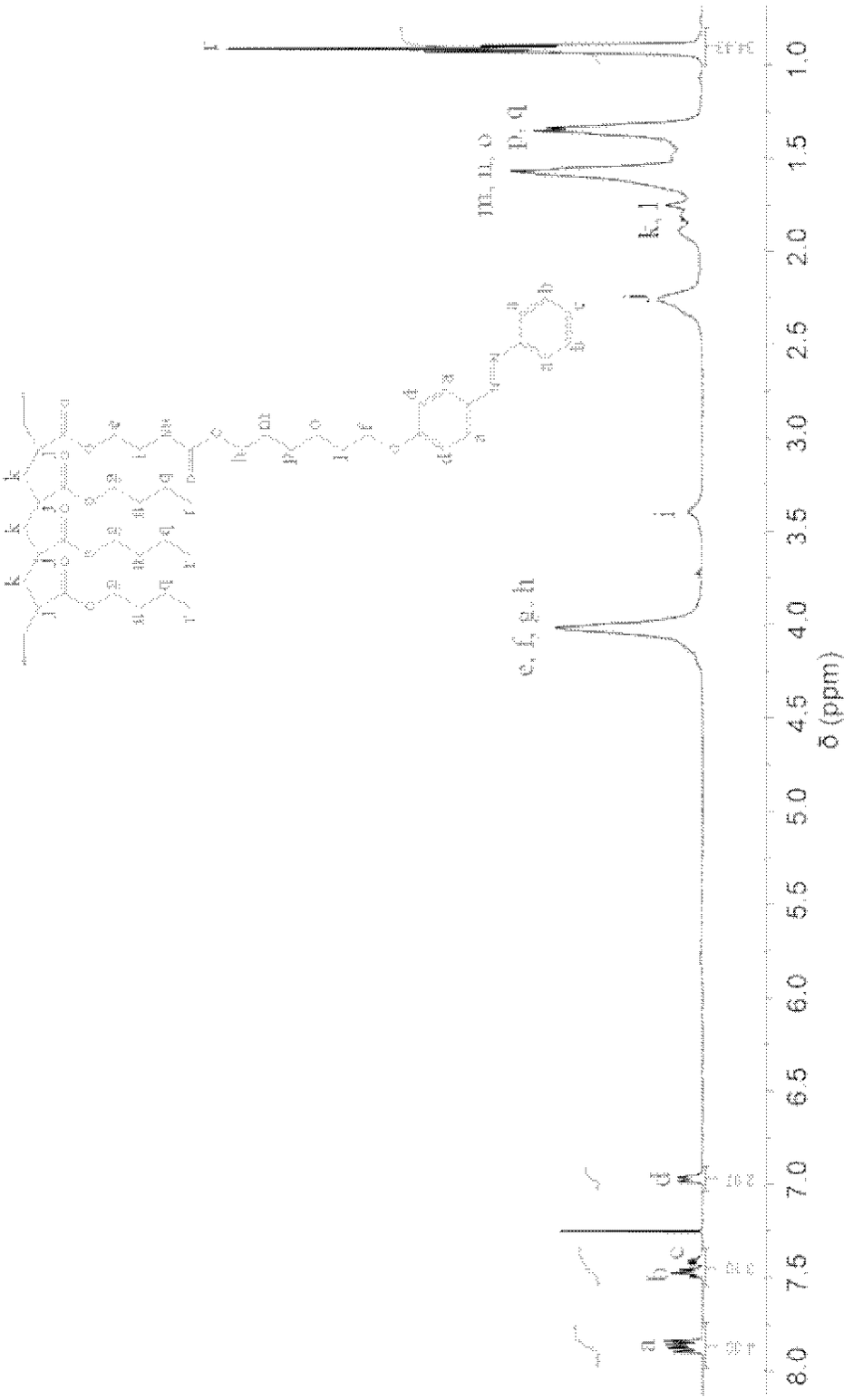

Figure 2-9. ^{1}H-NMR spectrum of Azo-polymer.

세한대학교

3.2. Transition in Appearance of the Switchable PSA

The switchable PSA was prepared by blending Azo-polymer with Azo-M **(Figure 2-10a)**. The switchable PSAs were named based on the Azo-M content (Azo-M-0, Azo-M-4, Azo-M-8 and Azo-M-12). The transparent Azo-polymer film became opaque when Azo-M was added. The film containing Azo-M became transparent after UV irradiation. Both films appeared dark yellow after UV irradiation **(Figure 2-10b)**. Changes in the optical properties and stickiness of the surface were observed, but phase transition (between the solid and liquid phases) was not observed.

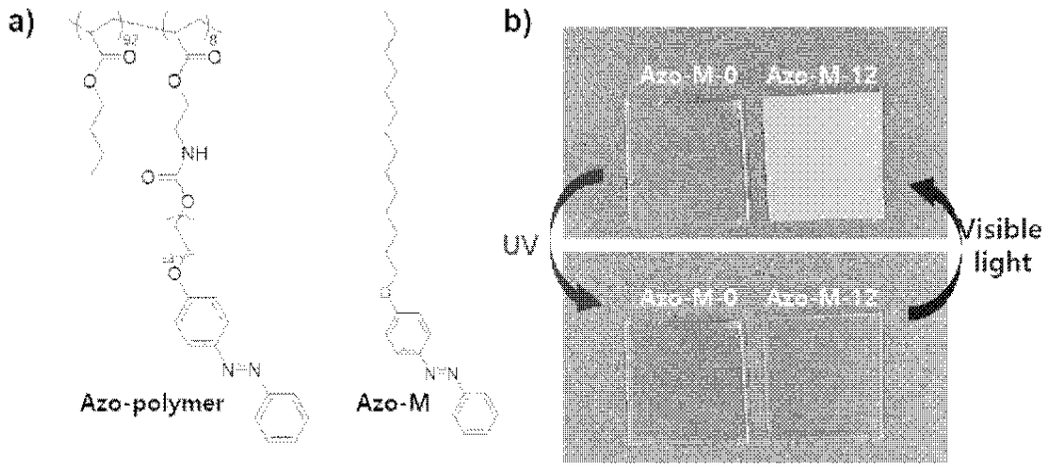

Figure 2-10. a) Chemical structures of Azo-polymer and Azo-M and b) transmittance and color change of the switchable PSA in the presence of the Azo-M upon photo-irradiation.

서울대학교 SEOUL NATIONAL UNIVERSITY

3.3. Adhesion Switchability Evaluated with Probe Tack Test

The probe tack was measured to determine the adhesion switchability and switching time of the switchable PSA (according to the UV and Vis irradiation time). For Azo-M-0, the initial value was 2.6 N. This tack value could be maintained even when the UV irradiation time was increased to 2 min **(Figure 2-11a)**. Since only 4 mol% of Azo-M (Azo-M-4) was added, the initial probe tack was reduced to zero. The surface had a non-sticky film-like state. The tack value, which was zero, dramatically increased to 4 N when the sample was subjected to UV irradiation for a short time of 15 s. The value could be maintained (at 4 N) for 2 min. However, further change in the maximum value and switching time was not observed even when the content of the Azo-M was increased. The Vis irradiation test was conducted after irradiating the sample with UV light for 30 s **(Figure 2-11b)**. Azo-M-0 exhibited no change in adhesion force even when it was irradiated with Vis for 2 min. For the Azo-M-containing PSAs, the tack value reached the minimum value after 15 s of Vis irradiation. The initial value (0 N) was reached again.

서울대학교 SEOUL NATIONAL UNIVERSITY

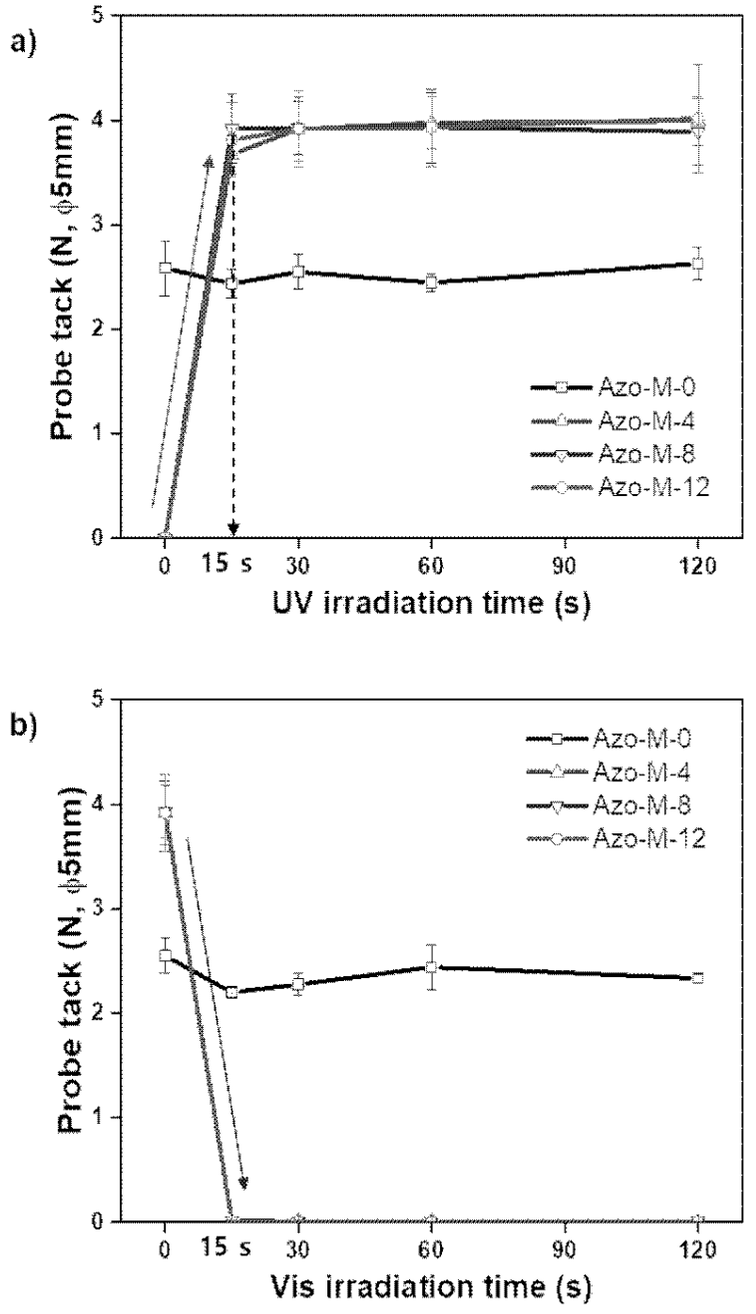

Figure 2-11. Probe tack according to a) UV and b) Vis irradiation time.

서울대학교

Further, we studied the repeatability of adhesion switching **(Figure 2-12)**. The PSA could be switched between its on and off states up to 30 times. During the process, the switchable PSA could be completely switched off. The tack forces of the UV irradiated PSA were in the range of 4 ± 0.2 N. The range was within the measurement error, and it was evaluated that there was no change in the adhesive force according to the cycle. In summary, a repeatable switch between the non-sticky film and sticky PSA states could be achieved by mixing Azo-polymer with Azo-M. A high adhesion force (4 N) was achieved within a short UV irradiation time (switching time: 15–30 s).

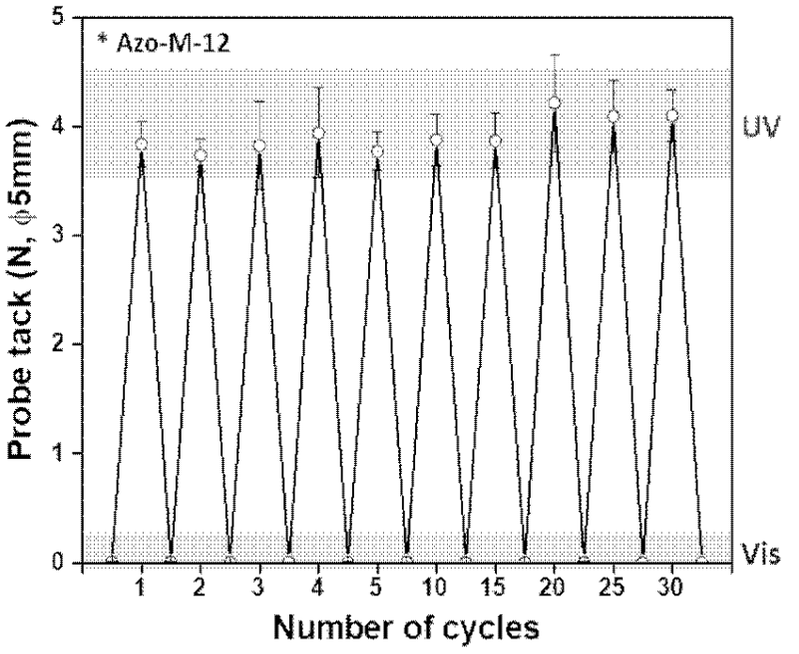

Figure 2-12. Adhesion switching repetitive test conducted with Azo-M-12.

서울대학교

Kendall defined the probe tack force (F) of an infinitely thick elastic material as follows:

$$F = \sqrt{\frac{8\pi}{(1-\nu^2)} E\omega a^3}, \quad (1)$$

where ν denotes the Poisson's ratio, E denotes Young's modulus, and ω denotes the work of adhesion when using a rigid probe of diameter 2a (Kendall, 1971).

Further, ω can be calculated as

$$\omega = \gamma_a + \gamma_s - \gamma_{as}, \quad (2)$$

where γ_a, γ_s and γ_{as} denote the surface energy of the adhesive, substrate and interface (of the adhesive and substrate), respectively. Based on equation (1), a change in the modulus and chemical characteristics of the PSA can cause a change in the adhesion force if external conditions such as temperature, thickness, adhesion area and test speed are kept constant. Therefore, we studied the modulus and chemical characteristic transition of the switchable PSA in the presence of photo-stimulus.

서울대학교

3.3. Photo-isomerization of Azobenzene Moiety in the Switchable PSAs (UV/Vis spectrometer)

We used UV/Vis spectroscopy to observe the photo-isomerization occurring in the PSA during UV and Vis irradiation. We expected that the photo-isomerization of the azobenzene moiety could lead to the physical and chemical transitions in the switchable PSA. The stable trans-azobenzene moiety has a strong absorption band near 350 nm due to the transition from the bonding (π) orbital to the antibonding (π^*) orbital. Meanwhile, the isomerized azobenzene moiety to the cis-form has a predominant absorption band at 440nm due to the transition from the nonbonding (n) orbital to the antibonding (π^*) orbital (Kumar, *et al.*, 1989, Serra, *et al.*, 2008).

Even in the initial state of Azo-M-0, a spectrum corresponding to the trans-form is observed because of the azobenzene moiety present in the polymer chain. In other samples, the absorption intensity of the trans-isomer increased with an increase in the Azo-M content **(Figure 2-13)**. There was little or no absorption (cis-form) in the 440 nm region in the initial state. Regardless of the Azo-M content, most trans-isomers were converted to the cis-form after only 15 s of UV irradiation. The trend of cis to trans isomerization caused by Vis irradiation was the same. When azobenzene groups form a highly ordered crystalline structure in a solid phase, the photo-isomerization of azobenzene is difficult to achieve because the free volume is not sufficient (Akiyama and Yoshida, 2012, Tsuda, *et al.*, 1964). In this study, it is considered that butyl groups of Azo-polymer and long alkyl substituent of the Azo-M contributed to securing free volume that can cause rapid photo-isomerization.

서울대학교

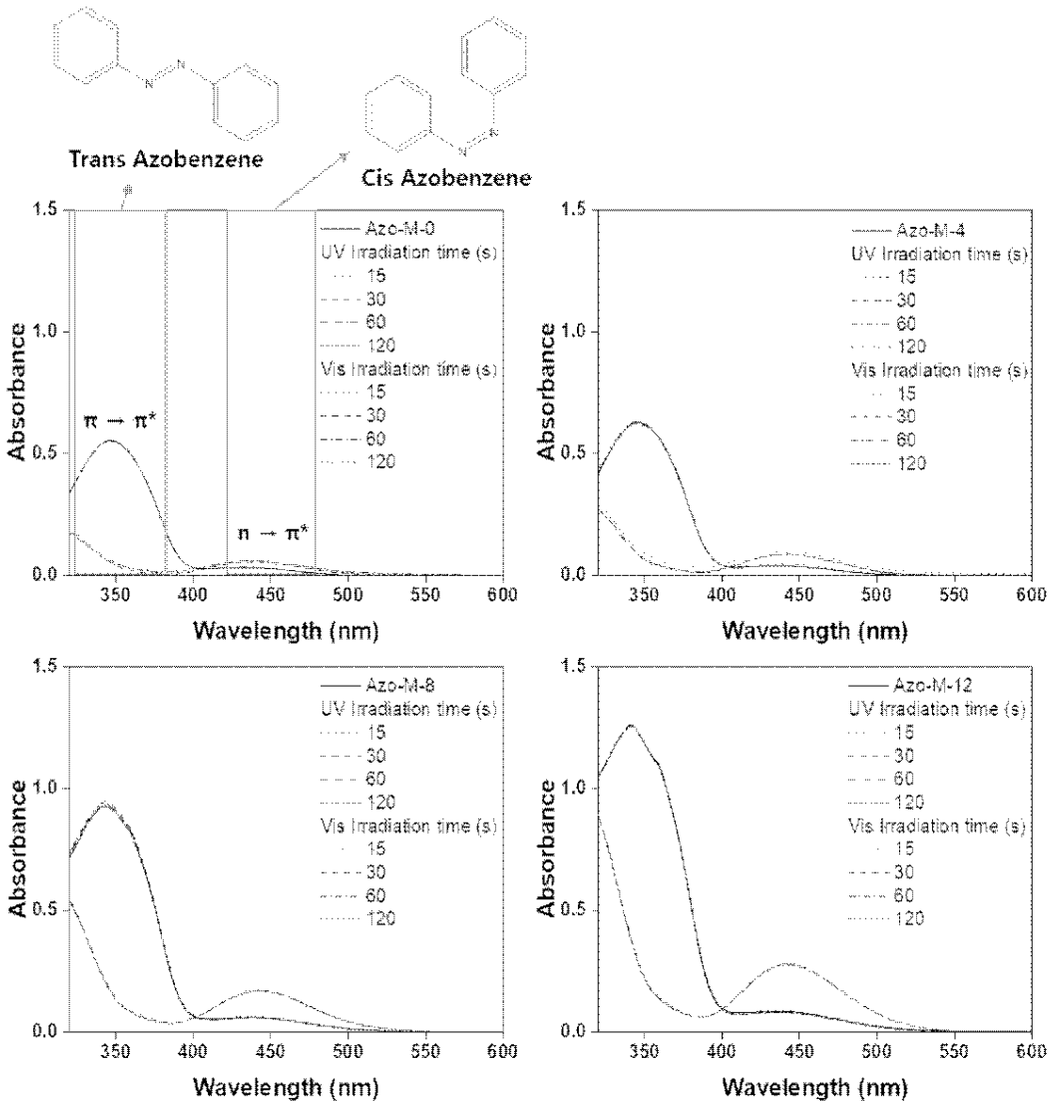

Figure 2-13. UV/Vis absorption spectral profiles of the switchable PSAs for observing the photo-isomerization of the azobenzene moiety.

서울대학교
SEOUL NATIONAL UNIVERSITY

3.4. Transition in Physical Properties of the Switchable PSAs

3.4.1. Logarithmic Damping Ratio

The influence of rapid photo-isomerization on the physical characteristics of the PSAs was confirmed by the RPT and shear modulus evaluation. The RPT has been used for evaluating curing behavior and viscoelastic properties of polymer coating materials or adhesives (Chiu and Wu, 2007, Hwang, *et al.*, 2013, Moon, *et al.*, 2012, Zhang, *et al.*, 2012). In this study, the RPT method is used to measure PSA viscoelastic properties by detecting the attenuation of the pendulum's amplitude via the displacement sensor after oscillating the pendulum placed on the PSA film with a magnetic force **(Figure 2-14a)**. The logarithmic damping ratio of the material can be evaluated. The higher damping ratio of a material indicates the quick attenuation of the amplitude of the pendulum and the low modulus of the material. As shown in **Figure 2-14b**, Azo-M-0 has similar damping ratios (approximately 1.0) regardless of the irradiation conditions (UV or Vis irradiation). The damping ratios of the samples were observed to be the same as the damping ratio recorded for Azo-M-0 (i.e., approximately 1.0) when the Azo-M-4, 8 and 12 samples were irradiated with UV light. However, these values decreased when the azobenzene groups in Azo-M existed in their trans-form in the initial state and post Vis irradiation. The gap in the damping ratio (between the UV and Vis irradiation) increased with an increase in the Azo-M content (from 4 to 12 mol%). This result indicates that Azo-M-0 and other UV-irradiated samples dissipate energy rapidly. The dissipation can be attributed to their soft and sticky nature. The Vis-irradiated Azo-M-4, 8 and 12 samples became harder as the Azo-M content increased and the kinetic energy of the pendulum could be retained for a longer period of time.

서울대학교

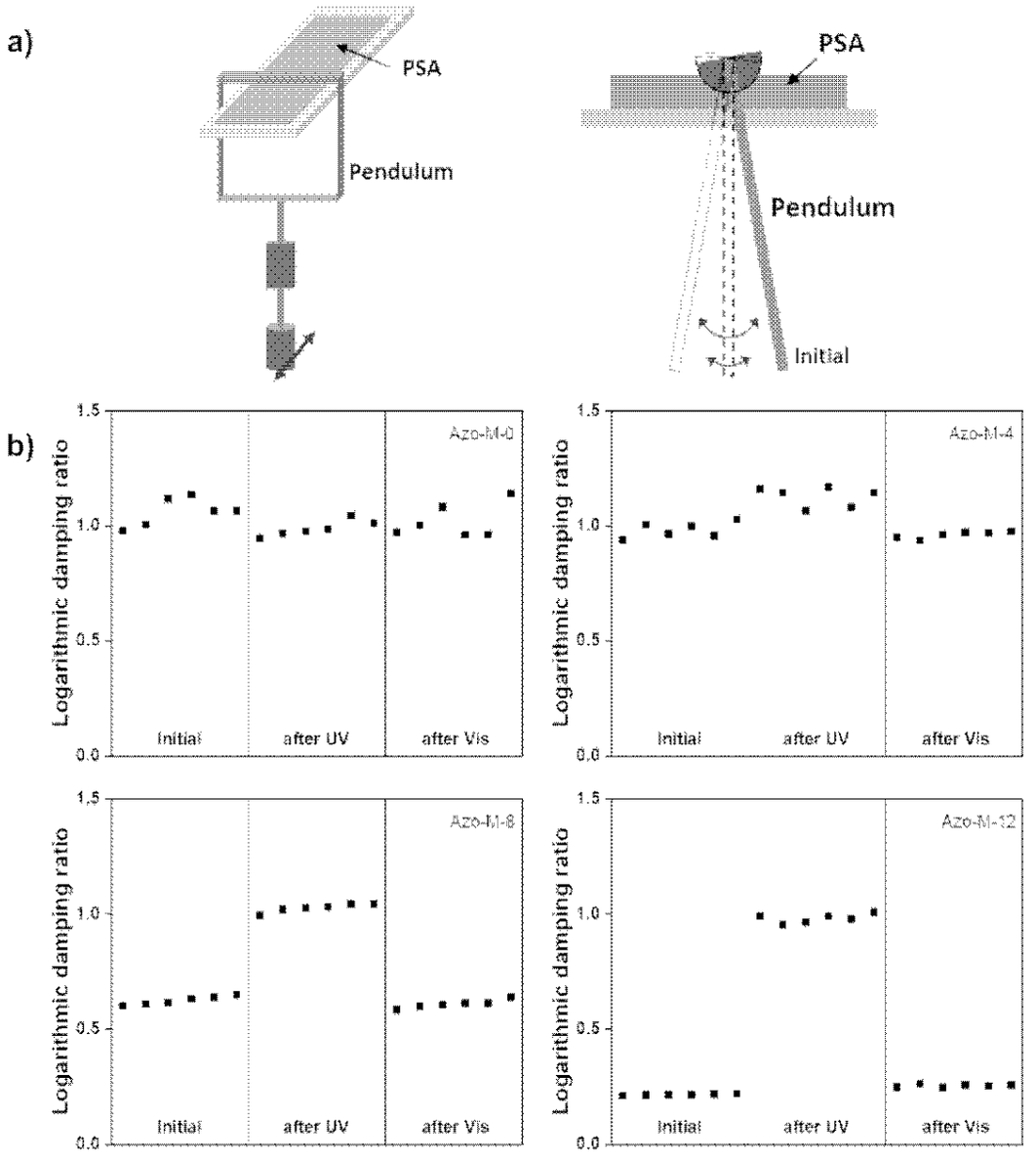

Figure 2-14. a) Schematic representation of the RPT measurement method, b) logarithmic damping ratio of the switchable PSAs obtained through the RPT.

서울대학교
SEOUL NATIONAL UNIVERSITY

3.4.2. Shear Modulus

We conducted a lap shear test using PMMA as a substrate to determine the shear modulus of the switchable PSA **(Figure 2-15)**. The Young's modulus and shear modulus of the PMMA are approximately 3 and 2 GPa, respectively. The PMMA substrates were 150 times thicker than the sandwiched switchable PSAs. Thus, we assumed no interference from the PMMA substrate when measuring the shear modulus of the PSA. Further, we used a DMA for precise testing.

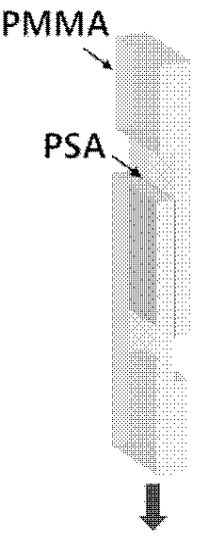

Figure 2-15. Schematic representation of the lap shear test.

The stress-strain curves of the "switched on" switchable PSAs presented a very short or no linear region after UV irradiation **(Figure 2-16a)**. Therefore, we determined the shear modulus as the slope of the tangent line in the low strain region below 2%. The shear modulus of the UV-irradiated Azo-M-0 was 27 kPa, and the modulus increased to 38 kPa in UV-irradiated Azo-M-4. However, the modulus decreased with an increase in the Azo-M content. The addition of Azo-M introduces aromatic groups that result in a higher modulus (higher than that of Azo-polymer). Azo-M was considered to play the role of a plasticizer with increased content due to the disturbance in the arrangement of the monomers caused by trans to cis isomerization.

The "switched off" switchable PSAs had a relatively long linear region in the stress-strain curves and a higher modulus than that of the "switched on" PSAs (except for Azo-M-0). The shear modulus increased with an increase in the Azo-M content. The modulus of Azo-M-12 was 78 kPa. Thus, the gap between the shear modulus of the "switched on" and "switched off" PSAs increased with

서울대학교

an increase in Azo-M content.

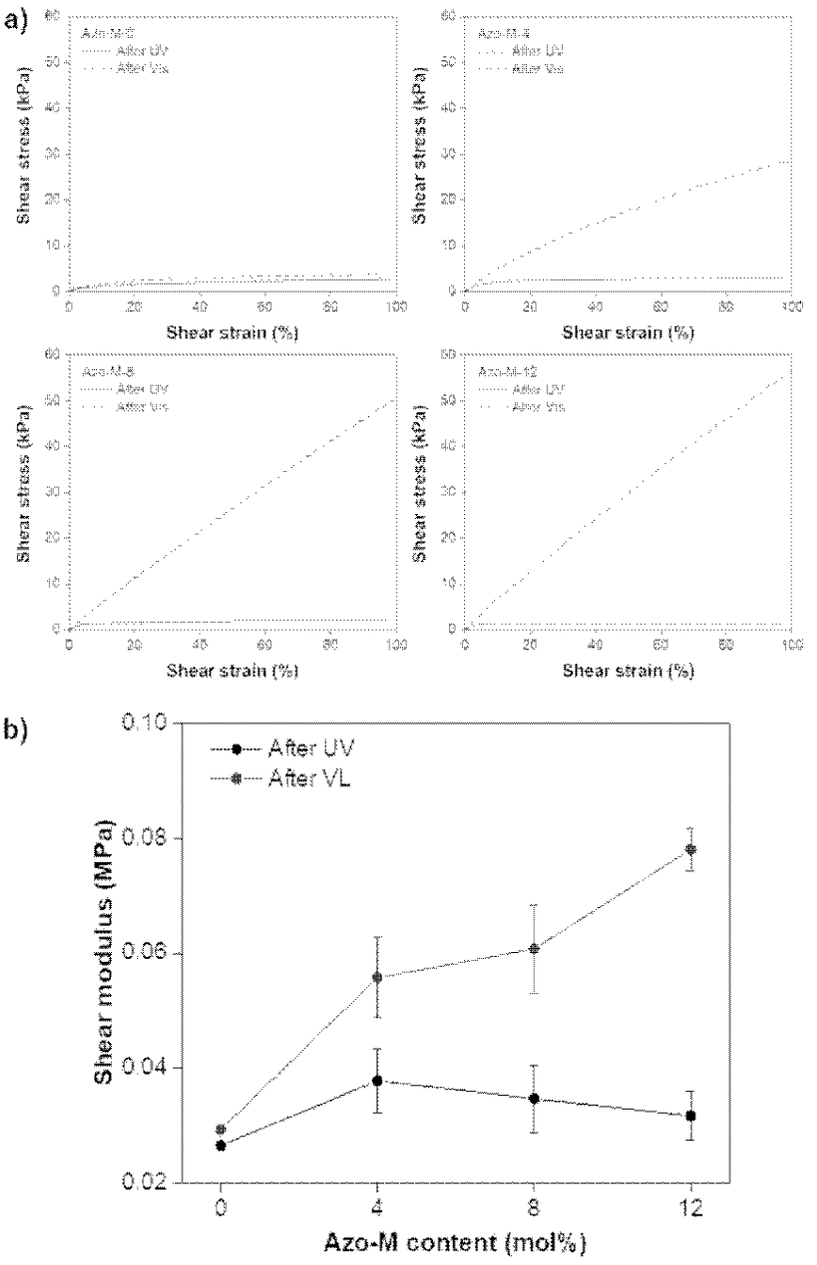

Figure 2-16. Changes in the a) lap shear stress and b) shear modulus of the switchable PSAs with UV and Vis irradiation.

서울대학교

3.5. Transition in Water Contact Angle of the Switchable PSAs

The water contact angle was measured to observe the changes in the chemical characteristics of the PSA surface. The contact angle of the Azo-M-0 was approximately 97° in the initial state, and this value was maintained even after the samples were subjected to UV and Vis irradiation **(Figure 2-17)**. When Azo-M was introduced, the contact angle became greater than 105° in the state where the azobenzene groups of the switchable PSAs existed in their trans-forms. The contact angle was lowered by trans-to-cis-isomerization under conditions of UV irradiation. The contact angles of Azo-M-4, which exhibited the largest change in contact angle, were 107° and 93°.

When the azobenzene moiety is isomerized (from trans to cis), it loses its symmetric structure. The dipole moment of the cis-isomer is higher than that of the trans-isomer. Therefore, the polar cis-azobenzene increased the surface energy of the PSA sample after UV irradiation, as shown by the decrease in the water contact angle (Ichimura, *et al.*, 2000). Meanwhile, low surface energy was observed for trans-azobenzene. The low surface energy can be attributed to the crystalline structure formed by π-π stacking between the azobenzene groups (Lim, *et al.*, 2006). The switching gap of the contact angles decreased as the content of Azo-M increased, but the change was insignificant (within 3°).

서울대학교 SEOUL NATIONAL UNIVERSITY

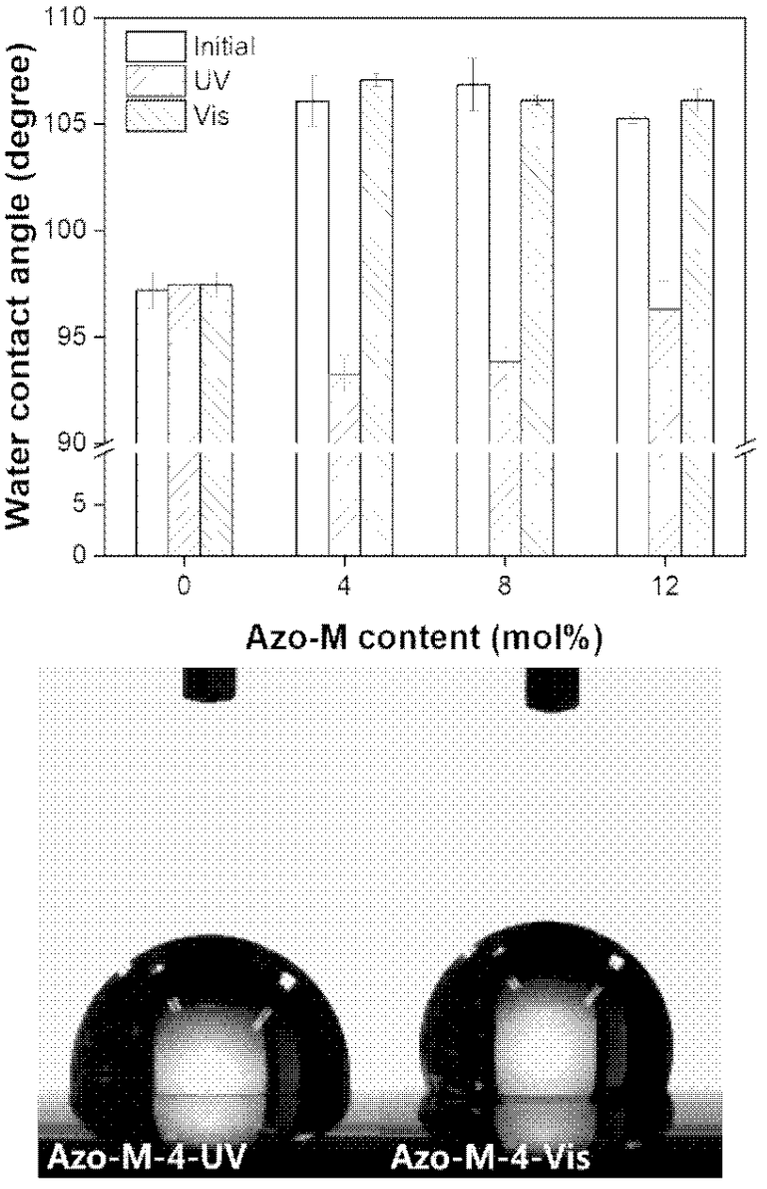

Figure 2-17. Transition of the water contact angle by UV and Vis irradiation.

In the "switched off" state, the modulus and hydrophobicity increased when Azo-M was added to Azo-polymer, and the probe tack decreased to zero. According to equation (1), an increase in the modulus induces an increase in the adhesive force. The zero tack value could not be explained only in terms of hydrophobicity because the correlation assumes an equilibrium state where the

서울대학교

probe and adhesive have completely adhered. A wetting process is necessary to achieve adhesion between the PSA and the substrate, and wettability depends on surface energy and modulus (Donatas, 1999). Unlike the wettability of liquid (which is determined by analyzing the surface energy), the wetting of the PSA is restricted by the modulus. Therefore, the restriction of the wettability of the PSA caused by the higher hydrophobicity and modulus induced the formation of the non-sticky surface and the "switched off" property. The decrease in the hydrophobicity and modulus (attributable to UV irradiation) made the switchable PSA sticky and wettable. The probe tack was unrelated to the Azo-M content despite the bigger modulus gap between the "switched on" and "switched off" states of the PSAs. It can be inferred from the results that 4 mol% of Azo-M is sufficient to switch off the probe tack. The differences in shear modulus cannot affect the probe tack results.

3.6. Transition in Crystalline Structure of Azobenzene by Photo-isomerization

3.6.1. XRD Patterns of the Switchable PSAs and DSC Curve of Azo-M

The XRD patterns of the switchable PSAs were recorded. The gentle slope in a wide range of 2θ in the XRD pattern indicates that Azo-polymer was amorphous **(Figure 2-18)**. As Azo-M was added, peaks were observed at 6.5°, 9.6°, 12.9°, 16.2°, 21.1° and 23.9°. The patterns showed that Azo-M formed its own crystalline structure in the switchable PSA because the crystalline patterns of the switchable PSAs matched the pattern recorded for Azo-M. We confirmed that the Azo-acrylate used to polymerize Azo-polymer had crystallinity using the DSC **(Figure 2-19)**. It had a mesophase which is characteristic of liquid

서울대학교

crystals between 29 °C and 67 °C, as shown during the cooling scan of the DSC measurement. However, the Azo-acrylate present in the polymer chain could not form a crystalline structure or mesophase in the PSA as their content was low (8 mol%) and due to interference from the co-monomer (BA).

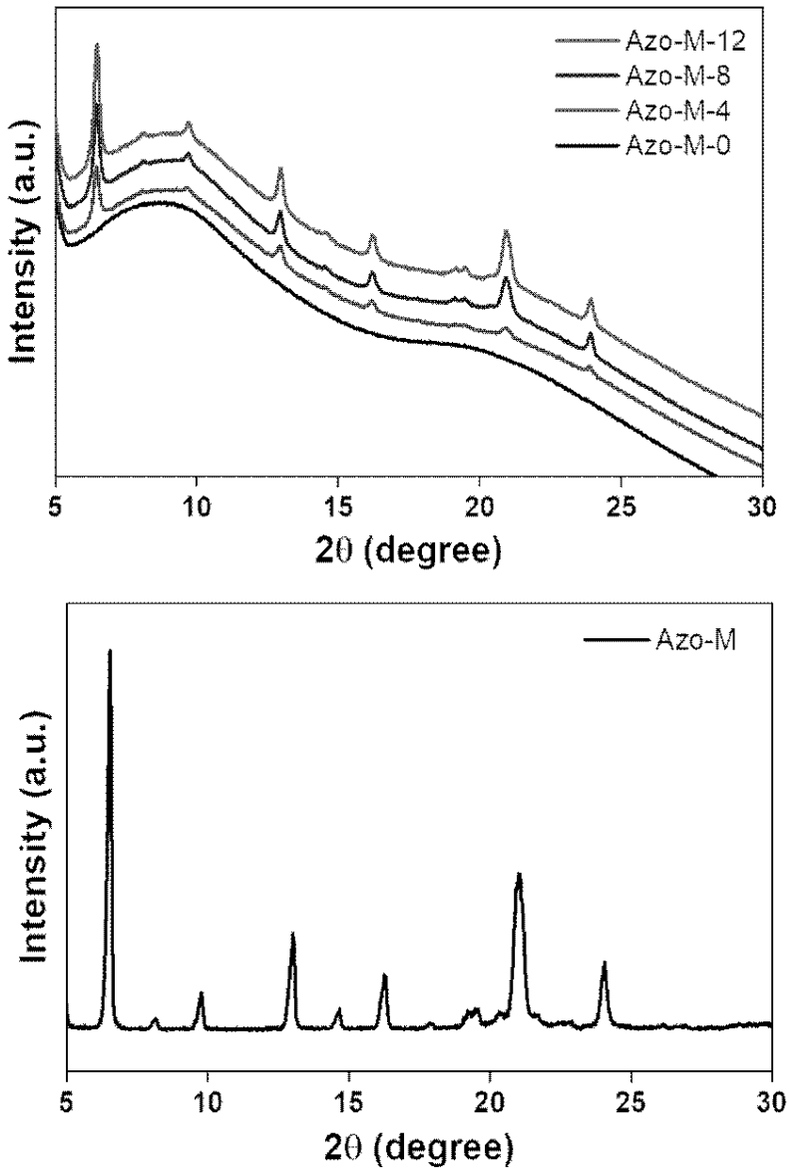

Figure 2-18. XRD patterns of the switchable PSAs and Azo-M.

서울대학교

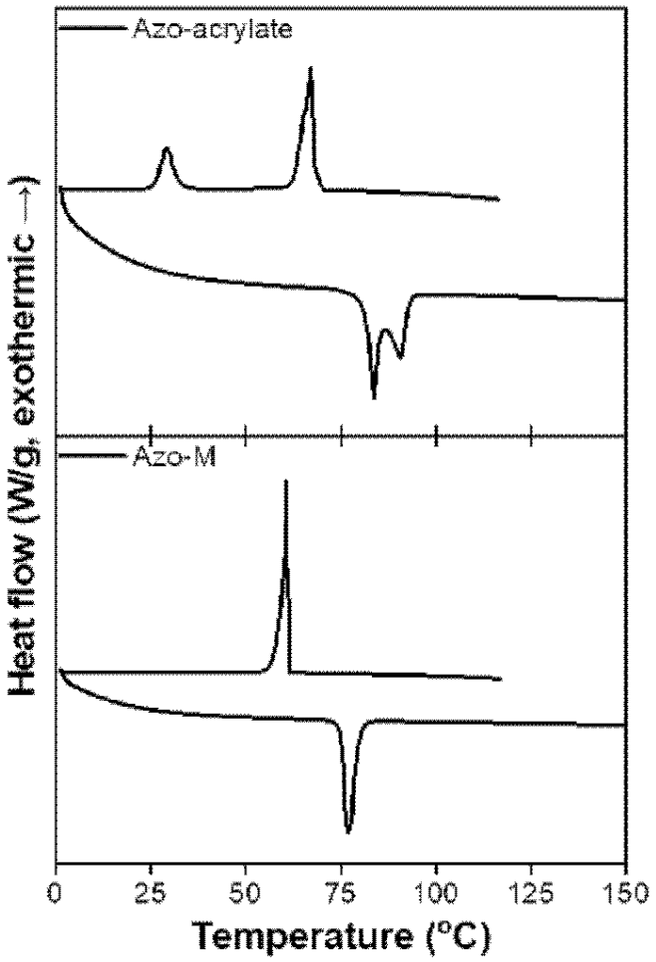

Figure 2-19. DSC profiles recorded for the Azo-acrylate and Azo-M.

3.6.2. POM Images of the Switchable PSAs

Further, we observed small and dense crystalline structures (formed in the switchable PSA) using a POM **(Figure 2-20)**. No crystalline structure was observed in the absence of Azo-M (as indicated by the XRD results). The crystalline structure disappeared in the POM image of the switchable PSA under conditions of UV irradiation. The trans-azobenzene has a planar structure and can be stacked easily, whereas the three-dimensionally distorted structure of the cis-azobenzene disturbs the molecular arrangement. This transition in

서울대학교

crystalline structure is expected to induce changes in hydrophilicity and the modulus that enable adhesion switching.

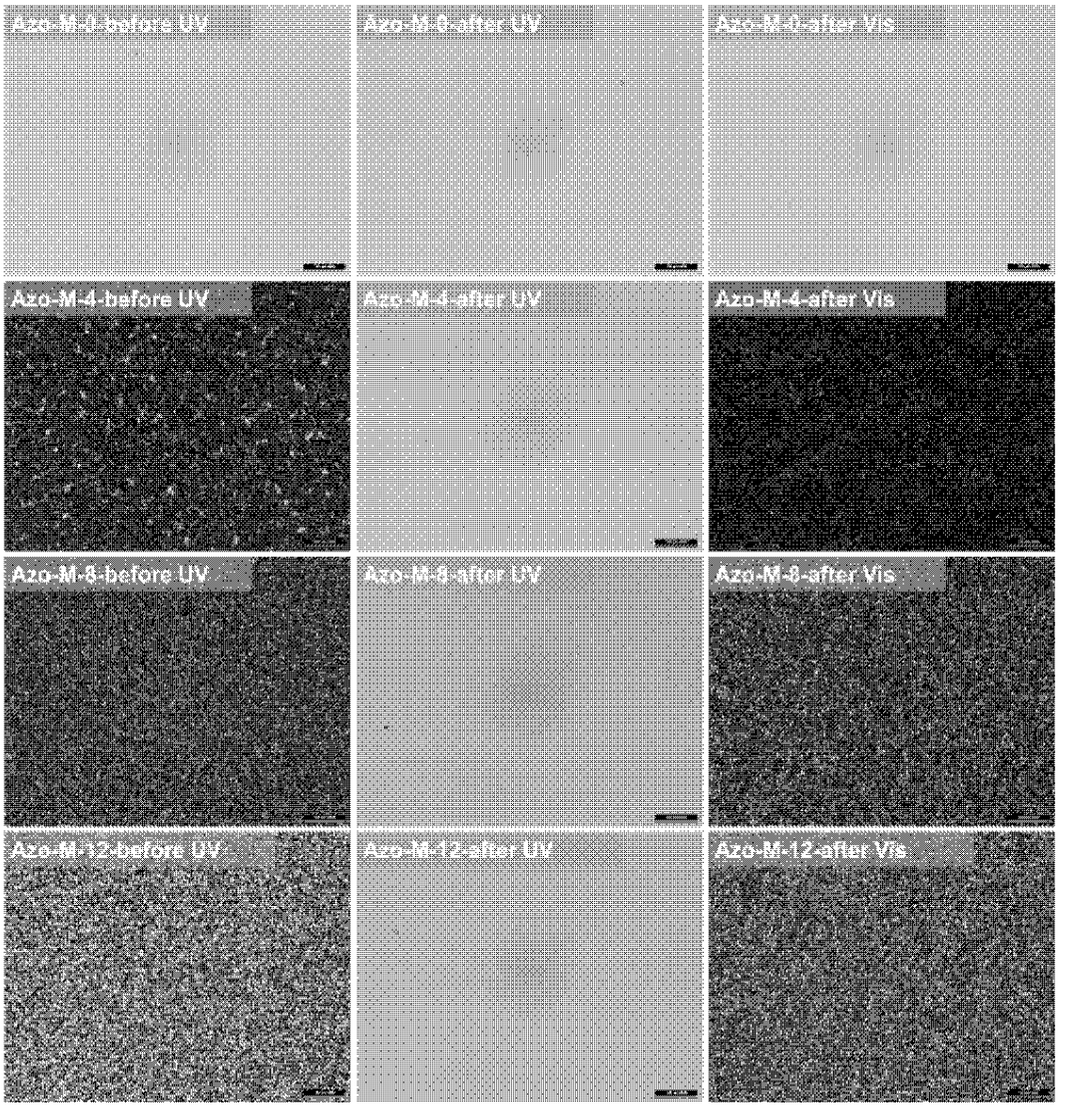

Figure 2-20. POM images of the switchable PSAs for observing the transition of crystalline structures under conditions of UV and Vis irradiation (×200).

서울대학교

3.7. Function of Azobenzene Side Groups in Azo Polymer in the Switchable PSAs

We attempted to convert Azo-polymer to poly(butyl acrylate) (PBA) to define the function of Azo-polymer in the switchable PSA. The Azo-M contents were set to 12, 16 and 20 (mol%), considering that 8 mol% of the azobenzene moiety was present in Azo-polymer. Nonuniformly stained films were obtained **(Figure 2-21a)**. When we tested the switchable probe tack, marks were left on the surface of the PSA and residue was left on the probe **(Figure 2-21b)**. We confirmed that Azo-M could be stably dispersed and fixed in the switchable PSA by making it interact with the azobenzene moiety in Azo-polymer.

서울대학교

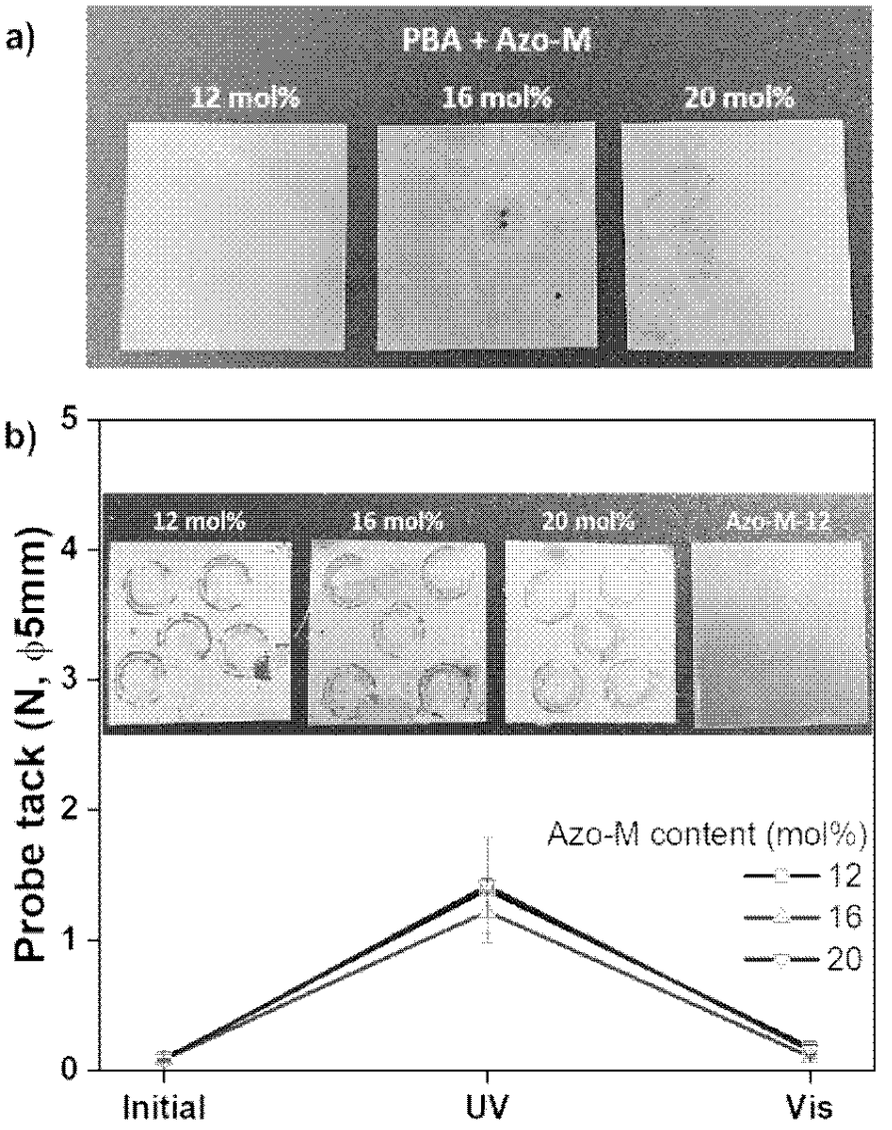

Figure 2-21. a) Images of nonuniform switchable PSA with PBA, b) probe tack of nonuniform switchable PSAs and surface comparison of switchable PSAs after probe tack test.

서울대학교

3.8. Influence of Heat Generated by UV irradiation Process in Adhesion Switching

The UV intensity for switching on the switchable PSAs, 120 mW/cm^2, was quite a strong irradiation condition. Also, the UV irradiation was conducted in an enclosed system. Therefore, it was expected that considerable heat could be generated during the UV irradiation process. The crystalline structure of Azo-M can be melted at high temperatures, and the photo-isomerization rate or efficiency of the azobenzene groups can be affected by the temperature condition. Thus, it was necessary to define the influence of heat in photo-isomerization and adhesion switching. When the temperature change of the PSA surface was tracked over time (**Figure 2-22**), the temperature increased to 58.6 ℃ and 70.8 ℃ after 30 s and 60 s of UV irradiation, respectively. The both

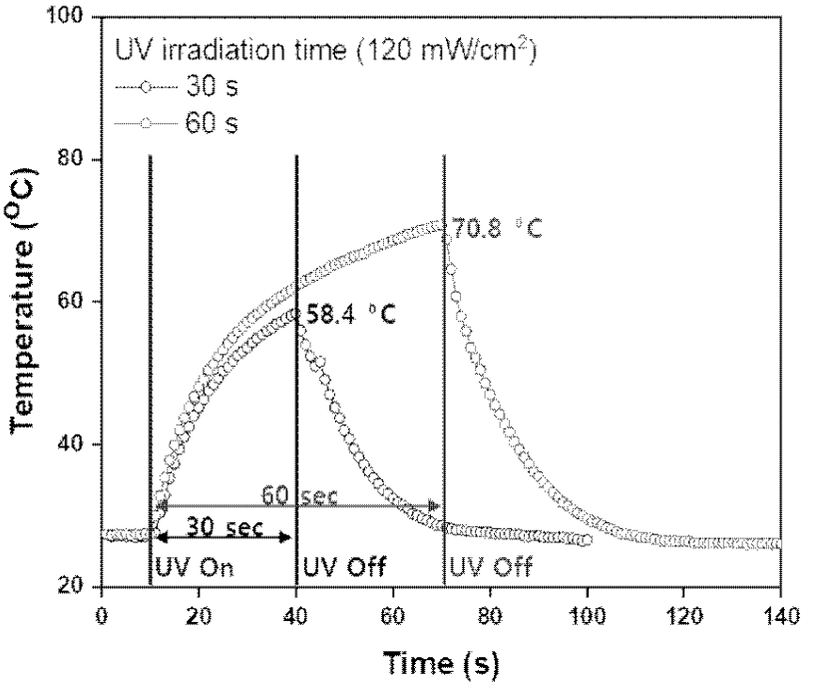

Figure 2-22. Surface temperatures of Azo-M-12 according to UV irradiation time.

서울대학교

temperatures were below the onset temperature of the melting peak of Azo-M in the DSC curve **(Figure 2-19)**. The high temperature did not induce any phase transition of Azo-M in the switchable PSAs because the PSAs were exposed to UV light for 30 s in this study.

We also evaluated whether temperature affects the isomerization of the azobenzene moiety and probe tack force. To clearly determine the effect of temperature, we kept the PSA at 70 °C for up to 5 min and monitored the isomerization of the azobenzene moiety through a UV/Vis spectrometer **(Figure 2-23)**. Even when the PSA was kept at 70 °C for 5 min, there was no increase in the absorption spectrum of n → π* near 450 nm, which could indicate trans-to-cis isomerization. A decrease in the π → π* absorption spectrum near 360 nm was not observed but rather increased slightly. It means that cis-to-trans isomerization occurred when the PSA was left at a high temperature. The reason for this situation is that the cis-to-trans isomerization

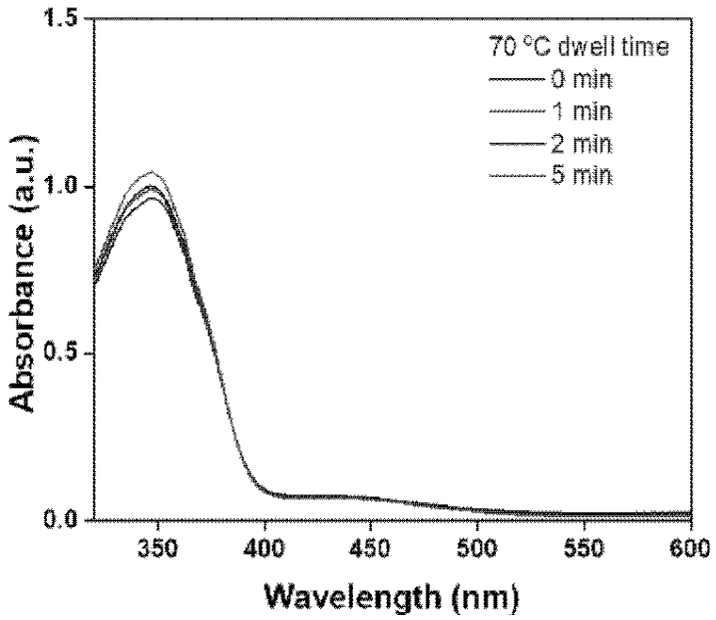

Figure 2-23. UV/vis absorption spectra of Azo-M-12 according to dwell time in high temperature.

서울대학교

of azobenzene occurs not only with visible light but also with thermal stimulus. Probe tack force was also maintained according to the dwell time at 70 °C **(Figure 2-24)**. These results indicate that the heat generated during UV irradiation did not cause trans-to-cis isomerization or adhesion changes. There is also a possibility that azobenzene moiety can be easily isomerized into cis-form in the crystalline structure due to a decrease in the modulus of the matrix polymer and an increase in the kinetic energy of molecules in high temperature. However, it was considered that the temperature increase due to the high energy of the UV radiation is inevitable.

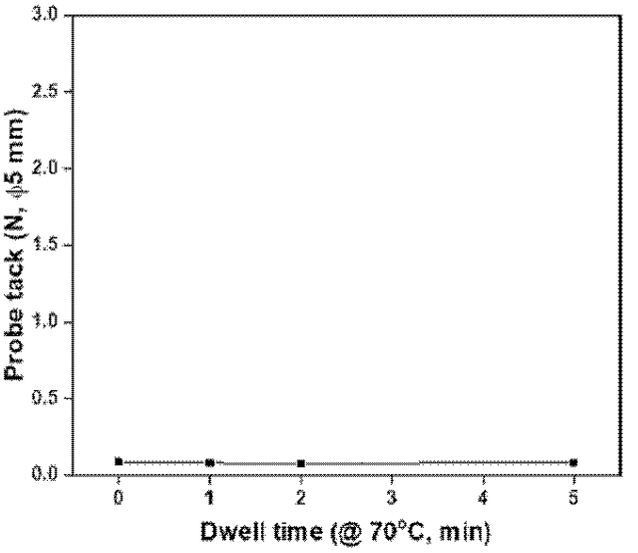

Figure 2-24. Probe tack of Azo-M-12 according to dwell time in high temperature.

서울대학교

3.9. Adhesion Switchability Evaluated with Peel Test

Adhesion switchability in the adhered state to a substrate is necessary for the switchable PSA to mediate the transfer process. Therefore, we conducted a 180° peel test to evaluate the property of adhesion switchability even in the adhered state to the substrate **(Figure 2-25a)**. The peel strength of the "switched on" Azo-M-4 was the highest as 8.3 N/25mm, and the peel strength is close to that of general PSA, 10 N/25mm. It means that the switchable PSA had sufficient adhesive strength as PSA. The peel strength tended to decrease as the Azo-M content increased. All samples showed a reduction in adhesive strength when irradiated with Vis. However, the peel strength did not drop to zero, unlike the probe tack results. The switching ratio (F_{high}/F_{low}; where F_{high} denotes the peel strength of the "switched on" PSA, and F_{low} denotes the peel strength of the "switched off" PSA) of Azo-M-4 was 1.8. The ratio increased with a decrease in F_{high}; The switching ratio of Azo-M-12 was 7.9, and the peel strength decreased to almost zero, 0.4 N/25mm.

Contrary to the probe tack results, which suggested that the Azo-M content and adhesion were not related, the peel test showed that as the Azo-M content increased, the adhesion forces of the "switched on" PSA decreased, and the switching ratio increased. Kendall defined the peel strength as follows (Kendall, 1975):

$$F_p = Etb[\sqrt{(1-cos\theta)^2 + \frac{2\omega}{Et}} - (1-cos\theta)], \quad (3)$$

where t denotes the adhesive thickness, b denotes the adhesive width, and θ denotes the peeling angle. In the case of the probe tack test, the adhesion

서울대학교 SEOUL NATIONAL UNIVERSITY

switching occurred with transition in PSA's wettability because the PSA surface was opened during adhesion switching. However, in the case of the peel test, the adhesion switching occurs after wetting of the "switched on" PSA to the adherent. Thus, the adhesion follows Kendall's model. While the decrease of PSA surface energy by Vis irradiation results in an adhesion decrease, the increase in modulus induces increasing in the peel strength in equation (3). Thus, it was expected that the decrease in peel strength by Vis irradiation was induced by the decrease in surface energy and not modulus but other factors. Although the mechanism was not defined clearly in this study, it was expected that the decrease in adhesion area due to shrinkage by Azo-M's crystallization was the factor of peel strength decrease.

We also conducted a 90° peel test with Azo-M-12, which had the highest switching ratio and the lowest peel strength after Vis irradiation **(Figure 2-25b)**. It could endure when the "switched on" PSA was attached to the silicone wafer and was loaded with binder clips. However, when the attached PSA was irradiated with Vis, the PSA detached immediately. In conclusion, the peel test confirmed that the switching characteristic was achieved even when the switchable PSA was attached to the substrate. Thus, we believed it could be used as a mediator in the transfer process.

서울대학교

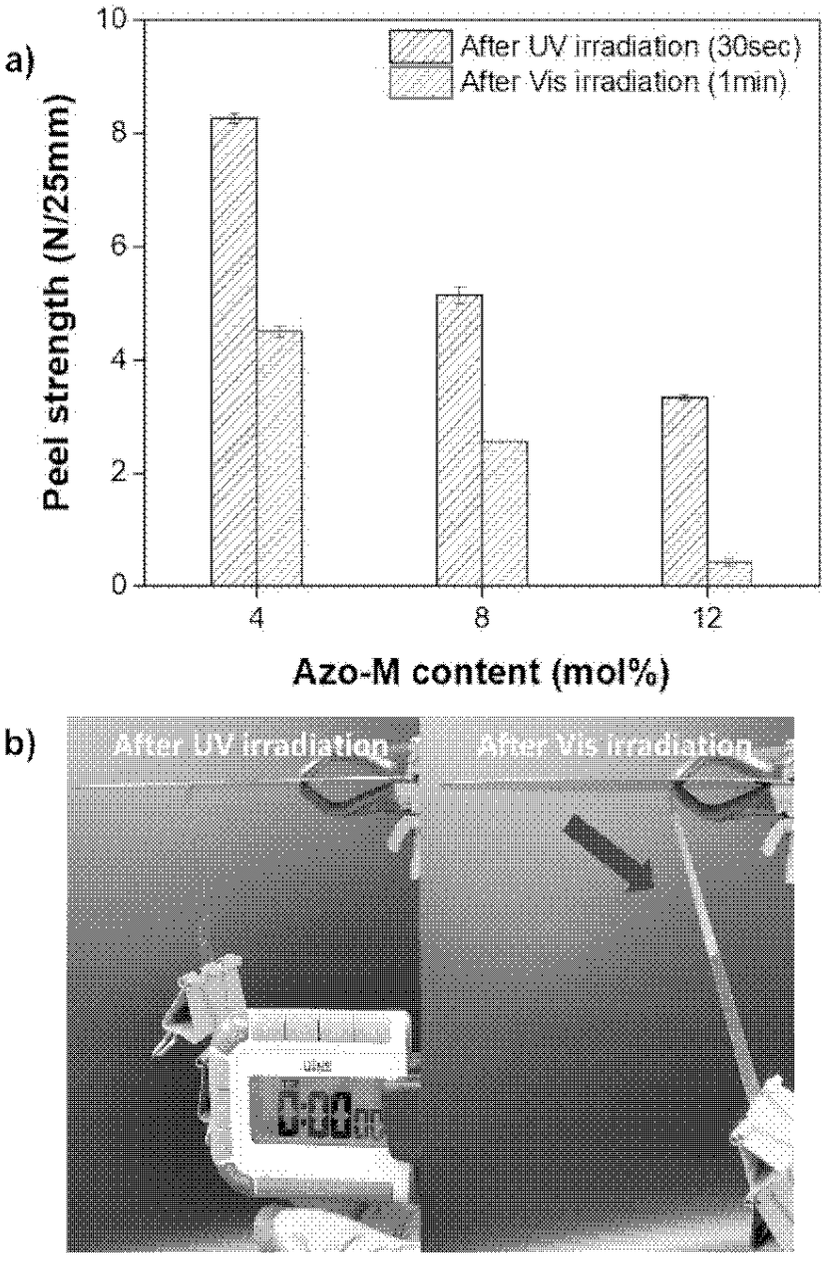

Figure 2-25. a) Changes in the 180° peel strength of the switchable PSAs with UV and Vis irradiation and b) images captured during the adhesion switching test by 90° peel test conducted with Azo-M-12. The Vis irradiated switchable PSA was peeled off immediately after the start of the test.

서울대학교

3.10. Mini-LEDs Transfer Test using Azo-M-12

We investigated if the switchable PSA can be used to transfer mini-LEDs. The mini-LEDs were arrayed on the carrier PSA. We transferred the mini-LEDs from the carrier PSA as the donor to the PDMS as an acceptor **(Figure 2-26a)**. The width and length of the mini-LED were 100 μm and 200 μm, respectively **(Figure 2-26b)**. The adhesion forces evaluated by the probe tack test of the donor and acceptor were approximately 0.8 N and 1.4 N, respectively **(Figure 2-27)**.

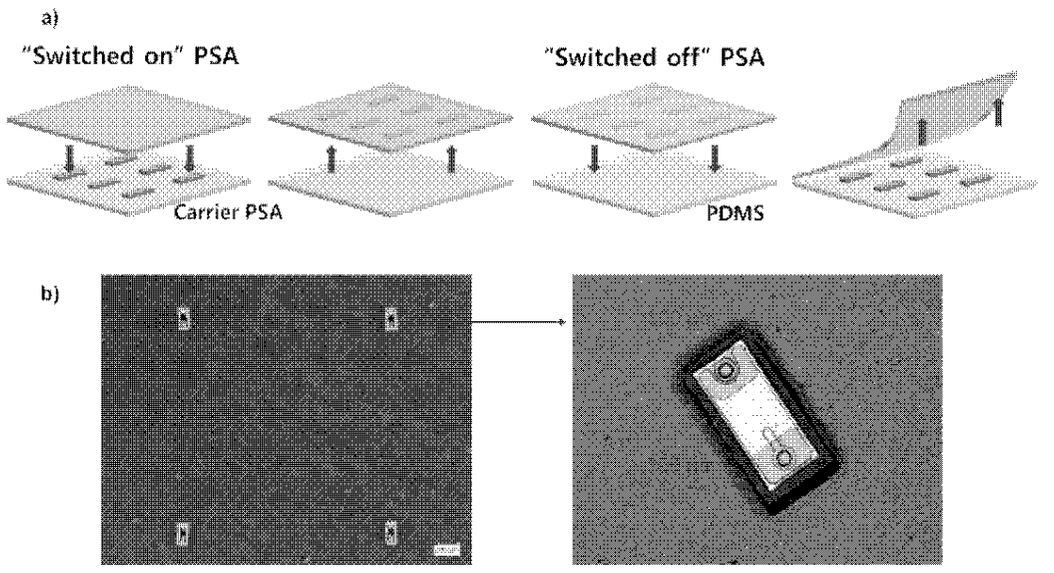

Figure 2-26. a) Schematic representation of the mini-LED transfer test method using switchable PSA (donor: carrier PSA, accepter: PDMS), b) confocal and optical microscopy images of the mini-LEDs.

서울대학교 SEOUL NATIONAL UNIVERSITY

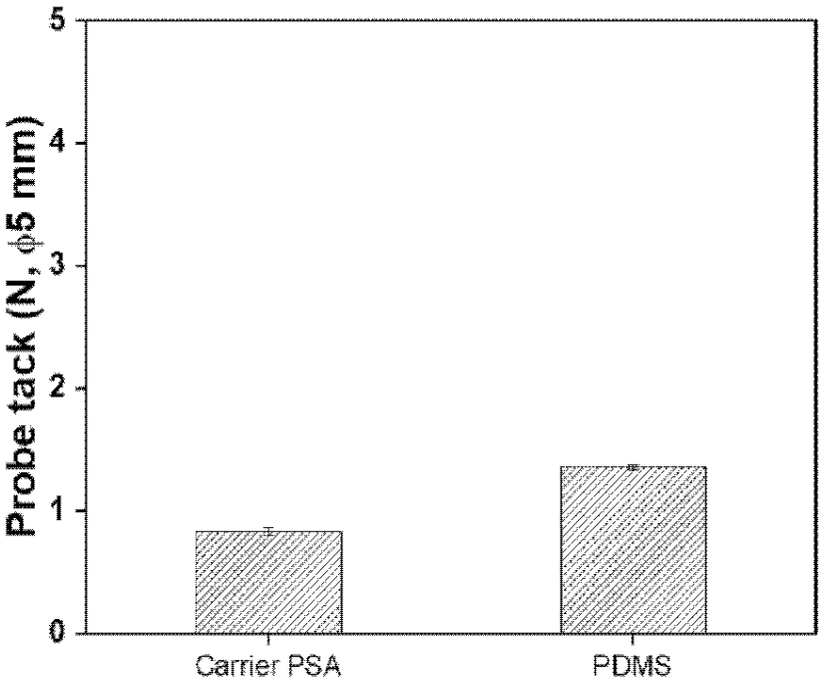

Figure 2-27. Probe tack forces of mini-LED carrier PSA and PDMS.

The transfer process is shown in **Figure 2-28**. We conducted the experiments with Azo-M-12 because it exhibited the maximum switching ratio. When the UV irradiated switchable PSA picked up the mini-LEDs, the mini-LEDs were successfully transferred to the switchable PSA. Then, the switchable PSA was placed onto the PDMS and then peeled off post Vis irradiation. The mini-LEDs were successfully transferred onto the PDMS substrate. Further, we examined the property of selective transfer by local UV irradiation using a photomask. The UV irradiated parts appeared dark yellow. It was confirmed that only the mini-LEDs located under the UV irradiated parts were transferred to the switchable PSAs.

서울대학교

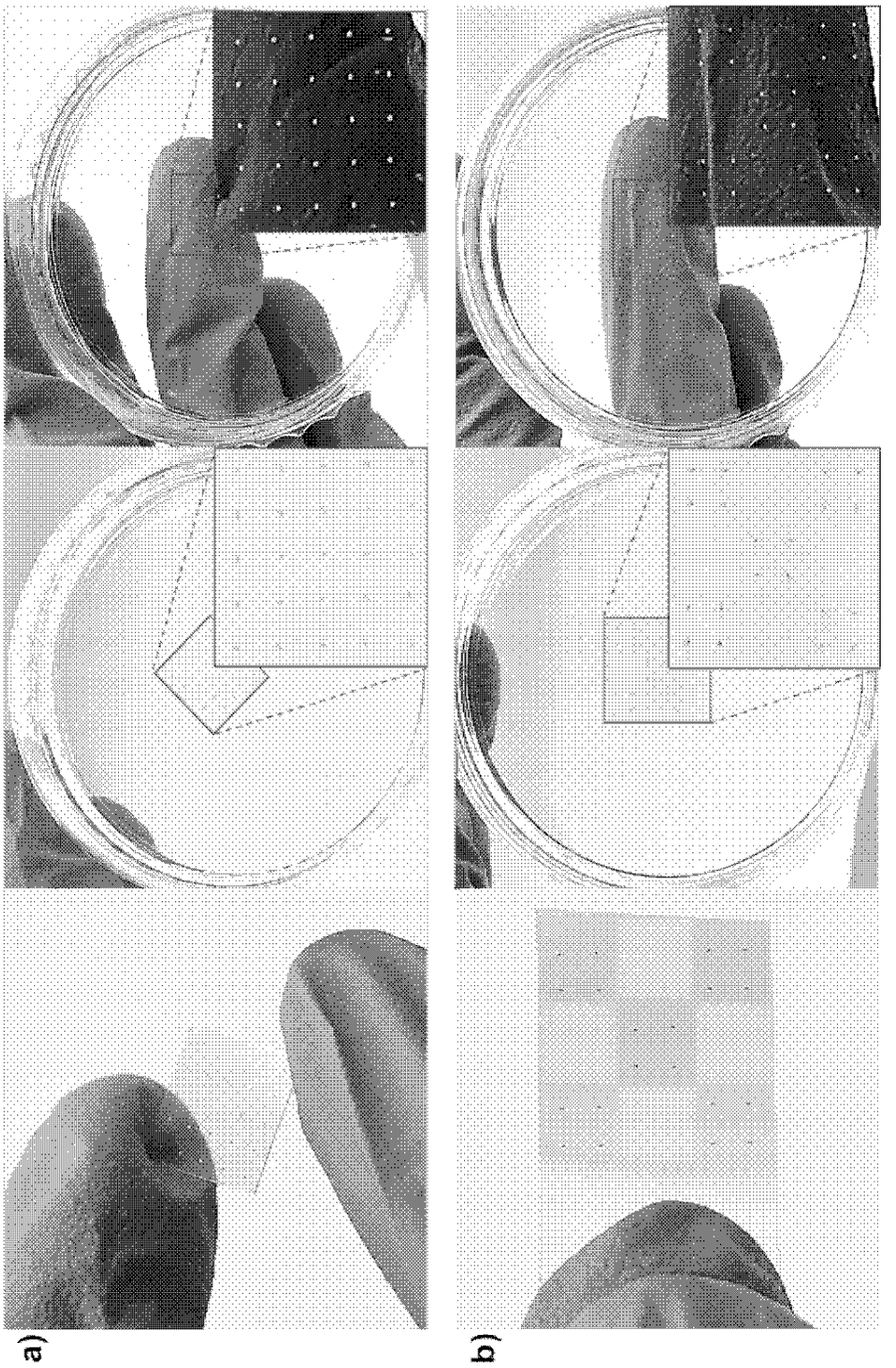

Figure 2-28. a) mini-LED transfer test using Azo-M-12, b) selective transfer by the partial adhesion switching of Azo-M-12 using a photomask.

서울대학교

4. Conclusions

We polymerized azobenzene-containing acrylic polymer (Azo-polymer) and synthesized azobenzene-containing low molecular weight compounds (Azo-M). The photo-responsive switchable PSA was fabricated with a mixture of Azo-polymer and Azo-M. The Azo-polymer was used as a matrix polymer of the PSA and allowed Azo-M to be uniformly and stably dispersed in the PSA. Also, the Azo-M was applied as a photo-responsive additive. The modulus and surface energy were tuned with UV and Vis irradiation. The change in the properties can be attributed to the crystalline structure transition exhibited by Azo-M (via photo-isomerization). The switchable PSAs exhibited the property of fast adhesion switching and a high switching ratio without phase transition between the solid and liquid states. Repetitive adhesion switching without a loss in adhesion force was also achieved. The novel switchable PSA can be potentially used as a selective and reusable transfer film for micro-scaled electronic devices. Especially, they can be used to realize mini-LED and micro-LED transfer processes. However, this study was limited to the synthesis and characterization of a polymer and monomer with a specific structure and the preliminary mini-LED transfer test. Thus, the influences of various azobenzene-containing compounds (differing in their chemical structures) will be described in other chapters.

서울대학교 SEOUL NATIONAL UNIVERSITY

Chapter 3

Influence of Hydrocarbon Chain Length of Azo-compounds in Photo-responsive Adhesion Switching Efficiency

서울대학교 SEOUL NATIONAL UNIVERSITY

1. Introduction

An adhesive is a material used to attach two substrates; it is generally known as a material that is applied in a liquid state and cured into a solid through the use of moisture, heat or light, forming an adhesive bond. Pressure-sensitive adhesives (PSAs) maintain their stickiness under service temperature conditions and can form an adhesion without curing (Creton and Ciccotti, 2016). To achieve adhesion without a liquid-to-solid phase transition, a PSA has to have a T_g that is 25–45 °C lower than service temperature (Creton, 2003) and the appropriate viscoelastic properties (Chang, 1991). T_g is a characteristic of amorphous polymers and is the temperature at which molecular segments comprising several molecules begin to move. The wetting of an adhesive on the substrate is essential for adhesion. The relatively low PSA T_g allows them to be wetted at the service temperature and form an adhesive bond in the absence of a phase transition. Chang published a study on the viscoelastic window of PSAs (Chang, 1991). They were found to have specific storage modulus (G') and loss modulus (G") ranges and to have characteristics and applications that can be determined by G' and G".

Thus, when the T_g and viscoelastic properties of a PSA are determined by the chemical composition or film fabrication process, the adhesive force is fixed under constant environmental conditions such as temperature and humidity. General adhesives maintain their adhesive force after being cured. However, there is growing interest in adhesives that can be released from a substrate upon user demand, thereby enabling multi-functionality. This type of adhesive, i.e., switchable adhesives, is attached to the substrate with a strong force and can be easily detached in response to external stimuli such as heat, light, water and electromagnetic force (Croll, *et al.*, 2019).

서울대학교

Heat is the most common stimulus for adhesion switching. Because the mechanical properties of the base polymer are temperature-dependent, the adhesive strength can be changed by heating or cooling it. Alternatively, an excessive temperature change is necessary to control the adhesive strength of general adhesives. In the case of conventional PSAs, a significant change in adhesive force can be achieved by applying a temperature that is at least 30–40 °C lower or higher than T_g (Kamperman, et al., 2012). As such, liquid crystal polymers or liquid crystal elastomers have been used to reduce the temperature range required for adhesion switching (Cho, *et al.*, 2003, De Crevoisier, *et al.*, 1999, Ohzono, *et al.*, 2019, Ohzono, *et al.*, 2020). Adhesion switching is induced by a change in the mechanical or chemical properties of the comprising materials (Croll, *et al.*, 2019). Thus, due to their better molecular mobility than dried materials, many researchers have opted to use hydrogel systems to obtain the desired switchable adhesion characteristics. The adhesion properties of hydrogels can be controlled by modulating the molecular conformation or reversible bonding phases, particularly heat-, pH- and solvent-dependent host-guest interactions or coordination with metal ions (Gao, *et al.*, 2019, La Spina, *et al.*, 2007, Nakamura, *et al.*, 2014, Yamaguchi, *et al.*, 2012, Zheng, *et al.*, 2012, Zheng, *et al.*, 2013). The frequency dependence of elastomer stamp (Meitl, *et al.*, 2005) or cross-linking by UV light (Boyne, *et al.*, 2001, Ebe, *et al.*, 2003, Lee, *et al.*, 2015) can be applied in the electronics manufacturing process to enable rapid adhesion switching that does not damage the substrate. There are also switchable adhesives that utilize shape-memory polymers (Eisenhaure, *et al.*, 2013), solvent wettability (Sim, *et al.*, 2015), and magneto-rheological materials (Kim, *et al.*, 2019, Testa, *et al.*, 2020). However, the applicability of switchable adhesives that require heat, solvent or hydrated conditions is limited. In addition, irreversibly cross-linked adhesives cannot be reused; other methods also have limitations, such as a slow switching speed or narrow adhesive force

서울대학교

modulation range.

Thus, we have studied photo-sensitive materials with rapid adhesion switching characteristics and a wide adhesive force modulation range in the dried state. Some compounds have photo-reversible bonds in the dried state (Kaur, *et al.*, 2014). A photo-reversible cycloaddition reaction of anthracene moiety has been applied in studies to realize re-workable adhesives (Akiyama, *et al.*, 2018, Liu, *et al.*, 2020, Shen, *et al.*, 2020). Although these compounds with reversible reactions form stable bonded structures, they require long-term stimulation for bond transition. We have applied an azobenzene moiety to fabricate the photo-responsive adhesive.

The azobenzene group isomerizes from the trans-form to the cis-form in response to UV radiation and returns to the trans-form under visible light. Although trans-azobenzene has a planar symmetric structure, cis-azobenzene has a three-dimensionally bent asymmetric structure (Goulet-Hanssens, *et al.*, 2020). For this reason, the intermolecular arrangement and polarity of the azobenzene moiety can be converted by photo-isomerization. Some studies have been conducted on switchable adhesives that incorporate an azobenzene moiety as an acrylic polymer side chain (Akiyama, *et al.*, 2014, Akiyama, *et al.*, 2016, Ito, *et al.*, 2018, Ito, *et al.*, 2018, Kortekaas, *et al.*, 2020, Zhou, *et al.*, 2019). However, these adhesives have limitations in terms of repeated usage because separation tends to occur during the solid-to-liquid phase transition.

Our previous study prepared PSA capable of adhesion switching without solid/liquid phase transition; they comprise mixtures of a copolymer of butyl acrylate and azobenzene-containing acrylate and a low molecular weight compound containing an azobenzene moiety (Lee, *et al.*, 2021). The azobenzene-containing compound had a chemical structure in which the para position of azobenzene was substituted with a hydrocarbon chain. The isomerization of azobenzene moiety is influenced by its substituent, polymer

서울대학교

containing azobenzene groups, and the environment of the surrounding matrix by electronic and steric effects (Barrett, *et al.*, 1995, Gegiou, *et al.*, 1968, Rau, *et al.*, 1988, Titov, *et al.*, 2016). Thus, we studied the influence of the substituent's steric effect on photo-isomerization of azobenzene moiety and adhesion switching by varying the hydrocarbon chain length of the substituent in this study. Our novel switchable PSA is triggered by UV and visible light irradiation and is capable of repeated adhesion switching without any loss of adhesive force. It was found to obtain a large adhesive force even at low UV intensity and under the condition of a short exposure time of 30 s. Here, we also report on the mechanism of adhesion switching and the influence of the UV intensity on the switchable PSAs.

서울대학교

2. Experimental

2.1. Materials

The following were purchased from Sigma-Aldrich: 4-phenylazophenol (98%), 1-chlorohexane (99%), 1-chlorodecane (98%), dibutyltin dilaurate (DBTDL, 95%) and butyl acrylate (>99%). Potassium carbonate (>99%), potassium iodide (>99.5%), 6-chloro-1-hexanol (>96%), 1-chlorotetradecane (>98%) and 1-chlorooctadecane (>98%) were purchased from Tokyo Chemical Industry Co., Ltd. The following were purchased from Samchun Chemicals Co., Ltd.: 2,2'-azobisisobutyronitrile (98%), 2-butanone (MEK, 99.5%), N,N-dimethylformamide (DMF, 99.5%), tetrahydrofuran (THF, 99.9%), methanol (99.5%), n-hexane (96%), acetone (99.5%) and ethyl acetate (EA, 99.5%). Lastly, 2-Isocyanatoethyl acrylate (Karenz AOI, Showa Denko) was used as the isocyanate-containing acrylic monomer.

2.2. Synthesis of Azobenzene-containing Acrylic Monomer and Low Molecular Weight Compounds

2.2.1. 6-(4-(Phenyldiazenyl)phenoxy)hexan-1-ol

The method was based on a procedure described by Zhou (Zhou, *et al.*, 2016). Briefly, 4-phenylazophenol (3.568 g, 0.018 mol) and potassium carbonate (2.488 g, 0.018 mol) were added to DMF (15 ml). After dissolving the mixture under the condition of stirring at room temperature for 30 min, potassium iodide (7.5 mg, 0.045 mmol) and 6-chloro-1-hexanol (3.689 g, 0.027 mol) were added to the solution. Synthesis was carried out over a period of 24 h and at 110 °C.

서울대학교

The reaction solution was poured into cold water, and the precipitate was filtered. After recrystallizing the filtered compound in n-hexane, the compound was filtered and dried at room temperature under vacuum.

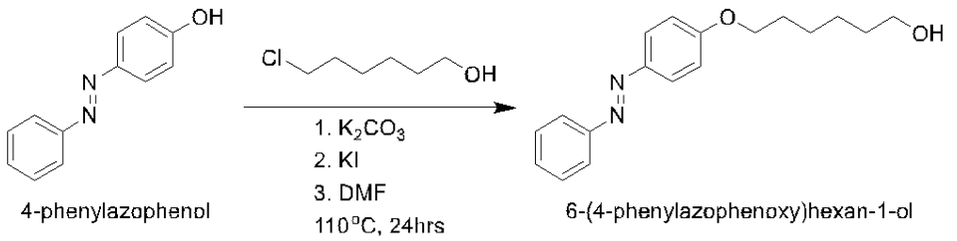

Figure 3-1. Synthesis of 6-(4-(Phenyldiazenyl)phenoxy)hexan-1-ol.

2.2.2. 2-((((6-(4-(phenyldiazenyl)phenoxy)hexyl)oxy) carbonyl)amino)ethyl acrylate (Azo-acrylate)

After dissolving 6-(4-(phenyldiazenyl)phenoxy)hexan-1-ol (2.000 g, 0.007 mol) in MEK (15 ml) at room temperature, 2-isocyanatoethyl acrylate (1.976 g, 0.014 mol) was added to the solution. The mixture was stirred under N2 purging conditions for 20 min. DBTDL (0.019 g) was diluted in MEK and added to the solution. The reaction mixture was maintained at 40 °C for 6 h. The reacted solution was poured into cold n-hexane, and the precipitate was filtered. The filtered compound was dried at room temperature under vacuum.

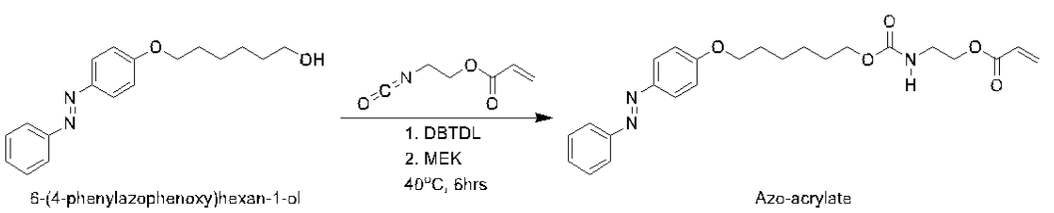

Figure 3-2. Synthesis of Azo-acrylate.

서울대학교

2.2.3. Low Molecular Weight Azobenzene Compounds (Azo-compounds)

The synthesis method for 6-(4-(phenyldiazenyl)phenoxy) hexan-1-ol was used to synthesize four low molecular weight azobenzene compounds (Azo-compounds), i.e., 1-(4-(hexyloxy)phenyl)-2-phenyldiazene (Azo-C6), 1-(4-(decyloxy)phenyl)-2-phenyldiazene (Azo-C10), 1-(4-(tetradecyloxy)phenyl)-2-phenyldiazene (Azo-C14) and 1-(4-(octadecyloxy)phenyl)-2-phenyldiazene (Azo-C18); note that alkyl chloride (1-chlorohexane, 1-chlorodecane, 1-chlorotetradecane and 1-chlorooctadecane) was used instead of 6-chloro-1-hexanol. After dissolving 4-phenylazophenol (1.982 g, 0.010 mol) and potassium carbonate (1.382 g, 0.010 mol) in DMF (9 ml), potassium iodide (4.2 mg, 0.025 mmol) and the corresponding alkyl chloride (0.015 mol) were added to the solution. Synthesis was carried out over a period of 24 h at 110 °C. The reaction solution was poured into cold water, and the precipitate was filtered. The filtered compound was recrystallized in methanol (Azo-C6), n-hexane (Azo-C10) or acetone (Azo-C14 and Azo-C18). The recrystallized compound was filtered and dried at room temperature under vacuum.

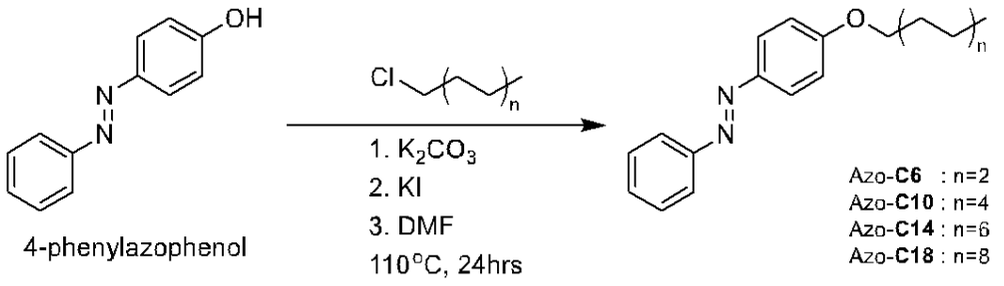

Figure 3-3. Synthesis of Azo-compounds.

서울대학교

2.3. Polymerization of the BA/Azo-acrylate Co-polymer (Azo-polymer)

After removing the inhibitor of BA using neutral aluminum oxide, BA (1.5 g, 0.012 mol) and Azo-acrylate (0.572 g, 1.3 mmol) were added to EA (5 mL). After stirring the mixture for 1 min at 70 °C to dissolve the Azo-acrylate powder, N2 gas was blown into the solution for 20 min at room temperature. AIBN (0.01 g) was added to the solution, and the solution was stirred at 70 °C for 1.5 h. Tetrahydrofuran (THF, 5 mL) was poured into the polymerized solution to prevent gelation caused by the interaction between the azobenzene moieties. The polymer solution was washed and dissolved with methanol and THF, respectively. The process was repeated thrice. The dissolved solution was poured on a silicone-release film and dried at 70 °C.

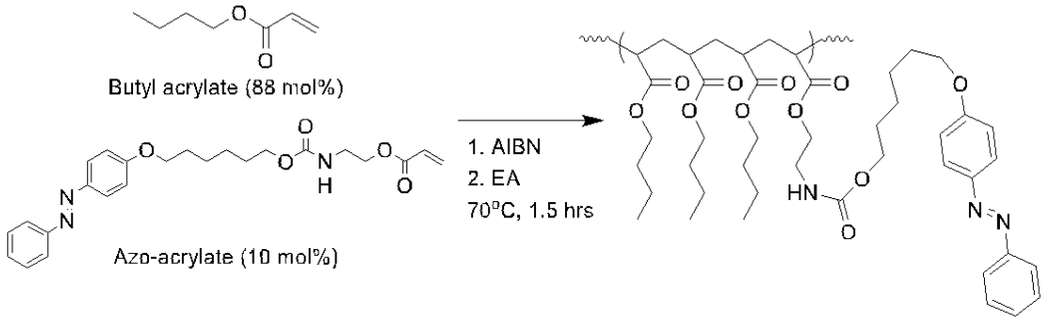

Figure 3-4. Polymerization of Azo-polymer.

2.4. Preparation of the Switchable PSA Specimens

After dissolving Azo-polymer in THF, 12 mol% of one of the four Azo-compounds was added to the polymer solution. The content of Azo-compound was calculated in consideration of the number of butyl acrylate and Azo-acrylate molecules in Azo-polymer. The Azo-compounds were dissolved in

서울대학교

their respective polymer solution using a vortex mixer. After using a 120 μm coating applicator to cast each mixture on a corona-treated polyethylene terephthalate (PET) film (50 μm), the films were dried at 100 °C for 20 min in a convection oven. After being cooled, the dried films were irradiated with UV light (365 nm LED lamp, 125 mW/cm^2, 30 s) and visible light (50 W white LED lamp, 30 s). The thicknesses of the switchable PSAs were 6–7 μm, as measured by using a digital micrometer (S-Mike_Pro, Sylvac). The lap shear test specimen was prepared using the same method, using a silicone-release PET film (50 μm) instead of the corona-treated PET film. According to the type of Azo-compound, the PSA samples were named SP-6, SP-10, SP-14 and SP-18 **(Table 3-1)**.

Table 3-1. Compositions of solution mixtures applied to cast the switchable PSAs.

	Azo polymer	THF	Azo-C6	Azo-C10	Azo-C14	Azo-C18
Azo polymer	0.1 g (88 mol% of butyl and azobenzene pendant groups)	1 ml	-	-	-	-
SP-C6			25.1 mg (12 mol%)	-	-	-
SP-C10			-	30.1 mg (12 mol%)	-	-
SP-C14			-	-	35.1 mg (12 mol%)	-
SP-C18			-	-	-	40.1 mg (12 mol%)

서울대학교 SEOUL NATIONAL UNIVERSITY

2.5. Characterization

2.5.1. Nuclear Magnetic Resonance (NMR) Spectroscopy

A 400 MHz NMR spectrometer (JNM-ECX400, JEOL) was used to record the 1H-NMR spectra. The operating temperature was room temperature, and tetramethylsilane ($\delta = 0$ ppm) was used as a reference to determine the chemical shift.

2.5.2. Adhesion Switchability Test

The adhesive forces of the switchable PSAs were evaluated by applying a probe tack test. The tack forces were measured by operating a texture analyzer (TA.XT plus, Stable Micro Systems) and a 500 N load cell at 25 °C (RH: 50 ± 10%). A cylindrical 5 mm-diameter stainless-steel probe was used. The UV and visible light irradiated specimens were measured after 10 s and 30 s for temperature stabilization. The probe was in contact with each PSA specimen for 1 s, applying a force of 100 g_f; the contact speed was 0.2 mm/s. After the probe was detached from the specimen at a speed of 10 mm/s, the maximum force was taken as the probe tack value. An average of five measurements was used for each specimen.

2.5.3. UV/Vis Spectroscopy

The azobenzene moiety photo-isomerization was monitored using a UV/Vis spectrometer (UV-1601PC, Shimadzu) to record the UV/Vis absorption spectrum; the scan range was 300–600 nm. The UV/Vis absorption of the 50

서울대학교 SEOUL NATIONAL UNIVERSITY

μm-thick corona-treated PET film was applied as the spectrum baseline to record the absorption spectrum of the switchable PSAs cast on the PET film.

2.5.4. Lap Shear Test

A lap shear test was conducted to measure the shear modulus of each switchable PSA. The PSA cast on the release film was transferred to a poly(methyl methacrylate) (PMMA) substrate with dimensions of 6 mm × 20 mm × 1 mm (width × length × thickness) after UV irradiation (125 mW/cm^2, 30 s). The adhesive area was 6 mm × 20 mm (width × length). After another PMMA substrate was attached, visible light was applied for 30 s. Two pieces of PMMA with dimensions of 6 mm × 6 mm × 1 mm were attached to each end of the substrate with an instant adhesive. The shear stress was measured using dynamic mechanical analysis (DMA, Q800, TA Instruments). The test was conducted in strain ramp mode at 25 °C; the test speed was 1%/s. This test was applied three times for each specimen; the average value was used.

2.5.5. Water Contact Angle Measurement

A drop-shape analyzer (DSA 100, KRÜSS) was used to measure the water contact angle of each PSA surface at 25 °C (RH: 50 ± 10%). The contact angle was measured 10 s after 5 μL of water droplets were dropped onto the surface. An average of five measurements was used for each specimen.

서울대학교

2.5.6. DSC Measurement

The T_g of the switchable PSAs and phase-transition temperatures of the Azo-compounds were measured by loading each PSA (2–3 mg) onto a sample pan (Tzero Pan, 901683.901, TA Instruments) and applying differential scanning calorimetry (DSC, Q200, TA Instruments). After being cooled to −50 °C at 30 °C/min, the temperature of each specimen was maintained for 2 min. The DSC curve was recorded as the specimen was heated to 50 °C at a rate of 5 °C/min. A photo-thermal DSC method was used to measure the T_g of each UV-irradiated switchable PSA. Although the cooling and heating rates were the same, each specimen was irradiated with UV light during the cooling and isothermal steps. The heating step was carried out under dark conditions. A spot UV curing system (S2000-XLA, OmniCure) with a 320–500 nm filter was used for UV irradiation. The UV intensity at the specimen surface was 75 mW/cm^2. The Azo-compounds (1–2 mg) were loaded onto the Tzero Pan. After each specimen was heated to 150 °C at 30 °C/min and subjected to a 3 min isothermal process, the data were recorded as it was cooled to 0 °C and heated to 200 °C at 10 °C/min.

서울대학교

3. Results and Discussion

3.1. Results of Synthesis and Polymerization

3.1.1. Synthesis of 6-(4-(Phenyldiazenyl)phenoxy)hexan-1-ol

The yield of the synthesis of 6-(4-(Phenyldiazenyl)phenoxy)hexan-1-ol was 51.9%. The chemical structure was defined by the ^{1}H-NMR spectrum. However, the NMR spectrum of the synthesized compound is omitted in this chapter.

3.1.2. Synthesis of Azo-acrylate

The yield of the synthesis of Azo-acrylate was 72.4%. The chemical structure was defined by the ^{1}H-NMR spectrum. The NMR spectrum of the synthesized compound is omitted in this chapter.

3.1.3. Synthesis of Azo-compounds

The synthesis yields of Azo-C6, Azo-C10, Azo-C14 and Azo-C18 were 50.3%, 56.7%, 75.6% and 64.3%, respectively. The chemical structures were defined by the ^{1}H-NMR spectra **(Figure 3-5, 3-6, 3-7 and 3-8)**. It was confirmed that the starting material, PAP, did not exist in the compound through the absence of a peak near 10 ppm corresponding to phenol of PAP. The analysis of the NMR spectrum is as follows.

서울대학교

Azo-C6 ^{1}H NMR (400 MHz, DMSO-d6, δ): 7.82 (m, 4H, Ar H), 7.52 (m, 3H, Ar H), 7.08 (m, 2H, Ar H), 4.02 (t, 2H, OCH_2), 1.70 (m, 2H, $OCH_2\underline{CH_2}$), 1.40 (m, 2H, $OCH_2CH_2\underline{CH_2}$), 1.26 (m, 4H, $OCH_2CH_2CH_2\underline{CH_2CH_2}$), 0.84 (m, 3H, $OCH_2CH_2CH_2CH_2CH_2\underline{CH_3}$)

Azo-C10 ^{1}H NMR (400 MHz, DMSO-d6, δ): 7.89 (m, 4H, Ar H), 7.46 (m, 3H, Ar H), 7.00 (m, 2H, Ar H), 4.03 (t, 2H, OCH_2), 1.81 (m, 2H, $OCH_2\underline{CH_2}$), 1.47 (m, 2H, $OCH_2CH_2\underline{CH_2}$), 1.30 (m, 12H, $OCH_2CH_2CH_2\underline{(CH_2)_6}$), 0.88 (m, 3H, $OCH_2CH_2CH_2(CH_2)_6\underline{CH_3}$)

Azo-C14 ^{1}H NMR (400 MHz, Chloroform-d, δ): 7.89 (m, 4H, Ar H), 7.46 (m, 3H, Ar H), 7.00 (m, 2H, Ar H), 4.03 (t, 2H, OCH_2), 1.81 (m, 2H, $OCH_2\underline{CH_2}$), 1.47 (m, 2H, $OCH_2CH_2\underline{CH_2}$), 1.30 (m, 20H, $OCH_2CH_2CH_2\underline{(CH_2)_{10}}$), 0.88 (m, 3H, $OCH_2CH_2CH_2(CH_2)_{10}\underline{CH_3}$)

Azo-C18 ^{1}H NMR (400 MHz, Chloroform-d, δ): 7.89 (m, 4H, Ar H), 7.46 (m, 3H, Ar H), 7.00 (m, 2H, Ar H), 4.03 (t, 2H, OCH_2), 1.82 (m, 2H, $OCH_2\underline{CH_2}$), 1.47 (m, 2H, $OCH_2CH_2\underline{CH_2}$), 1.30 (m, 28H, $OCH_2CH_2CH_2\underline{(CH_2)_{14}}$), 0.88 (m, 3H, $OCH_2CH_2CH_2(CH_2)_{14}\underline{CH_3}$)

서울대학교 SEOUL NATIONAL UNIVERSITY

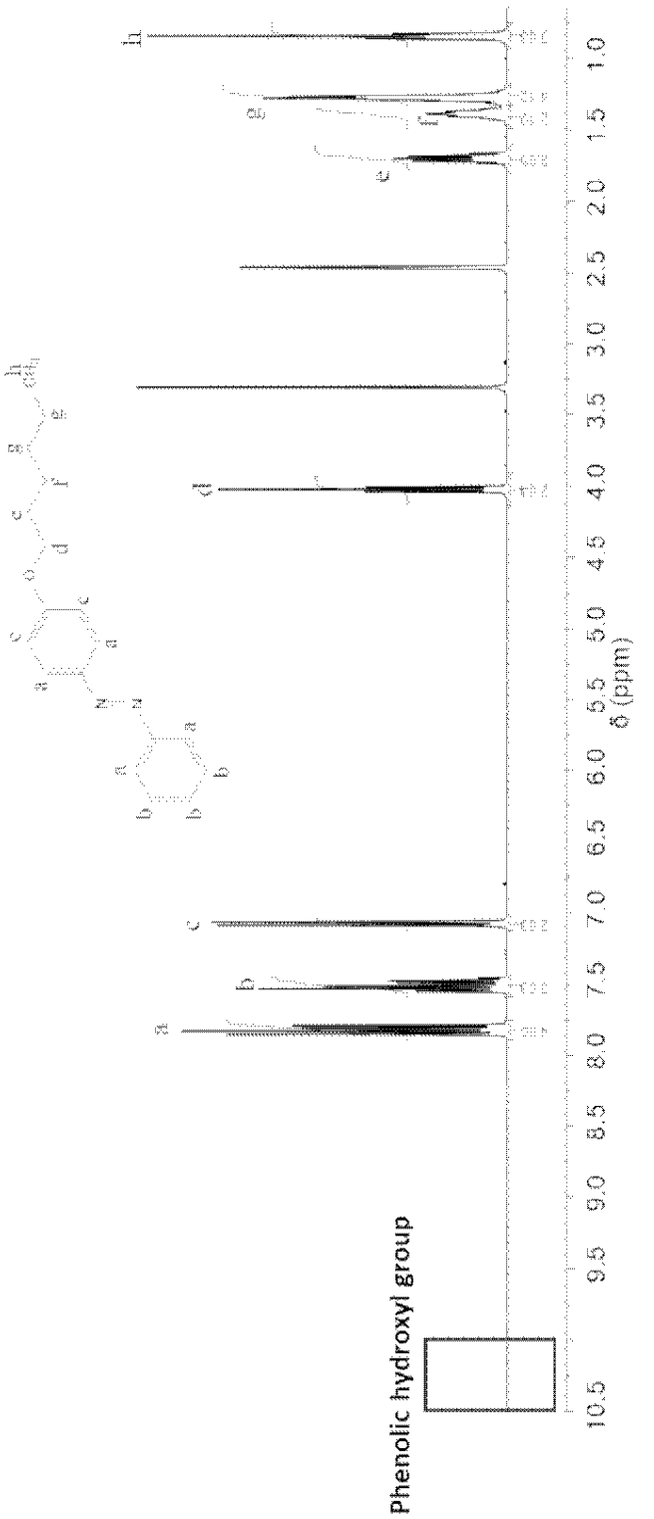

Figure 3-5. ^{1}H-NMR spectrum of Azo-C6.

세한대학교

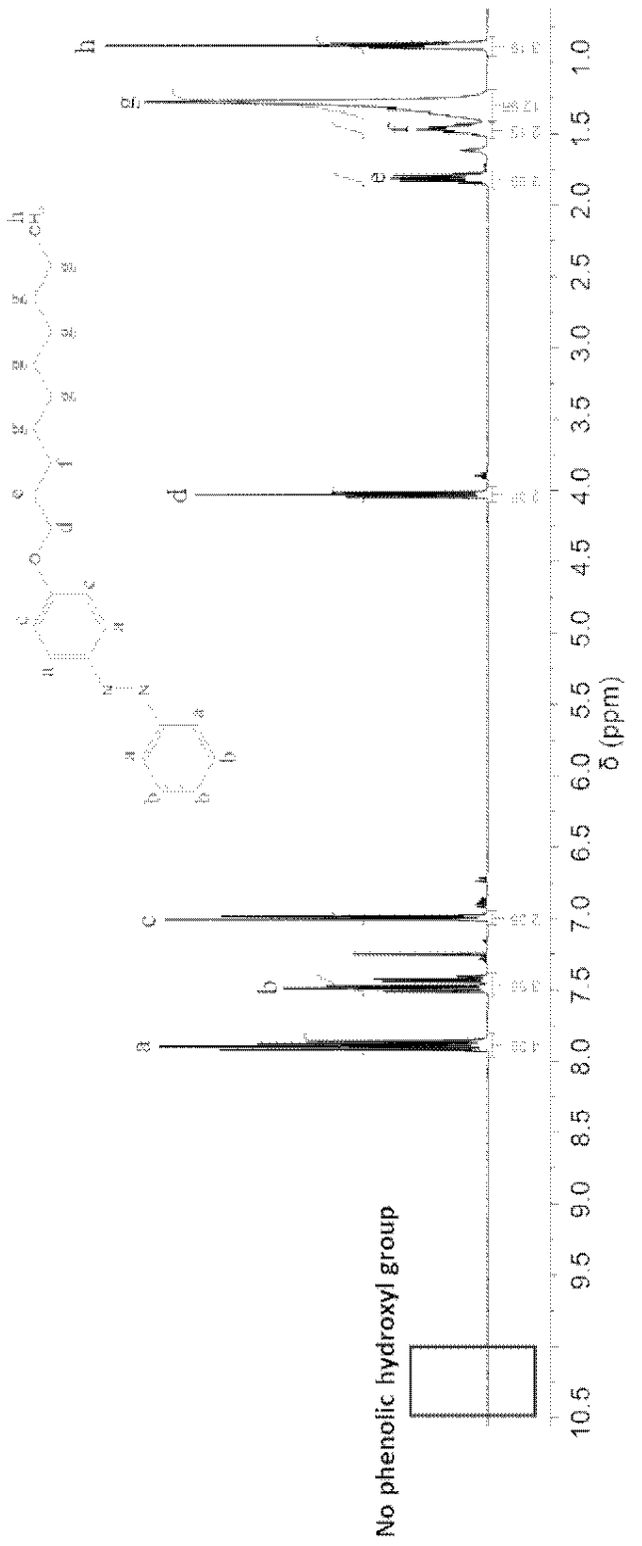

Figure 3-6. ^{1}H-NMR spectrum of Azo-C10.

서울대학교
Seoul National University

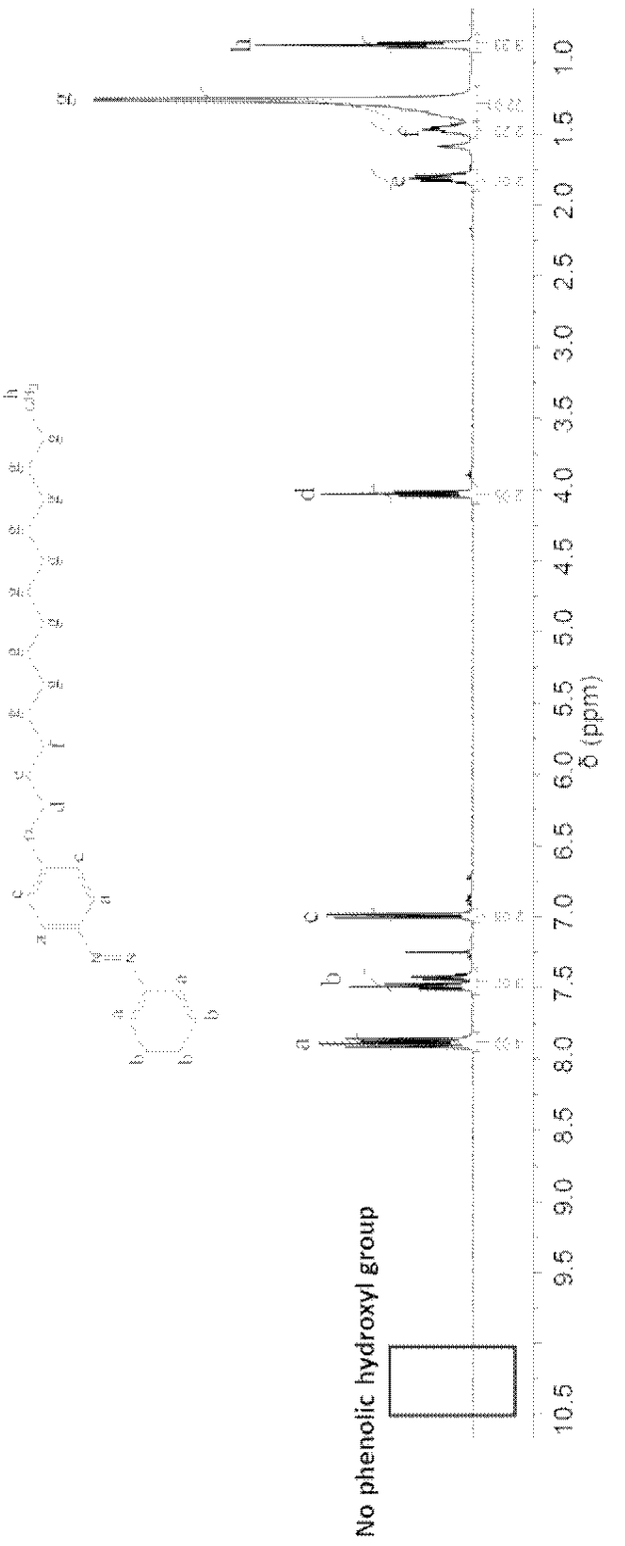

Figure 3-7. ^{1}H-NMR spectrum of Azo-C14.

서울대학교

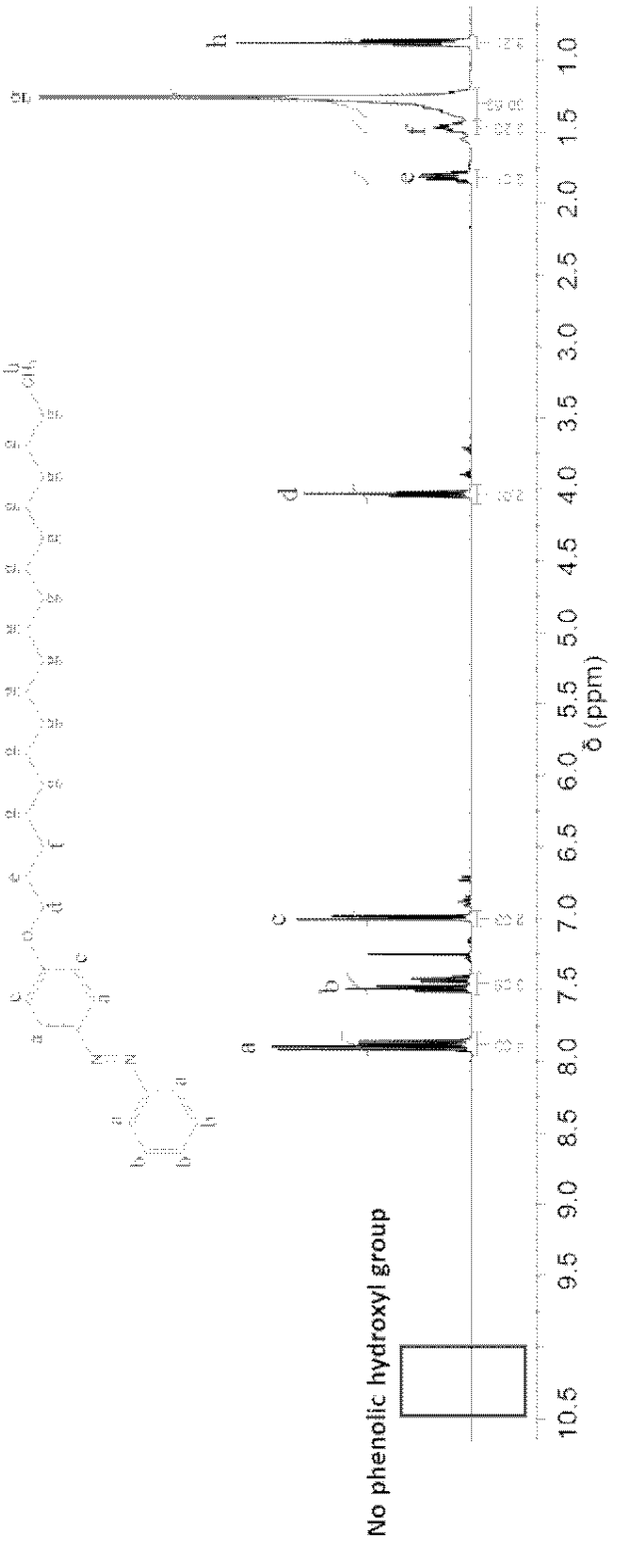

Figure 3-8. ^{1}H-NMR spectrum of Azo-C18.

서울대학교

3.1.4. Polymerization of Azo-polymer

Unreacted BA and Azo-acrylate in polymerized Azo-polymer solution were removed by washing with methanol and THF. The removal of unreacted monomers was confirmed through the absence of acrylate's double bond at 5.5-6.5 ppm of the NMR spectrum.

The ratio of Azo-acrylate monomer included in the polymerized chains among 10 mol% of azo-acrylate added for polymerization was calculated through the NMR spectrum, and the equation is as follows:

$$C_{azo} = \frac{I_{7.89ppm}/4}{I_{0.88ppm}/3 + I_{7.89ppm}/4}$$

where C_{azo} denotes the content of Azo-acrylate in washed Azo-polymer, $I_{7.89ppm}$ denotes the intensity of peak at 7.89 ppm corresponding to the azobenzene side chain, and $I_{0.88ppm}$ denotes the intensity of peak at 0.88 ppm corresponding to CH_3 of the butyl side chain. The calculated C_{azo} was 8 mol%.

The M_n, M_w and PDI of Azo-polymer measured with gel permeation chromatography (GPC) were 42,000, 147,000 and 3.5, respectively.

서울대학교 SEOUL NATIONAL UNIVERSITY

3.2. Adhesion Switching Characteristics of Switchable PSAs

Probe tack tests were applied to evaluate the adhesion switching characteristics of the switchable PSAs. Because the intermolecular interaction and arrangement are dependent on the chain length, the influence of the compound hydrocarbon chain length on the switching characteristics was evaluated by measuring the tack value variation according to UV intensity. The UV irradiation time was 30 s. After applying the probe tack test to each UV-irradiated specimen, all specimens were irradiated with visible light to "switch off" the adhesive force; then, the adhesive force was measured again to evaluate whether reversible switching was possible **(Figure 3-9a)**. In **Figure 3-9b**, the results of the "switched off" adhesive forces were omitted to highlight the trend with respect to UV intensity.

The Azo-polymer, which had a 2.2 N tack value before UV irradiation, exhibited no change in adhesion, even when the UV intensity was increased. Specifically, there was no change in the adhesion or switching characteristics even when Azo-C6 was added (SP-C6). The adhesive forces of Azo-polymer and SP-6 were maintained even when under visible light irradiation **(Figure 3-9a)**. Alternatively, when an Azo-compound had more than 10 of hydrocarbon chain length, an initial adhesive force was not detected before UV irradiation. In the case of SP-10, weak adhesion was detected when 12 mW/cm^2 of UV radiation was applied; the strength of the adhesion began to increase at 25 mW/cm^2 rapidly. The tack force gradually increased at UV intensities above 25 mW/cm^2 but tended to begin saturating at 100 mW/cm^2. The tack force increased to 4.4 N under the UV radiation condition of 125 mW/cm^2. Additionally, longer hydrocarbon chains of the Azo-compound necessitated stronger UV intensities for adhesion. The adhesive forces of SP-C14 and SP-C18 sharply increased at 50 and 100 mW/cm^2, respectively **(Figure 3-9b)**. The

서울대학교

tack value also decreased as the length of the hydrocarbon chain increased. The adhesive forces of SP-C10, SP-C14 and SP-C18 sharply declined in response to visible light irradiation **(Figure 3-9a)**.

Thus, adhesion switching was possible when the Azo-compound had more than 10 of hydrocarbon chain length. Furthermore, as the hydrocarbon chain length increased, the UV intensity required for adhesion switching increased, and the adhesive force decreased. Reversible adhesion switching was possible for SP-10, SP-14 and SP-18. Note that the 30-cycle adhesion switching repetition test for SP-C10, which had the highest tack force, confirmed no decrease in the adhesive force **(Figure 3-10)**.

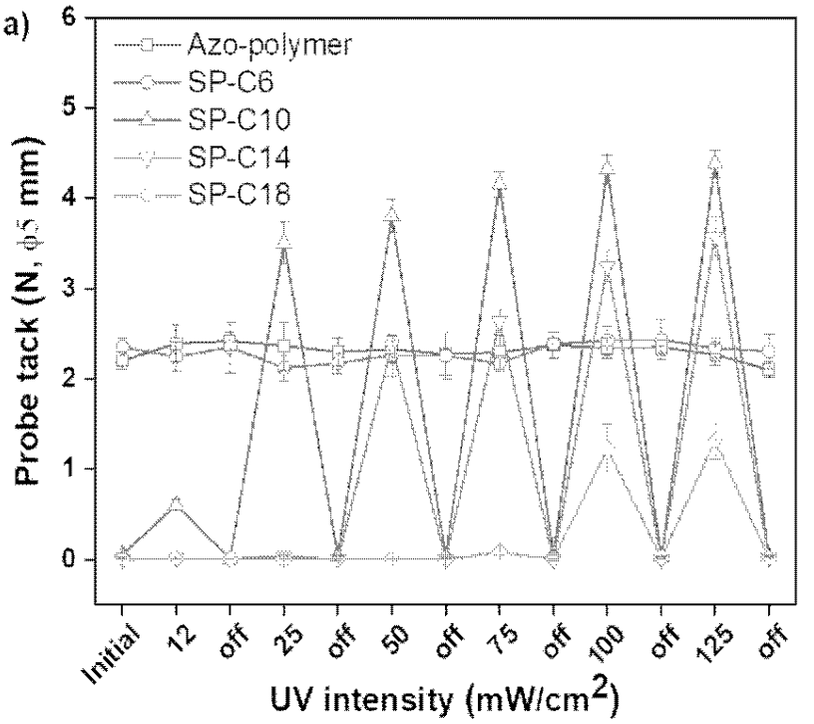

Figure 3-9a. Probe tack force of the switchable PSAs as a function of UV irradiation intensity, including "switched off" adhesive force of the PSAs.

서울대학교

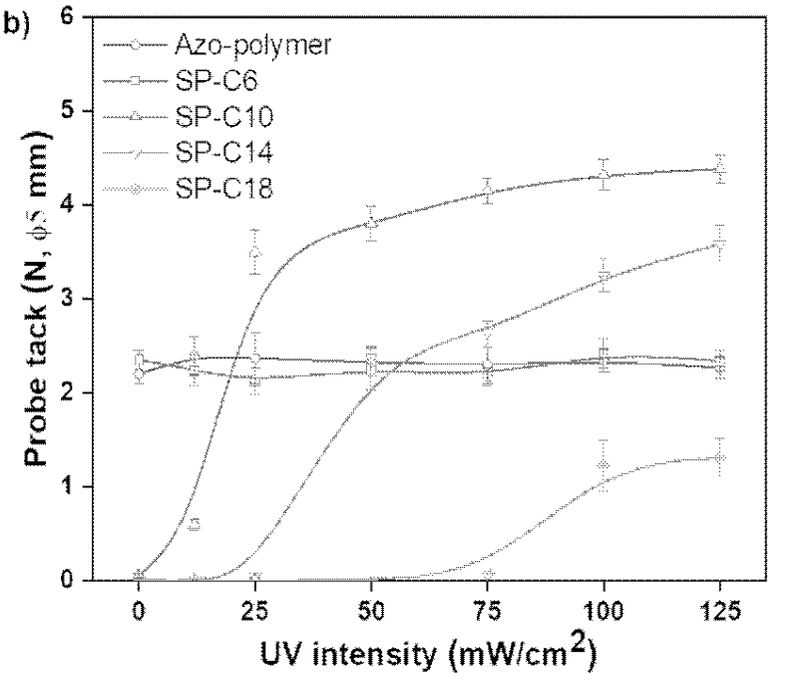

Figure 3-9b. Probe tack force of the switchable PSAs as a function of UV irradiation intensity.

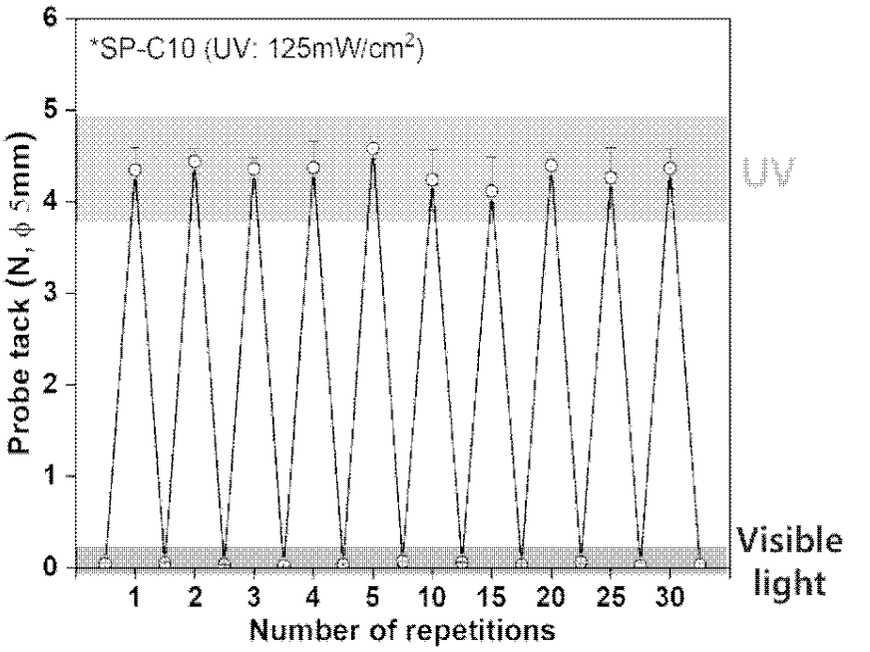

Figure 3-10. 30-cycle adhesion switching test results for SP-C10 (UV irradiation time: 30 s).

서울대학교

As mentioned, adhesion was enabled by wetting the adhesive on the substrate. Although the wetting of an ideal solid with a low-viscosity liquid can be simply explained by surface energy, complex factors must be considered to determine the wetting of a viscoelastic material. In particular, the modulus is the main factor in determining the wetting of viscoelastic material (Donatas, 1999). The modulus limits its wetting, and materials with a high modulus have poor wettability.

After adhesion was initially established by wetting, the response of a PSA to various external forces that try to separate it is expressed as an adhesive force. The equation for the probe tack force F is as follows:

$$F = \sqrt{2\pi^2 K\gamma a^4/t}, \quad (1)$$

where K is the bulk modulus, γ is the interfacial surface energy, a is the radius of the probe, and t is the thickness of the adhesive (Kendall, 1971). According to equations (1), the surface energy and modulus affect the adhesive properties of PSAs. In contrast to wettability, an increase of the modulus in the adhesion-formed state increases probe tack force. Thus, we monitored the photo-isomerization of the azobenzene moiety in each switchable PSA under various UV radiation conditions and evaluated the photo-isomerization-induced changes in each PSA's modulus and surface energy.

서울대학교

3.3. Photo-isomerization of Azobenzene Moiety

Because any change in adhesive force in response to UV or visible light irradiation was expected to be related to the photo-isomerization occurring between the trans- and cis-forms of the azobenzene moiety, the isomerization was measured at different UV intensities by using a UV/Vis spectrometer. The photo-isomerization of the azobenzene moiety was monitored by focusing on the $\pi \rightarrow \pi^*$ and $n \rightarrow \pi^*$ absorption bands. Stable trans-azobenzene tended to have a $\pi \rightarrow \pi^*$ absorption band near 360 nm, whereas the cis-form had a lower-energy absorption band ($n \rightarrow \pi^*$) near 450 nm (Ladanyi, *et al.*, 2017).

Figure 3-11 shows the UV/Vis spectra of the switchable PSAs according to UV intensity. The UV irradiation time was 30 s as in the probe tack test. The photo-isomerization process was quantified based on the absorbance near 360 nm, the primary absorption band of trans-azobenzene. However, as shown in **Figure 3-11**, the 360 nm absorbance of the switchable PSAs was out of the measurement range. In order to obtain a trans-azobenzene absorption band that is within the measurable range, it is necessary to measure much thinner switchable PSAs. However, because more light intensity is attenuated through thicker materials according to the Beer-Lambert law, the photo-isomerization process may be carried out differently for relatively thinner switchable PSAs. Thus, we obtained the UV/Vis spectra of the PSA films with the same thickness as applied in the probe tack test and monitored the photo-isomerization trend by focusing on the $n \rightarrow \pi^*$ absorption band near 450 nm.

In the case of Azo-polymer, isomerization of the azobenzene pendants in the polymer chain was observed. Regarding the isomerization results for the trans- to cis-form, absorption near 450 nm and 360 nm increased and decreased, respectively. The changes in both absorption bands revealed saturation at 25 mW/cm^2. It means that most azobenzene groups in Azo-polymer were

서울대학교 SEOUL NATIONAL UNIVERSITY

isomerized at 25 mW/cm^2. The degree of SP-C6 isomerization increased gradually at 12 and 25 mW/cm^2; it was saturated at 50 mW/cm^2. The UV intensity associated with isomerization saturation in the switchable PSAs increased with the increasing length of the Azo-compound hydrocarbon chain. In the case of SP-C18, the degree of photo-isomerization gradually increased up until a UV intensity of 100 mW/cm^2; additionally, under 125 mW/cm^2 UV radiation conditions, the absorbance near 450 nm was lower than that in the cases of the other switchable PSAs. More energy was required for photo-isomerization of the azobenzene as the aliphatic chain length increased. Although photo-isomerization of the azobenzene group was observed in all specimens, the adhesion switching was possible only in SP-C10, SP-C14 and SP-C18. It could be defined through the evaluation of chemical and mechanical characteristics.

서울대학교

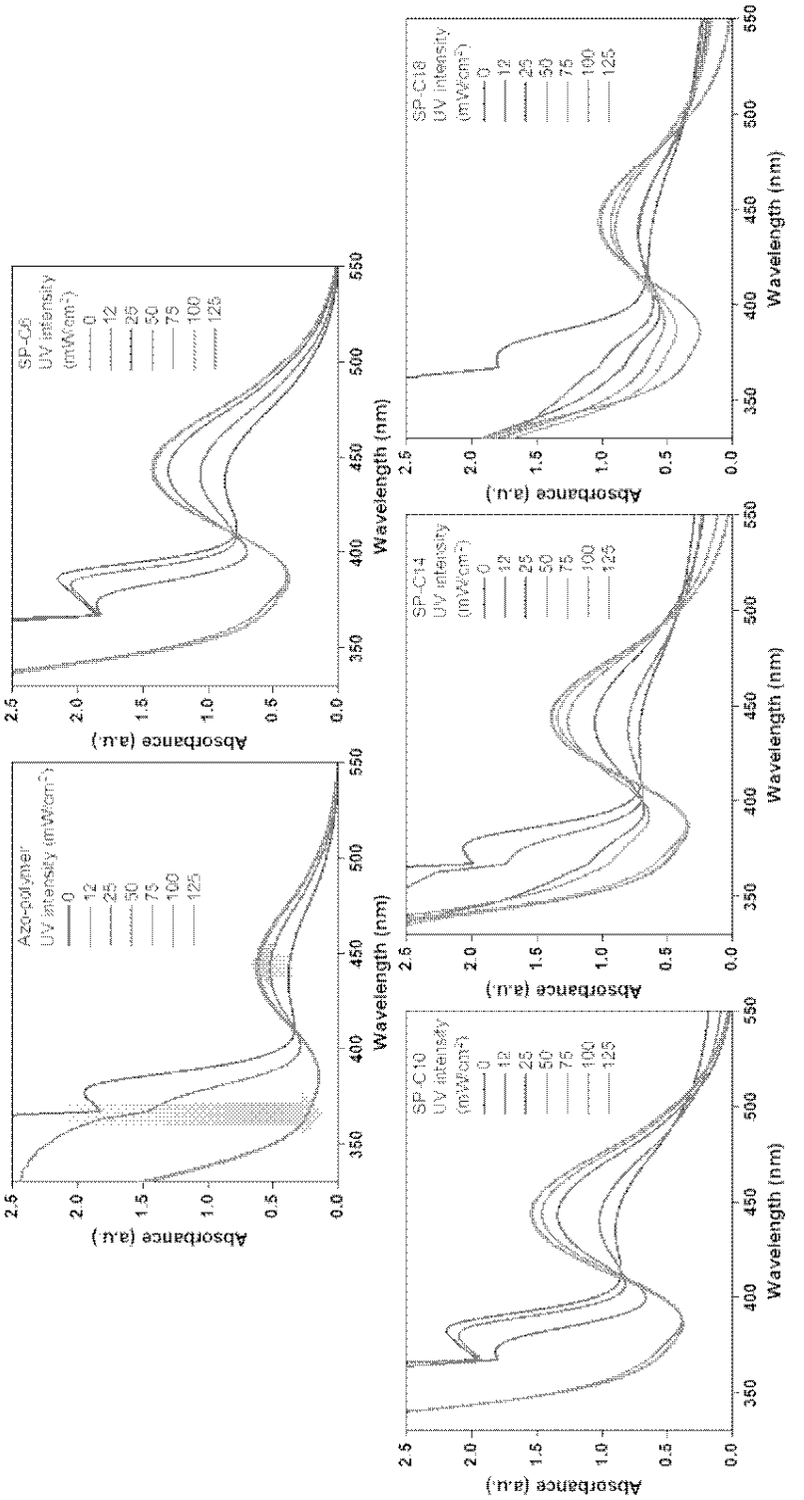

Figure 3-11. UV/Vis spectra of the switchable PSAs according to UV intensity (UV irradiation time: 30 s).

서울대학교

3.4. UV light-induced Changes in T_g, Shear Modulus and Water Contact Angle of the Switchable PSAs

3.4.1. T_g Measurement with DSC

As mentioned in the Introduction, a PSA must have a low T_g to have adhesive properties at the service temperature. Thus, the T_g values for the pre- and post-UV-irradiated switchable PSAs were measured using DSC **(Figure 3-12)**. UV irradiation shifted the initial T_g of Azo-polymer from −10.2 °C to −16.3 °C. It was considered that the interaction between the trans-azobenzene pendant groups was weakened as they were isomerized into the cis form because the size and flexibility of polymer side groups are factors that determine T_g (Jenekhe, *et al.*, 1993). When the azobenzene pendant groups existed in the trans-state, there were interactions between the pendants groups due to their planar structure and the π-π interaction. The interactions limit the mobility of the side groups. Alternatively, when they were isomerized to cis-form, the interactions were reduced due to their bent structure; the T_g could be shifted to a lower temperature.

For SP-C6, the initial-state T_g was −16.0 °C, which was lower than the initial T_g of Azo-polymer. Azo-C6 was expected to disperse between the polymer chains and act as a plasticizer. The Azo-polymer and SP-C6, which did not have adhesion switchability, had the initial-state T_g; this was not clearly detectable in the DSC curves for SP-C10 and SP-C14, although there was a slight slope transition in the DSC curves of SP-C10 and SP-C14. However, under UV irradiation, SP-C10 and SP-C14 were measured to have clear T_g transitions of −15.6 °C and −15.5 °C, respectively. The manifestation of T_g by UV radiation constitutes one of the reasons that the adhesive forces of SP-C10 and SP-C14 were "switched on". Under DSC measurement, the transition in the heat flow

서울대학교

curve slope is detected at a specific temperature range by a segmental movement of a polymer molecule. It is defined as T_g. Thus, the phenomenon that clearly distinguished T_g became non-detectable by external stimuli signified that the molecular mobility of the switchable PSA became constrained. The SP-C18 had a non-sticky surface in the initial state. However, it had a relatively clear T_g than those of SP-C10 and SP-C14 even before UV radiation in the DSC curve. The initial-state T_g of SP-C18 (−14.6 °C), which was between those of Azo-polymer (-10.2 °C) and SP-C6 (-16.0 °C), and a small magnitude of gradient change in the DSC curve were results of the partial incompatibility between SP-C18 and Azo-polymer.

서울대학교

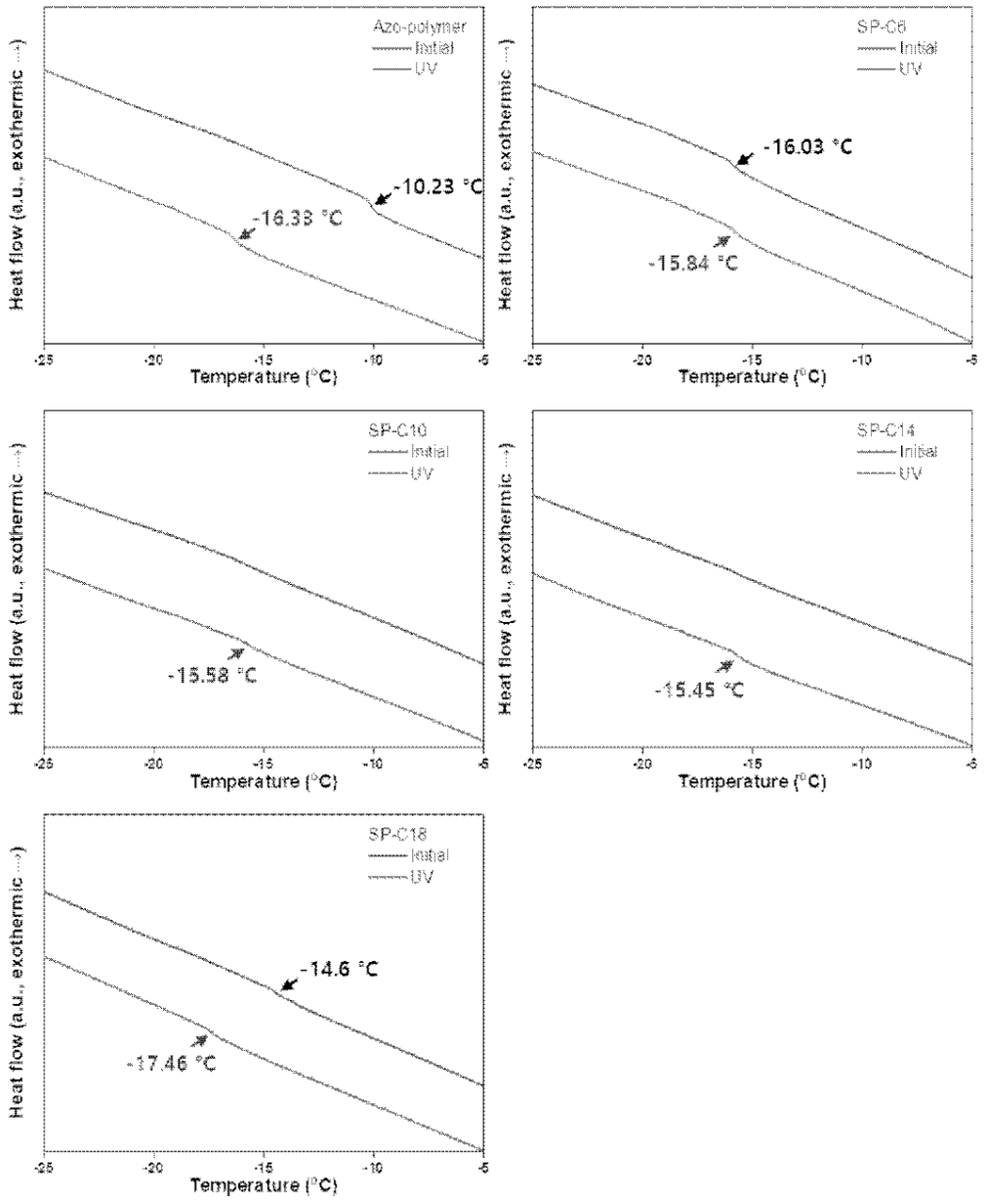

Figure 3-12. Pre- and post-UV exposure DSC curves for the switchable PSAs.

서울대학교
SEOUL NATIONAL UNIVERSITY

3.4.2. Shear Modulus

Figure 3-13 shows the lap shear test results for the switchable PSAs. The Azo-polymer and SP-C6 had low moduli within the 10–20 kPa range, even before UV exposure. The lower shear modulus of SP-C6 compared to that of Azo-polymer is attributable to the plasticizing effect of Azo-C6, as indicated by the DSC results. The pre-UV-exposure shear moduli of SP-C10, SP-C14 and SP-C18 were 79, 112 and 106 kPa, respectively, which were much higher than those of Azo-polymer and SP-C6. As the hydrocarbon chain length of the Azo-compound increased, the modulus tended to increase; however, the modulus of SP-18 is thought to have been lower than that of SP-14 because of the lower compatibility between Azo-C18 and Azo-polymer. In the cases of the specimens that exhibited adhesion switching characteristics, i.e., SP-C10, SP-C14 and SP-C18, the shear modulus decreased as the UV intensity increased. In particular, there was an intensity range in which the modulus rapidly decreased (0–25 mW/cm^2 for SP-C10, 25–50 mW/cm^2 for SP-C14 and 25–75 mW/cm^2 for SP-C18); this range coincided with the range in which the tack forces and absorbance of the cis-azobenzene moiety rapidly increased. SP-C10 and SP-C14 had shear moduli below 10 kPa after UV irradiation at 125 mW/cm^2. Alternatively, SP-C18, which had a narrow adhesion modulation range, had a relatively high shear modulus (25 kPa) even after UV irradiation at 125 mW/cm^2.

서울대학교 SEOUL NATIONAL UNIVERSITY

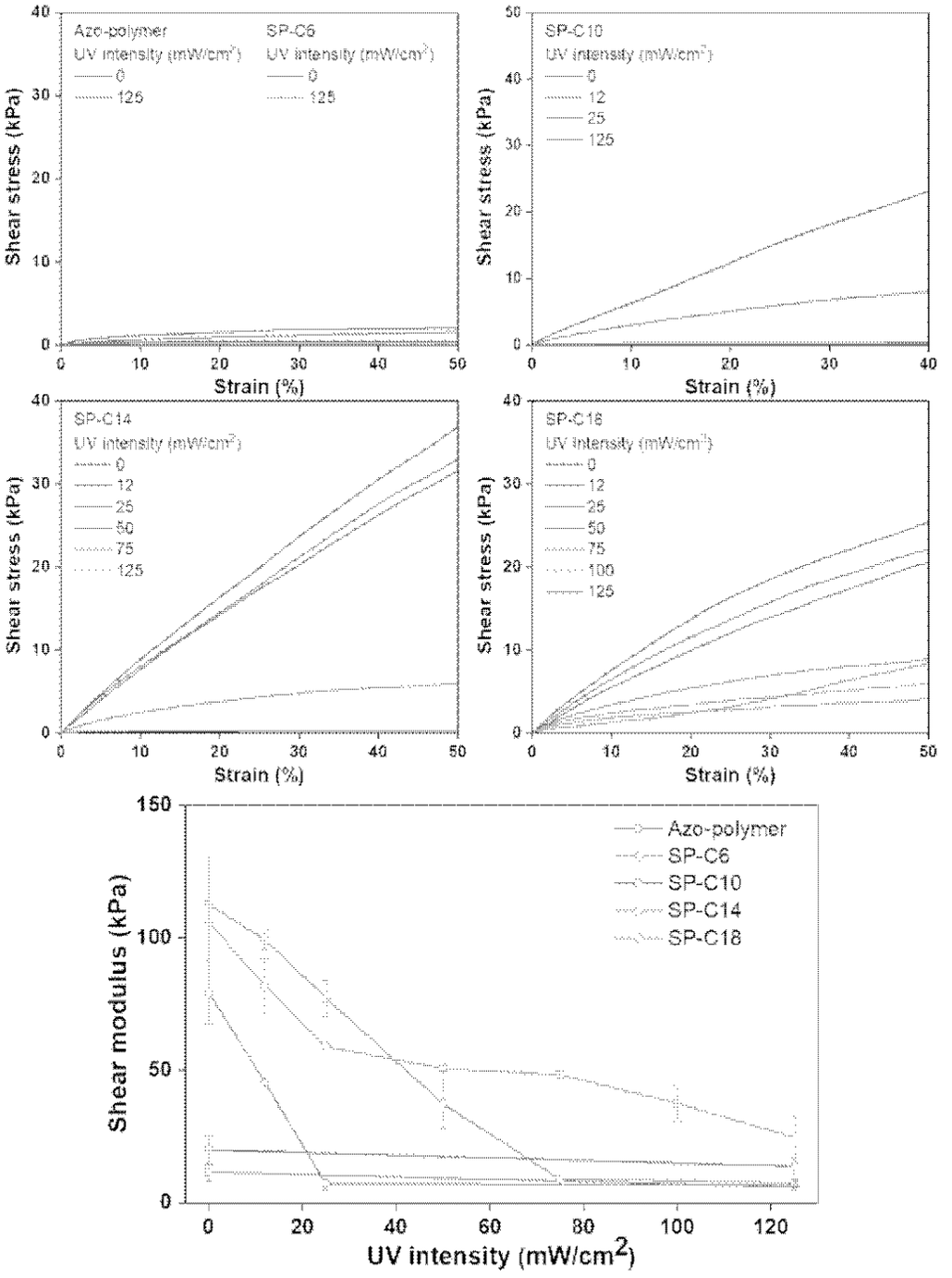

Figure 3-13. Stress-strain curves and shear modulus results for the switchable PSAs according to UV intensity.

서울대학교

3.4.3. Water Contact Angle

The chemical characteristics of the switchable PSAs were evaluated in terms of their water contact angles. The contact angles of Azo-polymer and SP-C6 were 93–94°; they were maintained even under the conditions of UV and visible light exposure **(Figure 3-14)**. The initial contact angles of SP-C10, SP-C14 and SP-C18 increased to 101.4°, 105.5° and 105.9°, respectively. In general, an increase in the water contact angle means a decrease in surface energy. The contact angles of SP-C10 and SP-C14 decreased to 93° after UV irradiation (125 mW/cm^2); this value was similar to those for Azo-polymer and SP-6. The results of measuring the contact angles of SP-C10, SP-C14 and SP-C18 according to the UV intensity revealed that the contact angles for each switchable PSA decreased within a specific intensity range in a way that was similar to the shear modulus results (0–25 mW/cm^2 for SP-C10, 25–50 mW/cm^2 for SP-C14 and 50–100 mW/cm^2 for SP-C18, **Figure 3-15**).

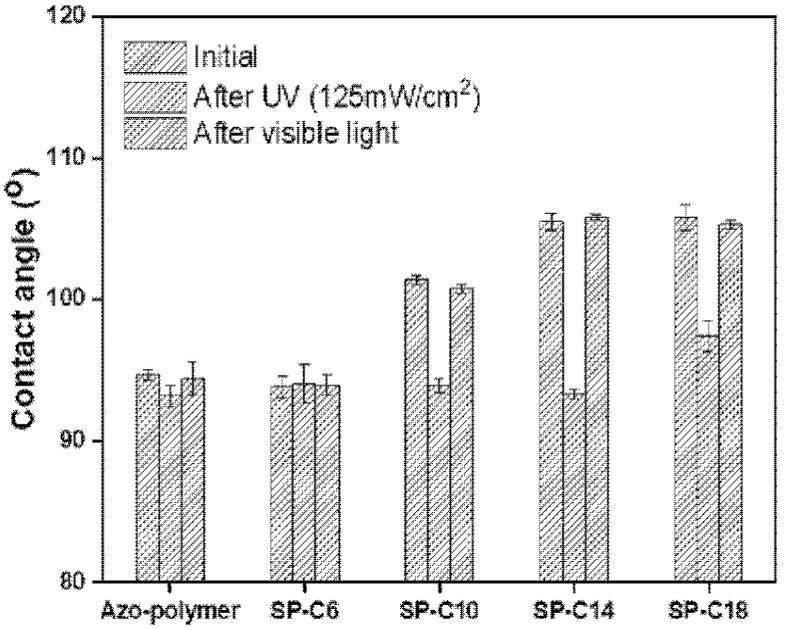

Figure 3-14. Transition in water contact angle of the switchable PSAs.

서울대학교

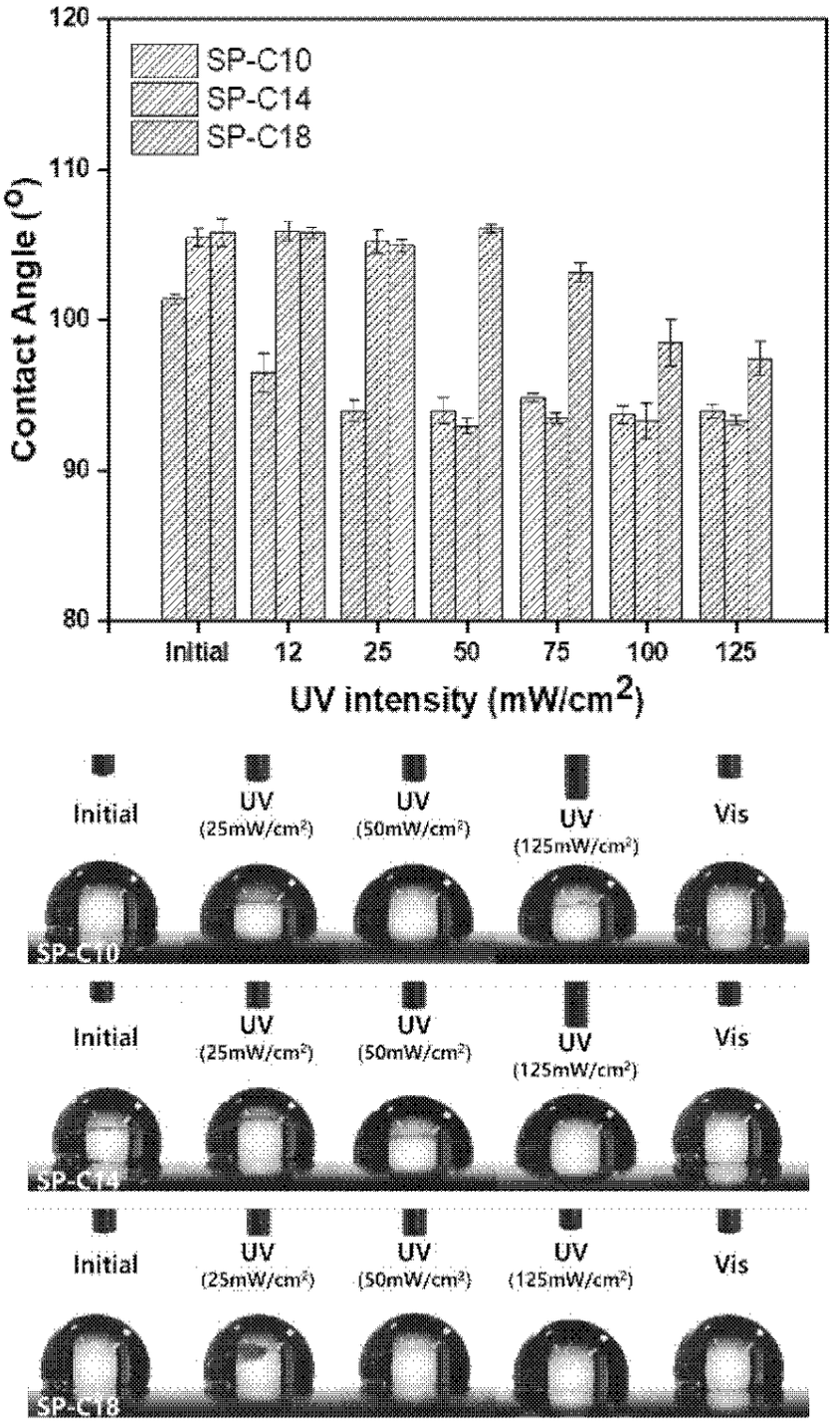

Figure 3-15. Changes in water contact angle of the switchable PSAs according to UV irradiation intensities.

서울대학교

In the cases of the PSAs that were found to be capable of adhesion switching (i.e., SP-C10, SP-C14 and SP-C18), the changes in T_g, shear modulus and contact angle were confirmed to have been induced as a result of the UV exposure. The deactivation of the adhesive force in the initial and visible light-irradiated states of the switchable PSAs was attributable to the non-detectable T_g, an increase in the shear modulus and a decrease in surface energy. A decrease in surface energy can decrease the adhesive force in both cases of wetting and equation (1). However, the visible light-irradiated switchable PSA shear modulus values were 4–6 times larger than that of Azo-polymer; this higher modulus resulted in less wetting, which is considered to be the main cause of adhesion deactivation. The non-detectable T_g in the DSC curves also verified that the molecular mobility of the PSA was restricted and insufficient to form wetting on the substrate. Alternatively, when UV irradiation was applied to the switchable PSAs, the photo-isomerization of the azobenzene moiety from the trans- to cis-form induced clear T_g transition and caused the modulus to decrease, and surface energy to increase. These complex changes led to the activation/deactivation of the adhesive forces of the switchable PSAs.

서울대학교

3.5. Transition in the Crystalline Structures of the Switchable PSAs

Changes in the crystalline structure are believed to be the primary reason for the changes in the T_g, modulus and surface energy that occurred during photo-isomerization of the azobenzene moiety in the switchable PSAs (Lee, *et al.*, 2021). As shown in **Figure 3-16**, Azo-polymer and SP-C6 were transparent in the initial state and maintained transparency under the condition of UV exposure. However, the "switched off" SP-10, SP-14 and SP-18 were opaque before UV irradiation. SP-C10 became transparent under low intensity (12–25 mW/cm^2) of UV radiation. SP-C14 became transparent at UV intensities above 50 mW/cm^2, whereas SP-C18 appeared to be partially transparent at 100 mW/cm^2 and was still not completely transparent at 125 mW/cm^2. The UV intensity ranges in which the film transparency changed were the same as those in which the adhesion, trans-to-cis photo-isomerization, shear modulus and contact angle of each PSA were rapidly changed. Because Azo-polymer was amorphous, it was transparent. The opaqueness of the amorphous Azo-polymer-containing switchable PSAs was attributable to the crystalline structure of each Azo-compound. When Azo-compounds form crystalline structures, light scattering and refraction occur by the crystalline structure. Therefore, the specimens appeared opaque.

In order to confirm the transparency change of the film quantitatively, the visible region transmittance spectra of the switchable PSAs according to UV irradiation intensity are shown in **Figure 3-17**. The low transmittance of 400–550 nm is due to n → π* absorption of the azobenzene groups. Therefore, the transparency of film specimens can be monitored through transmittance in wavelengths longer than 550 nm. **Figure 3-17** shows that Azo-polymer and SP-C6 had 100% transmittance regardless of UV irradiation. However, SP-10, 14 and 18 had low transmittance in the initial state, and in particular, the

서울대학교 SEOUL NATIONAL UNIVERSITY

transmittance of SP-C14 was the lowest at 55%. As previously described, SP-C10 became fully transparent with only 25 mW/cm^2 of UV intensity; SP-C14 and SP-C18 had 100% of transmittance over 75 and 100 mW/cm^2, respectively.

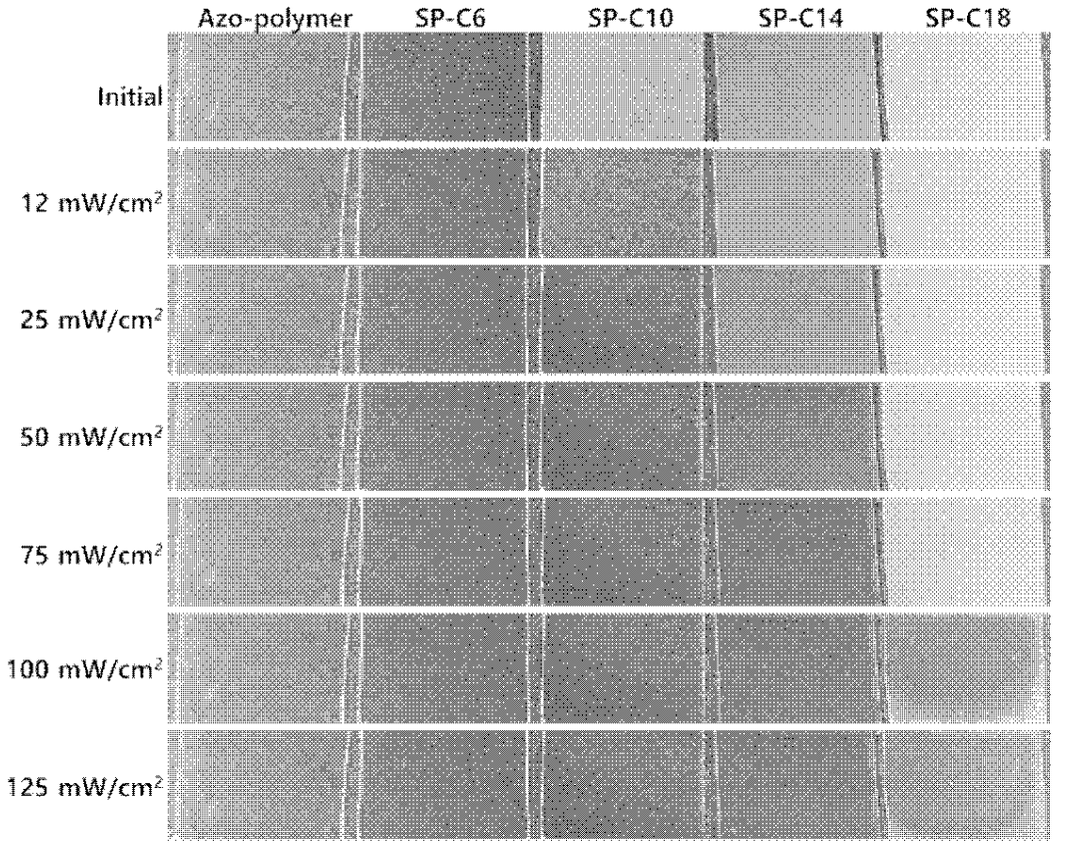

Figure 3-16. Transition in the transparency of the switchable PSAs according to UV intensity.

서울대학교

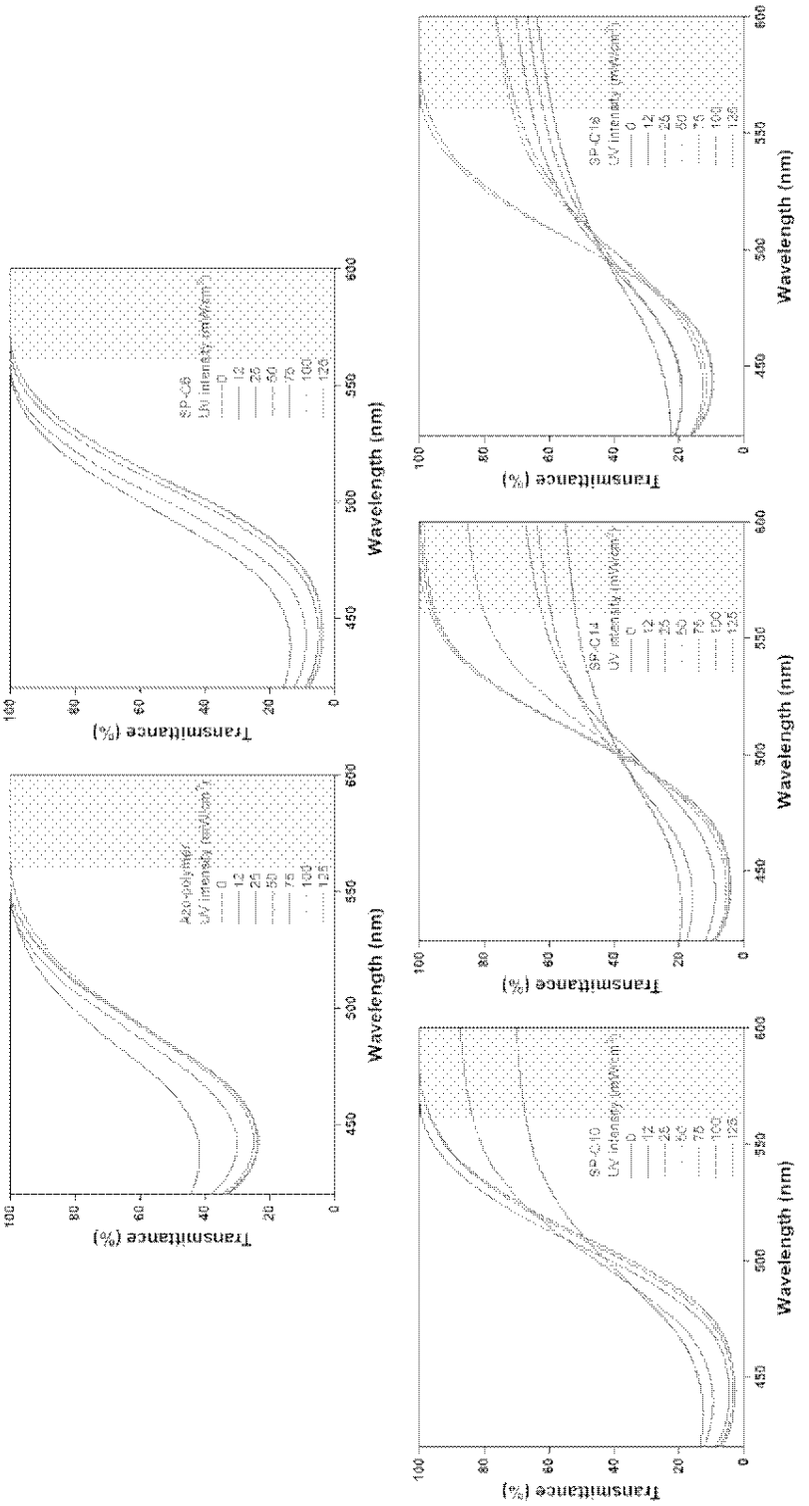

Figure 3-17. Transmittance in a visible wavelength range of the switchable PSAs according to UV intensity.

서울대학교

3.6. Reason for Difference in Photo-isomerization Efficiency according to Hydrocarbon Chain Length of Azo-compounds

From all data, it was obtained that the different UV intensity was required for transition in physical and chemical properties according to the chain length of the hydrocarbon substituent of Azo-compounds. The changes in properties were due to the transition in crystalline structure by photo-isomerization of the azobenzene groups. In other words, the photo-isomerization efficiency of azobenzene moiety changed according to the chemical structure changes in Azo-compounds. As shown in the UV/Vis absorption spectra in **Figure 3-11**, SP-C18, which has the longest chain, required twice as much UV energy as the shortest SP-C6 for full trans-to-cis photo-isomerization. The change in the photo-isomerization efficiency of azobenzene is due to the chemical factor by its substituent (Gegiou, *et al.*, 1968) or the physical factor of the surrounding matrix (Gegiou, *et al.*, 1968).

3.6.1. Difference in Photo-isomerization Efficiency by Chemical Factor

The photo-isomerization between trans- and cis-azobenzene is occurred with the excitation of electrons by light stimuli. The absorption wavelength and isomerization efficiency can be determined by the energy gap between the stable and the excited state for isomerization. A more specific energy state pathway for isomerization of azobenzene is shown in **Figure 3-18** (Brzozowski, *et al.*, 2001). The azobenzene is in the lowest singlet state S_0 of the trans-form in the absence of UV light. When it absorbs UV light, the azobenzene molecule is converted to an excited singlet state S_1. The molecule in the S_1 state undergoes a transition to triplet state T_1, which has a lower energy level, and

서울대학교

the molecule in the T_1 state return to the S_0 or moves to the T_1' state, which is a triplet state of the cis-azobenzene. The molecule in the T_1' state is finally stabilized in the S_0' of the cis-form. The cis-to-trans isomerization occurs in the opposite pathway or direct transition from the S_0' to S_0 by thermal relaxation without external stimulation.

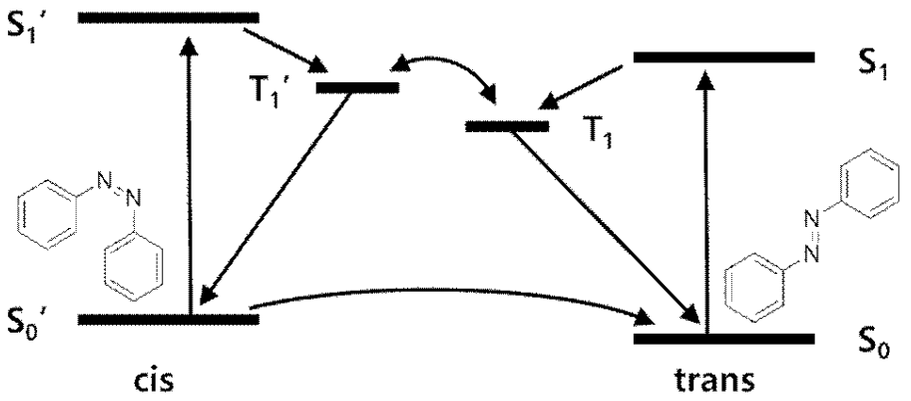

Figure 3-18. Energy state pathway for isomerization of azobenzene (Brzozowski and Sargent, 2001).

The chemical structure determines the energy gap between each energy level. In particular, in azobenzene, substituents' number, type and position determine the energy level (Dokic, *et al.*, 2009). All Azo-compounds have one hydrocarbon substituent at the para position **(Figure 3-19)**. The difference in hydrocarbon length was not expected to affect the electron distribution of azobenzene moiety. In order to confirm the expectation, the charges of PAP, Azo-C6 and Azo-C18 molecules were calculated. The calculation was performed using the extended Huckel model in PerkinElmer Chem3D software (Ver. 16.0.1.4, **Table 3-2)**. There was no charge change by substitution except for charge change of carbons 9, 10 and 11 adjacent to oxygen as the phenol group of PAP was replaced with the hydrocarbon chain. Furthermore, the chain

서울대학교

length of the substituent did not affect the charge of the azobenzene molecule.

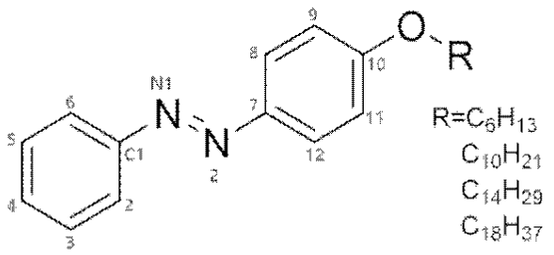

Figure 3-19. Chemical structure of Azo-compounds and atom numbers for charge calculation.

Table 3-2. Charge calculation of PAP, Azo-C6 and Azo-C18 by extended Huckel model in PerkinElmer Chem3D.

	PAP (R=H)	**Azo-C6 ($R=C_6H_{13}$)**	**Azo-C18 ($R=C_{18}H_{37}$)**
N1	0.419	0.420	0.420
N2	0.564	0.522	0.522
C1	0.132	0.114	0.114
C2	-0.193	-0.192	-0.192
C3	-0.058	-0.067	-0.067
C4	-0.257	-0.271	-0.271
C5	-0.024	-0.024	-0.024
C6	-0.204	-0.216	-0.216
C7	0.132	0.128	0.128
C8	-0.184	-0.182	-0.182
C9	**-0.065**	**-0.123**	**-0.123**
C10	**-0.279**	**0.071**	**0.071**
C11	**-0.032**	**-0.129**	**-0.129**
C12	-0.221	-0.239	-0.239

서울대학교

As a result of expectation and calculation, it was expected that the substitution of Azo-compounds did not influence photo-isomerization. It was defined by experimental data using a UV/Vis spectrometer. In the UV/Vis absorption spectra of the compounds in the THF solution, any shift in the resonance wavelength was absent **(Figure 3-20)**.

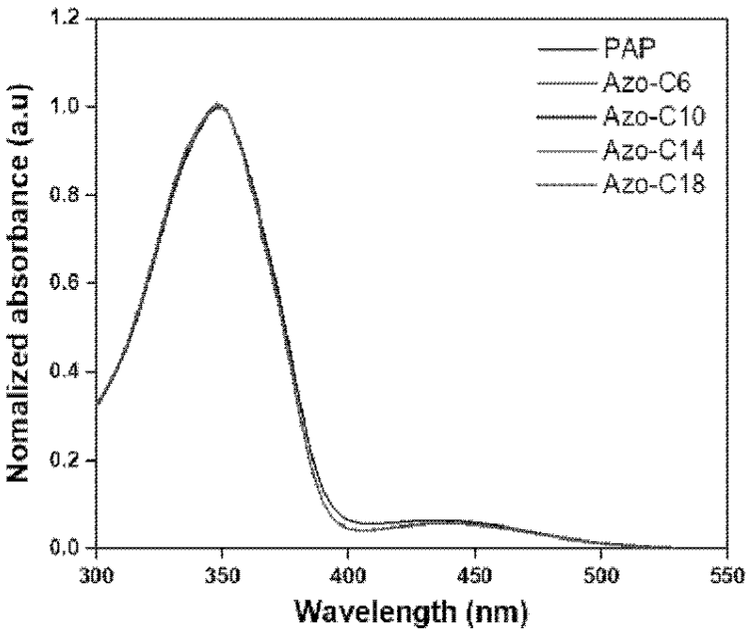

Figure 3-20. UV/Vis absorption spectra of Azo-compounds.

In addition, the Azo-compound solutions were exposed to 5 mW/cm^2 of UV light, and trans-to-cis isomerization was monitored **(Figure 3-21a)**. By calculating the saturated absorbance value of each compound as 100%, the trans-to-cis photo-isomerization yield according to the UV dose was shown in **Figure 3-21b**. The photo-isomerization yield was also not affected by the chemical structure of the compounds. As a result, it was determined that chemical factors did not cause the photo-isomerization efficiency of the switchable PSAs.

서울대학교

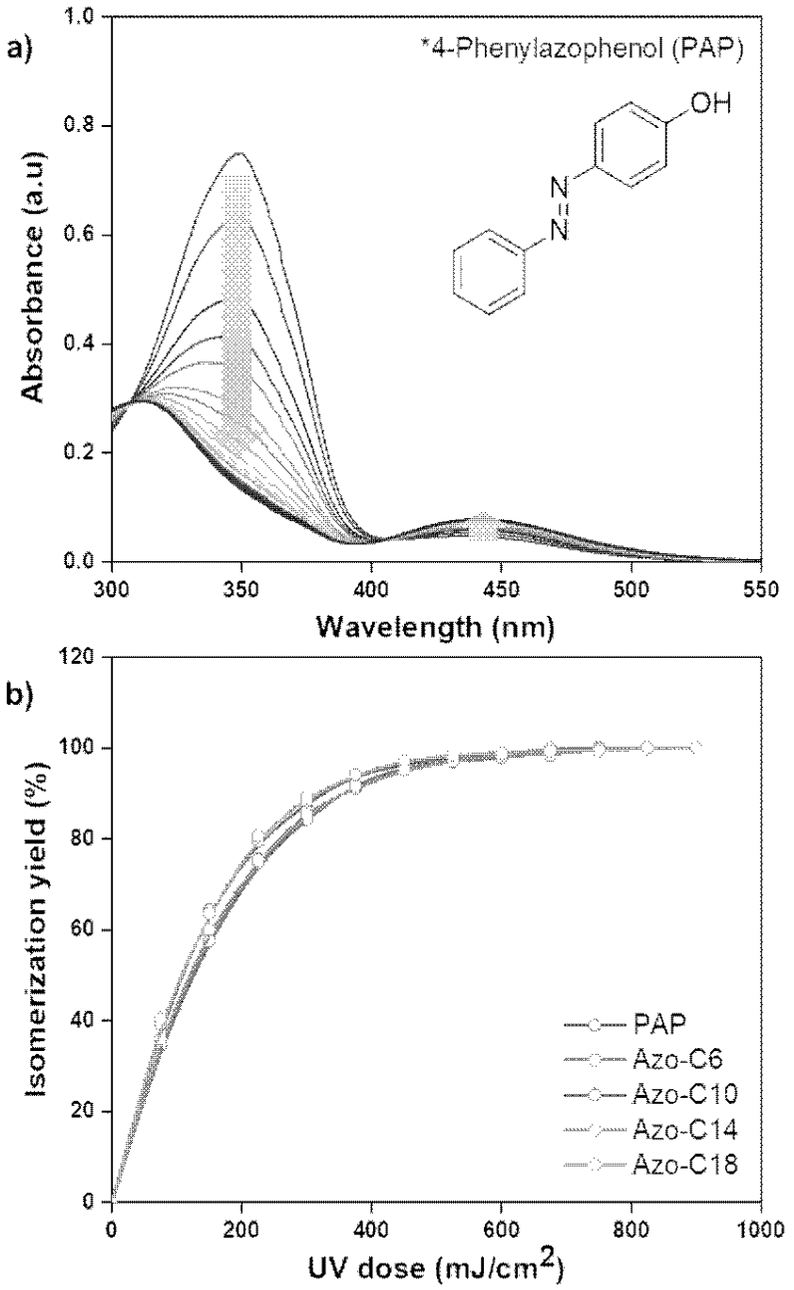

Figure 3-21. a) Monitoring of trans-to-cis photo-isomerization of PAP according to UV irradiation time by UV/Vis spectrometer, b) Trans-to-cis photo-isomerization yield of Azo-compounds according to UV dose.

서울대학교

3.6.2. Difference in Photo-isomerization Efficiency by Physical Factor of Surrounding Matrix

The photo-isomerization efficiency can be determined by the physical restriction of the surrounding matrix. The switchable PSAs consisted of Azo-polymer as a polymer matrix and Azo-compounds as photo-responsive additives. However, when the compounds formed crystalline structures, the azobenzene groups were stacked with each other and surrounded by not only Azo-polymer but also crystalline structures built with hydrocarbon chain substituents. Since Azo-polymer has a much lower modulus compared to the crystalline structures of Azo-compounds **(Figure 3-13)**, it was considered that the photo-isomerization of azobenzene would be predominantly limited by the crystalline structures of the compounds, not Azo-polymer.

Therefore, we evaluated the crystallinity of each Azo-compound by DSC curves **(Figure 3-22)**. Melting temperatures of Azo-C6, C10, C14 and C18 were 56.0 °C, 64.1 °C, 76.6 °C and 84.6 °C, respectively. Azo-C6 and Azo-C10, which have relatively short substituents, had one more small phase transition peak on each DSC curve at 38.1 °C and 42.0 °C, respectively. The small peaks were endothermic peaks due to partial molecular disorder. Many organic materials have a single phase transition between solid and liquid states. However, when the materials exhibit two or more phase transitions, they have intermediate phases, which are mesophases (Priestley, 1975). Azo-C6 and Azo-C10 had the mesophase between the two phase-transition peaks. It means that the two compounds have a relatively weak molecular arrangement. However, as the length of the hydrocarbon substituent increased (Azo-C14 and Azo-C18), the phase-transition temperature increased, and the mesophase disappeared.

서울대학교

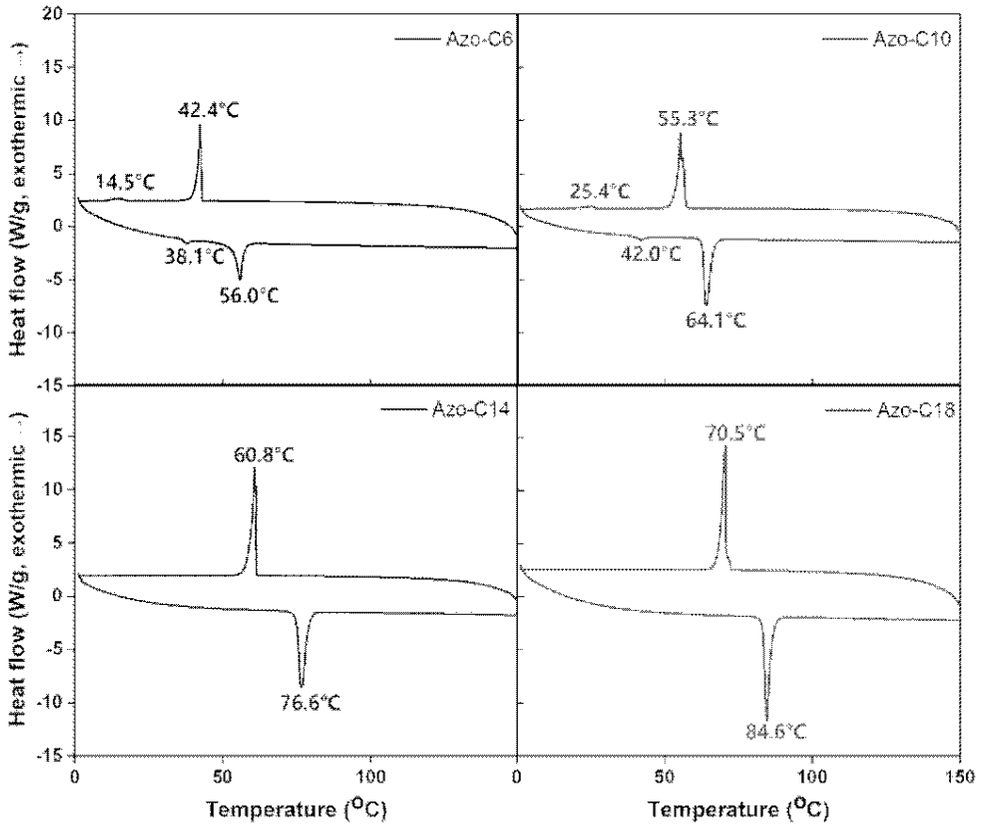

Figure 3-22. DSC curves and phase transition temperatures of Azo-compounds.

We also calculated the melting enthalpies of Azo-compounds with the DSC curves. The melting enthalpy is the energy required for a substance to change from a solid to a liquid state. The energies required to disarrange the ordered structures of Azo-compounds were compared through the melting enthalpy, and it was considered that the compound with high melting enthalpy would require more energy for trans-to-cis photo-isomerization of azobenzene. The melting enthalpies of Azo-C6, Azo-C10, Azo-C14 and Azo-C18 obtained via integration of the phase-transition peaks were 20.1 kJ/mol, 38.3 kJ/mol, 51.2 kJ/mol and 62.5 kJ/mol, respectively **(Figure 3-23b)**.

서울대학교

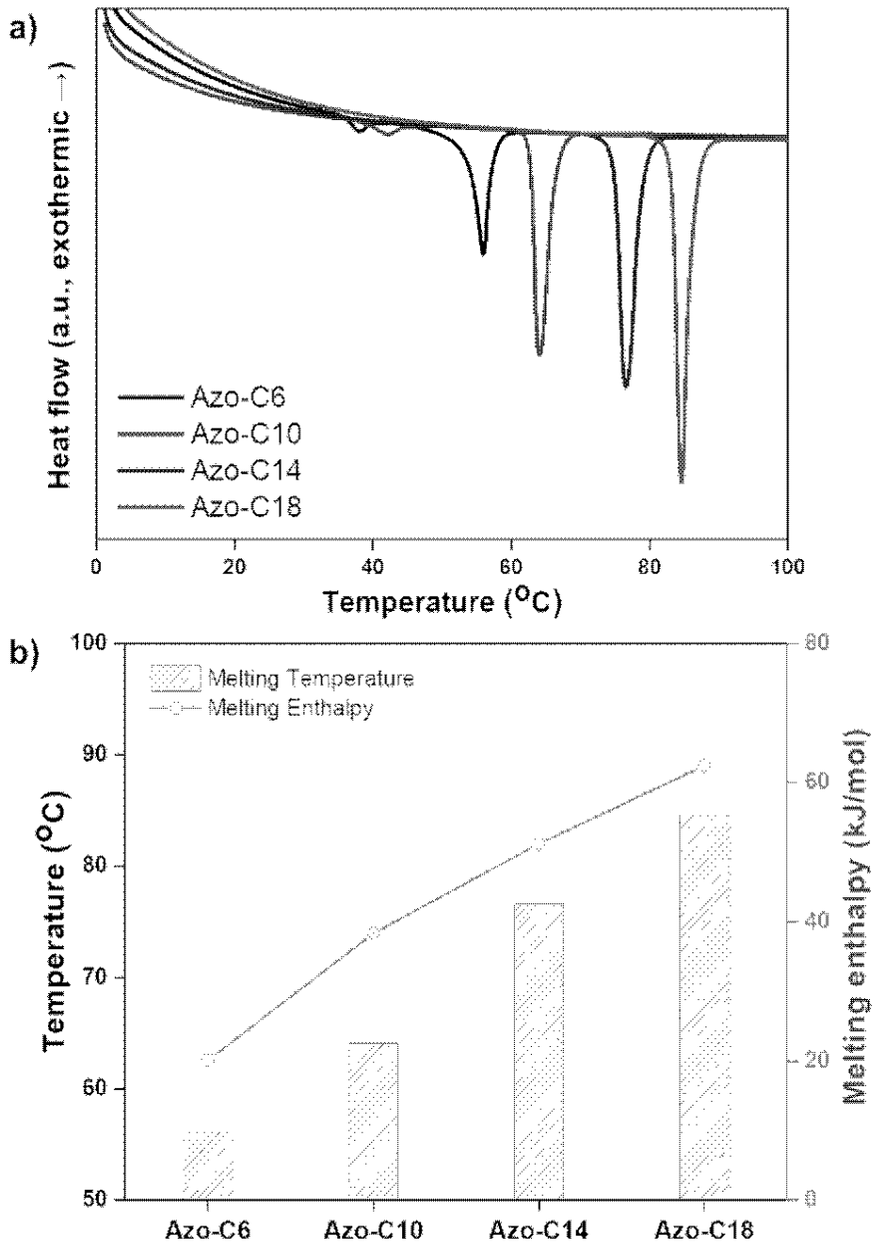

Figure 3-23. a) Comparison of melting peaks of Azo-compounds, b) melting temperatures and enthalpy according to the hydrocarbon chain length of Azo-compounds.

서울대학교

The intermolecular interactions of Azo-compounds were the π-π interaction of the azobenzene moiety and the dispersion interaction of the hydrocarbon chains. Thus, as the length of the hydrocarbon chain increased, the intermolecular interaction and crystalline structure became stronger. It led to an increase in the melting temperature and enthalpy. SP-C6 did not exhibit adhesion switching characteristics because Azo-C6, which had a relatively weak intermolecular interaction, did not form a crystalline structure in Azo-polymer. Alternatively, Azo-C10, C14 and C18 formed a crystalline structure, and adhesion switching was realized by a transition in the crystalline structure by UV and visible light radiation **(Figure 3-24)**. The crystalline structures formed by the interaction between Azo-C10, C14 and C18 molecules are stronger than the molecular arrangement of amorphous Azo-polymer and SP-C6. The crystalline structures require more stress for deformation and induce an increase in shear modulus. The surface energy is also reduced due to the intermolecular stacking of the crystalline structure formed by the dispersion interaction of the hydrocarbon chain and the π-π interaction of azobenzene (Lim, *et al.*, 2006).

The reason that the UV intensity required for the switchable PSAs to activate their adhesive forces increased as the azo-compound aliphatic chain length increased is believed to be related to the energy required to induce phase switching in the crystalline structures of Azo-compounds. The isomerization of the azobenzene moiety was affected by the phase and viscosity of the surrounding substances. Isomerization is known to become difficult when the viscosity surrounding the azobenzene moiety increases (Gegiou, *et al.*, 1968). Furthermore, the photo-isomerization from trans- to cis-azobenzene may not be possible if it exists in the solid phase (Tsuda and Kurata, 1964). Thus, photo-isomerization may be related to molecular mobility and free volume. Consequently, Azo-C10-containing SP-C10, which had a low melting enthalpy

서울대학교

and a mesophase, was capable of adhesion switching at a lower UV intensity than SP-C14 and SP-C18.

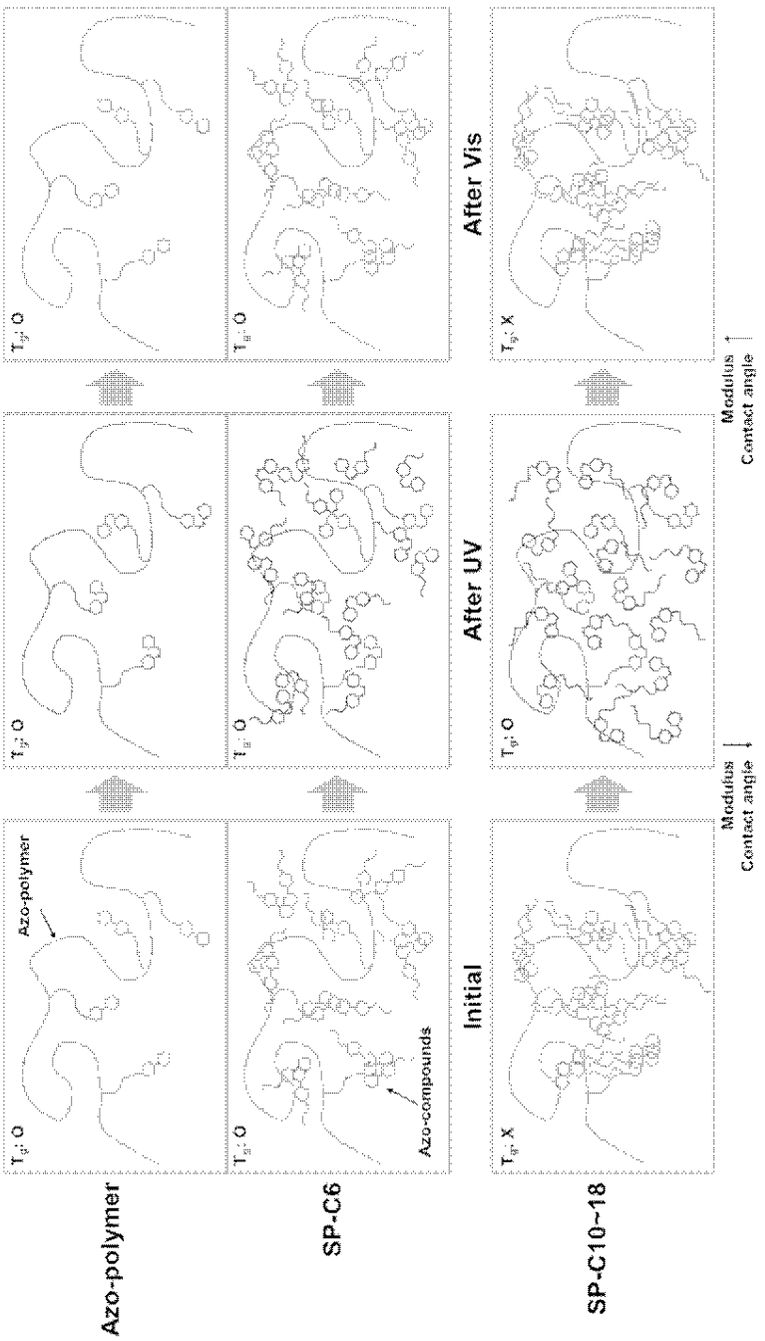

Figure 3-24. Schematic illustration of crystalline structure formation of Azo-compounds and transition in crystalline structure by light irradiation.

서울대학교

4. Conclusions

Azo-compounds with substituents with different hydrocarbon chain lengths were synthesized on the azobenzene group. The switchable PSAs were prepared by mixing the compounds with an Azo-polymer. When the aliphatic chain length exceeded 10, adhesion switching was possible. Moreover, longer chain lengths necessitated stronger UV intensity for adhesion switching. It is related to the phase-transition temperature and melting enthalpy of the compounds. Changes in the crystalline structure of Azo-compound in the polymer matrix were induced due to UV exposure, and the adhesive forces of the switchable PSA were activated in response to the detection of T_g, a decrease in the shear modulus, and an increase in surface energy. In the case of SP-C10, adhesion switching was possible at a relatively low UV intensity of 25 mW/cm^2, even under a short UV irradiation time of 30 s. In addition, there was no loss of adhesive force even after 30 continuous cycles of adhesion switching. The adhesive force of the PSAs was activated by trans-to-cis isomerization of azobenzene moiety. Thus, the activated adhesive properties cannot be maintained permanently because of the metastable nature of the cis-azobenzene. However, it can be applied to processes requiring short-term adhesive force since it was confirmed that the adhesive properties were maintained during the probe tack test (within a few minutes). It is expected that our novel switchable PSA, which is reusable and capable of rapid switching even at low UV intensities, can be applied in the transfer printing process in the electrical and electronic industries.

서울대학교 SEOUL NATIONAL UNIVERSITY

Chapter 4

UV Laser Process for Adhesion Switching and Selective Mini-LED Transfer

서울대학교 SEOUL NATIONAL UNIVERSITY

1. Introduction

Recently, many researchers have studied switchable adhesives. Whereas traditional adhesives have a stationary adhesive force, the switchable adhesives have adhesive properties that can change in response to external stimuli. Due to these unique properties, the switchable adhesives have been used in various fields, such as medical, display and semiconductor industries. The adhesion switching is achieved through changes in the material's surficial, mechanical and geometric properties (Croll, *et al.*, 2019), and the change in the properties can be realized through stimuli-responsive dynamic linkages (Gao, *et al.*, 2019, Heinzmann, *et al.*, 2014, Yamaguchi, *et al.*, 2012, Zheng, *et al.*, 2013) or chemical moieties such as azobenzene (Akiyama, *et al.*, 2014, Akiyama, *et al.*, 2016, Ito, *et al.*, 2018, Ito, *et al.*, 2018) and anthracene (Akiyama, *et al.*, 2018, Liu, *et al.*, 2020, Shen, *et al.*, 2020). Previously studied materials could be activated under limited conditions such as hydration, heat and long switching times, and they had limitations related to reuse. Therefore, we presented studies on switchable PSAs that improve these limitations (Lee, *et al.*, 2021, Lee, *et al.*, 2021).

Laser (light amplification by stimulated emission of radiation) is a light source that emit coherent and amplified light. The light emitted from the laser has higher directional, energy density and focusing properties due to identical wavelength, frequency and phase of photons (Dubey, *et al.*, 2008). Therefore, the laser system is applied to various industries, and in particular, it is used in various processes in the semiconductor industry, which requires the most minute and precise process (Rahim, *et al.*, 2017). In addition, the laser-driven transfer processes were also studied (Eisenhaure and Kim, 2016, Saeidpourazar, *et al.*, 2012). In these studies, the selective transfer was achieved by local light irradiation to fine areas using the laser as a light source.

서울대학교

Transfer printing is the electronic device manufacturing process that transfers circuits or devices fabricated on a substrate to another substrate. The process has been required to manufacture flexible and stretchable electronic devices. The inorganic substrate should be replaced with the organic substrate for flexibility, and the substitution makes the transfer printing necessary in the manufacturing process. The circuits or devices cannot be fabricated on the organic substrate directly and should be transferred from the inorganic substrate due to the vulnerability of organic materials to chemicals and high temperatures (Linghu, *et al.*, 2018). In addition, the transfer process is used when the electronic components cannot be directly formed on a substrate due to a complicated process.

The micro-LED display manufacturing is a representative process including the transfer process. Millions of individual micro-LEDs are fabricated on different substrates and then transferred onto a circuit during display manufacturing (Li, *et al.*, 2020). Various types of switchable adhesives have been studied as transfer mediators. Polydimethylsiloxane (PDMS) stamp using the frequency dependence of the PDMS is a representative type (Kim, *et al.*, 2009, Lee, *et al.*, 2005, Meitl, *et al.*, 2005). However, the stamp has the limitations of vulnerability to contamination and difficulty in selective transfer. Other transfer processes using ultraviolet (UV) tapes (Pan, *et al.*, 2020), thermal release films (Yan, *et al.*, 2017), and magnetorheological elastomers (Kim, *et al.*, 2019) were studied. However, no material was capable of selective transfer and reusing simultaneously.

Our previous studies proposed azobenzene-containing photo-responsive switchable PSAs (Lee, *et al.*, 2021, Lee, *et al.*, 2021). The adhesive force of the switchable PSA was activated with UV light irradiation and deactivated with visible light irradiation. We used an LED lamp as a light source for the UV light irradiation and realized selective LEDs transfer to the PDMS substrate using a

서울대학교

photo-mask (Lee, *et al.*, 2021). However, it was difficult to achieve precise and micropatterned adhesion switching with the LED light source. Therefore, in this study, the ns pulsed UV laser system was used as the light source, and the switchable PSA that is applicable to the laser process was fabricated by mixing the azobenzene-containing acrylic polymer and low molecular weight azobenzene compounds. The photo-responsive adhesion switching efficiency of the switchable PSA was improved by chemical modification in azobenzene's substituent and the addition of a UV absorber. The UV absorber also enhanced resistance to laser-induced surface damage of the switchable PSA. We derived optimum laser process conditions for adhesion switching, and the micropatterned adhesion switching and small-scaled selective mini-LEDs transfer were realized with the laser process.

서울대학교

2. Experimental

2.1. Materials

The following were purchased from Sigma-Aldrich: 4-phenylazophenol (98%), 1-chlorohexane (99%), dibutyltin dilaurate (DBTDL, 95%) and butyl acrylate (>99%). Potassium carbonate (>99%), potassium iodide (>99.5%), 6-chloro-1-hexanol (>96%), 1-chlorotetradecane (>98%) and hexyl isocyanate (>98%) were purchased from Tokyo Chemical Industry Co., Ltd. The following were purchased from Samchun Chemicals Co., Ltd.: 2,2'-azobisisobutyronitrile (98%), 2-butanone (MEK, 99.5%), N,N-dimethylformamide (DMF, 99.5%), tetrahydrofuran (THF, 99.9%), methanol (99.5%), n-hexane (96%), acetone (99.5%) and ethyl acetate (EA, 99.5%). 2-Isocyanatoethyl acrylate (Karenz AOI, Showa Denko) was used as the isocyanate-containing acrylic monomer. N-(2-Ethoxyphenyl)-N'-(2-ethylphenyl)oxamide (OA, SABOSTAB® UV 312), Three types of UV absorbers, 2-(2-hydroxy-5-methylphenyl)benzotriazole (BTA, SONGSORB® 1000) and 2-Hydroxy-4-n-octoxybenzophenone (BP, SONGSORB® 8100), were provided from Songwon Industrial Co., Ltd. SYLGARD 184 (Dow Corning) was used as the PDMS acceptor in the mini-LED transfer test.

서울대학교

2.2. Synthesis of Azobenzene-containing Acrylic Monomer and Low Molecular Weight Compounds

2.2.1. 6-(4-(Phenyldiazenyl)phenoxy)hexan-1-ol

The method was based on a procedure described by Zhou (Zhou, *et al.*, 2016). Briefly, 4-phenylazophenol (3.568 g, 0.018 mol) and potassium carbonate (2.488 g, 0.018 mol) were added to DMF (15 ml). After dissolving the mixture under the condition of stirring at room temperature for 30 min, potassium iodide (7.5 mg, 0.045 mmol) and 6-chloro-1-hexanol (3.689 g, 0.027 mol) were added to the solution. Synthesis was carried out over a period of 24 h and at 110 °C. The reaction solution was poured into cold water, and the precipitate was filtered. After recrystallizing the filtered compound in n-hexane, the compound was filtered and dried at room temperature under vacuum.

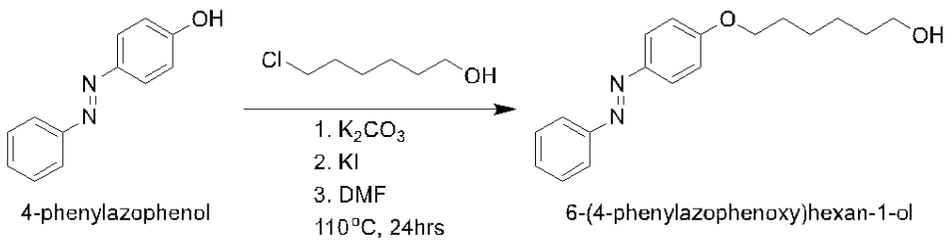

Figure 4-1. Synthesis of 6-(4-(Phenyldiazenyl)phenoxy)hexan-1-ol.

서울대학교 SEOUL NATIONAL UNIVERSITY

2.2.2. 2-((((6-(4-(phenyldiazenyl)phenoxy)hexyl)oxy)carbonyl)amino)ethyl acrylate (Azo-acrylate)

After dissolving 6-(4-(phenyldiazenyl)phenoxy)hexan-1-ol (2.000 g, 0.007 mol) in MEK (15 ml) at room temperature, 2-isocyanatoethyl acrylate (1.976 g, 0.014 mol) was added to the solution. The mixture was stirred under N_2 purging conditions for 20 min. DBTDL (0.019 g) was diluted in MEK and added to the solution. The reaction mixture was maintained at 40 °C for 6 h. The reacted solution was poured into cold n-hexane, and the precipitate was filtered. The filtered compound was dried at room temperature under vacuum.

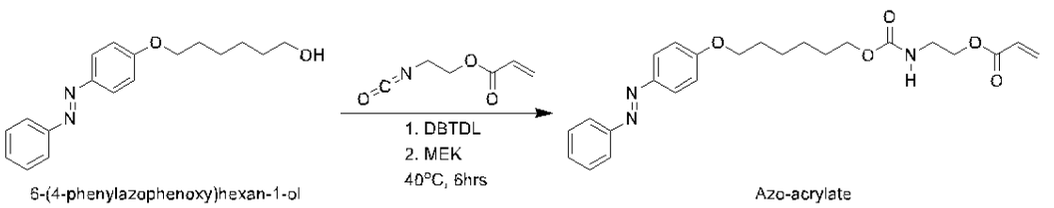

Figure 4-2. Synthesis of Azo-acrylate.

서울대학교

2.2.3. Low Molecular Weight Azobenzene Compounds (Azo-compounds)

The synthesis method for 6-(4-(phenyldiazenyl)phenoxy) hexan-1-ol was used to synthesize three azobenzene-containing compounds (Azo-compounds), i.e., 1-(4-(hexyloxy)phenyl)-2-phenyldiazene (Azo-C6) and 1-(4-(tetradecyloxy)phenyl)-2-phenyldiazene (Azo-C14); note that alkyl chloride (1-chlorohexane and 1-chlorotetradecane) was used instead of 6-chloro-1-hexanol. After dissolving 4-phenylazophenol (1.982 g, 0.010 mol) and potassium carbonate (1.382 g, 0.010 mol) in DMF (9 ml), potassium iodide (4.2 mg, 0.025 mmol) and the corresponding alkyl chloride (0.015 mol) were added to the solution. Synthesis was carried out over a period of 24 h at 110 °C. The reaction solution was poured into cold water, and the precipitate was filtered. The filtered compound was recrystallized in methanol (Azo-C6) or acetone (Azo-C14). The recrystallized compound was filtered and dried at room temperature under vacuum.

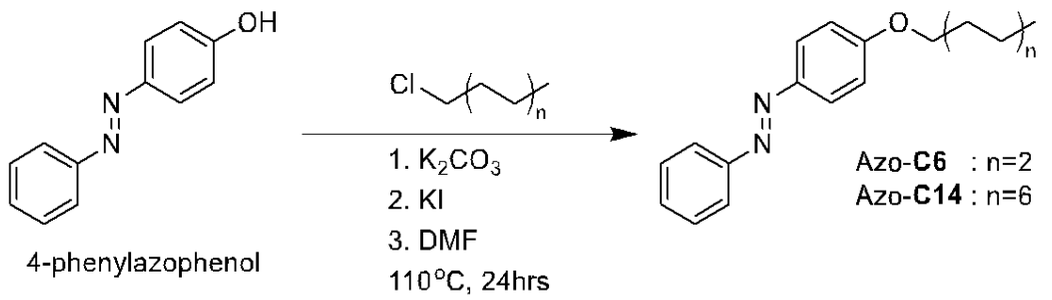

Figure 4-3. Synthesis of Azo-compounds.

서울대학교

2.2.4. 6-(4-(phenyldiazenyl)phenoxy)hexyl hexylcarbamate (Azo-U)

The synthesis method for Azo-acrylate was used to synthesize 6-(4-(phenyldiazenyl)phenoxy)hexyl hexylcarbamate (Azo-U); note that hexyl isocyanate was used instead of 2-isocyanatoethyl acrylate. After dissolving 6-(4-(phenyldiazenyl)phenoxy)hexan-1-ol (1.500 g, 0.005 mol) in MEK (15 ml) at room temperature, hexyl isocyanate (1.272 g, 0.010 mol) was added to the solution. The mixture was stirred under N_2 purging conditions for 20 min. DBTDL (0.019 g) was diluted in MEK and added to the solution. The reaction mixture was maintained at 60 °C for 6 h. The reacted solution was poured into cold n-hexane, and the precipitate was filtered. The filtered compound was dried at room temperature under vacuum.

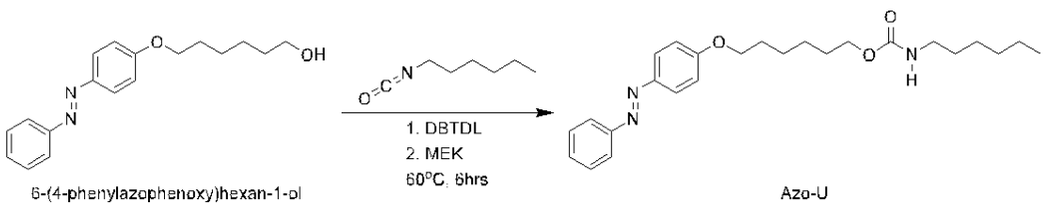

Figure 4-4. Synthesis of Azo-U.

서울대학교

2.3. Polymerization of the BA/Azo-acrylate Co-polymer (Azo-polymer)

After removing the inhibitor of BA using neutral aluminum oxide, BA (1.5 g, 0.012 mol) and Azo-acrylate (0.572 g, 1.3 mmol) were added to EA (5 mL). After stirring the mixture for 1 min at 70 °C to dissolve the Azo-acrylate powder, N_2 gas was blown into the solution for 20 min at room temperature. AIBN (0.01 g) was added to the solution, and the solution was stirred at 70 °C for 1.5 h. Tetrahydrofuran (THF, 5 mL) was poured into the polymerized solution to prevent gelation caused by the interaction between the azobenzene moieties. The polymer solution was washed and dissolved with methanol and THF, respectively. The process was repeated thrice. The dissolved solution was poured on a silicone-release film and dried at 70 °C.

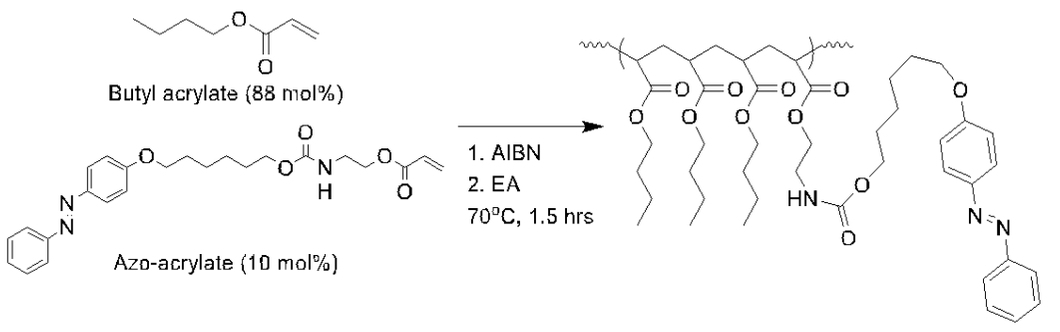

Figure 4-5. Polymerization of Azo-polymer.

서울대학교

2.4. Preparation of the Switchable PSA Specimens

Five switchable PSAs were prepared according to the type and combination of Azo-compounds (including Azo-U). SP-C14 contained 12 mol% of Azo-C14, and the three PSAs were named SP-C6_C14-1_9, SP-C6_C14-3_7 and SP-C6_C14-5_5 according to the mixing ratio of Azo-C6 and Azo-C14. The mixing ratio was the mole ratio of the two compounds, and the total content was 12 mol%. SP-U contained 12 mol% of Azo-U **(Table 4-1)**. After dissolving Azo-polymer in THF, 12 mol% of single or mixed Azo-compounds was added to the polymer solution. The content of Azo-compounds was calculated in consideration of the number of butyl acrylate and Azo-acrylate molecules in Azo-polymer. The Azo-compounds were dissolved in their respective polymer solution by using a vortex mixer. After using a 120 μm coating applicator to cast each mixture on a corona-treated polyethylene terephthalate (PET) film (50 μm), the films were dried at 100 °C for 20 min in a convection oven. After being cooled, the dried films were irradiated with UV light (365 nm LED lamp, 125 mW/cm^2, 30 s) and visible light (50 W white LED lamp, 30 s) because the trans- and cis-azobenzene ratio and the molecular arrangement of Azo-compounds formed by the drying process would be different from those formed by UV and visible light irradiation. The thicknesses of the switchable PSAs were 6–7 μm, as measured by using a digital micrometer (S-Mike_Pro, Sylvac).

SP-U was modified with the addition of a UV absorber (BTA). The switchable PSAs were SP-U-Ab10, 20, 30, 40 and 50, depending on the content of the absorber (10, 20, 30, 40 and 50 (mol%)). The content was calculated as the molar ratio with Azo-U in SP-U **(Table 4-1)**.

서울대학교 SEOUL NATIONAL UNIVERSITY

Table 4-1. Compositions of solution mixtures applied to cast the switchable PSAs.

	Azo polymer	THF	Azo-C6	Azo-C14	Azo-U
SP-C14	0.1 g (88 mol% of butyl and azobenzene pendant groups)	1 ml	-	35.1 mg (12.0 mol%)	-
SP_C6_C14-1_9			2.5 mg (1.2 mol%)	31.6 mg (10.8 mol%)	-
SP-C6_C14-3_7			7.5 mg (3.6 mol%)	24.6 mg (8.4 mol%)	-
SP-C6_C14-5_5			12.6 mg (6.0 mol%)	17.6 mg (6.0 mol%)	-
SP-U			-	-	38.0 mg (12.0 mol%)

	Azo polymer	THF	Azo-U	BTA
SP-U	0.1 g	1 ml	38.0 mg (12.0 mol%)	-
SP-U-Ab10				2.0 mg
SP-U-Ab20				4.0 mg
SP-U-Ab30				10.0 mg
SP-U-Ab40				15.0 mg
SP-U-Ab50				20.0 mg

2.5. Preparation of the PDMS Acceptor

The PDMS resin and curing agent (resin : curing agent = 10 : 0.5) were mixed using a paste mixer (ARE-310, THINKY) operated at 2,000 rpm. The process proceeded for 3 min (mixing: 2 min, deforming: 1 min). The mixture was poured into a petri dish, and the sample was cured at 80 °C (curing time: 12 h).

서울대학교 SEOUL NATIONAL UNIVERSITY

2.6. Characterization

2.6.1. Nuclear Magnetic Resonance (NMR) Spectroscopy

A 400 MHz NMR spectrometer (JNM-ECX400, JEOL) was used to record the 1H-NMR spectra. The operating temperature was room temperature, and tetramethylsilane ($\delta = 0$ ppm) was used as a reference to determine the chemical shift.

2.6.2. Adhesion Switchability Test

The adhesive forces of the switchable PSAs were evaluated by applying a probe tack test. The tack forces were measured by operating a texture analyzer (TA.XT plus, Stable Micro Systems) and a 500 N load cell at 25 °C (RH: 50 ± 10%). A cylindrical 5 mm-diameter stainless-steel probe was used. The probe was in contact with each PSA specimen for 1 s, applying a force of 100 g_f; the contact speed was 0.2 mm/s. After the probe was detached from the specimen at a speed of 10 mm/s, the maximum force was taken as the probe tack value. An average of five measurements was used for each specimen.

2.6.3. UV/Vis Spectroscopy

The azobenzene moiety photo-isomerization was monitored using a UV/Vis spectrometer (UV-1601PC, Shimadzu) to record the UV/Vis absorption spectrum; the scan range was 300–600 nm. Azo-compounds were measured as a solution state in THF; the molality of the Azo-compound solution was 0.035 mol/kg, and a spectrum baseline was obtained with THF in a quartz cuvette.

서울대학교 SEOUL NATIONAL UNIVERSITY

2.6.4. DSC Measurement

The Azo-compounds (1.5–2.0 mg) were loaded onto the Tzero Pan (Tzero Pan, 901683.901, TA Instruments) and applied differential scanning calorimetry (DSC, Q200, TA Instruments). After each specimen was heated to 150 °C at 30 °C/min and subjected to a 3 min isothermal process, the data were recorded as it was cooled to 0 °C and heated to 150 °C at 10 °C/min.

2.7. UV Laser System

The UV laser test was conducted through joint research with Korea Institute of Machinery & Materials (KIMM) **(Figure 4-6)**. The wavelength of the laser system was 355 nm. The laser system emitted a pulsed laser beam, and the pulse width was 19 ns with a 90 kHz of repetition rate. The focal length was 160mm; The beam size at the focal point was 7.2 μm.

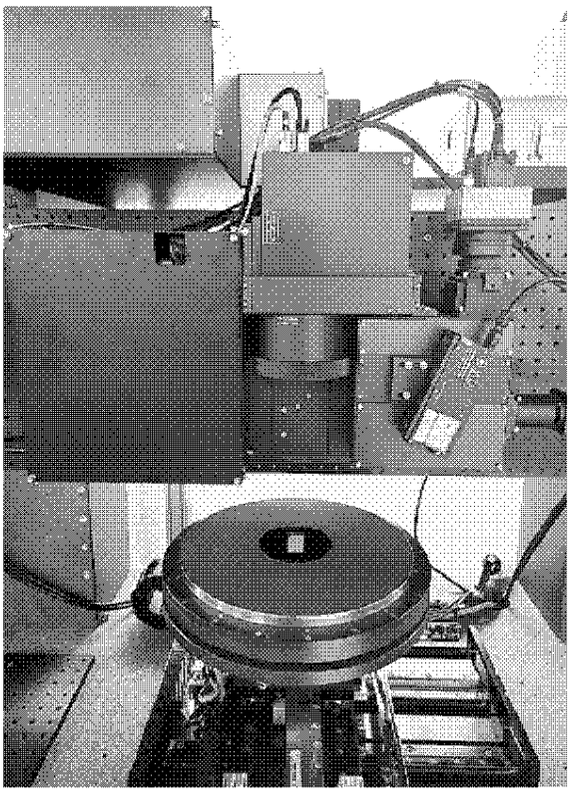

Figure 4-6. UV laser system (KIMM).

서울대학교

3. Results and Discussion

3.1. Results of Synthesis and Polymerization

3.1.1. Synthesis of 6-(4-(Phenyldiazenyl)phenoxy)hexan-1-ol

The yield of the synthesis of 6-(4-(Phenyldiazenyl)phenoxy)hexan-1-ol was 53.2%. The chemical structure was defined by the ^{1}H-NMR spectrum. However, the NMR spectrum of the synthesized compound is omitted in this chapter.

3.1.2. Synthesis of Azo-acrylate

The yield of the synthesis of Azo-acrylate was 77.6%. The chemical structure was defined by the ^{1}H-NMR spectrum. The NMR spectrum of the synthesized compound is omitted in this chapter.

3.1.3. Synthesis of Azo-compounds

The synthesis yields of Azo-C6 and Azo-C14 were 54.8% and 61.8%, respectively. The chemical structure was defined by the ^{1}H-NMR spectrum. The NMR spectrum of the synthesized compound is omitted in this chapter.

서울대학교 SEOUL NATIONAL UNIVERSITY

3.1.4. Synthesis of Azo-U

The synthesis yield of Azo-U was 77.0%. The chemical structure was defined by the ^{1}H-NMR spectrum **(Figure 4-7)**. The analysis of the NMR spectrum is as follows.

δ = 7.82 (dd, 4H, Ar H), 7.50 (dt, 3H, Ar H), 7.08 (m, 2H, Ar H), 7.00 (m, 1H, NH), 4.03 (t, 2H, Ar-OCH_2), 3.90 (t, 2H, $\underline{CH_2}OOCNH$), 2.89 (m, 2H, $NH\underline{CH_2}$), 1.72 (m, 2H, Ar-$OCH_2\underline{CH_2}$), 1.44 (m, 6H, Ar-$OCH_2CH_2\underline{CH_2CH_2CH_2}$, $NHCH_2\underline{CH_2}$), 1.18 (m, 6H, $NHCH_2CH_2\underline{CH_2CH_2CH_2}$), 0.80 (m, 3H, $NHCH_2CH_2CH_2CH_2CH_2\underline{CH_3}$)

서울대학교 SEOUL NATIONAL UNIVERSITY

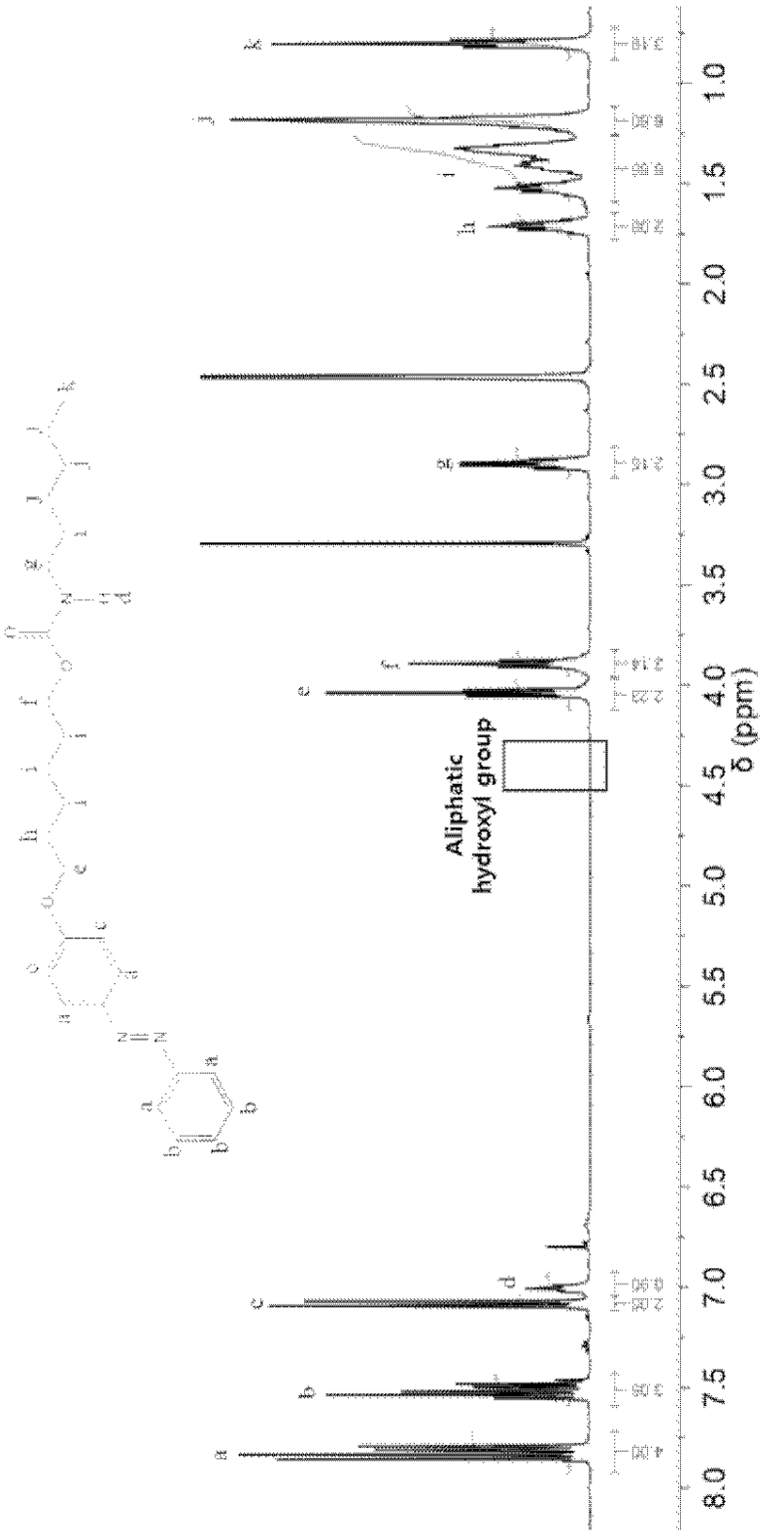

Figure 4-7. ^{1}H-NMR spectrum of Azo-U.

세종대학교 Sejong University

3.1.5. Polymerization of Azo-polymer

Unreacted BA and Azo-acrylate in polymerized Azo-polymer solution were removed by washing with methafnol and THF. The removal of unreacted monomers was confirmed through the absence of acrylate's double bond at 5.5-6.5 ppm of the NMR spectrum.

The ratio of Azo-acrylate monomer included in the polymerized chains among 10 mol% of azo-acrylate added for polymerization was calculated through the NMR spectrum, and the equation is as follows:

$$C_{azo} = \frac{I_{7.89ppm}/4}{I_{0.88ppm}/3 + I_{7.89ppm}/4}$$

where C_{azo} denotes the content of Azo-acrylate in washed Azo-polymer, $I_{7.89ppm}$ denotes the intensity of peak at 7.89 ppm corresponding to the azobenzene side chain, and $I_{0.88ppm}$ denotes the intensity of peak at 0.88 ppm corresponding to CH_3 of the butyl side chain. The calculated C_{azo} was 8 mol%.

The M_n, M_w and PDI of Azo-polymer measured with gel permeation chromatography (GPC) were 38,000, 165,000 and 4.3, respectively.

서울대학교 SEOUL NATIONAL UNIVERSITY

3.2. Adhesion Switching of SP-C14 with UV Laser

3.2.1. Selection of Switchable PSA for a UV Laser Test

In our previous study, we synthesized four azobenzene-containing compounds according to a hydrocarbon chain length of substituent on the para position of the azobenzene group; the substituent lengths were 6 (Azo-C6), 10 (Azo-C10), 14 (Azo-C14) and 18 (Azo-C18) (Lee, *et al.*, 2021). Switchable PSAs were fabricated with a mixture of Azo-polymer and the azobenzene-containing compound (SP-C6, SP-C10, SP-C14 and SP-C18). SP-C10 showed the highest UV efficiency for switching on the adhesive force. However, its adhesive force was not fully switched off immediately after visible light irradiation **(Figure 4-8)**; The SP-C10 required an additional 25 s after visible light exposure for zero adhesive force. Whereas SP-C14 had lower photo-isomerization efficiency than SP-C10, its adhesive force could be fully switched off to zero immediately after visible light irradiation. The stable and immediate switching on/off property is a primary function of photo-responsive PSA. Thus, we conducted an adhesion switching test by UV laser with SP-14.

서울대학교

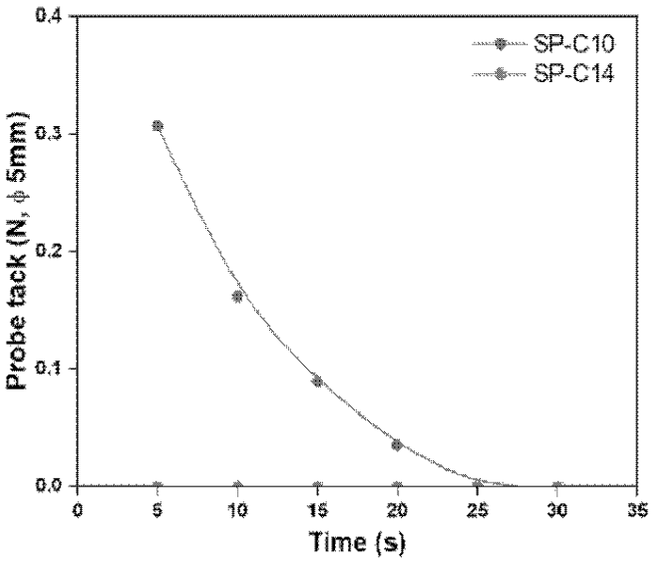

Figure 4-8. Probe tack forces of SP-C10 and SP-C14 according to the dwell time after visible light irradiation.

3.2.2. UV Laser Adhesion Switching Test

The laser irradiation and process parameters are briefly presented in **Figure 4-9**. The laser radiated through a focus lens is focused on a specific point, a focal point; Light energy is concentrated into the narrowest area at the focal point. When the specimen is placed on the focal point, it is irradiated with the highest energy density light. The beam size and energy density can be controlled by defocusing length from the focal point. The light intensity is also adjusted with output power. Since the beam size controlled by the defocusing length is several to several hundred μm, it scans from end to end of the irradiation area to irradiate a large area. The scan speed and pitch determine the beam overlap rate. An ns pulsed UV laser system was used in this study. Thus, the repetition rate of pulsed light can be controlled. In short, the laser irradiation parameters are power, defocusing length (beam size), scan speed, pitch and repetition rate.

서울대학교

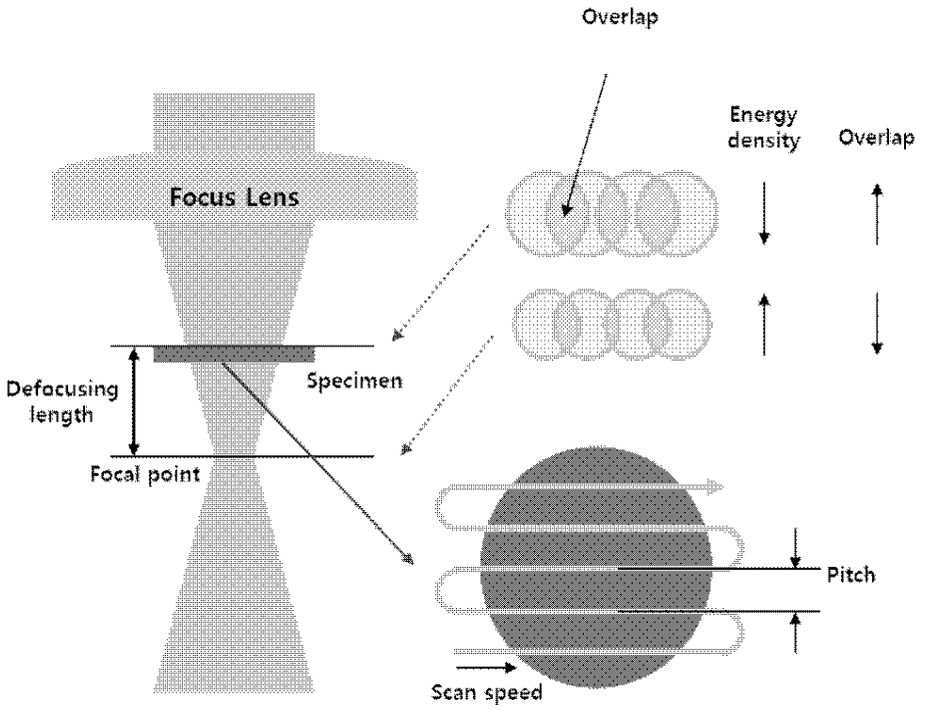

Figure 4-9. Schematic illustration of the laser irradiation process parameters.

Probe tack results of the UV laser adhesion switching test are presented in **Table 4-2**. The process conditions are classified into two-part. The repetition rate and beam size were fixed in condition no. 1–6, and the power, scan speed and repetition rate were fixed in condition no. 7–14.

The yellow SP-14 was turned to white under exposure to UV laser with condition no. 1. Since the azobenzene group is a yellow chromophore, the color transition to white was considered a result of a change in the chemical structure of the chromophore. Under condition no. 2, in addition, the marks left by the laser scanning path were observed through an optical microscope **(Figure 4-10)**. As the laser power decreased, no obvious surface damage was observed (conditions no. 3 and 4, **Figure 4-11**). However, the tack forces were 0.22 N and 0.12 N, which were significantly lower than the maximum force (3.58 N) of SP-14 in our previous study using an LED UV light source (Lee, *et al.*, 2021).

서울대학교 SEOUL NATIONAL UNIVERSITY

Table 4-2. Probe tack results according to the variation of UV laser process parameters.

Condition No.	Power (mW)	Scan speed (m/s)	Repetition rate (kHz)	Beam size (μm)	Tack force (N)
1	80	0.50	50	13	**Surface damage**
2	40	0.50			**Surface damage**
3	30	0.50			**0.22**
4	10	0.50			**0.12**
5	10	0.25			**0.15**
6	10	0.05			**0.18**

Condition No.	Power (mW)	Scan speed (m/s)	Repetition rate (kHz)	Defocusing length (μm)	Tack force (N)
7	40	2	300	600	**0.27**
8				800	**0.25**
9				900	**0.15**
10				1100	**0.03**
11				1200	**0.00**
12				1600	**0.00**
13				2000	**0.00**
14				2400	**0.00**

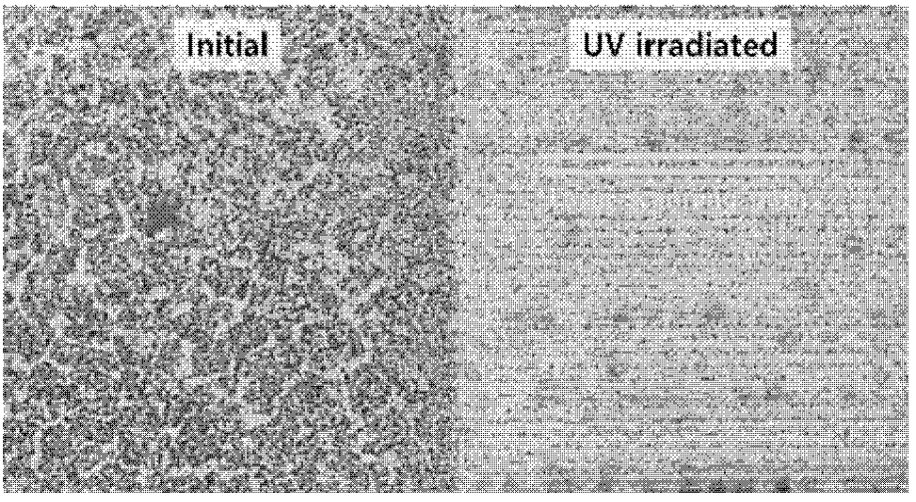

Figure 4-10. Optical microscope image of the UV laser irradiated SP-14 with process condition no. 2 (×100).

서울대학교 SEOUL NATIONAL UNIVERSITY

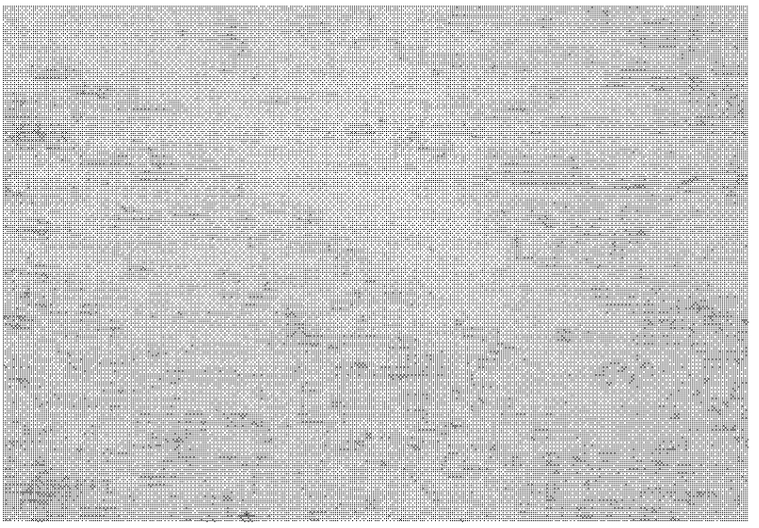

Figure 4-11. Optical microscope image of the UV laser irradiated SP-14 with process condition no. 3 (×100).

The decrease in scan speed of the UV laser induces an increase in overlapped area of the beam. Thus, the tack force increased at a slower scan speed (condition no. 4–6). The tack force of SP-14 decreased with an increase in the defocusing length (condition no. 7–14) because a longer defocusing length enlarges the beam size and weakens the energy density of the UV light. Although it was possible to observe the correlation between each process parameter and adhesive force, SP-14 had very low probe tack values under all process conditions.

The intensity of UV light emitted through the laser system was strong enough. It could damage the chemical structure of the azobenzene groups. The low adhesive force of SP-14 in various energy densities and doses, which were adjusted with process parameters, was expected to be related to the UV irradiation time. The ns pulsed UV laser does not emit light continuously, as shown in **Figure 4-12**. The pulsed laser system has a microsecond scaled interval between light emissions. However, the light emission time, tens of

서울대학교 SEOUL NATIONAL UNIVERSITY

nanoseconds, is much shorter than the interval time. Furthermore, since the laser scans the exposure area at high speed, the exposure time to UV light per unit area is extremely short. Therefore, SP-14 could not secure enough time to isomerize and break the crystalline structures of Azo-C14 under the UV laser system.

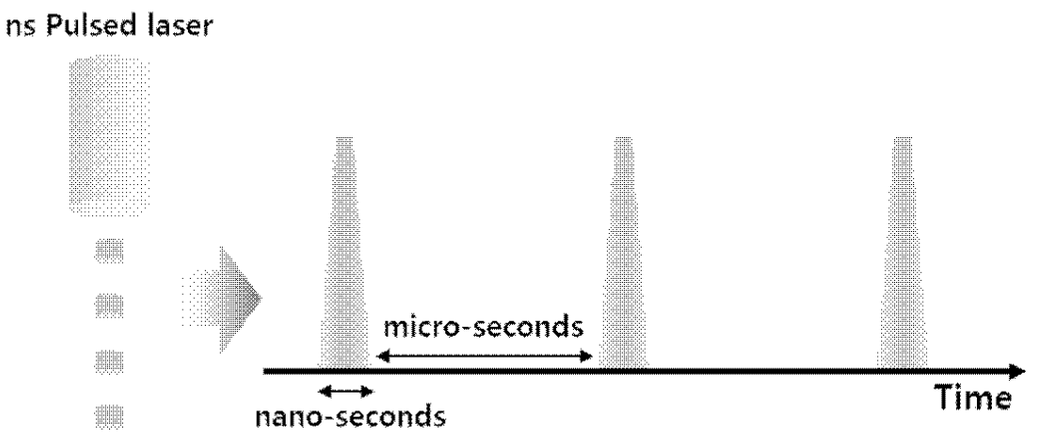

Figure 4-12. Schematic illustration of pulsed light emission of ns pulsed laser.

In order to activate the adhesion of switchable PSA in the pulsed UV laser system, it was expected that the isomerization and crystalline structure dissolution of Azo-compound should be possible even at a short time and low intensity. Therefore, we tried to realize a switchable PSA capable of adhesion switching under the UV laser system through modification of Azo-C14.

서울대학교

3.3. Experimental Strategy for Improving Photo-isomerization Efficiency of the Switchable PSA

The photo-isomerization of the azobenzene group is affected by its substituent type, number and position (Dokic, *et al.*, 2009) and by the viscosity and modulus of the surrounding substance (Gegiou, *et al.*, 1968). In our previous research, the melting temperature and enthalpy of Azo-compound were closely related to the photo-isomerization efficiency of the azobenzene-containing switchable PSA (Lee, *et al.*, 2021). Thus, we tried to weaken the crystalline structure of Azo-C14 to improve the photo-isomerization efficiency of the switchable PSA.

3.3.1. Azo-compound mixture of Azo-C6 and Azo-C14

Azo-compound can be easily stacked with pi-pi interaction between the azobenzene groups and van der Waals interaction between hydrocarbon substituents. In particular, Azo-C14 formed a stronger crystalline structure than Azo-C6 and Azo-C10 with its longer chain (Lee, *et al.*, 2021). Thus, we fabricated switchable PSAs with mixtures of Azo-C6 and Azo-C14. It was expected that Azo-C6, which has a shorter substituent, causes irregular arrangement between Azo-C14 molecules. The inhomogeneity of molecular arrangement would weaken the crystalline structure and improve photo-isomerization efficiency.

서울대학교

3.3.2. Introduction of Functional Group in Middle of Hydrocarbon Chain of Azo-compound

In addition to mixing Azo-compounds, we also introduce the urethane functional group in the middle of the hydrocarbon chain of Azo-C14. Although the urethane group can form hydrogen bonds, it was considered that it could interfere with packing between hydrocarbon chains. Thus, we synthesized Azo-U by the urethane reaction between 6-(4-(Phenyldiazenyl)phenoxy)hexan-1-ol and hexyl isocyanate.

3.3.3. Addition of UV Absorber

Finally, we used a UV absorber as an additive to improve the switchable PSA's photo-isomerization efficiency. The UV absorber absorbs UV light in a specific wavelength range and converts light energy into thermal energy (Kim, *et al.*, 2018). We expected that the thermal energy converted from UV light by the absorber would raise the switchable PSA's internal temperature, which would make the dissolution of the crystalline structure easier.

서울대학교 SEOUL NATIONAL UNIVERSITY

3.4. Adhesion Switching Efficiency of the Switchable PSAs Including Mixtures of Azo-C6 and Azo-C14

3.4.1. Melting Temperatures and Enthalpies of Azo-C6 and Azo-C14 Mixtures

The melting temperature and enthalpy of each Azo-C6 and Azo-C14 mixture were measured through DSC measurement to predict the influence on the photo-isomerization efficiency (**Figure 4-13** and **Table 4-3**). Four mixtures were prepared according to the mixing ratio of Azo-C6 and Azo-C14, 1:9, 3:7, 5:5 and 7:3.

The melting temperatures of Azo-C14 and Azo-C6 were 76.3 °C and 57.8 °C, and the melting enthalpies of Azo-C14 and Azo-C6 were 52.6 kJ/mol and 25.3 kJ/mol, respectively. When the mixing ratio of Azo-C6 and Azo-C14 was 1:9, the main melting peak moved to a lower temperature (73.4 °C) than the peak of Azo-C14, and an additional phase transition peak appeared at 46.1 °C. Two phase transition peaks indicate an intermediate phase, mesophase (Priestley, 1975) or incompatibility between materials when two or more substances are mixed. However, both cases mean that the second phase transition occurs after the first phase transition of weak intermolecular arrangement at a relatively low temperature.

When the mixing ratio of Azo-C6 was increased, the intensity of the first melting peak was increased as the peak was fixed at 46 °C, and the second melting peak at a higher temperature converged towards the first peak. The phase transition of Azo-C6 molecules dominated the first melting temperature, and the second one was dominated by Azo-C14. However, both temperatures were lower than that of each Azo-compound, and it means the partial compatibility between Azo-C6 and Azo-C14 according to the mixing ratio. The

서울대학교 SEOUL NATIONAL UNIVERSITY

mixture had one phase transition temperature and good compatibility in a 7:3 mixing ratio.

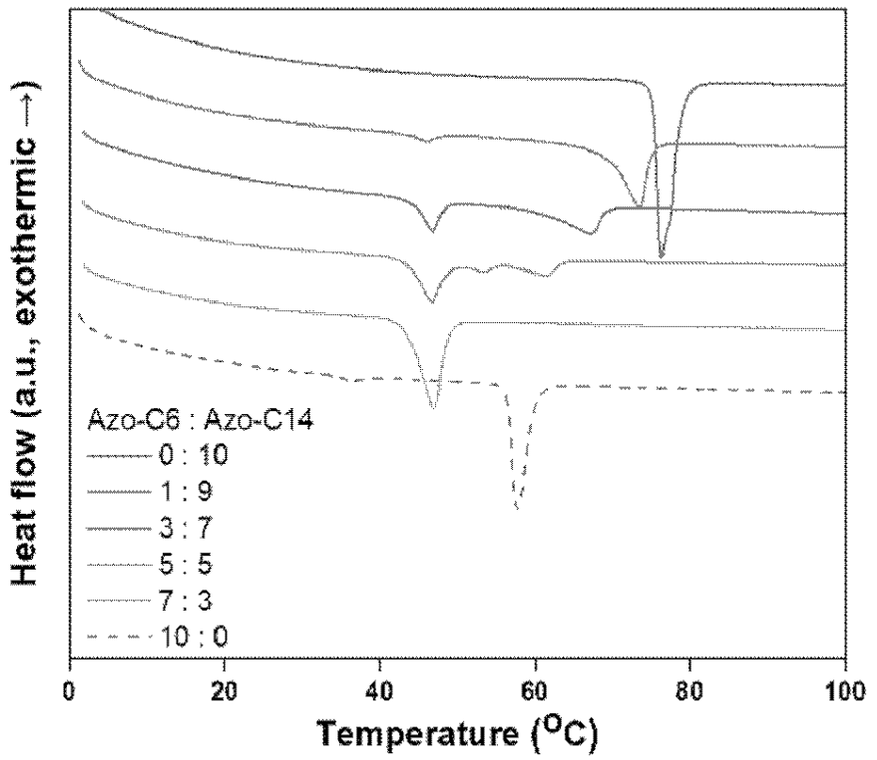

Figure 4-13. Comparison of DSC melting curves of Azo-C6 and Azo-C14 mixtures.

Table 4-3 Melting temperatures and enthalpies of Azo-C6 and Azo-C14 mixtures.

Azo-C6 : Azo-C14	T_m (°C)			Melting Enthalpy (kJ/mol)
0 : 10		76.3		52.6
1 : 9	46.1		73.4	34.0
3 : 7	46.8		67.1	24.5
5 : 5	46.7	53.4	61.6	25.6
7 : 3	47.0			28.4
10 : 0		57.8		25.3

서울대학교 SEOUL NATIONAL UNIVERSITY

Consequently, the melting temperatures of the mixtures decreased with the Azo-C6 ratio. It resulted from the weakening of the crystalline structure by compound mixing. Furthermore, the mixtures had a lower melting temperature than Azo-C6, depending on the mixing ratio. Melting enthalpy also decreased dramatically with mixing the compounds from 52.6 kJ/mol to 24.5 kJ/mol. However, the enthalpy was increased at 5:5 and 7:3 ratios, where the compatibility of Azo-C6 and Azo-C14 increased.

3.4.2. Adhesion Switching Properties of the Switchable PSAs including Azo-C6 and Azo-C14 Mixtures

We conducted a probe tack test with various UV irradiation intensities to evaluate the photo-isomerization efficiency of the switchable PSAs including Azo-C6 and Azo-C14 mixtures **(Figure 4-14)**. The UV exposure time was 5 s to observe short-time adhesion switching. The adhesive force of SP-C14 was not activated until 50 mW/cm^2 of UV light was irradiated. It had a low adhesive force of 0.2 N even at 75 mW/cm^2, and the prove tack force increased only to 2.0 N under 125 mW/cm^2 of UV irradiation intensity.

As the content of Azo-C6 in switchable PSA increased, it had higher probe tack force under the same UV intensity; The probe tack forces of SP-C6_C14-1_9 and SP-C6_C14-3:7 were 1.0 N and 1.7 N under exposure to 75 mW/cm^2 of UV light, and the maximum tack values were 2.4 N and 3.5 N at 125 mW/cm^2, respectively. However, the initial adhesive force of SP-C6_C14-5_5 was 0.2 N, which was not completely "switched off". Consequently, the photo-responsive adhesion switching efficiency was increased as the content of Azo-C6 increased. When the mixing ratio of Azo-C6 and Azo-C14 exceeded 5:5, the switchable PSA lost its switchability. However, the Azo-C6 and Azo-C14 mixture systems

서울대학교

did not lower the minimum UV intensity for activating adhesive force; 75 mW/cm^2 was the minimum UV intensity for adhesion switching in all specimens.

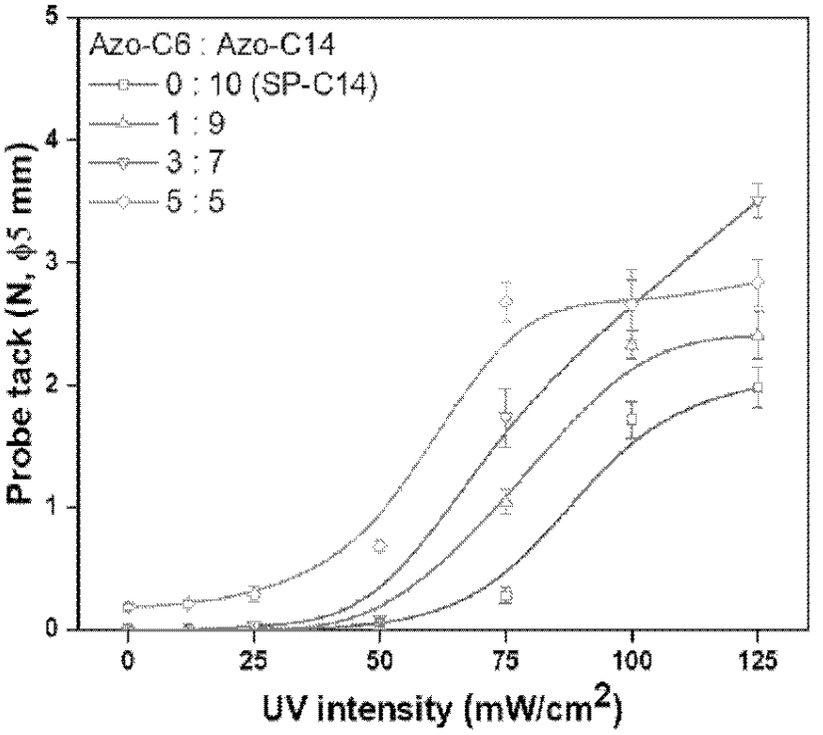

Figure 4-14. Probe tack forces of the switchable PSAs including Azo-C6 and Azo-C14 mixtures with various UV intensities.

3.5. Adhesion Switching Efficiency of the Switchable PSA with Azo-U

3.5.1. Melting Temperature and Enthalpy of Azo-U

Azo-U had two phase transition peaks at 65.2 °C and 97.5 °C **(Figure 4-15)**. The second phase transition temperature was higher than that of Azo-C14. The increase in melting temperature was due to hydrogen bonding of the urethane

서울대학교 SEOUL NATIONAL UNIVERSITY

groups in the substituent chain. However, Azo-U had the first phase transition temperature at a lower temperature than the melting temperature of Azo-C14. The melting enthalpy of Azo-U was 33.1 kJ/mol, which was lower than that of Azo-C14 (52.6 kJ/mol, **Table 4-4**).

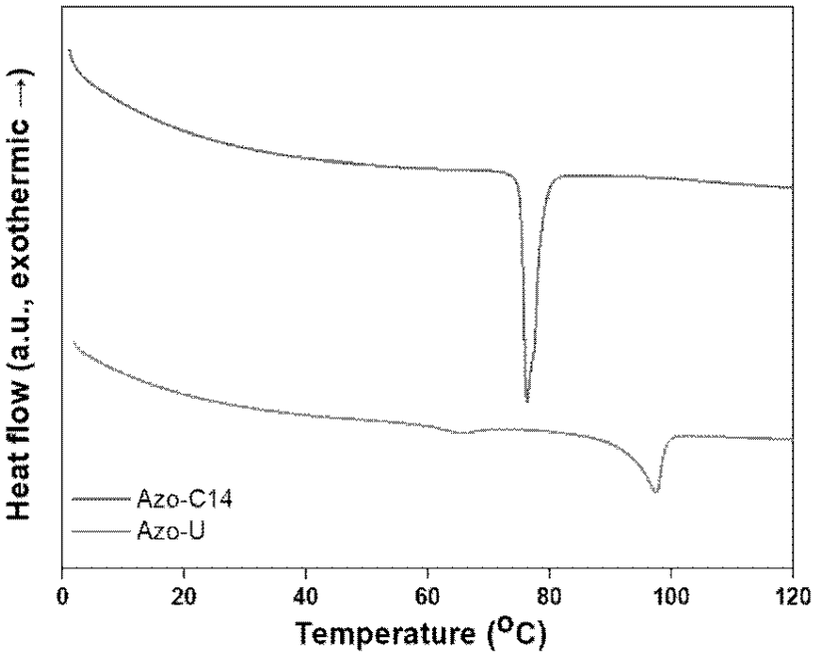

Figure 4-15. DSC melting curve of Azo-U.

Table 4-4 Melting temperature and enthalpy of Azo-U.

	T_m (°C)		Melting Enthalpy (kJ/mol)
Azo-C14	76.3		52.6
Azo-U	65.2	97.5	33.1

서울대학교 Seoul National University

3.5.2. Adhesion Switching Properties of SP-U

The adhesion switching efficiency was evaluated and compared with SP-C14, SP-C6_C14-1_9 and SP-C6_C14-3_7 **(Figure 4-16)**. The prove tack forces of SP-U were 0.3 N, 2.2 N, 4.2 N and 4.5 N from 50 mW/cm^2 to 125 mW/cm^2 of UV intensity. It had higher adhesive forces under all UV radiation conditions than other specimens. Especially, the adhesive property of SP-U was activated at 50 mW/cm^2, which did not activate the other specimen's adhesive force.

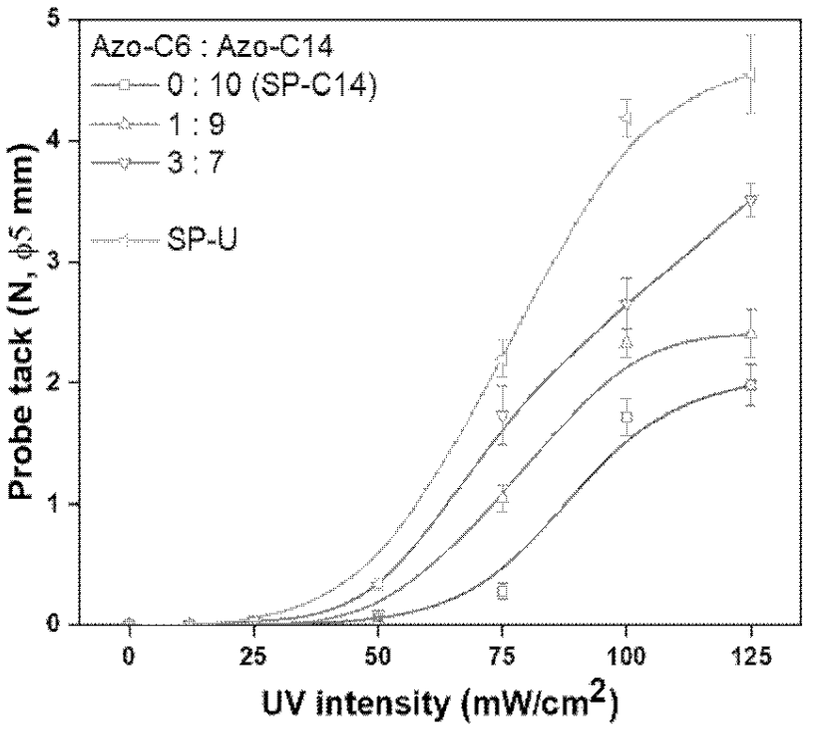

Figure 4-16. Probe tack forces of the SP-U with various UV intensities.

서울대학교 SEOUL NATIONAL UNIVERSITY

3.6. Adhesion Switching Efficiency of the Switchable PSAs with UV Absorber

3.6.1. UV Absorption Spectra of UV Absorbers

Three types of typical UV absorbers are presented in **Figure 4-17**. The chemical structures of the absorbers determine absorption wavelength and absorbance. Thus, we measured the UV absorption spectra of the UV absorbers and selected a proper absorber for the UV laser system **(Figure 4-17)**. Since the wavelength of the UV laser was 355 nm, an absorber with high absorbance for UV light at 355 nm wavelength was required. OA and BP had high absorbance for a relatively short wavelength. We chose BTA as the UV absorber for the UV laser study because of its highest absorption at 355 nm.

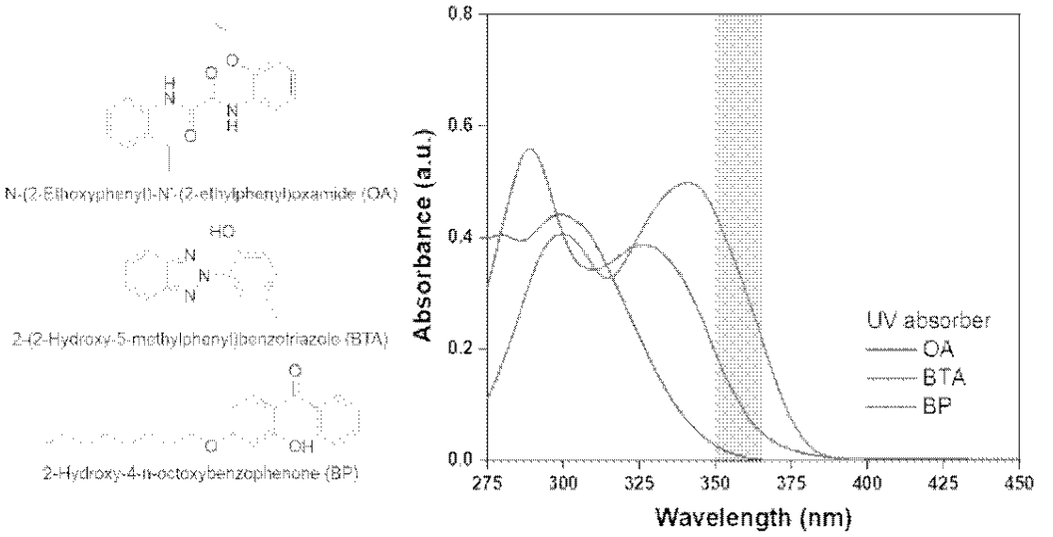

Figure 4-17. Chemical structures and UV absorption spectra of three UV absorbers.

서울대학교 SEOUL NATIONAL UNIVERSITY

3.6.2. Adhesion Switching Properties According to UV Absorber Content

SP-U had the highest adhesive forces and could be activated under the lowest UV intensity. Thus, we added the UV absorber, BTA, to the SP-U for further modification in photo-responsive adhesion switching efficiency **(Figure 4-18)**. SP-U-Ab10 shows the same probe tack tendency depending on UV intensities as SP-U. The adhesion switching efficiency increased as the absorber content increased up to 30 mol%. Although the maximum tack force of SP-U-Ab30 was reduced by 5% compared to that of SP-U, adhesion activation was possible even at 25 mW/cm^2. However, in SP-U-Ab40 and SP-U-Ab50, the adhesion switching efficiency decreased as the BTA content increased. The decrease in efficiency resulted from the inhibition of photo-isomerization of azobenzene as the amount of light absorbed by the absorber increased in the UV radiation process.

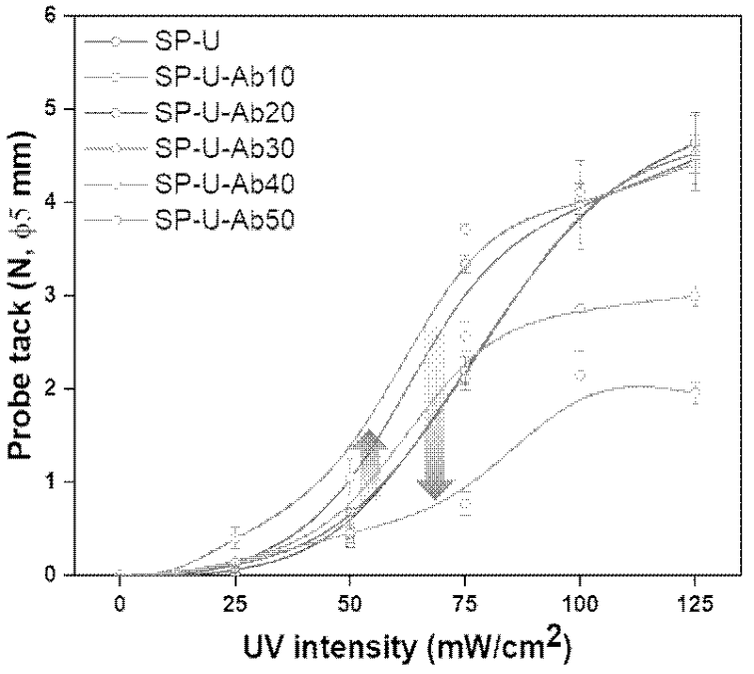

Figure 4-18. Probe tack forces of the SP-U with various UV intensities.

서울대학교

We predicted that light-to-heat energy transition by the addition of UV absorber could promote adhesion switching efficiency. Thus, we tracked specimen temperature during UV light irradiation process with a photo-DSC measurement **(Figure 4-19a)**. When specimens were irradiated with 75 mw/cm^2 of UV light, there was no difference in specimen temperature between SP-U-Ab30, which showed the highest adhesion switching efficiency, and SP-U. The specimen temperature increased by 2 °C in SP-U-Ab50. The increase in specimen temperature by the energy transition of the UV absorber was insignificant and would not stimulate dissolution of crystalline structure of Azo-U.

DSC melting curves of Azo-U and UV absorber mixtures were obtained as shown in **Figure 4-19b**. As the content of the absorber increased, the melting temperature gradually decreased. When 30 mol% of absorber was included, the melting temperature of Azo-U was 90.4 °C, which was 7 °C lower than that Azo-U itself. It was a result of the crystalline structure weakening of Azo-U in the multicomponent system as the melting temperature decreased in the Azo-compounds mixtures of Azo-C6 and Azo-C14. Consequently, the change in crystalline structure by addition of the UV absorber induced improvement of adhesion switching efficiency.

서울대학교

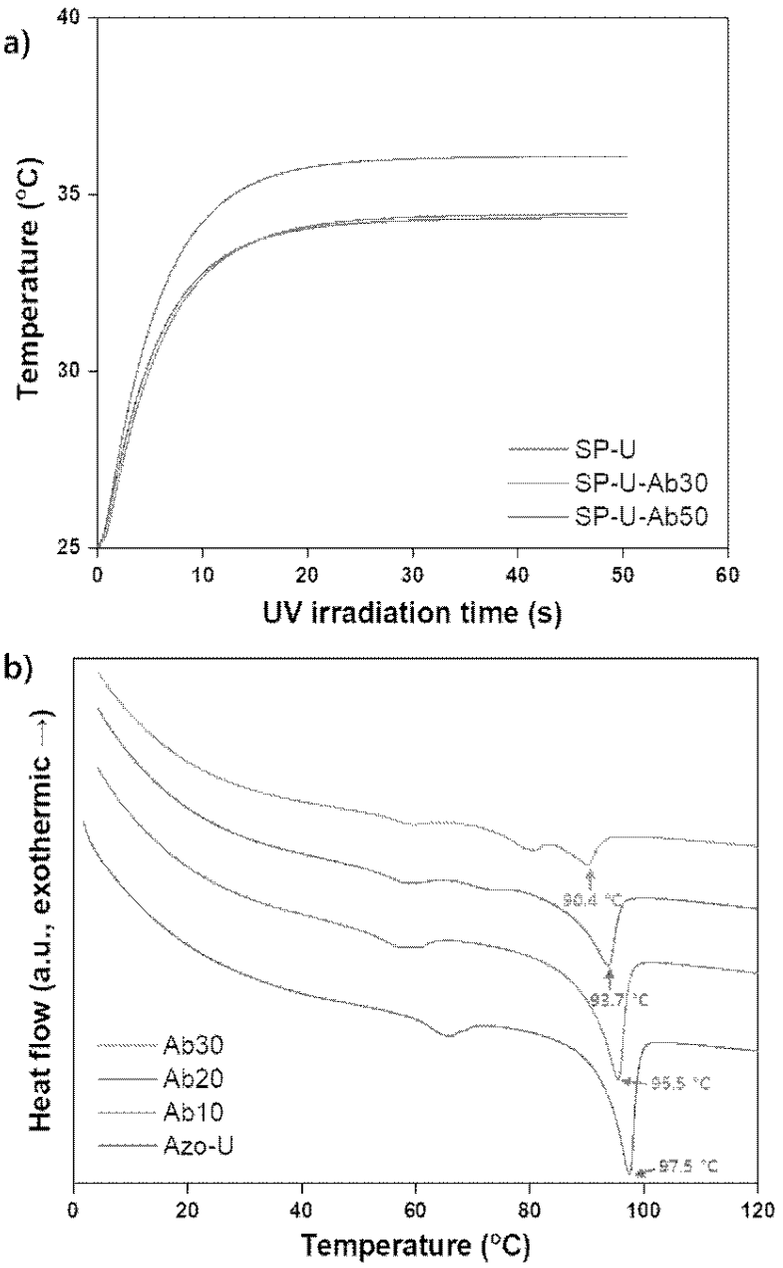

Figure 4-19. a) Temperature tracking of the switchable PSAs during UV light irradiation, b) melting curves of mixtures of Azo-U and the UV absorber.

서울대학교 SEOUL NATIONAL UNIVERSITY

The UV/Vis absorption spectra of Azo-U and the UV absorber were obtained to study the magnitude of UV light blocking by the absorber (**Figure 4-20**). The absorbance of 365 nm wavelength of Azo-U was higher than that of the UV absorber in the same molality solution. The absorbance at 365nm of BTA was 51% of that of Azo-U.

The absorbance of each Azo-U and the UV absorber in the switchable PSAs, SP-U-Ab10–50, was predicted with each absorption spectrum in **Figure 4-20 (Figure 4-21)**. The 10 mol% of UV absorber absorbed 5.7% of 365nm UV light comparing to Azo-U and did not induced change in adhesion switching efficiency in switchable PSA (**Figure 4-18**). SP-U-Ab40 and SP-U-Ab50, which showed low adhesion switching efficiency, had absorbance rates of 34.3% and 51.5%, respectively. The photo-isomerization of azobenzene groups and adhesion switching were inhibited due to the relatively high UV absorbance of the absorber in these two specimens.

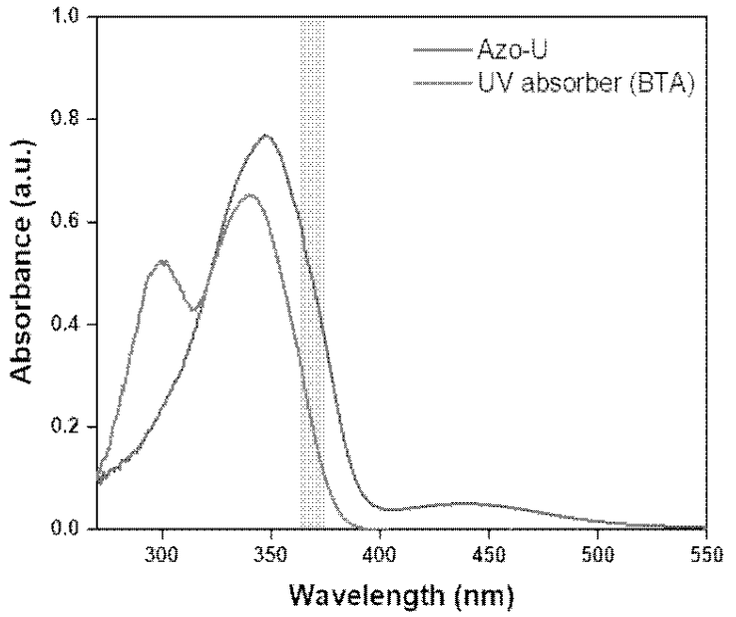

Figure 4-20. UV/Vis absorption spectra of Azo-U and UV absorber (BTA).

서울대학교

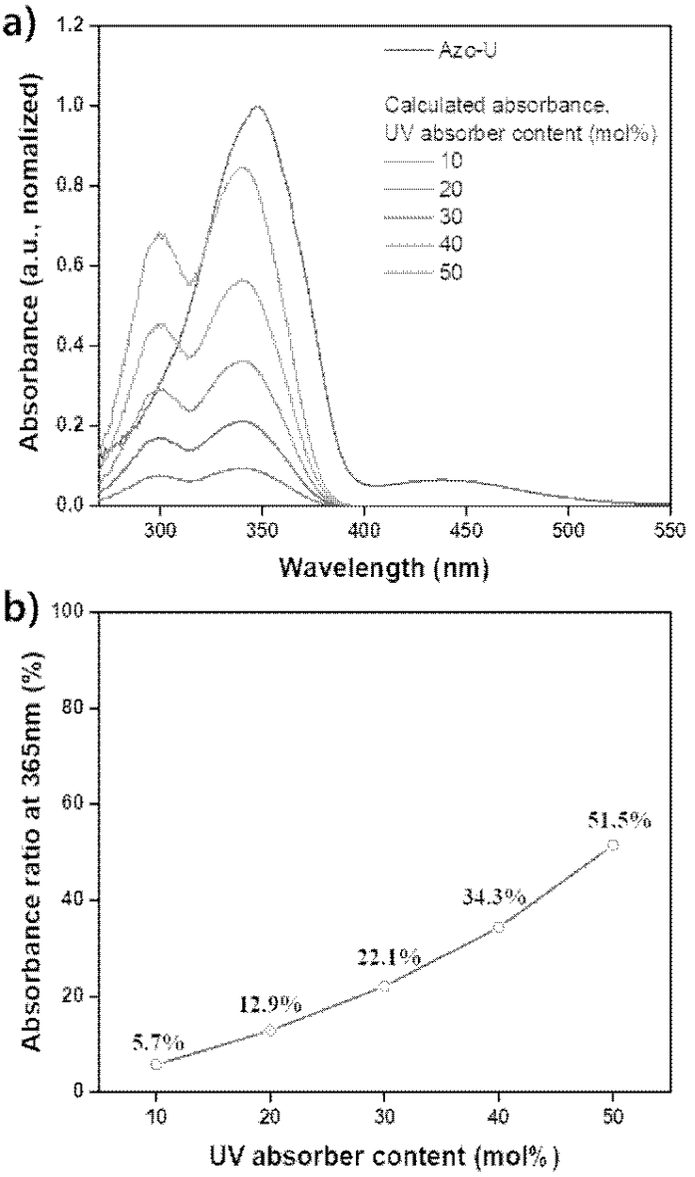

Figure 4-21. a) Comparison of normalized absorption spectrum of Azo-U and calculated absorption spectra of the UV absorber according to the absorber content, b) absorption ratio of the UV absorber at 365nm according to the content comparing to the absorption of Azo-U.

서울대학교
SEOUL NATIONAL UNIVERSITY

3.7. Adhesion Switching Test of SP-C14 and SP-U-Ab30 with UV Laser System

The alteration of Azo-compound from Azo-C14 to Azo-U and the addition of the UV absorber induced a significant increase in the adhesion switching efficiency of SP-C14 **(Figure 4-22)**. Consequently, SP-U-Ab30, which showed the highest efficiency, was used for the UV laser test.

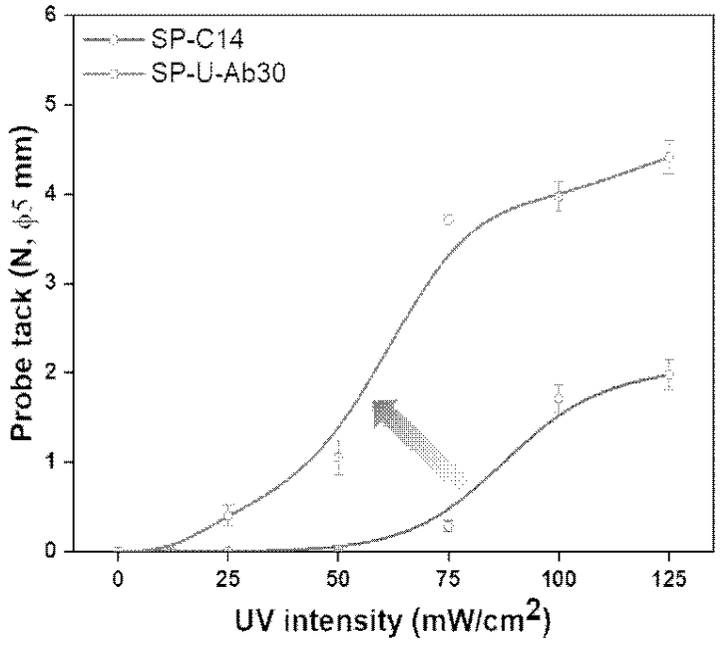

Figure 4-22. Modification in adhesion switching efficiency of SP-C14 with Azo-U and UV absorber.

서울대학교 SEOUL NATIONAL UNIVERSITY

3.7.1. Process Parameters of UV Laser System

The output power, repetition rate, beam size, pitch and scan speed were the process parameters of the UV laser system. The repetition rate was fixed as 90 kHz, the maximum rate that enabled stable irradiation in the laser system. The beam size, pitch and scan speed determine the overlap rate of the pulsed laser beam. Based on the scan progress direction, scan speed determines the distance between beams in the X-direction, and the pitch determines the distance in the Y-direction. This study set the pitch equal to the beam size to allow only the overlap between beams in the X-axis direction. Therefore, the overlap rate was calculated with repetition rate, scan speed and beam size as described in equation (1).

$$Overlap\ rate = \frac{Repetition\ rate\ (Hz)}{Scan\ speed\ (mm/s)} \times Beam\ size\ (mm), \qquad (1)$$

The light exposed from the laser system has the highest energy per unit area at the focal point. At the focal point, the beam size is minimum, and the increase in beam size and the decrease in energy per unit area occur simultaneously as the defocusing length increases. The laser is defined through the energy density because the adjustment of one process parameter varies various properties of the laser simultaneously. The energy density is calculated with the power, beam size, and overlap rate as follows:

$$\begin{aligned} &Energy\ density\ (J/cm^2) \\ &= Pulse\ energy\ density\ (J/cm^2) \times Overlap\ rate \\ &= \frac{Power\ (W)}{Repetition\ rate\ (kHz) \times Beam\ area\ (mm^2)} \times Overlap\ rate, \qquad (2) \end{aligned}$$

서울대학교 SEOUL NATIONAL UNIVERSITY

Table 4-5. Process conditions of UV laser adhesion switching test.

No.	Repetition rate (kHz)	Power (mW)	Beam Size (μm)	Scan speed (m/s)	Overlap rate	Pulse Energy density (mJ/m^2)	Energy density (J/m^2)
1	90	10	100	1	9	1.42	0.01
2				0.1	90		0.13
3				0.01	900		1.27
4			80	0.8	9	2.21	0.02
5				0.08	90		0.20
6				0.008	900		1.99
7			60	0.6	9	3.93	0.04
8				0.06	90		0.35
9				0.006	900		3.54
10			40	0.4	9	8.85	0.08
11				0.04	90		0.80
12				0.004	900		7.96
13			20	0.2	9	35.39	0.32
14				0.02	90		3.18
15	90	15	60	0.012	450	5.90	2.65
16				0.024	225		1.33
17				0.036	150		0.88
18	90	20	60	0.012	450	7.86	3.54
19				0.024	225		1.77
20				0.036	150		1.18
21				0.048	112		0.88
22				0.040	135		1.06
23				0.032	169		1.33
24				0.038	142		1.12
25				0.034	159		1.25
26	90	25	60	0.012	450	9.83	4.42
27				0.024	225		2.21
28				0.036	150		1.47
29				0.048	112		1.10
30				0.060	90		0.88
31				0.072	75		0.74
32				0.084	64		0.63
33	90	30	60	0.018	300	11.80	3.54
34				0.054	100		1.18
35				0.072	75		0.88
36				0.09	60		0.71

서울대학교 Seoul National University

3.7.2. Comparison of SP-C14 and SP-U-Ab30 in UV Laser Adhesion Switching Test

The adhesion switching properties of SP-C14 and SP-U-Ab30 using UV laser were evaluated in **Figure 4-23**. The power was fixed as 10 mW, and the pulse energy density varied from 1.4–35.4 mJ/cm^2 by adjusting the beam size. The scan speed determined the overlap rate of the UV beam as 9, 90 and 900. The 9 overlap rate means that the beam is irradiated 9 times at a point. At low overlap rates, 9 and 90, the adhesive force was not activated even at high pulse energy density, except that SP-U-Ab30 had an adhesive force of 0.3 N at 8.8 pulse energy density. Adhesion switching occurred in both SP-C14 and SP-U-Ab30 at all pulse energy densities from 1.4 mJ/cm^2 to 8.8 mJ/cm^2 with the 900 overlap rate. The adhesive force of SP-C14 increased with the increase of pulse energy density and was highest at 3.9 mJ/cm^2 (1.1 N), and it decreased at 8.8 mJ/cm^2. The activated adhesive force of SP-U-Ab30 increased with pulse energy density from 1.4 mJ/cm^2 to 8.8 mJ/cm^2. The maximum adhesive force was 1.1 N at 8.8 mJ/cm^2 pulse energy density. At 35.4 mJ/cm^2 pulse energy density, the 900 overlap rate test was not conducted. In order to overlap the 20 μm beam size 900 times, the scan speed had to be 2 mm/s and was too slow for the laser irradiation process.

In comparing SP-C14 and SP-U-Ab30, SP-C14 had higher tack forces at low pulse energy density, and SP-U-Ab30 had higher adhesive force at 8.8 mJ/cm^2 pulse energy density. The result was different from the test using the LED lamp; The adhesive force of SP-U-Ab30 was activated at a lower intensity and was higher than that of SP-C14. It was considered that the UV absorber hindered UV absorption of azobenzene groups rather than the light-to-thermal energy transition in the short UV pulse (19 ns) at low pulse energy density.

서울대학교 SEOUL NATIONAL UNIVERSITY

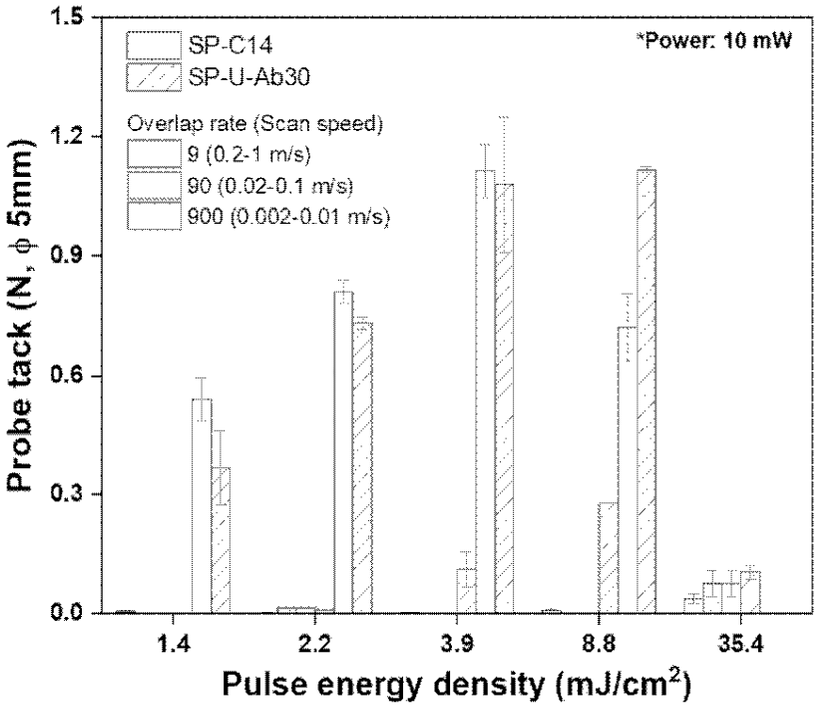

Figure 4-23. Adhesion switching test of SP-C14 and SP-U-Ab30 with UV laser according to pulse energy densities and overlap rates (power:10 mW).

The adhesion switching by laser system required a high overlap rate. However, the scan speed had to be slow for the high overlap rate. Thus, the laser output power was increased from 10 mW to 20 mW for the faster process **(Figure 4-24)**. The pulse energy density was fixed as 7.9 mJ/cm^2. The overlap rates were adjusted from 110 to 450 with 0.012–0.048 m/s of scan speeds. SP-C14 and SP-U-Ab30 had similar tack forces at overlap rates of 110, 225 and 450. However, the adhesive force of SP-U-Ab30 at a 150 overlap rate was twice higher than that of SP-C14. Furthermore, surface defects of SP-C14 were observed under all laser irradiation conditions **(Figure 4-25)**. The mark of the laser scan path was left on the surface, but the defect was not clearly observed in SP-U-Ab30. Especially, no defects remained on SP-U-Ab30 under the overlap rate of 150, which had the highest adhesive force **(Figure 4-25f)**.

서울대학교

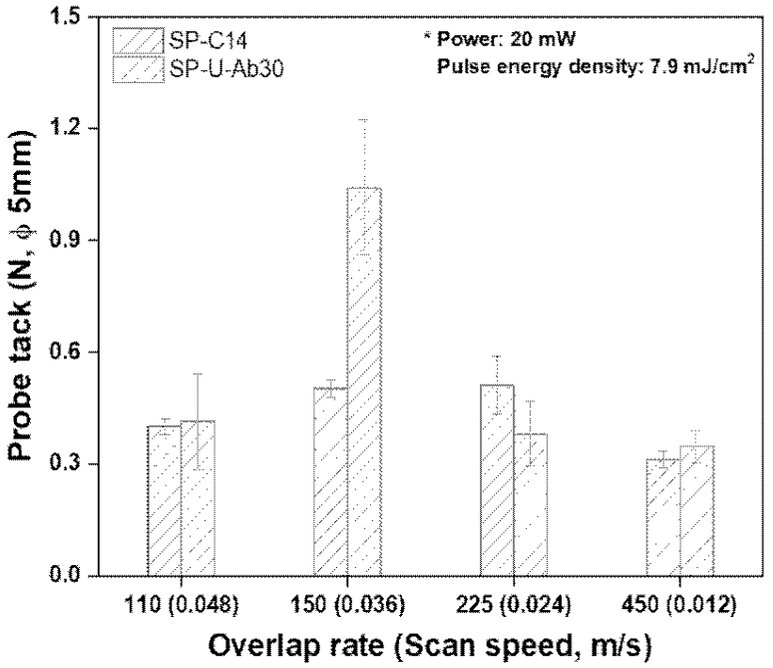

Figure 4-24. Adhesion switching test of SP-C14 and SP-U-Ab30 with UV laser according to overlap rates (power:20 mW, pulse energy density: 7.9 mJ/cm^2).

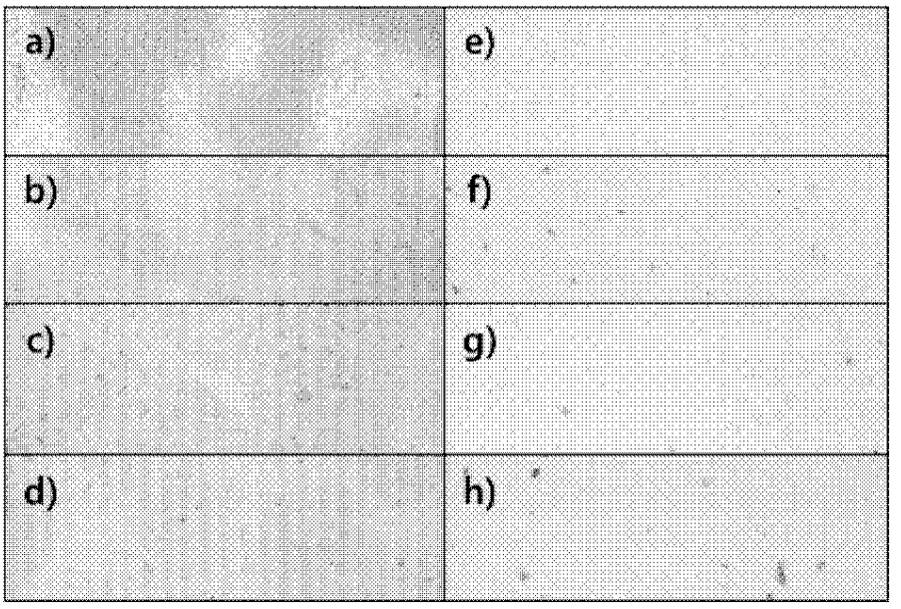

Figure 4-25. Optical microscope images of UV irradiated PSA surfaces. a), b), c) and d) were surfaces of SP-C14 irradiated with 110, 150, 225 and 450 overlap rates. e), f), c) and d) were surfaces of SP-U-Ab30 (×100).

서울대학교

Even in the adhesion switching test of 20 mW power laser irradiation, SP-U-Ab30 did not have higher adhesion switching efficiency than SP-C14. However, SP-U-Ab30 had stronger resistance to laser-induced surface defects than SP-C14. It was estimated that the UV absorber dispersed the high energy of the UV laser and prevented surface defects. The adhesive force of both switchable PSAs was sufficiently activated with 0.004–0.006 m/s of scan speed under a 10 mW power laser test. However, the adhesive force of SP-U-Ab30 could be activated to 1.0 N with 6 to 10 times faster scan speed (0.036 m/s) without surface defects under 20 mW power. Therefore, it was determined that the SP-U-Ab30 with laser defect resistance would be more suitable for the UV laser process, and additional tests were performed to optimize the process conditions with SP-U-Ab30.

3.7.3. Optimization of the UV Laser Radiation Conditions

The probe tack forces of SP-U-Ab30 were measured with various UV laser irradiation conditions, and the adhesive forces were plotted according to the energy density and power, as shown in **Figure 4-26**. The energy densities were in the range of 0.01–4.42 J/cm^2, and the powers were divided into three ranges: 10 mW, 15–20 mW and 25–30 mW. A linear relationship between the energy density and tack force was not observed. However, the switchable PSA had relatively high adhesive forces with a specific energy density range, 1.0-1.5 J/cm^2. In addition, low adhesive forces were measured in the overall energy density under high laser power, 25–30 mW. The relatively high adhesive forces were observed in the output power range of 15–20 mW. Consequently, the optimum process condition was described in **Table 4-6**, and the adhesive force was 1.0 N under the process condition.

서울대학교

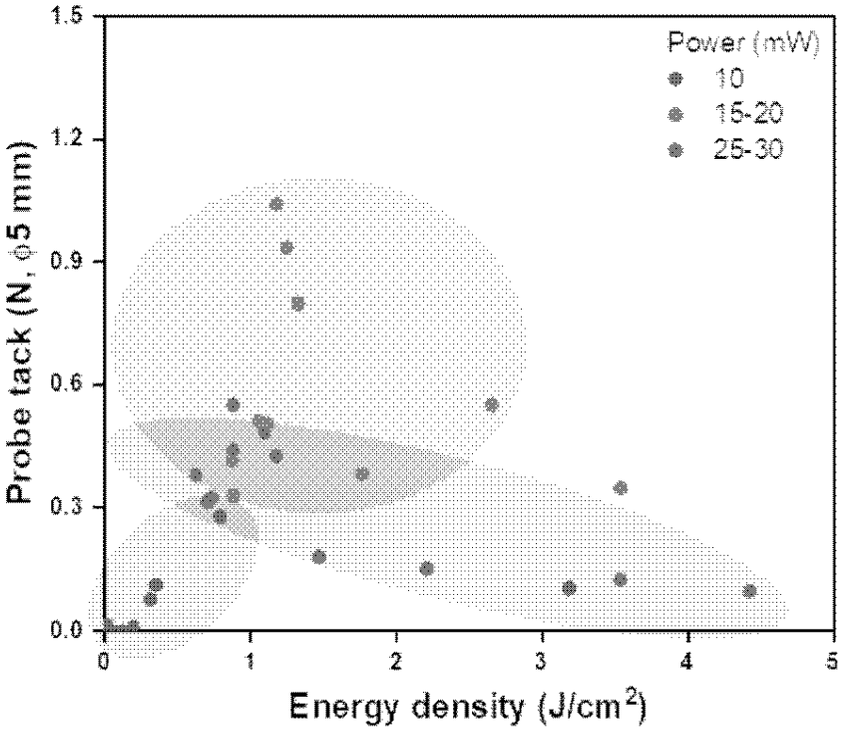

Figure 4-26. Photo-activated probe tack forces of SP-U-Ab30 plotted by the energy densities and powers of the UV laser radiation conditions.

Table 4-6. Optimum process condition of UV laser adhesion switching test.

No.	Repetition rate (kHz)	Power (mW)	Beam Size (μm)	Scan speed (m/s)	Overlap rate	Pulse Energy density (mJ/m^2)	Energy density (J/m^2)
20	90	20	60	0.036	**150**	**7.86**	**1.18**

서울대학교

3.8. Selective Mini-LED Transfer Process Using the UV Laser System

One of the advantages of using the laser system instead of an LED lamp is forming a micro-pattern on the switchable PSA. We fabricated a fine and complex pattern on the switchable PSA using the UV laser system, as shown in **Figure 4-27a**. The micro-patterned adhesion switching makes selective picking in mini-LEDs arrays possible. It enables the selective transfer of the mini-LEDs of a specific color or position on demand. 100 μm × 200 μm of LEDs were arranged with distances of 2mm in X- and Y-directions between each LED **(Figure 4-27b)**. The selective adhesion switching pattern consisted of a square pattern of 300 μm × 300 μm and 4mm distances in X- and Y-directions **(Figure 4-27c)**.

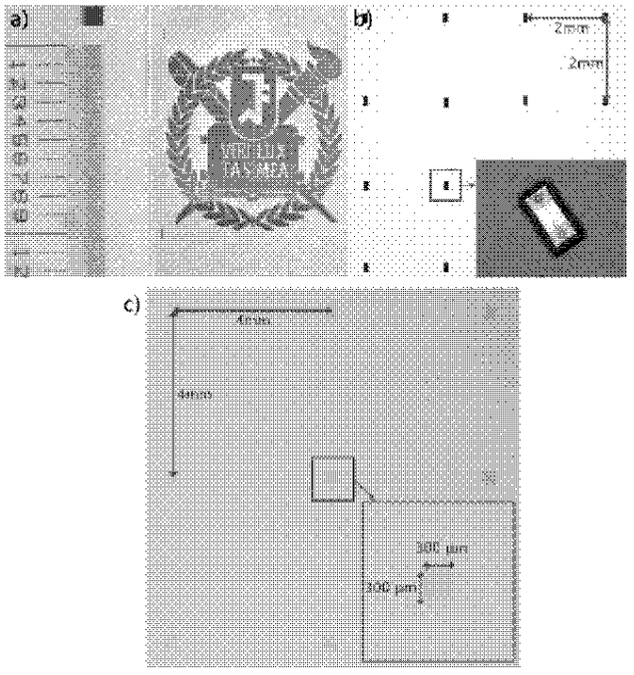

Figure 4-27. a) Fine pattern formed by UV laser irradiation, b) mini-LED and mini-LEDs array on the carrier PSA, c) surface of SP-U-Ab30 with micro-patterned selective adhesion switching.

서울대학교 SEOUL NATIONAL UNIVERSITY

We realized the selective transfer of mini-LEDs using SP-U-Ab30 with patterned adhesion activation **(Figure 4-28)**. The switchable PSA irradiated with UV laser was placed on a stage that can move Z-axis. After attaching the mini-LEDs array to a glass wafer, the glass wafer was placed on a surrounding vacuum chuck. The positions of the activated micro-pattern of the switchable PSA and mini-LEDs were aligned by moving the glass wafer in X- and Y-axis directions. The aligning process was conducted through observation with an optical microscope. The stage was raised in the z-direction to attach the mini-LED array to the PSA, and it was confirmed that the mini-LEDs were transferred only to the activated pattern. Finally, after switching off adhesive force using a visible light LED lamp, the mini-LEDs were successfully transferred to the PDMS substrate.

서울대학교 SEOUL NATIONAL UNIVERSITY

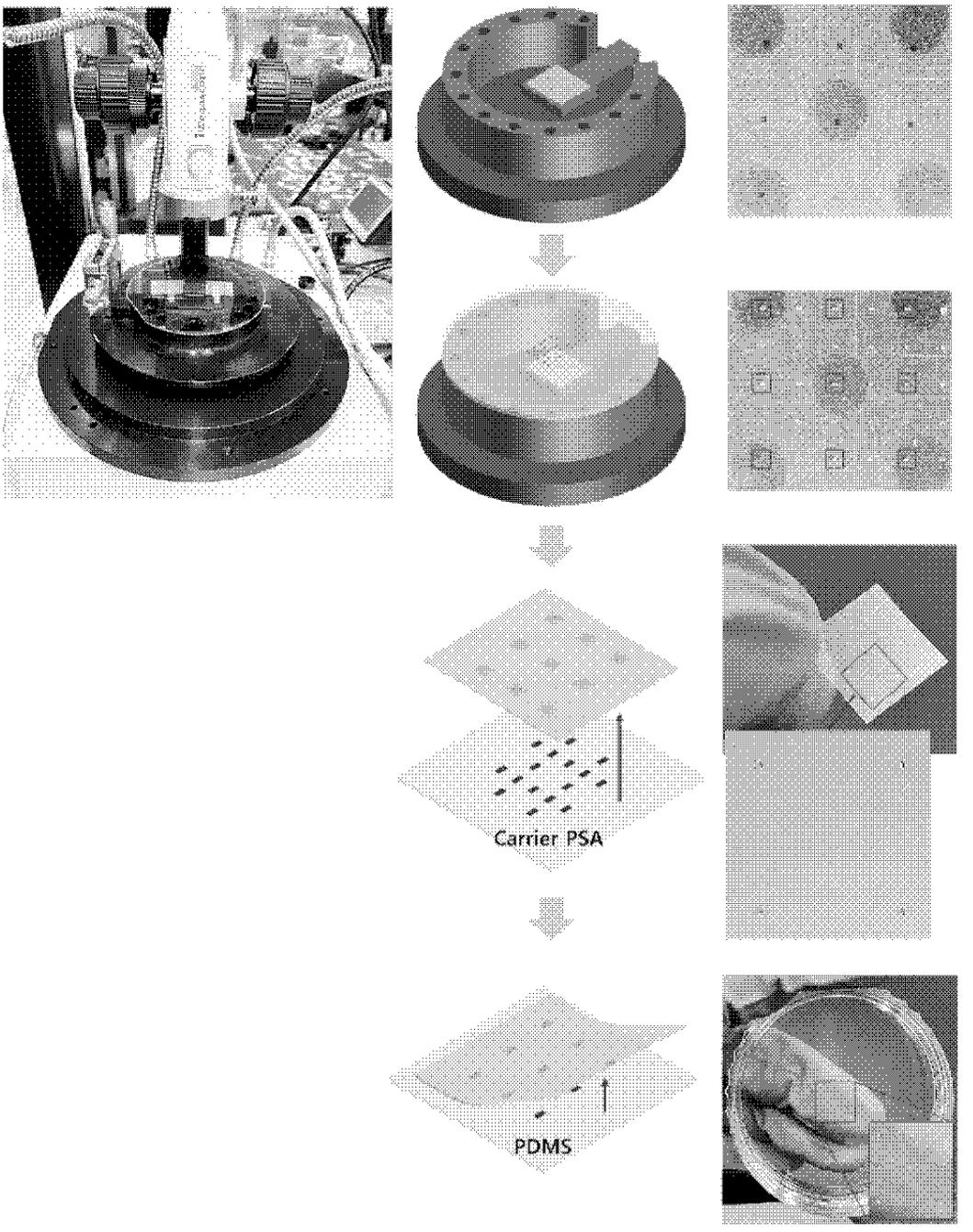

Figure 4-28. Selective mini-LED transfer process with SP-U-Ab30 using the UV laser system.

서울대학교

4. Conclusions

We fabricated switchable PSAs capable of adhesion switching through the 355 nm ns pulsed laser system and derived optimal laser irradiation conditions. We expected that switchable PSA should have high light-induced adhesion switching efficiency for the laser process because the pulsed UV laser is irradiated to a unit area for a very short time. Thus, we synthesized Azo-U and used the UV absorber as an additive to improve the photo-adhesion switching efficiency of previously studied SP-C14. SP-U-Ab30 was selected as a switchable PSA for the laser process. The adhesive force of SP-U-Ab30 could be activated at lower UV intensity and was higher under the same intensity than that of SP-C14. The UV laser irradiation process was controlled with four parameters, repetition rate, power, beam size and scan speed. The overlap rate and energy density were calculated through the parameters, and the characteristics of the laser were defined through these two factors. In the adhesion switching test using the UV laser, SP-U-Ab30 did not have better efficiency than SP-C14 but had higher resistance to laser-induced surface defects. We determined the optimal laser irradiation condition with SP-U-Ab30. Finally, we successfully realized the selective mini-LED transfer by micro-patterned adhesion switching. Although this study has limitations in that our transfer system was not applied to the large-scale transfer process and the manufacturing process of electronic devices, it is expected that our system has the potential for a new type of LED transfer method.

서울대학교 SEOUL NATIONAL UNIVERSITY

Chapter 5

Overall Conclusions

서울대학교
SEOUL NATIONAL UNIVERSITY

1. Overall Conclusions

The objective of this study was the realization of 1) photo-responsive, 2) switchable in the dried state and 3) reusable switchable PSA. In addition, it was also attempted to develop a fast and selective light irradiation process using the UV laser system. The switchable PSAs studied in this research had a non-sticky surface in the initial state; These adhesive forces were activated under exposure to UV light of 365 nm or 355 nm wavelength. Then, the activated switchable PSA was switched off again and returned to the initial state by irradiation with visible light. The UV-induced adhesion switching occurred within only 5 s with the LED lamp or 3 μs with the laser system. The adhesion switching was repeatable, and it was ensured that there was no change in adhesive force up to 30 times. The selective mini-LED transfer process was possible by partial UV irradiation on the switchable PSA. Consequently, the switchable PSA system was expected to be applied in the transfer process of microelectronic devices, including mini-LEDs.

1.1. Fabrication of Novel Photo-responsive Switchable PSA

The switchable PSAs consisted of azobenzene-containing acrylic polymer (Azo-polymer) as a matrix and low molecular weight compounds (Azo-compounds) as photo-responsive additives. Azo-polymer had 8 mol% of azobenzene and 92 mol% of butyl side groups. The T_g of Azo-polymer was low at -10.2 °C because of the high butyl acrylate ratio; It made the switchable PSA sticky in the "switched on" state and provided free volume required for the photo-isomerization of azobenzene groups. In addition, the 8 mol% of azobenzene groups interacted with Azo-compounds and enabled stable

서울대학교

dispersion of Azo-compounds in the switchable PSAs.

Five Azo-compounds, Azo-C6, Azo-C10, Azo-C14, Azo-C18 and Azo-U, were used in this study. The azobenzene groups of Azo-compounds were photo-isomerized between trans- and cis-form with UV and visible light irradiation even in the dried film state.

1.2. Adhesion Switching Mechanism and Influence of Chemical Structures of Azo-compounds

Azo-compounds formed crystalline structures in the switchable PSAs by pi-pi interaction of benzene groups and van der Waals force of hydrocarbon chain substituents. The UV-induced trans-to-cis isomerization of the azobenzene groups led to the dissolution of the crystalline structures. It caused transitions in mechanical properties, T_g and surface energy of the PSAs. Finally, the adhesion switching occurred.

The chemical structures of Azo-compounds determined the regularity of the molecular arrangement and solidity of the crystalline structures. Azo-C6, which had the shortest hydrocarbon chain as a substituent, did not form the crystalline structure in the PSA and did not induce adhesion switchability. Conversely, adhesion switching did not occur sufficiently in SP-C18 due to the high solidity of the crystalline structure of Azo-C18. By understanding the relationship between the solidity of the crystalline structure and adhesion switching properties, the efficiency of the photo-responsive adhesion switching could be improved. The efficiency improvement was realized by mixing two Azo-compounds or introducing a functional group in the substituent that disturbs the molecular packing of the hydrocarbon chain.

서울대학교

1.3. Influence of UV Light Emission Sources on the Adhesion Switching: LED Lamp and Laser System

The LED lamp irradiates UV light continuously to a large area, and the process condition is controlled by light intensity and irradiation time. The adhesion switching properties and process condition (intensity and time) had a linear relationship in the control range of this study; the switchable PSAs had high adhesive force at high UV intensity and long irradiation time. As the UV irradiation process for switchable PSA, the LED lamp enabled the large area irradiation process with the simplicity of process condition control.

On the other hand, the UV light is pulsed and concentrated in a very small area through the laser system. Since light is irradiated for only 19 ns in one pulse of UV irradiation, it was difficult to secure sufficient time for the switchable PSAs to induce crystalline dissolution by photo-isomerization. In addition, since the concentrated UV light had a high energy density, an increase in laser power damaged the PSA surface. Securing a high overlap rate in a low power condition made adhesion switching possible. However, there was no linear relationship between process parameters and adhesion switchability. The optimum condition was derived from a specific energy density and power range. As the UV irradiation process for switchable PSA, the laser system enabled the selective adhesion switching process for μm-scaled adherents because several to tens of μm patterns can be formed with the laser system.

서울대학교

References

서울대학교
SEOUL NATIONAL UNIVERSITY

Agolini, F. and Gay, F. P., 1970, Synthesis and properties of azoaromatic polymers, *Macromolecules*, **3** (3): 349-351

Akiyama, H. and Yoshida, M., 2012, Photochemically reversible liquefaction and solidification of single compounds based on a sugar alcohol scaffold with multi azo-arms, *Adv. Mater.*, **24** (17): 2353-2356

Akiyama, H., Kanazawa, S., Okuyama, Y., Yoshida, M., Kihara, H., Nagai, H., Norikane, Y. and Azumi, R., 2014, Photochemically reversible liquefaction and solidification of multiazobenzene sugar-alcohol derivatives and application to reworkable adhesives, *ACS Appl. Mater. Interfaces*, **6** (10): 7933-7941

Akiyama, H., Fukata, T., Yamashita, A., Yoshida, M. and Kihara, H., 2016, Reworkable adhesives composed of photoresponsive azobenzene polymer for glass substrates, *J. Adhes.*, **93** (10): 823-830

Akiyama, H., Okuyama, Y., Fukata, T. and Kihara, H., 2018, Reversible photocuring of liquid hexa-anthracene compounds for adhesive applications, *J. Adhes.*, **94** (10): 799-813

Barrett, C., Natansohn, A. and Rochon, P., 1995, Cis-trans thermal isomerization rates of bound and doped azobenzenes in a series of polymers, *Chem. Mater.*, **7**: 899-903

Barrett, C. J., Mamiya, J. I., Yager, K. G. and Ikeda, T., 2007, Photo-mechanical effects in azobenzene-containing soft materials, *Soft Matter*, **3** (10): 1249-1261

Beharry, A. A. and Woolley, G. A., 2011, Azobenzene photoswitches for

서울대학교 SEOUL NATIONAL UNIVERSITY

biomolecules, *Chem. Soc. Rev.*, **40** (8): 4422-4437

Bignozzi, M. C., Angeloni, S. A., Laus, M., Incicco, L., Francescangeli, O., Wolff, D., Galli, G. and Chiellini, E., 1999, Liquid crystal poly(glycidyl ether)s by anionic polymerization and polymer-analogous reaction, *Polym. J.*, **31** (11): 913-919

Boyne, J. M., Millan, E. J. and Webster, I., 2001, Peeling performance of a novel light switchable pressure-sensitive adhesive, *Int. J. Adhes. Adhes.*, **21** (1): 49-53

Brzozowski, L. and Sargent, E. H., 2001, Azobenzenes for photonic network applications: third-order nonlinear optical properties, *J. Mater. Sci.: Mater. Electron.*, **12** (9): 483-489

Chang, E. P., 1991, Viscoelastic windows of pressure-sensitive adhesives, *J. Adhes.*, **34** (1-4): 189-200

Chiu, H.-T. and Wu, J.-H., 2007, A Study on the curing behavior of silicone/polyurethane/epoxy blends by rigid-body pendulum rheometer, *Polym. Plast. Technol. Eng.*, **45** (9): 1081-1085

Cho, K., Cho, J. H., Yoon, S., Park, C. E., Lee, J.-C., Han, S.-H., Lee, K.-B. and Koo, J., 2003, Switchable tack in side-chain liquid crystalline polymers, *Macromolecules*, **36** (9): 2009-2014

Choi, M., Jang, B., Lee, W., Lee, S., Kim, T. W., Lee, H.-J., Kim, J.-H. and Ahn, J.-H., 2017, Stretchable active matrix inorganic light-emitting diode display

서울대학교

enabled by overlay-aligned roll-transfer printing, *Adv. Funct. Mater.*, **27** (11): 1606005

Creton, C., 2003, Pressure-sensitive adhesives: an introductory course, *MRS bull.*, **28** (6): 434-439

Creton, C. and Ciccotti, M., 2016, Fracture and adhesion of soft materials: a review, *Rep. Prog. Phys.*, **79** (4): 46601

Croll, A. B., Hosseini, N. and Bartlett, M. D., 2019, Switchable adhesives for multifunctional interfaces, *Adv. Mater. Technol.*, **4** (8): 1900193

De Crevoisier, G., Fabre, P., Corpart, J.-M. and Leibler, L., 1999, Switchable tackiness and wettability of a liquid crystalline polymer, *Science*, **285** (5431): 1246-1249

Ding, K., Avrutin, V., Izyumskaya, N., Özgür, Ü. and Morkoç, H., 2019, Micro-LEDs, a manufacturability perspective, *Appl. Sci.*, **9** (6): 1206

Dokic, J., Gothe, M., Wirth, J., Peters, M. V., Schwarz, J., Hecht, S. and Saalfrank, P., 2009, Quantum chemical investigation of thermal cis-to-trans isomerization of azobenzene derivatives: substituent effects, solvent effects, and comparison to experimental data, *J. Phys. Chem. A*, **113** (24): 6763–6773

Donatas, S., Handbook of pressure sensitive adhesive technology, 1999, Satas & Associates, Rhode Island, USA.

Dubey, A. K. and Yadava, V., 2008, Laser beam machining—A review, *Int. J. Mach. Tools Manuf.*, **48** (6): 609-628

서울대학교

Ebe, K., Seno, H. and Horigome, K., 2003, UV curable pressure-sensitive adhesives for fabricating semiconductors. I. development of easily peelable dicing tapes, *J. Appl. Polym. Sci.*, **90** (2): 436–441

Eisenhaure, J. and Kim, S., 2016, Laser-driven shape memory effect for transfer printing combining parallelism with individual object control, *Adv. Mater. Technol.*, **1** (7):

Eisenhaure, J. D., Xie, T., Varghese, S. and Kim, S., 2013, Microstructured shape memory polymer surfaces with reversible dry adhesion, *ACS Appl. Mater. Interfaces*, **5** (16): 7714-7717

Gao, Y., Wu, K. and Suo, Z., 2019, Photodetachable adhesion, *Adv. Mater.*, **31** (6): 1806948

Gegiou, D., Muszkat, K. A. and Fischer, E., 1968, Temperature dependence of photoisomerization. VI. Viscosity effect., *J. Am. Chem. Soc.*, **90** (1): 12-18

Gegiou, D., Muszkat, K. A. and Fischer, E., 1968, Temperature dependence of photoisomerization. V. Effect of substituents on the photoisomerization of stilbenes and azobenzenes, *J. Am. Chem. Soc.*, **90**: 3907-3918

Goulet-Hanssens, A., Eisenreich, F. and Hecht, S., 2020, Enlightening materials with photoswitches, *Adv. Mater.*, **32** (20): 1905966

Härth, M. and Schubert, D. W., 2012, Simple approach for spreading dynamics of polymeric fluids, *Macromol. Chem. Phys.*, **213** (6): 654-665

Heinzmann, C., Coulibaly, S., Roulin, A., Fiore, G. L. and Weder, C., 2014,

서울대학교

Light-induced bonding and debonding with supramolecular adhesives, *ACS Appl. Mater. Interfaces*, **6** (7): 4713-4719

Hvilsted, S., Andruzzi, F., Kulinna, C., Siesler, H. W. and Ramanujam, P. S., 1995, Novel side-chain liquid crystalline polyester architecture for reversible optical storage, *Macromolecules*, **28** (7): 2172—2183

Hwang, J. W., Kim, K. N., Lee, G. S., Nam, J. H., Noh, S. M. and Jung, H. W., 2013, Rheology and curing characteristics of dual-curable automotive clearcoats using thermal radical initiator derived from O-imino-isourea and photo-initiator, *Prog. Org. Coat.*, **76** (11): 1666-1673

Ichimura, K., Oh, S.-K. and Nakagawa, M., 2000, Light-driven motion of liquids on a photoresponsive surface, *Science*, **288** (5471): 1624-1626

Ito, S., Akiyama, H., Sekizawa, R., Mori, M., Yoshida, M. and Kihara, H., 2018, Light-induced reworkable adhesives based on ABA-type triblock copolymers with azopolymer termini, *ACS Appl. Mater. Interfaces*, **10** (38): 32649-32658

Ito, S., Yamashita, A., Akiyama, H., Kihara, H. and Yoshida, M., 2018, Azobenzene-based (meth)acrylates: controlled radical polymerization, photoresponsive solid–liquid phase transition behavior, and application to reworkable adhesives, *Macromolecules*, **51** (9): 3243-3253

Ito, S., Akiyama, H., Mori, M., Yoshida, M. and Kihara, H., 2019, Azobenzene-containing triblock copolymer adhesive based on light-induced solid–liquid phase transition: application to bonding for various substrates, *Macromol. Chem. Phys.*, **220** (12): 1900105

서울대학교 SEOUL NATIONAL UNIVERSITY

Ito, S., Akiyama, H., Sekizawa, R., Mori, M., Fukata, T., Yoshida, M. and Kihara, H., 2019, Azobenzene-containing block copolymers as light-induced reworkable adhesives: effects of molecular weight, composition, and block copolymer architectures on the adhesive properties, *J. Polym. Sci. A: Polym. Chem.*, **57** (7): 806-813

Izumi, A., Teraguchi, M., Nomura, R. and Masuda, T., 2000, Synthesis of poly(p-phenylene)-based photoresponsive conjugated polymers having azobenzene units in the main chain, *Macromolecules*, **33** (15): 5347-5352

Jenekhe, S. A. and Roberts, M. F., 1993, Effects of intermolecular forces on the glass transition of polymers, *Macromolecules*, **26**: 4981-4983

Kamperman, M. and Synytska, A., 2012, Switchable adhesion by chemical functionality and topography, *J. Mater. Chem.*, **22** (37):

Kaur, G., Johnston, P. and Saito, K., 2014, Photo-reversible dimerisation reactions and their applications in polymeric systems, *Polym. Chem.*, **5** (7): 2171-2186

Kendall, K., 1971, The adhesion and surface energy of elastic solids, *J. Phys. D: Appl. Phys.*, **4** (8): 1186

Kendall, K., 1975, Thin-film peeling - the elastic term, *J. Phys. D: Appl. Phys.*, **8** (13): 1449

Kim, J.-H., Kim, B.-C., Lim, D.-W. and Shin, B.-C., 2019, Control of adhesion force for micro LED transfer using a magnetorheological elastomer, *J. Mech.*

서울대학교

Sci. Technol., **33** (11): 5321-5325

Kim, J. U., Lee, S., Kang, S. J. and Kim, T. I., 2018, Materials and design of nanostructured broadband light absorbers for advanced light-to-heat conversion, *Nanoscale*, **10** (46): 21555-21574

Kim, T.-H., Carlson, A., Ahn, J.-H., Won, S. M., Wang, S., Huang, Y. and Rogers, J. A., 2009, Kinetically controlled, adhesiveless transfer printing using microstructured stamps, *Appl. Phys. Lett.*, **94** (11):

Kortekaas, L., Simke, J., Kurka, D. W. and Ravoo, B. J., 2020, Rapid photoswitching of low molecular weight arylazoisoxazole adhesives, *ACS Appl. Mater. Interfaces*, **12** (28): 32054-32060

Kumar, G. S. and Neckers, D. C., 1989, Photochemistry of azobenzene-containing polymers, *Chem. Rev.*, **89** (8): 1915-1925

La Spina, R., Tomlinson, M. R., Ruiz-Pérez, L., Chiche, A., Langridge, S. and Geoghegan, M., 2007, Controlling network–brush interactions to achieve switchable adhesion, *Angew. Chem.*, **119** (34): 6580-6583

Ladanyi, V., Dvorak, P., Al Anshori, J., Vetrakova, L., Wirz, J. and Heger, D., 2017, Azobenzene photoisomerization quantum yields in methanol redetermined, *Photochem. Photobiol. Sci.*, **16** (12): 1757-1761

Lee, K. J., Motala, M. J., Meitl, M. A., Childs, W. R., Menard, E., Shim, A. K., Rogers, J. A. and Nuzzo, R. G., 2005, Large-area, selective transfer of microstructured silicon: a printing- based approach to high-performance thin-

서울대학교 SEOUL NATIONAL UNIVERSITY

film transistors supported on flexible substrates, *Adv. Mater.*, **17** (19): 2332-2336

Lee, S.-W., Lee, T.-H., Park, J.-W., Park, C.-H., Kim, H.-J., Kim, S.-M., Lee, S.-H., Song, J.-Y. and Lee, J.-H., 2015, The effect of laser irradiation on peel strength of temporary adhesives for wafer bonding, *Int. J. Adhes. Adhes.*, **57**: 9-12

Lee, T.-H., Han, G.-Y., Yi, M.-B., Shin, J.-H. and Kim, H.-J., 2021, Photoresponsive, switchable, pressure-sensitive adhesives: influence of UV intensity and hydrocarbon chain length of low molecular weight azobenzene compounds, *RSC Advances*, **11** (59): 37392-37402

Lee, T. H., Han, G. Y., Yi, M. B., Kim, H. J., Lee, J. H. and Kim, S., 2021, Rapid photoresponsive switchable pressure-sensitive adhesive containing azobenzene for the mini-light emitting diode transfer process, *ACS Appl. Mater. Interfaces.*, **13** (36): 43364-43373

Li, J., Luo, B. and Liu, Z., 2020, Micro-LED mass transfer technologies, *2020 21st International Conference on Electronic Packaging Technology (ICEPT)*: 1-3, IEEE

Lim, H. S., Han, J. T., Kwak, D., Jin, M. and Cho, K., 2006, Photoreversibly switchable superhydrophobic surface with erasable and rewritable pattern, *J. Am. Chem. Soc.*, **128**: 14458-14459

Linghu, C., Zhang, S., Wang, C. and Song, J., 2018, Transfer printing techniques for flexible and stretchable inorganic electronics, *npj Flex. Electron.*,

서울대학교

2 (1): 1-14

Liu, Z., Cheng, J. and Zhang, J., 2020, An efficiently reworkable thermosetting adhesive based on photoreversible [4+4] cycloaddition reaction of epoxy-based prepolymer with four anthracene end groups, *Macromol. Chem. Phys.*, **222** (2):

Macosko, C. W., 1977, Adhesives rheology, *Adhes. Age*, **20** (9): 35-37

Maugis, D. and Barquins, M., Fracture mechanics and adherence of viscoelastic solids, 1980, in *Adhesion and adsorption of polymers*, Springer, Boston, USA.

Meitl, M. A., Zhu, Z.-T., Kumar, V., Lee, K. J., Feng, X., Huang, Y. Y., Adesida, I., Nuzzo, R. G. and Rogers, J. A., 2005, Transfer printing by kinetic control of adhesion to an elastomeric stamp, *Nat. Mater.*, **5** (1): 33-38

Moon, J.-I., Lee, Y.-H., Kim, H.-J., Noh, S.-M. and Nam, J.-H., 2012, Synthesis of elastomeric polyester and physical properties of polyester coating for automotive pre-primed system, *Prog. Org. Coat.*, **75** (1-2): 65-71

Morino, S. y., Kaiho, A. and Ichimura, K., 1998, Photogeneration and modification of birefringence in crosslinked films of liquid crystal/polymer composites, *Appl. Phys. Lett.*, **73** (10): 1317-1319

Nakamura, T., Takashima, Y., Hashidzume, A., Yamaguchi, H. and Harada, A., 2014, A metal-ion-responsive adhesive material via switching of molecular recognition properties, *Nat. Commun.*, **5** (1): 1-9

Norikane, Y., Tanaka, S. and Uchida, E., 2016, Azobenzene crystals swim on water surface triggered by light, *CrystEngComm*, **18** (38): 7225-7228

서울대학교

Ohzono, T., Saed, M. O. and Terentjev, E. M., 2019, Enhanced dynamic adhesion in nematic liquid crystal elastomers, *Adv. Mater.*, **31** (30): 1902642

Ohzono, T., Norikane, Y., Saed, M. O. and Terentjev, E. M., 2020, Light-driven dynamic adhesion on photosensitized nematic liquid crystalline elastomers, *ACS Appl. Mater. Interfaces*, **12** (28): 31992-31997

Pan, Z., Guo, C., Wang, X., Liu, J., Cao, R., Gong, Y., Wang, J., Liu, N., Chen, Z., Wang, L., Ishikawa, M. and Gong, Z., 2020, Wafer-scale micro-LEDs transferred onto an adhesive film for planar and flexible displays, *Adv. Mater. Technol.*, **5** (12): 2000549

Peng, Z., Wang, C., Chen, L. and Chen, S., 2014, Peeling behavior of a viscoelastic thin-film on a rigid substrate, *Int. J. Solids Struct.*, **51** (25-26): 4596-4603

Priestley, E. B., Liquid crystal mesophases, 1975, in *Introduction to liquid crystals*, Springer, Boston, MA.

Rahim, K. and Mian, A., 2017, A review on laser processing in electronic and MEMS packaging, *J. Electron. Packag.*, **139** (3): 030801

Rau, H. and Yu-Quan, S., 1988, Photoisomerization of sterically hindered azobenzenes, *J. Photochem. Photobiol. A: Chem.*, **42**: 321-327

Saeidpourazar, R., Li, R., Li, Y., Sangid, M. D., Lu, C., Huang, Y., Rogers, J. A. and Ferreira, P. M., 2012, Laser-driven micro transfer placement of prefabricated microstructures, *J. Microelectromech. Syst.*, **21** (5): 1049-1058

서울대학교

Saito, T., 1985, A theoretical approach to the pressure-sensitive adhesion, *日本接着会誌*, **21**: 228

Serra, F. and Terentjev, E. M., 2008, Effects of solvent viscosity and polarity on the isomerization of azobenzene, *Macromolecules*, **41** (3): 981-986

Shen, L., Cheng, J. and Zhang, J., 2020, Reworkable adhesives: fealable and fast response at ambient environment based on anthracene-based thiol-ene networks, *Eur. Polym. J.*, **137**:

Shin, J., Sung, J., Kang, M., Xie, X., Lee, B., Lee, K. M., White, T. J., Leal, C., Sottos, N. R., Braun, P. V. and Cahilla, D. G., 2019, Light-triggered thermal conductivity switching in azobenzene polymers, *Proc. Natl. Acad. Sci.*, **116** (13): 5973-5978

Sim, K., Chen, S., Li, Y., Kammoun, M., Peng, Y., Xu, M., Gao, Y., Song, J., Zhang, Y., Ardebili, H. and Yu, C., 2015, High fidelity tape transfer printing based on chemically induced adhesive strength modulation, *Sci. Rep.*, **5**: 16133

Sperling, L. H., Introduction to physical polymer science, 2005, John Wiley & Sons, New Jersey, USA.

Suh, J. B., Gent, A. N. and Kelly, S. G., 2007, Shear of rubber tube springs, *Int. J. Non Linear Mech.*, **42** (9): 1116-1126

Testa, P., Chappuis, B., Kistler, S., Style, R. W., Heyderman, L. J. and Dufresne, E. R., 2020, Switchable adhesion of soft composites induced by a magnetic field, *Soft Matter*, **16** (25): 5806-5811

서울대학교 SEOUL NATIONAL UNIVERSITY

Titov, E., Granucci, G., Gotze, J. P., Persico, M. and Saalfrank, P., 2016, Dynamics of azobenzene dimer photoisomerization: electronic and steric effects, *J. Phys. Chem. Lett.*, **7** (18): 3591-3596

Tsuda, M. and Kurata, K., 1964, Isomerization of cis-azobenzene in the solid phase, *Bull. Chem. Soc. Jpn.*, **37** (9): 1284-1288

Webster, I., 1997, Recent developments in pressure-sensitive adhesives for medical applications, *Int. J. Adhes. Adhes.*, **17** (1): 69-73

Yamaguchi, H., Kobayashi, Y., Kobayashi, R., Takashima, Y., Hashidzume, A. and Harada, A., 2012, Photoswitchable gel assembly based on molecular recognition, *Nat. Commun.*, **3** (1): 1-5

Yan, Z., Pan, T., Xue, M., Chen, C., Cui, Y., Yao, G., Huang, L., Liao, F., Jing, W., Zhang, H., Gao, M., Guo, D., Xia, Y. and Lin, Y., 2017, Thermal release transfer printing for stretchable conformal bioelectronics, *Adv. Sci.*, **4** (11): 1700251

Yi, H., Seong, M., Sun, K., Hwang, I., Lee, K., Cha, C., Kim, T.-i. and Jeong, H. E., 2018, Wet-responsive, reconfigurable, and biocompatible hydrogel adhesive films for transfer printing of nanomembranes, *Adv. Funct. Mater.*, **28** (18):

Zhang, Y., Yang, X., Zhao, X. and Huang, W., 2012, Synthesis and properties of optically clear silicone resin/epoxy resin hybrids, *Polym. Int.*, **61** (2): 294-300

서울대학교

Zheng, Y., Hashidzume, A., Takashima, Y., Yamaguchi, H. and Harada, A., 2012, Switching of macroscopic molecular recognition selectivity using a mixed solvent system, *Nat. Commun.*, **3** (1): 1-4

Zheng, Y., Hashidzume, A. and Harada, A., 2013, pH-responsive self-assembly by molecular recognition on a macroscopic scale, *Macromol. Rapid Commun.*, **34** (13): 1062-1066

Zhou, H., Xue, C., Weis, P., Suzuki, Y., Huang, S., Koynov, K., Auernhammer, G. K., Berger, R., Butt, H.-J. and Wu, S., 2016, Photoswitching of glass transition temperatures of azobenzene-containing polymers induces reversible solid-to-liquid transitions, *Nat. Chem.*, **9** (2): 145-151

Zhou, Y., Chen, M., Ban, Q., Zhang, Z., Shuang, S., Koynov, K., Butt, H.-J., Kong, J. and Wu, S., 2019, Light-Switchable Polymer Adhesive Based on Photoinduced Reversible Solid-to-Liquid Transitions, *ACS Macro. Lett.*, **8** (8): 968-972

Zosel, A., 1985, Adhesion and tack of polymers: Influence of mechanical properties and surface tensions, *Colloid Polym. Sci.*, **263** (7): 541-553

畑, 敏. and 植松, 市., 1947, 剥離の力學 (接着力の剥離試験法に關する研究)) I~ III (第 3 報) 剥離試驗機の試製と測定値の膜差について, *高分子化學*, **4**: 77-81

서울대학교 SEOUL NATIONAL UNIVERSITY

List of Publications

This Ph.D. dissertation is based on the following publications.

I. Lee, T. H., Han, G. Y., Yi, M. B., Kim, H. J., Lee, J. H. and Kim, S., 2021, Rapid photoresponsive switchable pressure-sensitive adhesive containing azobenzene for the mini-light emitting diode transfer process, *ACS Appl. Mater. Interfaces*, **13** (36): 43364-43373

II. Lee, T. H., Han, G. Y., Yi, M. B., Shin, J. H. and Kim, H. J., 2021, Photoresponsive, switchable, pressure-sensitive adhesives: influence of UV intensity and hydrocarbon chain length of low molecular weight azobenzene compounds, *RSC Advances*, **11** (59): 37392-37402

III. Lee, T. H., …., Kim, H. J., and Kim, S., Photoresponsive, switchable, pressure-sensitive adhesives: UV laser process for selective mini-light emitting diode transfer, **in preparation**

서울대학교 SEOUL NATIONAL UNIVERSITY

초 록

최근 사용자의 요구에 따라 접착력을 조절할 수 있는 점·접착소재에 - 한 연구들이 활발하게 진행되어 오고 있으며, 이러한 소재를 접착력 가변형 점·접착소재라고 한다. 접착력 가변형 점·접착소재는 외부자극에 반응해 접착력을 변화시키는 소재로, 부착 시 높은 접착력을 갖지만 탈착 시에는 낮은 접착력을 갖도록 하는 소재이다. 일상 생활이나 의료 산업에서 편의성을 위해 이러한 소재가 사용되기도 하지만, 최근 고도화된 전기전자 산업의 다양한 제조 공정에서 부품, 회로, 디바이스 등을 임시로 고정한 후 분리시키는 공정에 적용하기 위해 많은 연구들이 진행되고 있다.

하지만 기존에 연구된 소재들은 수분, 열, 장시간의 공정과 같이 산업에 적용하기 어려운 조건을 충족시켜야 하거나, 영구적인 반응이나 잔사 문제로 재사용이 어려운 한계를 가진다. 따라서, 위와 같은 한계점들을 극복할 수 있는 소재에 - 한 연구 필요성이 있었다.

이번 연구에서는 빛을 외부 자극으로 활용하기 위해 아조벤젠 그룹을 이용하였으며, 아조벤젠을 포함하는 아크릴 고분자와

서울대학교 SEOUL NATIONAL UNIVERSITY

저분자량의 아조벤젠 화합물을 혼합하여 빛에 반응하는 접착력 가변형 점착소재를 제조하였다. 이 점착소재는 초기 상태에서는 접착력이 없지만 365 nm 파장의 자외선을 조사하였을 때 접착력이 활성화 되었으며, 가시광선의 조사를 통해 다시 접착력이 없는 초기 상태로 돌아올 수 있었다. 이러한 접착력의 전환이 접착력의 변화없이 30회까지 반복됨을 확인하여 반복 사용이 가능함을 검증하였다.

분석을 통해 자외선과 가시광선에 의한 트랜스 아조벤젠과 시스 아조벤젠 사이의 광-이성질체화가 아조벤젠 화합물이 이루는 결정구조의 전환을 유도하며, 이 결정구조의 전환은 점착 소재의 물성, 표면 에Δ 지, 유리전이 온도의 전환을 동반시켜 최종적으로 접착력의 전환을 만들어 냄을 밝혀냈다. 또한, 각기 다른 길이의 탄화수소 사슬을 치환기로 갖는 아조벤젠 화합물들을 합성하여 점착소재를 제조하였는데, 이 연구를 통해 아조벤젠 화합물 결정구조의 견고한 정도가 접착력 전환을 위해 필요한 자외선의 세기와 시간을 결정하는 것을 밝혔다.

마지막으로는 자외선 레이저 장비를 통한 접착력 전환과 이를 통한 mini-LED의 선택적 전사공정에 - 한 연구를 진행했다. 자외선 레이저 장비는 미세한 패턴을 정교하게 형성시킬 수 있고, 빠른

서울대학교

공정이 가능하다는 장점을 갖는다. 이번 연구에서 자외선 흡수제를 포함하는 점착소재를 레이저 공정에 적용하였으며, 자외선 흡수제가 높은 에Δ 지의 레이저 빔으로 인한 표면 손상을 방지할 수 있었다. 레이저의 에Δ 지 밀도나 출력과 접착력 전환 특성 간에 선형 관계는 없었지만, 특정한 범위의 조건에서 최적 공정 조건을 ω 을 수 있었다. 이 공정 조건을 통해 점착소재에 패턴화된 접착력 전환이 가능했고, 선택적인 mini-LED 전사 공정을 성공적으로 구현했다.

위 연구들을 통해 새로운 접착력 가변형 점착소재를 제시하였으며, 이 점착소재는 광에 빠르게 반응하며 재사용이 가능한 장점을 가졌다. 또한, 레이저 공정을 이용하여 선택적인 mini-LED 전사 공정으로의 적용가능성을 제시하였다.

키워드 : 점착소재, 접착력 가변형 점착소재, 광 반응형, 아조벤젠, 광-이성질화체화, mini-LED, 자외선 레이저, 전사 공정

학 번 : 2013-21131

서울대학교